UNIVERSITÀ
DEGLI STUDI
FIRENZE

DOCTORAL PROGRAMME IN DRUG RESEARCH AND INNOVATIVE TREATMENTS

CYCLE XXXI

Coordinator: Prof. Teodori Elisabetta

"Effects of adenosine A_{2B} and A_3 receptor ligands on synaptic activity, oligodendrogenesis and dorsal root ganglia excitability *in vitro*"

Scientific–Disciplinary Sector: BIO/14

PhD student
Dr. Fusco Irene

Tutor
Prof. Pugliese Anna Maria

Coordinator
Prof. Teodori Elisabetta

Years 2015/2018

INDEX

ABSTRACT

The role of the neuromodulator adenosine and its receptors on cerebral ischemia, synaptic activity, oligodendrogenesis and dorsal root ganglia excitability was investigated by using different *in vitro* models with the specific purpose to individuate new class of neuroprotective agents for different pathological conditions.

Cerebral ischemia is a multifactorial pathology characterized by different events evolving in time. Adenosine levels in the brain increases dramatically during ischemia up to concentrations able to stimulate all its receptors, A_1, A_{2A}, A_{2B}, and A_3. The neuroprotective role of A_1 receptors (A_1AR_S) in this pathology is well established, but the use of selective A_1AR agonists is hampered by their undesirable peripheral side effects. Data in literature demonstrate that adenosine A_{2A} and A_3 receptors ($A_{2A}AR_S$, A_3ARs) play a controversial effects during ischemia, whereas the involvement of adenosine A_{2B} receptors (A_{2B}ARs) is not yet investigated.

On this basis, in a first part of this study we explored the role of A_{2B}AR on synaptic activity and cellular excitotoxcicity under physiological conditions and during *in vitro* ischemic-like insult (obtained by oxygen and glucose deprivation: OGD) in the CA1 region of rat hippocampus, a cerebral area particularly susceptible to ischemic insult. We conducted extracellular recordings of CA1 field excitatory post-synaptic potentials (fEPSPs) in acute hippocampal slices to monitor the impact of OGD insults on synaptic activity. Furthermore, the extent of histological damage was assessed on neurons and glia by immunohistochemistry. A severe, 7 min OGD induced the appearance of anoxic depolarization (AD), a clear sign of tissue damage, in all hippocampal slices tested and completely abolished fEPSPs that did not recover after return to normoxic condition. Seven minutes OGD was than applied in the presence of the selective A_{2B}AR antagonists MRS1754 (500 nM) or PSB603 (50 nM), separately administered 15 min before, during and 5 min after OGD. Both antagonists did not modify fEPSP amplitude under normoxia but prevented or delayed the appearance of AD and allowed significant recovery of neurotransmission within 10-15 min of normoxic reperfusion. The A_{2B}AR antagonism also counteracted the reduction of neuronal density in CA1 stratum pyramidale, decreased apoptosis at least up to 3 h after the end of OGD and maintained activated mTOR levels similar to those of controls, thus sparing neurons from the degenerative effects caused by the simil-ischemic conditions. Astrocytes significantly proliferated in CA1 stratum radiatum already 3 h after the end of OGD, possibly due to increased glutamate release. A_{2B}AR antagonism significantly prevented astrocyte modifications. The selective antagonists of the A_{2B}AR subtype may thus represent a new class of neuroprotective drugs in ischemia.

The A_{2B}ARs are also known to inhibit paired pulse facilitation (PPF), a form of short-term plasticity whose reduction reflects an increase in presynaptic glutamate release. The effect of A_{2B}ARs on PPF is known to be sensitive not only to A_{2B}AR blockade but also to the A_1AR antagonist DPCPX, indicating that it is mediated by A_1AR activation. In the second part of this study we confirmed the involvement of A_{2B}AR in PPF by using the prototypical selective agonist BAY606583. We also provide the first functional characterization of two newly synthesized non-nucleoside like A_{2B}AR agonists: P453 and P517, belonging to the amino-3,5-dicyanopyridine series. By means of extracellular recordings, we investigated their effect on PPF protocol at Schaffer collateral-CA1 synapses in rat acute hippocampal slices. We found that P453 and P517 mimicked the effect of BAY606583 in decreasing the PPF in all slices tested. This effect was prevented by two different A_{2B}AR antagonists PSB603 and MRS1754 and also by the A_1AR antagonist DPCPX. We conclude that P453 and P517 are functional A_{2B}AR agonists whose activation increases glutamate release at presynaptic terminals by counteracting the tonic A_1AR -mediated inhibition of synaptic transmission.

Multiple Sclerosis (MS) is the most frequent demyelinating disease in the Central Nervous System (CNS). Remyelination does occur, but is limited especially in chronic disease stages. Therefore, promotion of neuroprotective and repair mechanisms, such as remyelination, represents an attractive additional treatment strategy. A number of pathways have been identified that may contribute to ameliorate the impaired remyelination in MS lesions; among them are adenosinergic signaling and sphingosine kinase/sphingosine 1-phosphate signaling axis (SphK/S1P). Oligodendrocyte development involves progression from oligodendrocyte progenitor cells (OPCs) to mature oligodendrocytes. Both cellular types express each of the different adenosine receptor subtypes (A_1, A_{2A}, A_{2B} and A_3). Interestingly, treatment of OPCs in culture with adenosine promotes maturation and migration through A_1AR, without adverse effects on cell viability. Moreover, treatment of OPCs

in culture with selective A_{2A}AR agonists reduces outward K^+ currents and, by this mechanism, inhibits cell maturation into myelinating oligodendrocytes. A very recent study demonstrated that Fingolimod (FTY720), that has been approved as orally active drug for relapsing MS, modulates S1P receptors. A relationship between SphK1 activity and A_{2B}AR activation has been demonstrated in mouse normal and sickle erythrocytes *in vitro*.(Sun *et al*., Blood, 2015, 125(10):1643-52). In a third part of this study the role of A_{2B}AR and SphK/S1P signaling on oligodendrogenesis in rat cultured OPCs was investigated by patch clamp experiments coupled to Western Blot and Real Time PCR. In particular, we investigated the effects of A_{2B}AR ligands on: i) outward K^+ currents and ii) myelin basic protein (Mbp) and myelin-associated glycoprotein (MAG) expression at different times in culture. BAY606583 (0.1-30 µM) reduced the amplitude of outward potassium currents. This effect was blocked by MRS1706 (10 µM), a selective A_{2B}AR antagonist. Similar results were obtained in the presence of newly selective synthetized A_{2B}AR agonists P453and P517 and unselective A_{2B}AR agonist NECA, applied in conditions of A_1, A_{2A} and A_3AR block. The active form of Fingolimod named FTY720-phosphate (FTY720-P) at micromolar concentration mimicked and partially occluded the effect of BAY606583. When applied at nanomolar concentrations, FTY720-P produced an increase in outward potassium currents. SphK1 phosphorylation was enhanced after acute treatment with BAY606583, demonstrating an interaction between SphK/S1P pathway and A_{2B}AR activation. Chronic application (7 days) of BAY606583 (1-10 µM) or of P453 (50-100 nM) in cultured medium reduced OPC differentiation, as indicated by the decrease of the two genes target MAG and Mbp3, typically expressed by mature oligodendrocytes. FTY720-P (1 µM), mimicked the effect of 10 µM BAY606583 on OPC maturation. On the contrary, VPC96047 (0.5 µM), a pan-SphK inhibitor, and VPC96091 (0.5 µM) a selective SphK1 inhibitor, increased MAG and Mbp3 levels. These effects were abolished in the presence of 10 µM BAY606583. Our data shows that novel pathways activated by A_{2B}AR and SphK/S1P are involved in the maturation of OPCs.

In recent years, there have been further significant developments in understanding of the role of adenosine in nociception. It's known that A_1AR activation inhibits pain behaviours in different models of acute or chronic pain. Unfortunately, the therapeutic utility of A_1AR agonists is limited by their adverse cardiovascular effects. Of note, exciting preclinical observations designate the A_3AR as a powerful analgesic mediator in different *in vivo* rodent models of experimental neuropathic pain (Janes *et al.*, 2016, Br. J. Pharmacol., 173: 1253–67; Little *et al.*, 2015, Brain 138: 28–35), suggesting A_3AR agonists can be used for analgesia treatment without cardiovascular implications. The cellular mechanisms mediating pain relief on A_3AR activation remain largely unexplored. In the last part of this study, we investigated the expression and functional effects of A_3AR on the excitability of small-medium sized, capsaicin-sensitive, dorsal root ganglion (DRG) neurons isolated from 3-4 week-old rats. RT-PCR experiments and immunofluorescence analysis revealed A_3AR expression in DRG. Patch-clamp experiments demonstrated that two distinct A_3AR agonists, Cl-IB-MECA and the highly selective MRS5980, inhibited Ca^{2+}-activated K^+ (K_{Ca}) currents evoked by a voltage ramp protocol. This effect was dependent on a reduction of Ca^{2+} influx via N-type voltage-dependent Ca^{2+} channels (VDCCs) as Cl-IB-MECA significantly reduced Ca^{2+} currents activated by a 0 mV depolarization and this effect was sensitive to the N-type blocker PD173212 but not to the L-type blocker, lacidipine. The endogenous agonist adenosine also reduced N-type Ca^{2+} currents, and its effect was inhibited by 56% in the presence of A_3AR antagonist MRS1523, demonstrating that the majority of adenosine's effect is mediated by this receptor subtype. Current clamp recordings demonstrated that neuronal firing of rat DRG neurons was also significantly reduced by A_3AR activation in a MRS1523-sensitive but PD173212-insensitive manner demonstrating that firing inhibition was not dependent upon N-type Ca^{2+} channel inhibition. Intracellular Ca^{2+} measurements confirmed the inhibitory role of A_3AR on DRG neuronal firing. We conclude that pain-relieving effects observed upon A_3AR activation could be mediated through N-type Ca^{2+} channel block and action potential inhibition, as independent mechanisms in isolated rat DRG neurons. These findings support A_3AR-based therapy as a viable approach to alleviate pain in different pathologies.

INTRODUCTION

INTRODUCTION

1. Adenosine

Adenosine is a purine nucleoside indispensable for DNA synthesis: it is formed by an adenine and ribose molecule joined through an N9-glicosidic bond, which, in nervous system, is continually formed both at intracellular and extracellular level (Figure 1).

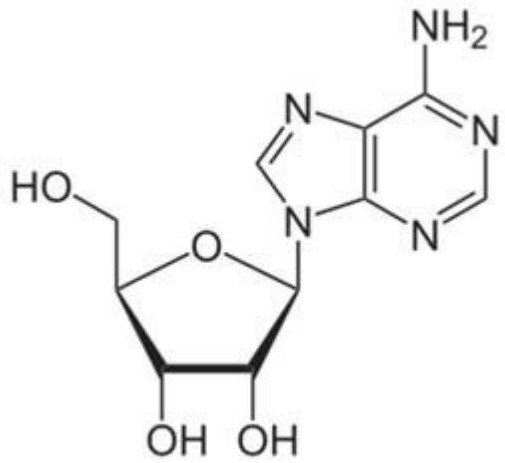

Figure 1: Adenosine structure formula. Its brute formula is C10H13N5O4 (Taken from: Ceruti *et al.*, 2004).

Adenosine play an essential role as neuromodulator also in biochemical processes and signal transduction, being correlates with molecules such as ATP, ADP and AMP. At central level, it carries out numerous actions: acts as an endogenous anticonvulsant, influences control of motility, pain, learning and memory (Pedata *et al.,* 2007). Moreover, adenosine has a further crucial role in the modulation of emotional states, conditioning social interactions and aggressive behaviours. In physiologic conditions, extracellular adenosine exercises an inhibition on synaptic transmission and this makes adenosine a highly protective neuromodulator. At the extracellular side, adenosine is produced from AMP (Adenosine monophosphate) which is dephosphorylated by the enzyme 5'-nucleotidase (5'-NT). Adenosine can also be formed through the breakdown of nucleotides which are released into extracellular space. The 5'-NT is inhibited by ATP and it has an elevated affinity towards AMP: for this reason, when the cell is exposed to an intense metabolic activity with increased ATP consumption and consequent elevated production of AMP, the enzyme has very high enzymatic activity (Pedata *et al.,* 2007). Therefore, during low energetic support conditions as in epileptic attacks, hypoxia or ischemia, production of adenosine is much raised (Latini and Pedata, 2001). Adenosine is a paramount chemical mediator which can activate determined biologic responses and its action mainly occurs through purinergic receptors activation. These every receptor is structurally composed by 7 amphipathic α-helices (TM 1-7), which consist of a sequence of 20-25 hydrophobic amino acids (Figure 2).

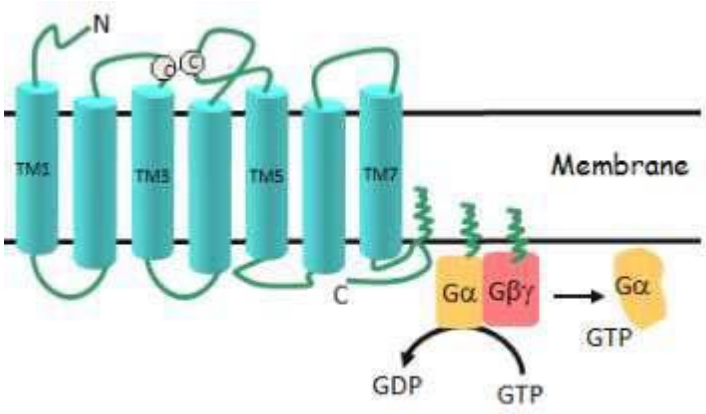

Figure 2: Seven transmembrane domain receptor (TM) coupled with a G-protein. The Gα, binding GTP, release itself and activates a biologic response (Taken from: Cristalli *et al.,* 2008).

The N-terminal portion is located at extracellular level whereas the C-terminal exposes toward the intracellular side; all the 7 domains are strictly interconnected via 3 intracellular (IL 1-3) and 3 extracellular loops (EL 1-3) (Cristalli *et al.,* 2008). The seven transmembrane domain receptors are always associated, at the intracellular side, with specific transduction heterotrimeric protein, defined G protein, which are activated after the interaction between the receptor and substrate.

The purine receptors have been classified in two categories by Burnstock in 1978, P1 and P2 (X, Y) receptors, the latter ones activated by ATP (Burnstock *et al.,* 1978). This distinction helped clarifying the incredible variety and complexity of purine-mediated effects observed till then and the ubiquitous presence of ecto-ATPases, enzymes catalysing extracellular nucleotides degradation. The presence of these enzyme on cell membranes incredibly complicated the scenario by forming ADP, AMP and adenosine from extracellular ATP (Zimmermann *et al.,* 1998), so that some of the actions of ATP were directly due to P2 receptor activation, whereas others were due to the indirect action of adenosine on P1 receptors. Both P1 and P2 subfamilies where later recognised to be further divided into different subtypes. P1 receptors were initially distinguished into two classes (A_1 and A_2 receptors) on the basis of their excitatory or inhibitory actions on adenylyl cyclase (van Calker *et al.,* 1979). Later work defined four different subtypes of P1 receptors: A_1, A_{2A}, A_{2B} and A_3 (Fredholm *et al.,* 2001). P2 receptors appeared to be more heterogeneous, with P2T, P2Z and P2U subtypes being proposed from different authors (Gordon, 1986; O'Connor *et al.,* 1991). Definitive classification came from Abbracchio and Burnstock (Abbracchio and Burnstock, 1994) who proposed that P2 purinoceptors should belong to two major families: P2X ligand-gated ion channel receptors and P2Y G-protein-coupled receptors. Cloning experiments supported this classification and helped subdividing P2 receptors into seven P2X and eight P2Y subtypes (King, 2002; North, 2002).

To date, it is well recognised that purinergic signalling plays a fundamental role in several biological systems, from invertebrates to mammals, and purinergic-mediated effects including both short-term (neurotransmission, endothelial-mediated vasodilatation, platelet aggregation) and long-term (cell proliferation, differentiation, migration and death) phenomenon have been demonstrated.

1.1 Adenosine and Synaptic Transmission

Recent experiments have focused much attention on adenine nucleotides as possible transmitters or neuro modulators in the mammalian brain. Although much of the work implicating adenosine or related compounds in 'purinergic transmission has been done with the peripheral nervous system (Burnstock, 1975).

The possible relevance to the function of the CNS has not been lost on workers in this area. Indeed, adenosine (or related adenine nucleotides) meet many of the criteria for consideration as putative transmitters; these compound sand the enzymes for their synthesis and degradation are ubiquitous in the nervous system, and are released in a calcium-dependent manner by either field stimulation or by activation of discrete synaptic systems (Pull and McIlwain, 1972; McIlwain and Pull, 1972; Deadwyler *et al.,* 1976) Adenosine and various derivatives have potent depressant actions at many levels of the neuroaxis when administered by microiontophoresis, with the hippocampus, cortex, and caudate being particularly sensitive (Kostopoulos *et al.,* 1975; Kostopoulos and Phillis, 1977; Taylor and Stone, 1978). In experiments using *in vitro* preparations and perfusion with these compounds, a marked reduction in the amplitude of monosynaptic evoked responses has been demonstrated (Kuroda *et al.,* 1976; Scholfield, 1978). Nevertheless, a convincing case has yet to be made for adenosine being the sole transmitter at any central synapse. Partly in response to this, and partly because many of the actions of adenosine are seen at synapses where adenosine is clearly not the primary transmitter (Ginsborg and Hirst, 1972; Miyamota and Breckenridge, 1974; Schubert *et al.,* 1976; Hayashi *et al.,* 1978). It has come to be regarded more as a putative neuromodulator than as a transmitter *per se* in the CNS. In addition to the powerful electrophysiological actions of adenosine, it is also one of the most potent elevators of cyclic adenosine 3',5'-monophosphate(cyclicAMP) levels in brain tissue (Sattin and Rall, 1970; Shimizu and Daly, 1970; Schultz, 1975). Because these increases in cyclicAMP can be blocked by a variety of antagonists, primarily methylxanthines (Sattin and Rall, 1970; Huang and Daly, 1972; Kuroda *et al.,* 1976; Mah and Daly, 1976) and because the increases in cyclicAMP can be potentiated by treatments which would be expected to raise extracellular adenosine concentrations, such as adenosine uptake blockers (Huang and Daly, 1974), it has been suggested that adenosine may exert its effects via an interaction with an adenylatecyclase-linked receptor located in the cell membrane (Huang *et al.,* 2006; Huang and Daly, 1974; Mah and Daly, 1976). In addition to directly increasing cyclicAMP levels, adenosine also potentiates the ability of other amines, most not ably noradrenaline (NA), to stimulate cyclicAMP formation. Thus, adenosine has clearly defined physiological effects, and biochemical evidence suggests an empirically defined adenosine receptor which is coupled to an adenylate cyclase, and which possibly interacts with other amine-sensitive adenylate cyclases.

2. Effects of extracellular purines

In virtually all peripheral tissues, extracellularly released nucleotides or nucleosides play important roles in a large number of physiological processes. In addition, the rapid breakdown of extracellular ATP to adenosine is responsible for a close interplay between ATP-ergic and adenosinergic systems whose clear dissection presents numerous experimental problems (Hussl and Boehm, 2006) (Figure 3).

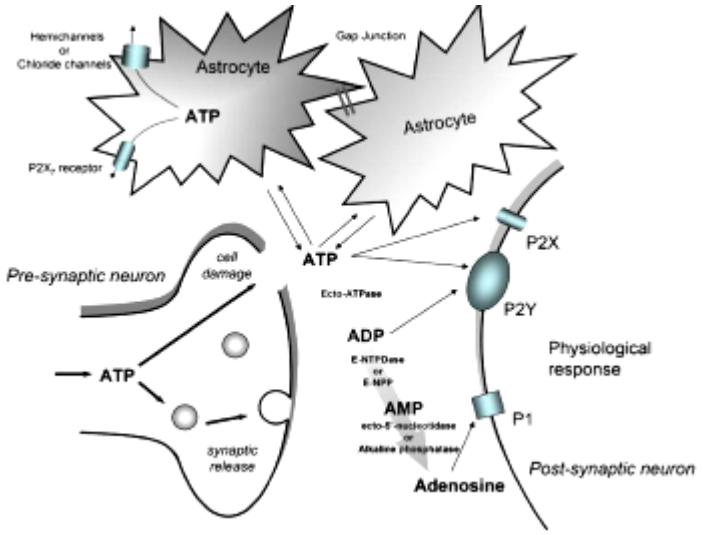

Figure 3: Purine-induced signaling pathway involves the activation of P1 adenosine and P2 purinergic receptors and purine hydrolysis by ectonucleotidases. The scheme demonstrates purinergic receptor activity present in glia-glia, neuron-glia, and neuron-neuron interaction during neurogenesis as well as in the metabolism of the adult brain (Taken from: Majumder *et al.*, 2007).

2.1 Purinergic receptors

Receptors for both ATP and adenosine are widely distributed in the nervous system as well as in other tissues. The notion that there are purinergic receptors, that is, proteins on the surface of cells that bind and respond to purines, was slow to evolve. The first evidence was the observation of cardiovascular physiological effects of purines. Drury and Szent-Gyorgyi (Drury and Szent-Györgyi, 1929), first noted effects of adenine nucleotides on cardiac and vascular tissues in 1929. Thirty-four years later, Berne (Berne, 1963) identified a physiological role for adenosine as a mediator of coronary vasodilation in response to myocardial hypoxia. In the 1970s, adenosine was found to stimulate cAMP formation in brain slices. Subsequently, physiological effects of adenosine on almost all tissues have been described. Based on the responses of various tissues to purines, Burnstock (Burnstock *et al.*, 1978) proposed that there are distinct receptors that bind adenosine or ATP, designated P1 and P2 receptors, respectively (see Figure 4). The existence of adenosine receptors was not widely accepted until the 1980s, when saturable binding sites for radioactive adenosine analogs were demonstrated in brain. The existence of adenosine receptors was proved unequivocally when the first adenosine receptors were cloned in 1990 (Maenhaut *et al.*, 1990).

Originally, the "P" in P1 and P2 was meant to designate purinergic receptors. However, it has been discovered that some of the P2 receptors bind pyrimidines, UTP or UDP, preferentially over the purine, ATP. Hence, the "P" in P2 is now used to designate purine or pyrimidine. Despite these exceptions, P1 and P2 receptors collectively are still generally referred to as purinergic receptors. In addition to adenosine, various synthetic adenosine analogs activate P1, but not P2, receptors and synthetic ATP or UTP analogs activate P2, but not adenosine, receptors. However, not all purines activate P1 or P2 receptors. For example, adenine, guanosine and uric acid do not activate P1 receptors. Inosine, the purine nucleoside product of adenosine deamination, generally has weak activity at P1 receptors but does activate A_3 adenosine receptors in ischemic tissues, particularly in rodent species (Jin *et al.*, 1997). This action of inosine may be physiologically significant because inosine accumulates to very high concentrations (>1 mM) in ischemic tissues. The development of synthetic compounds that activate P1 or P2 receptors has been important for elucidating how these receptors function because some of these compounds are more potent and selective than the parent purines and most are more stable than the short-lived endogenous compounds adenosine and ATP.

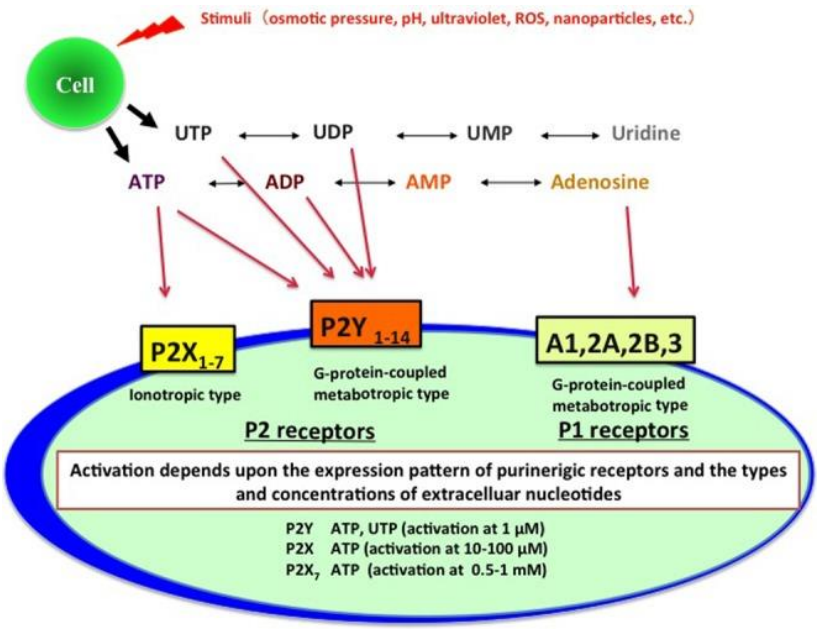

Figure 4: The purinergic receptor family. The purinergic receptors are divided into two major families: the P1, or adenosine, receptors and P2 receptors, which bind ATP and/or UTP. P1 and P2Y receptors are coupled to GTP-binding proteins. The P2X family of receptors are ligand-gated channels. Additional P2Y receptor subtypes have been claimed, but their identity as purinergic receptors is controversial. (Taken from: Siegel, 1999).

2.1.1 P1 receptors

Molecular cloning and pharmacological studies have identified four subtypes of adenosine P1 receptors: A_1, A_{2A}, A_{2B} and A_3 receptors (Fredholm *et al.*, 2001). All of them have already been cloned at least from rat, mouse and human. Structural data report a close similarity between adenosine receptors of the same subtype among mammalian species, excepte for A_3 receptors. This

subtype is the most recently discovered one, being cloned only in the last 15 years (Zhou *et al.*, 1992), and presents the largest variability. For instance, almost 30% difference in the amino acid sequence is found between humans and rats (Fredholm *et al.*, 2001).

All P1 receptors are metabotropic GPCR. Hence, A_1 and A_3 subtypes are associated with Gi activation, adenylyl cyclase inhibition and decrease of intracellular cAMP levels, while A_{2A} and A_{2B} receptors are linked to Gs proteins that activate the same enzyme increasing cAMP concentration in the cytosol. However, adenosine receptors have also been reported to couple to other G-proteins than Gs, modulating different second messenger systems (see Table 1). For instance, in addition to their effects on adenylate cyclase (and contrary to adenosine A_{2A} receptors) adenosine A_1, A_{2B} and A_3 receptors are also characterized by their stimulatory effect on phospholipase C (PLC) (Abbracchio *et al.*, 1995; Feoktistov and Biaggioni, 1997). Furthermore, A_1 and A_3 receptors can also activate phospholipase D (PLD) (Fredholm *et al.*, 2001). Several types of Ca^{2+} and K^+ channels are also activated (either by a direct G protein-channel interaction or by second messenger systems) after adenosine receptor stimulation, such as the inward rectifier GIRK channel Kir3.0 that is positively modulated by adenosine A_1 receptor activation (Takigawa and Alzheimer, 2002). A_1, A_{2A} and A_3 receptors present a particularly high affinity for the endogenous ligand, being activated by nanomolar concentrations of adenosine (Fredholm *et al.*, 2001) On the other hand, the affinity values of A_{2B} receptors for adenosine in binding and functional experiments are higher than 1 μM (Fredholm *et al.*, 2011). Under physiological conditions, extracellular adenosine concentrations are estimated to be in the range of 30 to 200 nM (see: Latini and Pedata, 2001;Frenguelli *et al.*, 2007). These levels are sufficient to activate A_1, A_{2A} and A_3 receptors subtypes, but not A_{2B}, which require higher concentrations (micromolar range) of adenosine to be activated. Such higher adenosine concentrations are only reached under pathological conditions, such as during hypoxia or ischemia *in vivo* (Pedata *et al.*, 2001) and *in vitro* (Latini *et al.*, 1999b).

Table 1. Characteristics and distribution of adenosine receptor subtypes in the Central Nervous System

Receptor subtypes	G-protein	G-protein coupling effect	Adenosine affinity	Distribution
A_1	$G_{i\ 1/2/3}$	↓ cAMP ↑ PLC, IP_3/DAG ↑Arachidonato,PLA_2 ↑ PLD	~100 nM	High levels in cortex, hippocampus, cerebellum. Intermediate levels in striatum and thalamus
A_{2A}	G_o G_s G_{olf} $G_{15/16}$	↑ cAMP ↑ cAMP ↑ IP_3	20-300 nM	High levels in striatum, nucleus accumbens and olfactory tubercle. Low levels in cortex and hippocampus
A_{2B}	G_s $G_{q/11}$	↑ cAMP ↑ PLC, IP_3/DAG, ↑ PLD	5-20 µM	Low level
A_3	$G_{i2/3}$ $G_{q/11}$	↓ cAMP ↑ PLC, IP_3/DAG ↑ PLD	25-290 nM	Widespread distribution. Higher levels in rat hippocampus and cerebellum.

(Taken from: Fredholm *et al.*, 2011)

2.1.2 A_{2B} adenosine receptors (A_{2B}AR)

A_{2B}AR show a low affinity for adenosine (EC_{50} = 5-20 µM; Beukers *et al.*, 2000; Fredholm *et al.*, 2001; Sachdeva and Gupta, 2013) and are associated, as the A_{2A}AR, to Gs protein; for these reason they were initially considered a receptor subtype with a little physiological importance (Sun and Huang, 2016). Recently we are beginning to understand the importance of this receptor and how much they are involved in many diseases. Moreover in physiological conditions, for their low affinity to adenosine, they are not activated; of contrary they are activated in pathological conditions, when adenosine reaches concentrations of micromolar order, therefore it represents an interesting therapeutic target. In addition to being coupled to Gs protein, the A_{2B}AR can be coupled to Gq protein (Gao *et al.*, 1999; Linden *et al.*, 1999; Panjehpour *et al.*, 2005), to the MAPK and arachidonic acid

pathway and to regulate the channels membrane ion probably through the βγ subunit of G protein (Donoso *et al.*, 2005; Schulte and Fredholm, 2003).

In general, A_{2B}AR are widely expressed in numerous tissues and organs, including the vascular system, smooth muscle, gastrointestinal tract, brain tissue and bladder (Wang and Huxley, 2006; Yaar *et al.*, 2005). However, the presence of these receptors is influenced by environmental stimuli, such as inflammation, cellular stress, trauma and hypoxia, which may increase their expression (Fredholm *et al.*, 2001; Hart *et al.*, 2009; Haskó *et al.*, 2009; Kolachala *et al.*, 2005; Kong *et al.*, 2006; Xaus *et al.*, 1999).

2.1.3 A_3 adenosine receptors (A_3AR)

The A_3AR have a high affinity for adenosine (EC_{50} = 300 nM) and are coupled to Gi proteins, whose activation inhibits the Adenylate Cyclase, stimulates the phospholipase C and B and induces the uptake of Ca^{2+} and its release from intracellular reserves (Sachdeva and Gupta, 2013).

Their activation can lead to both protective and harmful effects (Cheong *et al.*, 2013): in non-neuronal cells it was observed that a non-excessive activation prevents apoptosis mechanisms, while a persistent and intense activation induces toxic effects (Yao *et al.*, 1997). In general A_3AR are mainly expressed in the kidneys, lungs, heart, cerebral cortex and immune cells such as mast cells, eosinophils and neutrophils (Livingston *et al.*, 2004). These receptors show a significant difference between the various species under the pharmacological profile, the distribution and their function. In oligodendrocytes A_3AR represents the main cause of toxicity due to the action of adenosine; in fact, the selective 2-Cl-IB-MECA agonist induces apoptosis in oligodendrocytes, while the selective antagonist MRS 1220 is protective when the extracellular concentration of adenosine rises to 10 μM, as it occurs following ischemia (González-Fernández *et al.*, 2014). The toxic effect is due to the generation of reactive oxygen radicals (ROS) and the depolarization of the mitochondrial membrane (Brady *et al.*, 2004; Cao *et al.*, 2011), which leads to the release of pro-apoptotic proteins, activating the intrinsic pathway of apoptosis (González-Fernández *et al.*, 2014; Masino and Boison, 2013).

2.1.4 Pharmacology of P1 receptors

Since adenosine receptors have been studied for a long time, there are several useful pharmacological tools available at present. Numerous adenosine analogues have been developed that selectively bind one of the four different subtypes of P1 receptors. In human, rat and mouse tissues, the A_1 full agonist CCPA (and to a lesser extent CPA) and the antagonist DPCPX are highly selective compounds active at nanomolar concentrations. Allosteric enhancers for this receptor subtype (such as PD81723 and analogues) are also available and increase the agonist binding and its effects (Bruns and Fergus, 1990; van der Klein *et al.*, 1999).

NECA was long considered to be a selective A_2 agonist but it has been largely demonstrated that it is an unselective agonist at all P1 receptors, only slightly preferring A_{2A} subtypes (Fredholm *et al.*, 2001). However, based on evidence that 2-substitution of NECA molecule increased selectivity,

CGS21680 was developed as an A_{2A} selective agonist (Hutchison and Fox, 1989). This compound is less potent and selective in humans than in rats (Kull *et al.,* 1999), but it has been replaced by another recently developed A_{2A} agonist, ATL-146, which is 50 fold more potent than CGS21680 at the human receptor (Rieger *et al.,* 2001). Among the numerous A_{2A} antagonists, the most selective so far are SCH58261 and SCH442416 and the structurally related ZM241385 (Poucher *et al.,* 1995).

Potent A_{2B} agonists with affinity values in the low nanomolar range have been lacking till recently, when a new class of non-adenosine compounds (pyridine derivatives) has been synthesised by Beukers and colleagues (Beukers *et al.,* 2004). Among them, LUF5835 is a full agonist with an EC50 of 10 nM at human A_{2B}AR expressed in CHO cells. Unfortunately, its selectivity towards A_1AR and A_{2A}AR is not adequate to discriminate between them in native tissues. The situation is somewhat more favourable for antagonists, as some potent and relatively selective compounds have been found among anilide derivatives of xanthines with Ki values in the low nanomolar range, such as MRS1754 (Ji *et al.,* 2001), that is over 200-fold selective for A_{2B} *vs* all other P1 receptors (Kim *et al.,* 2000).

An emblematic feature of the adenosine A_3AR, the most recently discovered one, is its insensitivity to the antagonistic actions of methylxanthines, such as caffeine and theophylline, the traditional blockers of adenosine receptors (Fredholm, 1995). Hence, most A_3 antagonists are dihydropyridines, pyridines and flavonoids (Baraldi and Borea, 2000). Another class of highly selective compounds are isoquinoline and quinazoline derivatives, such as VUF5574 that presents a Ki value of 4 nM *vs* human A_3AR but not *vs* the rat isoform (van Muijlwijk-Koezen *et al.,* 2000). In this regard, it is worth noticing that significant species differences in the affinity of adenosine A_3 receptor antagonists have been noted, as expected from the high structural inter-species variability already mentioned. The affinity values of several A_3 blockers are typically more than 100-fold greater on human than rat receptors, as described for MRS1220. The unique rat-selective compound is the A_3 agonist MRS1523. In contrast, the affinity of the most widely used A_3 agonist, Cl-IB-MECA, does not vary beyond an order of magnitude between the species examined, at least among mammals. The high affinity (low nanomolar range) and selectivity (more than 100-fold *vs* A_1AR and A_{2A}AR) of this compound towards A_3AR turns it into the most used pharmacological tool for investigating A_3-mediated effects (Jeong *et al.,* 2003).

2.1.5 Distribution of P1 receptors

Receptor distribution provides helpful information on whether the endogenous agonist will exert significant effects in the intact organism. Thus, in this case, the rather low levels of adenosine present under basal physiological conditions and the 3-fold difference in receptor affinity for the agonist between the four P1 subtypes might suggest adenosine acts as a tonic modulator of normal cell functions or whether its role only becomes relevant during pathological conditions. As reported in Table 1, the highest levels of adenosine A_1AR are present in the CNS (Dixon *et al.,* 1996) with well known regional distributions (Schindler *et al.,* 2001) that will be examined in detail. High levels are also found in adrenal glands, eye and atria. Intermediate levels are also found in skeletal muscles,

liver, kidney, adipose tissue, gastrointestinal smooth muscles and bronchi. Lung and pancreas present low level of A_1AR expression (Fredholm *et al.,* 2001).

A_{2A} receptors are highly present in spleen, thymus, immune cells (leukocytes and granulocytes) and platelets. Lower levels are also found in the heart, lung and blood vessels. A_{2B} subtype is particularly abundant in the gastrointestinal tract, mainly in caecum, colon and urinary bladder. Other regions are lung, blood vessels and adipose tissue.

The A_3 subtype is mainly found in rat testis (Meyerhof *et al.,* 1991) and mast cells, in accordance with the fact that for a long time the unique role assigned to this receptor have been mast cell degranulation and histamine release. Intermediate levels are also found in the lung, spleen, thyroid and liver (Linden *et al.,* 1993; Salvatore *et al.,* 1993). Low levels of A_3AR are found in the brain (Dixon *et al.,* 1996) as described below.

2.1.6 CNS distribution of P1 receptors

There is much information on the distribution of the A_1AR and A_{2A}AR in the brain because excellent pharmacological tools, including radioligands, are available to exactly localise protein expression on cell membranes. In the case of A_{2B} and A_3 data are less impressive, and mostly related on the expression of the corresponding mRNAs that do not provide any information about the sub cellular districts of receptor distribution. It is true that mRNA expression and protein distribution often co localize, but occasionally do not exactly match. For example, in several brain regions, mRNA expression cannot be obviously detected even in areas where immunostaining for the receptor protein is observed. This is frequently due to the specialised expression of receptor proteins at nerve terminals, the protein synthesis taking place in the cell soma sometimes quite remote from the presynaptic region.

As already mentioned, the highest levels of A_1AR expression are found in the CNS, suggesting a particularly important role of adenosine in brain functions. Recently, by using [^{18}F]8-cyclopentyl-3-(3-fluoropropyl)-1-propylxanthine ([^{18}F]CPFPX) and PET imaging, A_1AR were quantified in the human CNS (Meyer *et al.,* 2005). The highest expression of A_1AR has been found in the cortex, hippocampus, cerebellum and dorsal horn of the spinal cord; intermediate levels in basal ganglia structures including the striatum (mRNA encoding A_1AR is present in large striatal cholinergic interneurones: (Dixon *et al.,* 1996) globus pallidus, subthalamic nucleus and thalamus (Fredholm *et al.,* 2001). An abundant expression of the adenosine A_1AR protein also occurs in the trigeminal ganglia, a finding supporting a role of this receptor in pain regulation (Schindler *et al.,* 2001). Neuronal A_1AR are localized both pre- and postsynaptically (Deckert and Jorgensen, 1988). In the hippocampus, a brain area in which A_1AR are abundant, subcellular analysis of nerve terminals revealed that A_1AR immunoreactivity is strategically located in the active zone of presynaptic terminals, as expected on the basis of the ability of A_1AR agonists to depress neurotransmitter release. It has also been demonstrated that A_1AR immunoreactivity is evident at postsynaptic sites together with NMDA receptor subunits NR1, NR2A and NR2B and with N-and P/Q-type calcium

channel immunoreactivity, emphasizing the importance of A_1AR in the control of dendritic integration (Lopes *et al.,* 2003). A_1AR can be found also extrasynaptically on dendrites (Rivkees *et al.,* 1995) and on the axonal fibres of the hippocampus (Swanson *et al.,* 1995). Activation of A_1AR along the axon may be a powerful extrasynaptic mechanism by which adenosine alters axonal electric transmission to inhibit neurotransmitter release (Swanson *et al.,* 1995).

A_{2A} receptors are principally located in the basal ganglia: in the caudate-putamen, nucleus accumbens and olfactory tubercle (Jarvis *et al.,* 1989; Rosin *et al.,* 1998). In particular, this receptor subtype is expressed on striatopallidal GABAergic-enkephalin neurones (where it co-localises with dopamine D_2 receptors), but not on GABAergic-dynorphin striatal neurones (Schulte and Fredholm, 2003). In the striatum the A_{2A}AR gene is found to a lesser extent also in large striatal cholinergic interneurones (Dixon *et al.,* 1996). A minor density of A_{2A}AR mRNA has been identified also in hippocampus and cortex (Cunha *et al.,* 1994; Dixon *et al.,* 1996). Besides postsynaptically, A_{2A}AR are also located presynaptically on different GABAergic, cholinergic, glutamatergic neurone types, although to a lesser extent (Hettinger *et al.,* 2001; Rosin *et al.,* 2003). In recent years, particular interest has been dedicated to study receptor dimerization, either in homomeric and heteromeric structures, since this phenomenon seems to frequently occur in numerous cell types and can modify the pharmacological profile of receptors and their functional role. Various lines of evidence indicate that such an interaction occurs in the striatum between A_{2A}AR adenosine and D_2 dopamine receptors, which usually co-localize in this brain region. This heterodimerization inhibits D_2 receptor functions (Ferre *et al.,* 1991), leading to co-aggregation and co-internalization of both proteins as a result of long-term exposure to A_{2A} or D_2 agonists (Hillion *et al.,* 2002).

Both A_1AR and A_{2A}AR are expressed in the brain not only in neurones but also on microglial cells (Fiebich *et al.,* 1996), astrocytes (Biber *et al.,* 1999; Rosin *et al.,* 2003), blood cells and vasculature (Phillis, 2004).

The distribution of A_{2B} AR and A_3AR in the CNS has been difficult to determine since central levels of mRNAs encoding these two adenosine receptors are extremely low, even below the detection limits of in situ hybridisation techniques. The more sensitive RT-PCR method was then successfully applied to this issue (Dixon *et al.,* 1996).

A_{2B} receptors are ubiquitously distributed in the brain and their mRNA has been detected in all rat cerebral areas studied (Dixon *et al.,* 1996; von Lubitz, 1999). Up to now, it has been difficult to relate A_{2B} receptors to specific physiological responses because of the paucity of A_{2B} selective agonists or antagonists.

The expression level of A_3AR in the brain is generally lower than that of the other subtypes (Ji *et al.,* 1994) and is highly species-dependent (Fredholm *et al.,* 2001, 2000). A_3AR are found in both neuronal and non-neuronal elements, i.e. astrocytes, microglia, and vasculature of the cerebral tissue (Zhao *et al.,* 1997) with widespread distribution. However, in the rat, a significant expression of A_3AR is found in cerebellum and hippocampus where they are mainly expressed at the presynaptic level (Lopes *et al.,* 2003).

2.1.7 Role of P1 receptors

P1 receptors exert important pathophysiological roles in a variety of tissue, from the cardiovascular system to the brain. At systemic level, adenosine acts as a negative chronotropic, inotropic and dromotropic modulator on heart functions by activating A_1AR. These effects are mainly due to the attenuation of the stimulatory actions of catecholamines on the heart functions carried on by A_1AR activation (Fraser *et al.,* 2003; Zablocki *et al.,* 2004). In contrast, the hypotensive effects exerted by adenosine in the periphery are attributed to A_{2A}AR activation, causing vasodilatation of blood vessels (Schindler *et al.,* 2005) and led, in the '60s-'70s, A_{2A} agonists to be tested in clinical trials as antihypertensive drugs. In addition, A_{2A}AR receptor stimulation also inhibits platelet aggregation (Varani *et al.,* 2000) and exhibits marked anti-inflammatory activities by inhibiting T-cell activation and proliferation, by reducing pro-inflammatory cytokine production and enhancing anti-inflammatory cytokine levels (Erdmann *et al.,* 2005; Lappas *et al.,* 2005). Less is known about the roles of A_{2B} and A_3AR in the periphery. One of the first described biological effects of adenosine A_3AR stimulation was degranulation of mast cells (Ramkumar *et al.,* 1993), suggesting a pro-inflammatory role of this receptor subtype. This hypothesis has been confirmed by subsequent studies demonstrating that A_3AR activation facilitates antigen-dependent histamine release from mast cells (Salvatore *et al.,* 2000). In addition, it has a demonstrated irritant effect in asthmatic lung mediated by A_3AR stimulation (Holgate, 2005), probably partnered, in eliciting this effect, by A_{2B}AR stimulation, that also mediates bronchoconstriction (Holgate, 2005). For this reason, mixed A_{2B} and A_3 antagonists have been proposed as candidates for the treatment of asthma (Press *et al.,* 2005).

2.1.8 P1 receptors and neurotransmission

The role of adenosine as a neuromodulator has long been known. In fact, many P1-mediated modulatory actions on presynaptic neurotransmitter release or postsynaptic neuronal excitability have been described. Under physiological conditions, adenosine exerts a tonic inhibition of synaptic transmission both *in vitro* or *in vivo* by stimulating A_1AR, as demonstrated in several brain regions such as the hippocampus, striatum and olfactory cortex (Latini and Pedata, 2001; von Lubitz, 1999). These mechanisms were studied in brain regions with a high concentration of A_1AR, such as the hippocampus. The inhibitory effect of adenosine A_1AR stimulation has a pre- and postsynaptic component. Activation of the presynaptic A_1AR reduces Ca^{2+} influx through the preferential inhibition of N-type and, probably, Q-type channels (Wu and Saggau, 1994; Yawo and Chuhma, 1993). Inhibition of presynaptic calcium currents decreases transmitter release (Prince and Stevens, 1992) and adenosine, by stimulation of A_1AR, has been found to inhibit the release of virtually all classical neurotransmitters: glutamate, acetylcholine, dopamine, noradrenaline and serotonin (see in Fredholm and Dunwiddie, 1988). In particular, a powerful suppression of glutamate release from presynaptic terminals has been described in the hippocampus (Burke and Nadler, 1988; Corradetti *et al.,* 1984), where adenosine A_1AR activation reduces the number of quanta released in the Schaffer collateral-commissural pathway (Lupica *et al.,* 1992).

The postsynaptic effect of A_1AR consists of a direct hyperpolarization of neurones via activation of GIRK channels (G protein-coupled inwardly-rectifying potassium channels) at the postsynaptic site (Takigawa and Alzheimer, 2002, 1999). In some brain regions, such as the hippocampus, the endogenous adenosine that is present in the extracellular space under physiological conditions exerts a tonic inhibition of excitatory neurotransmission by the activation of both pre- and post-synaptic A_1AR. Exogenous application of the selective A_1 antagonist DPCPX causes a 15% increase of synaptic potential amplitude in *in vitro* brain slices (Latini *et al.,* 1999b). This is an expected result in a brain region where extracellular adenosine concentration is found to be around 10-50 nM (Latini *et al.,* 1999b; Latini *et al.,* 1998) and A_1AR, whose affinity for adenosine is in the low nanomolar range, are highly expressed. These data are confirmed by the fact that, in slices taken from homozygous A_1AR knockout mice, no evidence was found for an endogenous inhibitory action of adenosine in the Schaffer collateral pathway in the CA1 region of the hippocampus or at the mossy fibre synapses in the CA3 region (Moore *et al.,* 2003). In addition, no inhibition of synaptic transmission was elicited by the application of exogenous adenosine (Johansson *et al.,* 2001). Opposite effects from A_1-mediated synaptic inhibition are elicited by A_{2A}AR activation, that has been shown to mediate excitatory actions in the nervous system (Latini *et al.,* 1996; Pedata *et al.,* 1984; Sebastião and Ribeiro, 1996; Spignoli *et al.,* 1984). Electrophysiological investigations into the role of A_{2A}AR in synaptic function under physiological conditions have shown that they increase synaptic neurotransmission. For example, in the hippocampus *in vitro*, A_{2A}AR stimulation results in a Ca^{2+}-dependent release of acetylcholine (Cunha *et al.,* 1995; Pedata *et al.,* 1984).

Furthermore, the application of CGS 21680, a selective A_{2A}AR agonist, decreases the ability of A_1AR agonists to inhibit excitatory neurotransmission (Cunha *et al.,* 1994; O'Kane and Stone, 1998). This effect supports the already proposed hypothesis that A_{2A}AR stimulation increases synaptic transmission through A_1AR desensitization (Dixon *et al.,* 1997).

Alternatively, another current theory is that A_{2A}AR increase excitatory amino acid release. In fact, the selective stimulation of adenosine A_{2A}AR augment the amount of glutamate released in hippocampus and striatum of young rats (Corsi *et al.,* 1999; Popoli *et al.,* 1995). In spite of the excitatory role in neurotransmission brought about by A_{2A}AR, the net effect of adenosine is an inhibitory tonus on neurotransmission, in accordance with observations suggesting that activation of A_{2A}AR requires a protracted stimulation to induce evident effects on synaptic transmission (Latini *et al.,* 1999a). It is worth noticing that the role of A_{2A}AR in the striatum is recently gaining interest inlight of their heterodimerization with D_2 dopamine receptors. The association between A_{2A}AR and D_2 receptors results in an antagonistic interaction which provided a rationale for evaluating A_{2A}-selective antagonists in Parkinson's disease, supported by epidemiological evidence indicating an inverse relationship between caffeine consumption and risk of developing this pathology (Ascherio *et al.,* 2001; Ross *et al.,* 2000). It was suggested that A_{2A} antagonists not only provide symptomatic relief but also decelerate dopaminergic neurone degeneration in patients (Xu *et al.,* 2005). Two different A_{2A} antagonists, istradefylleine (KW-6002) and a derivative of the anti-malarian

mefloquine (V2006), are respectively in Phase III and Phase II clinical trials for Parkinson's disease at present, with promising results (Chen *et al.,* 2013). Discrepancies about the role of adenosine A_3AR in the CNS are present in the literature. An excitatory role of A_3AR has been supported by evidence indicating that, in the rat hippocampus, their activation attenuates LTD and allows induction of LTP elicited by a subliminal weak-burst protocol (Costenla *et al.,* 2001). In addition, in the same brain area, A_3AR activation through a selective adenosine A_3 agonist has been shown to antagonizes the adenosine A_1AR -mediated inhibition of excitatory neurotransmission (Dunwiddie *et al.,* 1997). However, further electrophysiological studies refused this hypothesis, since several authors demonstrated that no significant interaction between A_1 and A_3AR occur in the rat cortex and hippocampus (Brand *et al.,* 2001; Lopes *et al.,* 2003). Additional evidence for an excitatory role of adenosine A_3AR came from studies carried out in "*in vitro*" hippocampal slices (Pugliese *et al.,* 2007) but, an inhibitory action has been attributed to A_3AR by Brand and colleagues (Brand *et al.,* 2001) who demonstrated that, in rat cortical neurones, the selective activation of this adenosine receptor subtype is involved in inhibition of excitatory neurotransmission, suggesting a synergistic action with the inhibitory effect of adenosine brought about by A_1AR activation. Despite results obtained by A_3AR stimulation, evidence that selective block of A_3AR does not affect neurotransmission in the CA1 region of the hippocampus under normoxic conditions, indicates that endogenous adenosine at physiological concentration does not exert tonic activation of A_3AR (Dunwiddie *et al.,* 1997; Pugliese *et al.,* 2003).

3. Brain ischemia

The word ischemia derived from Greek "ισχαιμία" ("Reduction of blood"), meaning the total lack of blood flow in an organ. Ischemia is not a disease ascribable to a unique cause. There are many factors that cause reduction or total arrest of blood flow: tachycardia, hypotension, extravascular compression, atherosclerosis, thromboembolism, gas embolism, vasoconstriction and adherent bridles, following surgery or chronic inflammation. In addition, exist ischemic event defined cryptogenic (without apparent cause) but normally at the bases of this condition there are many diseases, such as obesity, solid and blood tumours but also myocardial infarction, anaemia and granuloma. An unhealthy life style, such as smoking or consuming alcohol, considerably alter the predisposition to this pathological condition. Cerebral ischemia could be derived from a haemorrhagic or occlusive event, depending on the break of vessel and blood leak otherwise vessel occlusion due to presence of cellular material (Figure 5).

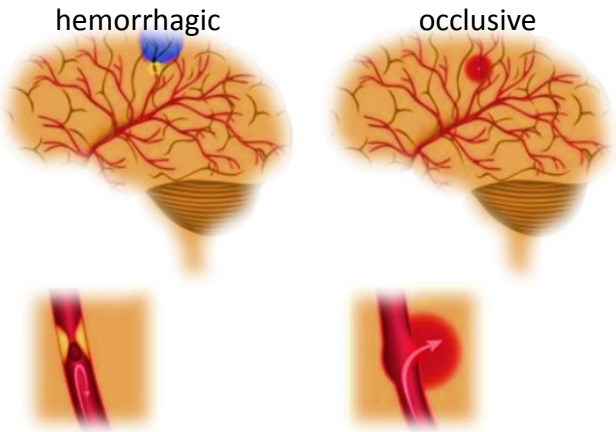

Figure 5: Etiopathological picture of both types of ischemia: on the left, in the figure ischemic stroke, representing the obstruction of a blood vessel; On the right haemorrhagic stroke, commonly known as cerebral haemorrhage, here with the breakdown of a blood vessel (Taken from Dirnagl *et al.,* 1999).

In 1970, cerebral ischemia was defined by OMS as "Neurological focal or global cerebrovascular injury syndrome persisting beyond 24 h or leading to death within 24 h" (24 h were chosen arbitrarily for distinguish it from transient ischemic attack). Thanks to this definition we could presume that the nervous tissue subjected to ischemic damage, if reached in appropriate time, can recover neuronal activity. For this, however, rapidity of intervention is indispensable and, given the high risk of death and disability which ischemia implicates, this disease is considered a medical emergency for which an immediate diagnosis is essential to be able to formulate an appropriate therapeutic intervention. Ischemia could involve both large or small vessels but the symptomatology is almost always the same and consist of feeling oppression, asphyxiation, spasm, formication (paresthesia), aphasia, dysarthria, hemiparesis, hemianopsia and migraine. Medical treatment known for cerebral ischemia are unfortunately too few and unfortunately, many drugs that have good results in the preclinical studies, are ineffective in clinical trials (De Keyser *et al.*, 1999). At the moment, the only drug approved to treat ischemia is tissue plasminogen activator (tPA), a specific enzyme that cleaves proteins which are present in the blood, such as fibrin, an essential protein in blood clotting, and thrombi. The main issue is that in order to perform such a vital function tPA must be necessarily administered in the first 3 h after the manifestation of the symptomatology.

3.1 Epidemiology

According to data of the Italian Ministry of Health (www.ministerodellasalute.it) worldwide cerebral ischemia is at the second place among lethal diseases in the industrialized countries and it is the third cause of disability among the elderly. In Italy, cerebral ischemia is the third cause of death after cardiac ischemia and neoplastic diseases: it causes 10-12% of annual deaths and it is the first ranked among invalidating diseases. Every year 196.000 cases of stroke occur in Italy, 20% of which are recurrent. The remaining 80% are all new recordable cases. Between the 10 and 20% of people hit by cerebral ischemia die within a month and a 10% die within the first year of life. Haemorrhagic

stroke mortality at the first month of the event equals to 50%. Only 25% of surviving patients to a stroke event recover completely, 75% survive with a certain form of disabilities, half of whom with a deficit as serious as they lost their selfsufficiency. The age in which cerebral stroke appears more frequently is around 55-60 years and its incidence increases with aging: young cases of cerebral stroke are much less frequent, about 7 cases/100.000/per year. The incidence rate among the elderly is around 6,5% and it mainly occurs in men than in women, 7,4% *vs* 5,9 respectively. It has been evaluated that demographic evolution, characterized by sensible aging of the population will lead to a significant increase in stroke cases in the next future, if the incidence should remain constant.

3.2 Physiopathology

The ischemic process results from a sequence of physiopathologic effects (Figure 6) which progress drastically through time and space, leading to cells death and consequently to the subsequent decline of brain damage.

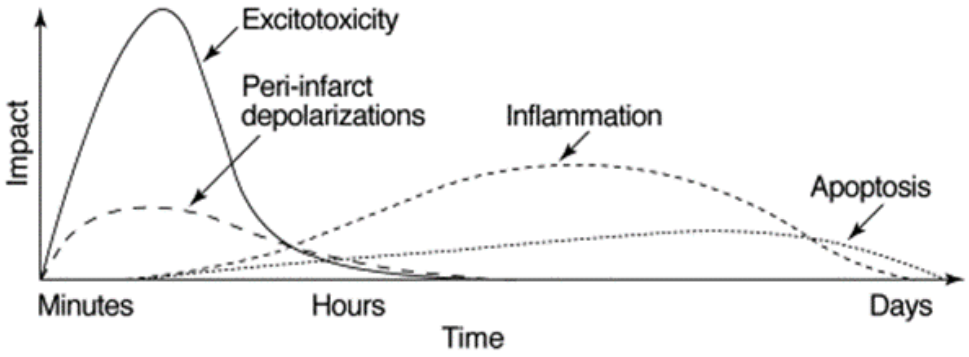

Figure 6: Representation of the various phases of ischemic insult, reported according to the time and intensity of the event (Taken from Dirnagl *et al.,* 1999).

In sequence, these are: excitotoxicity, peripheral depolarization, inflammation and cells death due to necrosis and apoptosis (Dirnagl *et al.,* 1999).

3.3 Excitotoxicity

Cells consume a substantial amount of oxygen and glucose, throughout catabolic processes to obtain the energy necessity for survival in the form of ATP. At the moment of the reduction of physiological concentration of oxygen and glucose, that occur during an ischemic insult, the cell necessarily looks for stock of energy due to the fact that it cannot produce energy by itself, and finds it in ATP. Given the disequilibrium between energy consumption and production the cell is forced to initiate the anaerobic metabolism that causes ATP depletion, transformation to AMP and the consecutive extracellular accumulation of adenosine. At intracellular level ATP has essential functions, of which is fundamental the operation of ATP-dependent pumps, such as the Na^+/K^+ which allows the active transport of Na^+ and K^+ through the plasma membrane. The increase of ATP causes a block of the

pump and consecutively a block of ions transport: thus, Na^+ accumulates in the intracellular side. This ionic distribution, strongly unbalanced, provokes an enormous depolarization at cellular level, making the membrane electrochemical potential more positive and causing the opening of other ion channels, such as the Ca^{2+}channel. Ca^{2+}, once inside the cell, contributes to the release of the neurotransmitters through the process of vesicle fusion, mediated by the protein of SNARE complex. The most widely released neurotransmitter in the ischemic process is glutamate, an amino acid and excitatory neurotransmitter which, if released in high concentration, lead to cellular toxicity. Glutamate, at postsynaptic level, activates AMPA, NMDA and Kainate receptors which further increase the intracellular concentrations of Na^+, K^+ and Ca^{2+} which further depolarize the cell membrane. The resulting cerebral oedema is caused by the increase of intracellular ionic concentration, which hence recall water from outside. Furthermore, the energy-dependent glutamate transporters are blocked and this contribute to the permanence of glutamate within inter-synaptic fissure and results in continuous receptors stimulation.

In addition, the intracellular messenger Ca^{2+}, activates a cascade of events (such as the synthesis of NO, characteristic of inflammation) which conduce to the onset of tissue damage (Beckman and Koppenol, 1996; Iadecola, 1997) and to the subsequent necrosis of the tissue (Dirnagl *et al.,* 1999). Among the most remarkable events of ischemia are the activation of enzymes which break down the cytoskeleton protein (Furukawa *et al.,* 1997), lipases activation, such as the phospholipase A2 (PLA2) and consequently activation of cyclooxygenase (COX2, involved in inflammation). It is possible to identify two ischemic areas (Figure 7): the focal area which undergoes a severe reduction of cerebral blood flow (CBF) and where neurons are continuously exposed to depolarization is defined the "ischemic core" (Hossmann, 1994). This causes rapid necrosis due to cytoskeleton destruction or to proteolysis. The perifocal area, named ischemic penumbra or "penumbra", can maintain, in the first periods after the ischemic attack, the physiologic metabolism of the tissue thanks to the perfusion of collateral anastomotic vessels (Astrup *et al.,* 1981; Hossmann, 1994; Obrenovitch, 1995). Lacking a properly pharmacologic treatment or reperfusion, the ischemic penumbra may advance toward an infarcted condition caused by ischemia and apoptosis.

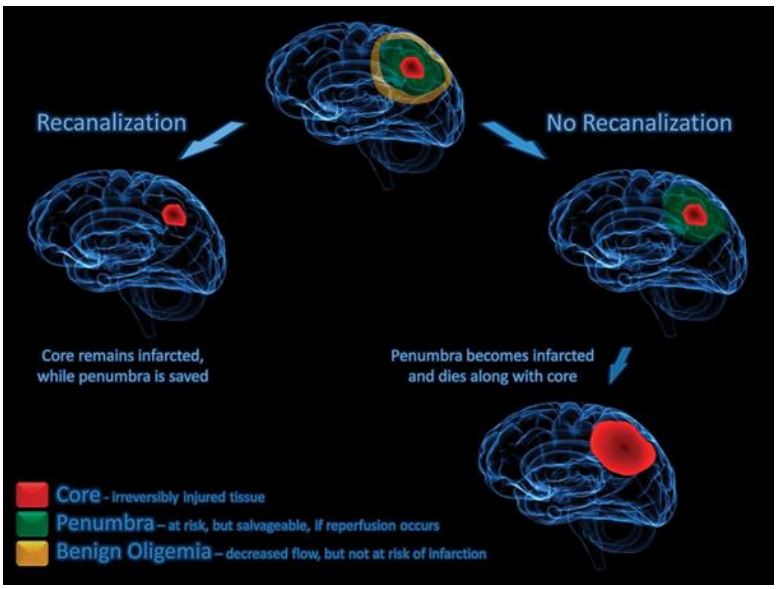

Figure 7: Representation of Ischemic Areas: The core, in red, is the first affected area during an ischemic insult. Penumbra, in green, for the first time remains perfused by the vessel connections, but without perfusion or drugs becomes infarct (Taken from Astrup *et al.*, 1981; Hossmann, 1994; Obrenovitch, 1995).

3.4 Anoxic depolarization

A typical consequence of a cerebral hypoxic/ischemic insult is the appearance of anoxic depolarization (AD), a rapid and regenerative wave of depolarization that propagates in the brain tissue. A similar response occurs in cerebral grey matter under normoxic conditions, as a consequence of neuronal hyper-excitability (for example during epileptic discharges) and is called spreading depression (SD). These two events are strictly correlated and present the same diagnostic criterion: an accelerating, regenerative, all-or-none type depolarization spreading out from a restricted core of grey matter into the surrounding tissue (Somjen, 2001).

SD was described for the first time by Aristides Leão, in 1944, who recorded a cortical electrogram (ECoG) of epileptic discharges obtained by "tetanic" stimulation in anesthetized rabbits. Leão noticed that, immediately after the induced seizure, an unexpected silencing of the ongoing normal electrical activity occurred, and hypothesised that SD and propagation of focal seizures were related phenomena generated by the same cellular elements (Leão, 1944). These first observations, later confirmed by others (Harreveld and Stamm, 1953), have been later supported by detailed investigations demonstrating that SD is caused by a "negative slow voltage variation" in the cortical surface that was identical to the voltage shift recorded after a few min of blood flow deprivation in the cerebral cortex (Leão, 1947) By reaching a maximal amplitude of -15 mV, this surface potential shift was astonishingly large compared with other brain waves recorded by ECoG and attracted the interest of a number of neurologists. Similarly, severe hypoxia or, more generally, sudden energy failure induce an SD-like response, and "spontaneous" waves of SD emanate from the border of an ischemic core and propagate into the surrounding brain areas (the "penumbra"). To date, SD and AD have been recorded in almost all brain regions, with high similarity and reproducibility among *in vivo* and *in vitro* experiments, but they are more readily provoked in some brain areas than in others.

The CA1 region of the hippocampal formation is considered the most susceptible zone, closely followed by the neocortex (Somjen, 2001).

Under normoxic conditions, SD can be triggered by a number of different stimuli and chemicals. Among the chemical agents, noteworthy are K^+ ions, glutamate, and acetylcholine, because these molecules are normally present in the brain, and ouabain because it reflects the reduced function of the membrane Na^+-K^+-ATPase during high energy demand or low energy supply and ultimately raises extracellular K^+ concentration, which is known to play a key role in this phenomenon. When ion-selective microelectrodes became available in the '60s, allowing to measure "real time" ion concentration changes in live tissues, it was soon reported an overflow of K^+ ions from the cortical surface during both SD (Brinley *et al.,* 1960) and AD (Vyskocil *et al.,* 1972). This K^+ overload is also accompanied by a precipitous drop in extracellular Cl^- and Na^+ levels and a passive release of organic anions from the cell cytoplasm including glutamate (Davies, 1995). This sequence of events suggests that during AD or SD, intra- and extracellular ion concentrations equilibrate and the electrochemical gradient across the cell membrane, which is essential for living functions, is lost. This hypothesis is also supported by the nearly complete depolarization that accompanies these events (Collewijn and Harreveld, 1966), typical of cells exposed to high extracellular K^+ concentrations as during SD or AD. In fact, as expressed by Grafstein in the "potassium hypothesis" of SD (Grafstein, 1956), K^+ released during intense neuronal firing accumulates in the restricted interstitial space of brain tissue and depolarizes the different cells that released it, resulting in a vicious circle that leads to neuronal hyperexcitability.

Further progresses in describing SD- and AD-related phenomena were made by using intracellular sharp microelectrodes to measure resting membrane potential before, during and after the passage of SD or AD waves (Collewijn and Harreveld, 1966; Müller and Somjen, 2000). The "all-or-none" nature of both events was confirmed by the observation that, once started, the amplitude of membrane depolarization was independent of the severity of the triggering event (Müller and Somjen, 2000). When membrane potential recordings were made simultaneously from stratum radiatum and stratum pyramidale of CA1 hippocampal slices, cell depolarization always began earlier and was of larger amplitude and longer duration in the layer of dendritic trees than in cell somata, suggesting that the triggering region was the dendritic layer and from there the depolarization spreads to the cell bodies (Herreras and Somjen, 1993a). A detailed analysis of the time course of different AD-related events in the hippocampus demonstrated that the onset of voltage changes was usually preceded by increased neuronal excitability that produced a "shower of population spikes" reflecting synchronized firing of pyramidal neurons (Grafstein, 1956; Herreras and Somjen, 1993b). This neuronal hyperactivity, also recorded during *in vivo* experiments (Rosenblueth and García Ramos, 1966), was shown to be strictly related to glutamate-induced excitotoxicity, since the voltage changes produced during AD or SD were greatly reduced by NMDA receptor antagonists (Herreras and Somjen, 1993a), that are well known neuroprotective agents against ischemia-induced damage of the brain tissue in experimental models (Calabresi *et al.,* 2000; Lee *et al.,* 1999). In addition, the

exogenous application of glutamate to the cortical surface is able to induce SD (van harreveld and schade, 1959). Evidence indicates, however, that a much reduced but still substantial ion gradient remains across the plasma membrane during AD (Müller and Somjen, 2000).

The massive redistribution of ions between the intra- and extracellular compartment during AD and SD leads to significant changes in cell homeostasis, reflected by the prominent cell swelling that accompany both phenomena. Leão himself firstly described a transient increase in tissue electrical impedance accompanying SD (Leão, 1951) and this was soon confirmed by others (Hoffman *et al.*, 1973; Ochs and Hunt, 1960). The major effect was the increase in tissue resistance, and was confirmed by morphological studies to be caused by swelling of cells leading to shrinkage of the interstitial space (Kow and van Harreveld, 1972; van harreveld and schade, 1959). Another parameter usually measured to monitor *in vitro* induced SD or AD is the intrinsic optical signal (IOS). Cell swelling produces a marked change in intracellular volume that is reliably associated with a decrease in light scattering (Aitken *et al.*, 1999), attributable to the dilution of scattering particles in the cytosol (BARER, 1953). This sequence of events leads to a pronounced increase in the IOS of brain tissue, as reported for the first time by Snow et al in hippocampal slices during SD (Snow *et al.*, 1983). This new approach permitted a detailed real-time two-dimensional mapping (not reachable with microelectrodes) of SD and ADspread, simultaneously recorded with other parameters (for example membrane potential or extracellular K^+ concentration), as exemplarily reported by Obeidat and Andrew (Obeidat and Andrew, 1998). Again, in hippocampal slices, the IOS triggered by AD or SD was stronger and occurred more rapidly in the dendritic layer of stratum radiatum than in the somatic region of stratum pyramidale (Aitken *et al.*, 1998; Müller and Somjen, 1999).

In spite of the many similarities between SD and AD events, some differences have also been described. For example, depolarization in SD is "self-limiting" and is followed by complete restoration of neuronal functions as soon as neurons recover their resting membrane potential, without any "irreversible side effects" at least after sparce SD events. On the contrary, after an AD, membrane potential and neuronal functions only recover if oxygen is restored soon after the onset of depolarization (Lipton, 1999) since oxidative energy (O2 and ATP consumption) is required to restore ion gradients (Wang *et al.*, 2003). If the ischemic insult persists during AD manifestation, neuronal damage will become irreversible and only a partial recovery of brain tissue functionality can be achieved. This seems to be mainly due to the deleterious role of a protracted intracellular Ca^{2+} rise, an event typically recorded during ischemia. In this regard it may be argued that, during normoxic SD, neurons gain as much Ca^{2+} as during AD but do not encounter such irreversible damage because membrane depolarization is self-limiting and only lasts for a few seconds. In fact, it has been demonstrated that if neurones are forced to remain depolarized for extended periods after SD triggering, even in well-oxygenated tissues they do not regain function (Herreras and Somjen, 1993b; Kawasaki *et al.*, 1988). Accordingly, if Ca^{2+} is removed from the bathing solution before oxygen is withdrawn, neurons recover their functions following a period of hypoxia that otherwise would have caused irreversible damage (Siesjö and Bengtsson, 1989). It appears that intracellular

Ca^{2+} levels must remain elevated for a critical length of time to initiate the reactions that result in irreversible cell injury (Deshpande *et al.,* 1987; Morley *et al.,* 1994). It follows that any treatment that postpones the onset of AD should extend the time limit of cell recovery. This concept has been largely confirmed by both *in vivo* and *in vitro* studies and represents the basis of the present work to investigate the effect of different drugs acting on purinergic systems during ischemia. On this basis, we monitored AD appearance in hippocampal slices as an index of irreversible tissue damage induced by *in vitro* ischemia and we investigated the role of purinergic receptors during a severe insult in the DG.

3.5 Adenosine and brain ischemia

Hypoxic-ischemic insult to the brain generally causes necrosis, although in most cases there exists also a process of delayed and apoptotic type injury in the region (penumbra) surrounding the area of most severe damage (Honig and Rosenberg, 2000; Lo, 2008; Schaller *et al.,* 2003). Stroke is today evaluated as the second most common cause of death and a major cause of long-term disability worldwide. Ischemic stroke commonly accounts for approximately 80% of all stroke cases, and is caused from occlusion of amajor cerebral artery by a thrombus or an embolism, which leads to loss of cerebral blood flow, a condition of hypoxia and glucose deprivation (oxygen, glucose deprivation: OGD) and subsequently tissue damage in the affected region (Gibson, 2013). Brain injury results from a complex sequence of pathophysiological events consequent to hypoxia/ischemia that evolve over time. The major pathogenic mechanisms of this cascade include: primary acute mechanisms of excitotoxicity and periinfarct depolarizations followed by activation of resident immune cells, i.e microglia, and production or activation of inflammation mediators (Dirnagl *et al.,* 1999). A complex interplay of biochemical and molecular mechanisms involving practically any cell type of the brain, concept of "the neurovascular unit," partakes in either salvage or demise of the tissue after a stroke (Dirnagl, 2012). Although after ischemia a precocious activation of resident immune cells may be neuroprotective and supportive for regeneration, protracted neuroinflammation is now recognized as the predominant mechanism of secondary brain injury progression.

Activated microglial cells proliferate, migrate and by production of inflammatory substances (Buttini *et al.,* 1996; Gebicke-Haerter *et al.,* 1996; Gomes *et al.,* 2013; Orr *et al.,* 2009; Rebola *et al.,* 2011) and chemokines trigger an inflammatory response (Dirnagl *et al.,* 1999). Pro-inflammatory mediators and oxidative stress give rise to the endothelial expression of cellular adhesion molecules (Huang *et al.,* 2006; Stoll *et al.,* 1998) and to an altered permeability of the blood brain barrier (BBB) that allows infiltration of leukocytes (neutrophils, lymphocytes and monocytes) (Huang *et al.,* 2006; Iadecola and Anrather, 2011; Stoll *et al.,* 1998) that on their turn exacerbate neuroinflammation and ischemic damage (Haskó and Pacher, 2008). Correlations among neutrophil accumulation, severity of brain tissue damage and neurological outcome have been reported by Akopov (Akopov *et al.,* 1996). Studies in the human brain after ischemic stroke confirm that neutrophils intensively accumulate in the regions of cerebral infarction (Akopov *et al.,* 1996; Dirnagl *et al.,* 1999). In the

last years basic research yielded numerous pharmacologic agents leading to the identification of more than 1000 molecules with brain-protective effects in animal models of brain ischemia and to the implementation of more than 250 clinical trials. However, drugs have failed to be efficacious during clinical trials and the only successful pharmacological treatment approved to date is tissue plasminogen activator that aims to decrease ischemia associated thrombosis risk. Yet, because of the narrow therapeutic time-window involved, thrombolytic application is very restricted in clinical settings (Chen *et al.,* 2014). Aspirin, other antiplatelets, and anticoagulants are used as preventive therapy of stroke (Albers *et al.,* 2011; Ginsberg, 2009; Macrez *et al.,* 2011; Moskowitz *et al.,* 2010; Young *et al.,* 2007). In this review, we summarize the studies that have contributed to current understanding of the mechanisms by which ATP and adenosine modulate tissue damage in brain ischemia models.

3.5.1 P1 receptors and cerebral ischemia

Ischemic stroke is the third leading cause of death in industrialised countries (The Group of Eight (G8)), with a mortality rate of around 30%, and it is the major cause of long-lasting disabilities. It is caused by a transient or permanent reduction in cerebral blood flow due to the occlusion of a major brain artery, either by an embolus or by local thrombosis. An effective therapy for this pathology does not exists yet. Several neuroprotective drugs have been developed and successfully tested in animal stroke models, but most of them failed to be efficacious in clinical trials (De Keyser *et al.,* 1999). A typical example concerning clinical failure of experimental models is provided by the class of NMDA receptor antagonists, that, in spite of promising results in animal models (Calabresi *et al.,* 2000; Lee *et al.,* 1999), failed to provide neuroprotection in clinical studies on patients (Caplan, 1998.; Plum, 2001). As reported above, the extracellular adenosine concentration under physiological conditions, calculated by different experimental approaches, is usually relatively constant in a range between 30-200 nM in brain tissue (see: Latini and Pedata, 2001) After ischemia, adenine nucleotides are released into the extracellular compartment and rapidly metabolized to adenosine by NTPDases and e5'-NTs ubiquitously expressed on the cell surface (Melani *et al.,* 2012, 2005). Both *in vivo* and *in vitro* studies largely demonstrate that adenosine concentration dramatically increases during cerebral ischemia (Hagberg *et al.,* 1987; Latini *et al.,* 1999b; Melani *et al.,* 2003, 1999; Pearson *et al.,* 2006) reaching values around 3 μM, able to activate all 4 subtypes of adenosine receptors. Adenosine initially derives from extracellular ATP degradation (Melani *et al.,* 2012), thereafter adenosine is released per sè from cells. This is principally due to the rapid and massive depletion of intracellular ATP occurring under metabolic stress conditions, such as hypoxia or ischemia, that lead to an accumulation of AMP, which in turn is degraded to adenosine. The rate of adenosine production thus exceeds its deamination to inosine or its rephosphorylation to AMP (Deussen, 2000) leading to a concentration gradient from the intra- to the extracellular space that causes adenosine to be released by the membrane transporter proteins (ENTs). Therefore, extracellular adenosine concentrations

greatly increase reaching micromolar values during hypoxic/ischemic conditions. *In vitro* studies demonstrated that during ischemia adenosine reaches values as high as 30 μM (Latini *et al.,* 1999b). A neuroprotective role of extracellular adenosine during cerebral ischemia has long been recognised by different authors. In fact it is largely known that adenosine-potentiating agents, which elevate endogenous adenosine by either inhibiting its metabolism (Lin and Phillis, 1992) or preventing its reuptake (Dux *et al.,* 1990), offer protection against ischemic neuronal damage in different *in vivo* ischemia models. Furthermore, adenosine infusion into the ischemic striatum during medial cerebral artery (MCA) occlusion significantly ameliorates the neurological outcome and reduces the infarct volume after transient focal ischemia (Kitagawa *et al.,* 2002). For all these reasons, many authors have indicated adenosine and its receptors as possible targets for therapeutic implementation in the treatment of stroke. All these protective effects of adenosine during cerebral ischemia are mainly due to adenosine A_1 receptor stimulation, that causes a reduction of Ca^{2+} influx, thus inhibiting the presynaptic release of excitatory neurotransmitters (Corradetti *et al.,* 1984; Pedata *et al.,* 1993; Zetterström and Fillenz, 1990) and in particular of glutamate, whose over-stimulation of NMDA receptors during ischemia is one of the principal mechanisms of neuronal excitotoxicity (Choi, 1990). In addition, by directly increasing the K^+ and Cl^- ion conductances at postsynaptic level, adenosine stabilises the neuronal membrane potential and reduces the neuronal hyper-excitability caused by increased glutamate release during ischemia (Tominaga *et al.,* 1992). The consequent reduction in cellular metabolism and energy consumption (Tominaga *et al.,* 1992) and a moderate lowering of the body/brain temperature (Gourine *et al.,* 2004) are protective events under ischemic conditions. Accordingly, *in vitro* models demonstrated that selective A_1AR stimulation reduces neuronal damage following hypoxia and/or glucose deprivation in primary cortical or hippocampal cell cultures (Daval and Nicolas, 1994) and brain slices (Dux *et al.,* 1990; Marcoli *et al.,* 2003; Mori *et al.,* 1992; Newman *et al.,* 1998; Tanaka *et al.,* 1997). Although data converge in demonstrating a neuroprotective effect of adenosine through A_1AR during ischemia, the clinical utility of selective A_1 agonists is hampered by unwanted central and peripheral effects i.e. sedation, bradycardia, hypotension (White *et al.,* 1996).

The role of A_{2A}AR in cerebral ischemia has been recently studied. Several data support an opposite, deleterious, role of A_{2A}AR during ischemic brain injury in comparison to adenosine A_1AR. In 1994, Gao and Phillis (Gao and Phillis, 1994) demonstrated for the first time that the non-selective A_{2A}AR antagonist CGS15943 reduces cerebral ischemic injury in the gerbil following global forebrain ischemia. Thereafter, many reports have confirmed the neuroprotective role of A_{2A}AR antagonists in different models of ischemia. The selective A_{2A}AR antagonist CSC, as well as the less selective antagonists CGS15943 and CP66713, were able to ameliorate hippocampal cell injury during global forebrain ischemia in gerbils (Phillis, 1995; Von Lubitz *et al.,* 1995). In agreement with these observations, hippocampal activation of A_{2A}AR during *in vitro* oxygen and glucose deprivation (OGD) may reduce the beneficial effects mediated by A_1AR and, in addition, increase glutamate outflow, thus contributing to the excitotoxic damage. These mechanisms explain the protective

effects of A_{2A} selective antagonists during OGD insults (Latini *et al.,* 1999a). Similarly, the selective A_{2A} receptor antagonist SCH58261 reduced ischemic brain damage in a rat neonatal model of hypoxia/ischemia (Bona *et al.,* 1997) and in an adult rat model of focal cerebral ischemia (Melani *et al.,* 2003; Monopoli *et al.,* 1998). Studies in genetically manipulated mice definitely confirmed the neuroprotective role of A_{2A}AR antagonists on ischemic brain damage. In fact, in A_{2A}AR knockout mice subjected to focal cerebral ischemia, the cerebral damage and neurological deficits were attenuated (Chen and He, 1999). The beneficial effects brought about by A_{2A} antagonists are mainly attributed to the blockade of A_{2A}AR located presynaptically on glutamatergic terminals (Hettinger *et al.,* 2001; Rosin *et al.,* 2003) thus reducing the excitotoxic damage (Marcoli *et al.,* 2003). In fact, selective activation of adenosine $A_{2A}AR_S$ has been demonstrated to promote glutamate release under normoxic and ischemic conditions (Corsi *et al.,* 1999; O'Regan *et al.,* 1992; Popoli *et al.,* 1995; Simpson *et al.,* 1992). In addition, recent data suggest that bone marrow derived cells, injected into rat brains (Yu *et al.,* 2004), and native microglial cells (Melani *et al.,* 2006) are important targets for A_{2A} antagonist-mediated neuroprotection against ischemic damage. Furthermore, we have recently demonstrated in the model of oxygen-glucose deprived hippocampal slices that two selective adenosine A_{2A}AR antagonists, ZM 241385 and SCH 58261 (with less efficacy), are protective during OGD in the CA1 region by delaying the appearance of anoxic depolarization (AD), astrocyte activation, and by improving neuronal survival and recovering synaptic activity under slice reperfusion with oxygenated-glucose-containing artificial cerebrospinal fluid (aCSF) (Pugliese *et al.,* 2009). The major protective effect of A_{2A}AR antagonists has been attributed to a reduction of glutamate outflow from neurons (Marcoli *et al.,* 2003; Pedata *et al.,* 2005, 2003) and therefore, to reduced excitotoxic damage.

Few studies, due to the paucity of A_{2B} selective agonists and antagonists, indicate a possible role for A_{2B} receptors during brain ischemic damage. In the stratum radiatum of CA1 hippocampal slices, the number and immunostaining density of immunoreactive cells for A_{2B}AR were increased after ischemic preconditioning (Zhou *et al.,* 2004). In human astroglial cells, the selective A_{2B}AR antagonist MRS 1706 completely prevents the elongation of astrocytic processes, a typical morphological hallmark of *in vivo* reactive astrogliosis which represents a deleterious process induced by selective stimulation of A_{2B}AR (Trincavelli *et al.,* 2004).

The few studies present in the literature concerning the role of A_3AR in cerebral ischemia are rather contradictory. The effects of A_3AR stimulation appear to depend on drug administration (acute *vs* chronic), dosage and timing of treatment with respect to the onset of the ischemic insult. Since information present in the literature about the role of $A_{2A}AR_S$ during cerebral ischemia in DG is scarce at present, we recently focused our attention on this matter in the present work.

In particular, we investigated the role of this adenosine receptor subtype by evaluating the effect on the synaptic and proliferative response of the DG to a severe OGD in acutely isolated rat hippocampal slices. It is well known that the DG is more resistant (Wang *et al.,* 2005) than the CA1 region to an ischemic episode, probably because of its major resistence to excitotocity and to its regenerative

capacity, even in adulthood (Altman, 1962; Altman and Das, 1965; Bartley *et al.,* 2005) due to the presence of multipotent neural stem cells localized in the SGZ (Yamashima *et al.,* 2007). These cells are able to proliferate and differentiate into neurons, astrocytes and oligodendrocytes (Sharp *et al.,* 2002) as a response to multiple factors, including hypoxic-ischemic injury (Liu *et al.,* 1998; Takagi *et al.,* 1999).

A typical electrophysiological parameter usually monitored during OGD is a rapid anoxic depolarization (AD) of a sizeable population of brain cells. This event appears as a consequence of prolonged ischemic episodes and is strictly correlated with irreversible neuronal and glial damage (Somjen, 2001), also contributing to the increase in cell damage in the so called "ischemic penumbral area" (Touzani *et al.,* 2001).

Distinct sections will be devoted to describing this crucial event, commonly considered an index of irreversible neuronal ischemic damage, and on adult neurogenesis and oligodendrogenesis after cerebral ischemia.

3.5.2 $A_{2B}AR_S$ in brain ischemia

A_{2B}AR is expressed at low levels in the rat brain (Dixon *et al.,* 1996; Fredholm *et al.,* 2000; Puffinbarger *et al.,* 1995; Li *et al.,* 2017)and has a low-affinity for adenosine. However it might be activated during conditions of hypoxia or ischemia when the extracellular adenosine levels rise (Koeppen *et al.,* 2011; Popoli and Pepponi, 2012). Because of paucity of A_{2B} selective agonists and antagonists (see Müller and Jacobson, 2011) few studies are present on the role of $A_{2B}AR_S$ in brain ischemia. In the stratum radiatum of CA1 hippocampal slices, the number and density of $A_{2B}AR_S$ on cells showing distinct morphological characteristics of astrocytes, are increased after ischemic preconditioning (Zhou *et al.,* 2004). In primary murine astrocytes, the expression of A_{2B}AR is strongly stimulated by LPS in concert with hypoxia and inhibited by adenosine, through A_1 and A_3AR subtypes (Gessi *et al.,* 2013). In human astroglial cells, a selective A_{2B} antagonist, N- (4-acetylphenyl)-2-[4-(2,3,6,7-tetrahydro-2,6-dioxo-1,3-dipropyl- 1H-purin-8-yl) henoxy]acetamide (MRS1706), completely prevents elongation of astrocytic processes (a morphological hallmark of *in vivo* reactive astrogliosis) induced by selective stimulation of $A_{2B}AR_S$ (Trincavelli *et al.,* 2004). A short-term TNF-alpha treatment induces A_{2B}AR desensitization in human astroglial cells (Trincavelli *et al.,* 2008). These results suggested that in the acute phase of brain ischemia that is characterized by both cytokine and adenosine high release, A_{2B}AR desensitization on astroglia might represents a cell defence mechanism (Trincavelli *et al.,* 2008).

Few studies have investigated the role of A_{2B}AR in brain ischemia *in vivo*. In a recent paper, it was reported that a selective A_{2B}AR antagonist, N-(4-cyanophenyl)-2-[4-(2,3,6,7-tetrahydro-2,6-dioxo-1,3-dipropyl-1H-purin-8-ylphenoxy]-acetamide (MRS1754), reduced the ceramide production in astrocytes and attenuated inflammatory responses and neuronal damage after global cerebral ischemia (Gu *et al.,* 2013). This effect was related to an early reduction of p38 MAPK activation. In fact, A_{2B}AR plays a key role in the rapid activation of p38 and in the subsequent inflammatory process (Koscsó *et al.,* 2012; Wei *et al.,* 2013). Altogether experiments indicated that antagonism of

A_{2B} receptor located on brain cells might be protective from ischemic brain damage. Recent introduction of new pharmacological and genetic tools led to understand a role of A_{2B}AR in the regulation of inflammation, immunity and tissue repair (Crespo *et al.,* 2013; Feoktistov and Biaggioni, 2011; Hinz *et al.,* 2014; Ortore and Martinelli, 2010). Besides brain cells, $A_{2B}AR_S$ are present on endothelial and blood immune cells and in most cases are coexpressed with $A_{2A}AR_S$. A_{2B}AR transcripts are found in neutrophils (Fredholm *et al.,* 1996) lymphocytes (Gessi *et al.,* 2005) and platelets (Amisten *et al.,* 2008). Moreover, $A_{2A}AR_S$ are expressed on the surface of endothelial cells (Feoktistov *et al.,* 2002) and regulate every aspect of endothelial inflammatory processes. Hypoxia is an important stimulus for the upregulation of A_{2B}AR expression via the oxygen-regulated transcription factor, HIF-1a (hypoxia inducible factor), in endothelial cells (Eltzschig *et al.,* 2003). Vascular permeability was significantly increased in vascular organs of A_{2B}AR KO mice subjected to ambient hypoxia. By contrast, hypoxia-induced vascular leak was not accentuated in A_1, A_{2A} or A_3AR KO mice, suggesting a specific role of A_{2B}AR in endothelial cells (Eckle *et al.,* 2008).

In agreement, A_{2B}AR KO mice showed increased basal levels of TNF-a and expression of adhesion molecules such as ICAM-1, P-selectin and E-selectin in lymphoid cells, resulting in increased leukocyte rolling and adhesion (Yang *et al.,* 2006). A_{2B}AR KO mice exposed to hypoxia exhibit increased neutrophil infiltration into hypoxic tissues revealing an inhibitory role for $A_{2B}AR_S$ in neutrophil transmigration *in vivo* (Eckle *et al.,* 2008). Attenuation of hypoxia-associated increases in tissue neutrophil numbers appeared to depend largely on hematopoietic cell A_{2B}AR signalling (Eckle *et al.,* 2008; Yang *et al.,* 2006). Pharmacological studies in fact indicate that $A_{2B}AR_S$ on neutrophils contribute to their decreased adhesion to endothelial cells and transmigration in tissue parenchyma (Eckle *et al.,* 2008; Eltzschig *et al.,* 2004). All together these studies indicate that, similarly to the A_{2A}AR, after ischemia a damaging role is exerted by A_{2B}AR located on brain cells while A_{2B}AR located on endothelial and blood immune cells is implicated in dampening vascular adhesion signals and hypoxia-induced inflammation (Koeppen *et al.,* 2011). A further possible role of A_{2B}AR in hypoxia/ischemia might be secondary to promotion of an angiogenic response because activation of A_{2B}AR by adenosine increases endothelial cell proliferation, chemotaxis and capillary tube formation (Adair, 2005; Grant *et al.,* 2001). Exposure of human umbilical vein endothelial cells to hypoxia increases expression of A_{2B}AR which upon stimulation promotes the release of vascular endothelial growth factor (VEGF) (Feoktistov *et al.,* 2004).

4. Neurodegenerative deseases

Neurodegeneration is a feature of many debilitating, incurable diseases that are rapidly rising in prevalence, such as Parkinson's disease. There is an urgent need to develop new and more effective therapeutic strategies to combat these devastating diseases. Models – from cell-based systems, to unicellular organisms, to complex animals – have proven to be a useful tool to help the research community shed light on the mechanisms underlying neurodegenerative diseases, and these advances have now begun to provide promising therapeutic avenues.

Neurodegenerative diseases represent a major threat to human health. These age-dependent disorders are becoming increasingly prevalent, in part because the elderly population has increased in recent years (Heemels, 2016). Examples of neurodegenerative diseases are Alzheimer's disease, Parkinson's disease, Huntington's disease, Multiple sclerosis, frontotemporal dementia and the spinocerebellar ataxias. These diseases are diverse in their pathophysiology, with some causing memory and cognitive impairments and others affecting a person's ability to move, speak and breathe (Abeliovich and Gitler, 2016; Canter *et al.*, 2016; Taylor *et al.*, 2016; Wyss-Coray, 2016).

Effective treatments are desperately needed but will only come with a deep understanding of the causes and mechanisms of each disease.

One way to learn about how a disease works is to develop a model system that recapitulates the hallmark characteristics of the disease. Powerful experimental model organisms such as the mouse, fruit fly, nematode worm, and even baker's yeast have been used for many years to study neurodegenerative diseases and have provided key insights into disease mechanisms (Auluck and Bonini, 2002; Boillée *et al.*, 2006; Bruijn *et al.*, 1998; Cooper *et al.*, 2006; Krobitsch and Lindquist, 2000; Outeiro and Lindquist, 2003; Yamamoto *et al.*, 2000).

CNS disorders are a group of diseases with significant socioeconomic impact and growing relevance due to the increase in life expectancy of the world population. Since only symptomatic or palliative therapies are currently available for most of these diseases, the development of innovative therapeutic strategies is an unmet need. CNS disorders, traditionally dichotomized between early-onset neurodevelopmental and late-onset neurodegenerative diseases, are associated with dysfunction of neuronal activity due to perturbations at the synapse level (Torres *et al.*, 2017).

They may therefore be collectively regarded as diseases of the synapse or synaptopathies. Synaptic defects are causally associated with early appearing neurological diseases, including autism spectrum disorders (ASD), schizophrenia (SCZ) and bipolar disorder (BP). On the other hand, in late-onset degenerative pathologies, such as Alzheimer's (AD), Parkinson's (PD) and Huntington's (HD) diseases, synaptopathy is thought to be the inevitable end-result of an ongoing pathophysiological cascade. However, understanding the initiation and contribution of synaptic dysfunction in neurological disorders has been challenging because of (i) limited and usually late-stage access to human tissue, and (ii) inadequate recapitulation of key features of the human diseases in existing experimental animal models. Recent advances in cell reprogramming technologies that allow generation of human induced pluripotent stem cells (hiPSCs) (Takahashi *et al.*, 2017), from somatic cells of patients with a variety of diseases have opened new perspectives for studying the pathogenesis of CNS disorders. The establishment of robust protocols for directing the differentiation of hiPSCs into various neuronal cell types has permitted disease-in-a-dish modelling and analysis of the phenotypic characteristics of numerous CNS pathologies. More recently, the development of three-dimensional (3D) organoid cultures has created new possibilities for studying disease emergence and progression in the closest situation to the human brain (Pașca, 2018).

Due to these revolutionizing technologies it is now possible to shed light into cellular and molecular mechanisms underlying neuronal dysfunction in patient cells and follow over time the emergence of disease phenotypes, particularly those appearing early.

4.1 Multiple sclerosis

Multiple sclerosis (MS) is a chronic disease of the CNS that mainly presents in young adults, creating a substantial health-care burden at individual, family and community levels (Ontaneda *et al.,* 2017). MS is primarily considered to be an immune-mediated disease and is characterized by focal areas of inflammatory demyelination that spread in the brain and in the spinal cord with time, driven by an infiltration of lymphocytes. According to this view, the first years of relapsing–remitting MS (RRMS), the form of MS that many individuals with the disease initially develop, are characterized by recurrent episodes of neurological dysfunction from which the individual usually recovers (Compston and Coles, 2002), and the frequency of such episodes can be even markedly reduced by treatments that modulate or suppress the immune system (Comi *et al.,* 2017).

The classic pathological hallmark of MS was long considered to be the presence of focal white matter demyelinating lesions. However, with time, it became clear that pathological changes are also detectable in normal-appearing white matter, as well as in the CNS grey matter, with the presence of focal grey matter lesions and grey matter atrophy (Filippi *et al.,* 2012). Neuronal axons are affected in the early stages of MS (Calabrese *et al.,* 2015). Over time, axonal damage and diffuse microglial activation dominate MS-related pathological changes and are accompanied by progressive, mostly untreatable, accumulation of neurological disability affecting many functional domains from mobility to cognition. Neuropsychological dysfunction, despite its precocious identification by Charcot, was overlooked for a long time in individuals with MS (Charcot J.M., 1877). However, in the past three decades, cognitive impairment has been increasingly investigated and it is now recognized to be a core feature of the MS clinical picture, with a negative influence on physical independence and competence in daily activities (Chiaravalloti and DeLuca, 2008; Langdon, 2011). Current available MS therapies target immune modulation with some efficacy, however, concomitantly with adverse side effects (English and Aloi, 2015).

Oligodendrocytes, are the myelin-producing cells in the CNS. Damaged oligodendrocytes no longer generate myelin and remyelination requires generation of new mature oligodendrocytes from the differentiation of oligodendrocyte precursor cells (OPCs) (Dawson *et al.,* 2003). These cellular resources are especially active after demyelinating episodes in early phases of MS. Indeed, OPCs actively proliferate, migrate to and repopulate the lesioned areas. Ultimately, efficient remyelination is accomplished when new oligodendrocytes reinvest nude neuronal axons, restoring the normal properties of impulse conduction. As the disease progresses, this fundamental process fails. Multiple causes seem to contribute to such transient decline, including the failure of OPCs to differentiate and enwrap the vulnerable neuronal axons. For example, the observation that OPCs are present in MS lesions but fail to differentiate into mature oligodendrocytes (Chang *et al.,* 2000; Levine and

Reynolds, 1999) suggests that the remyelination process is blocked at a premyelinating stage in demyelinating lesions.

Unfortunately, despite its high prevalence and considerable impact, the precise mechanisms underlying cognitive impairment in MS are still largely unknown, and efficacious treatments for this aspect of the disease are lacking. Pathological changes in CNS white matter and specific neuronal grey matter structures could play a crucial role in the pathogenesis of MS-related cognitive impairment (DeLuca *et al.*, 2015). Alterations in the physiological crosstalk between the immune and nervous systems might also have a role, as such crosstalk modulates synaptic transmission and the induction of synaptic plasticity in the CNS (Di Filippo *et al.*, 2008).

5. Oligodendrogenesis

Stroke-induced oligodendrogenesis in ischemic brain has not been broadly studied (Dewar *et al.*, 2003). Oligodendrocytes, myelin forming cells in the CNS, are vulnerable to cerebral ischemia (Dewar *et al.*, 2003; Pantoni *et al.*, 1996). Stroke acutely induces mature oligodendrocyte damage, leading to loss of myelin, which is associated with loss of axons (Dewar *et al.*, 2003; Pantoni *et al.*, 1996).

However, during stroke recovery there is a significant increase in generation of OPCs and some of them become mature myelinating oligodendrocytes in peri-infarct gray and white matter where sprouting axons are present (Zhang *et al.*, 2011).

An increase in mature myelinating oligodendrocytes observed after stroke in the adult brain likely result from new oligodendrocytes differentiated from OPCs. During development, mature oligodendrocytes (OLGs) are generated by cells of the embryonic ventricular zone in the brain and spinal cord, giving rise to OPCs that proliferate and migrate throughout the CNS (Richardson *et al.*, 2006). These OPCs can then terminally differentiate into mature OLGs during a step-by-step process characterized by the downregulation of precocious markers (such as the membrane chondroitin sulfate proteoglycan, NG2, and the PDGF receptor-alpha (PDGFRα)) and the acquisition of immature OLG antigens such as O4, followed by myelin specific structural proteins (i.e., myelin basic protein (Mbp)). Furthermore, early undifferentiated bipolar OPCs acquire a more complex morphology with many branched processes, culminating in the formation of membrane sheaths that wrap around axons (de Castro and Bribián, 2005). It has been demonstrated that $NG2^+$ OPCs (also called polydendrocytes) are still present in the adult CNS generating a lot of interest on these cells as a reservoir of OLGs to repair demyelinated lesions (Nishiyama *et al.*, 1999; Windrem *et al.*, 2004). It has been indeed reported that, under specific conditions, NG2 cells can give rise to neurons and astrocytes (Nishiyama *et al.*, 2009). This indicates that polydendrocytes exhibit additional properties apart from their assumed functions as OPCs, although this concept is currently a highly debated topic. NG2 cells have been also demonstrated to make multiple contacts with the axonal membrane at nodes of Ranvier (Butt *et al.*, 1999) and with synaptic terminals (Ong and Levine, 1999), suggesting a role in surveillance of neuronal activity and raising the question of whether adult NG2 cells may be

capable of responding to or influencing neuronal activity (Butt *et al.*,2002.; Butt and Dinsdale, 2005; Nishiyama *et al.*, 2002.). In this respect, several data indicate that, similarly to mature OLGs, these cells respond to neuronal activity and to neurotransmitters (Butt and Dinsdale, 2005).

5.1 Purinergic signalling in Oligodendrogenesis

Purinergic signaling (exerted by adenosine and ATP) has recently emerged as one of the main pathways that regulate myelination in both the PNS and CNS. In the CNS, neurons and multiple types of glia are in close proximity, so that a signal such as ATP released by a neuron could exert effects on many nearby cells (Figure 8).

OLGs have an essential role in efficient neurotransmission in the CNS. Myelin sheaths produced by differentiated OLGs wrap and insulate axon segments, and small, electrically conductive nodes of Ranvier are spaced between myelin internodes. This arrangement allows rapid saltatory conduction of action potentials along myelinated axons and is crucial for proper nervous system development and function. Impaired myelination has been implicated in neuropsychiatric disorders and cognitive disabilities (Haroutunian *et al.,* 2014). Furthermore, the extensive physical interaction between OLs and axons allows for OLGs to be involved in maintaining neuronal homeostasis. OLGs assist with axonal energy metabolism by exporting lactate, an energy substrate; through myelin membranes (Saab *et al.,* 2013).

In addition to OLGs, OPCs also contact axonal segments in the CNS. Ultrastructural studies have revealed synapse- like structures between axons and OPCs, with synaptic vesicles in the axon and structures resembling postsynaptic densities in the OPC process (Bergles *et al.,* 2000).

More recently, live, *in vivo* imaging has demonstrated synaptic vesicle accumulation along axonal segments during contact with OPC processes (Hines *et al.,* 2015). In this study, synaptic vesicle release along unmyelinated axon segments promoted myelin sheath formation. Growing evidence points to neuronal activity and neurotransmitter release affecting OPC proliferation, migration, and differentiation, as well as myelin formation (Almeida and Lyons, 2017; Fields, 2015; Gallo *et al.*, 2008). Furthermore, continuous myelin remodeling throughout adulthood points to a need for continuous communication between neurons, OPCs, and OLGs (Sampaio-Baptista and Johansen-Berg, 2017). Since ATP is released from neurons in an activity- dependent manner, ATP (or its derivatives ADP and adenosine) may be involved in the ongoing communication between neurons and myelinating glia.

In CNS, myelination is regulated by extracellular signals and intracellular factors acting on both the various steps of OLG maturation and axonal activity (Emery, 2010). In detail, adenosine has been reported to inhibit OPC proliferation in the presence of the mitogenic agent PDGF and to promote cell differentiation towards premyelinating oligodendrocytes, thus globally increasing myelination, as shown by the rise of Mbp^+ oligodendrocytes in DRG/OPC treated co-cultures. Of note, the percentage of myelinating Mbp^+ oligodendrocytes was lower in co-cultures treated with the

adenosine receptor antagonists alone, suggesting that endogenous sources of adenosine are sufficient to promote differentiation effects (Stevens *et al.*, 2002).

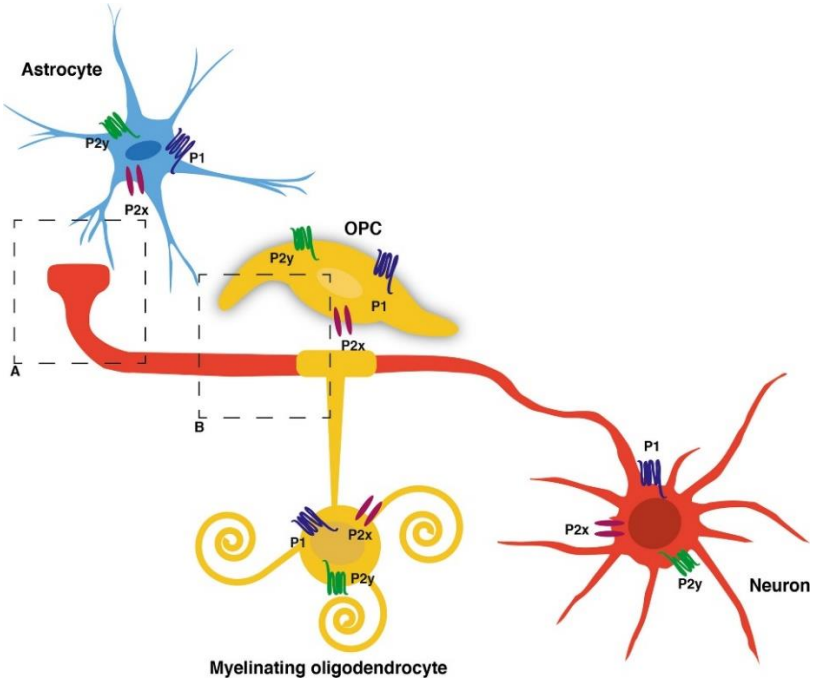

Figure 8: Overview of purinergic signaling in CNS cells. Schematic of CNS neuron/glial interactions and purinergic receptor expression. It should be noted for neurons and glial cells: expression of receptor subtypes varies across brain regions and with development. (Taken from: Welsh and Kucenas, 2018).

5.1.1 Role of P1 receptors in Oligodendrogenesis

Evidence for the role of purinergic signaling in regulating OPCs, OLGs, and myelination comes largely from *in vitro* studies.

Concerning oligodendrocytes, it has been demonstrated that purines exert multiple effects including increased motility, proliferation and differentiation of cultured OPCs (for a review see in: (Coppi *et al.*, 2015). Among purines, adenosine is a neuromodulator of the CNS, where it acts on four subtypes of P1 purinergic receptors (A_1, A_{2A}, A_{2B}, A_3) (Fredholm *et al.*, 2011). It is known that OPCs express all these receptors (see Table 2), as detected by RT-PCR in cultured OPCs, including A_{2B}AR (Stevens *et al.*, 2002, see Figure 9). To date, a functional role has been attributed only to A_1 and $A_{2A}AR_S$ (Coppi *et al.*, 2015). We elucidated the role of $A_{2A}AR_S$ on oligodendrogenesis, demonstrating that their selective activation decreases outward rectifying, sustained, I_K currents and inhibits *in vitro* OPC differentiation towards mature, myelinating oligodendrocytes, without affecting cell division (Coppi *et al.*, 2013a). Conversely, adenosine, through the activation of A_1AR seems to be a primary activity-dependent signal inhibiting the proliferation and promoting differentiation of premyelinating progenitors into myelinating oligodendrocytes (Stevens *et al.*, 2002) and stimulating OPC migration (Othman *et al.*, 2003). The functional role of the A_{2B}AR in oligodendrocytes has not yet been clarified. Among adenosine receptors, the A_{2B}AR is the least studied and still remains the most

enigmatic adenosine receptor subtype because of the relatively low potency of adenosine at this receptor (EC_{50} value of 24 μM) (Fredholm *et al.,* 2011) and the very few specific agonists that have been described so far. However, there is a growing interest in $A_{2B}AR_S$ in recent years, as it has been shown to play a role in inflammation and cancer and is even considered a promising new pharmacotherapeutic target. Of particular note is that in the brain during different pathological conditions, such as cerebral ischemia, extracellular adenosine is elevated to levels sufficient for $A_{2B}AR$ activation (Pedata *et al.,* 2016).

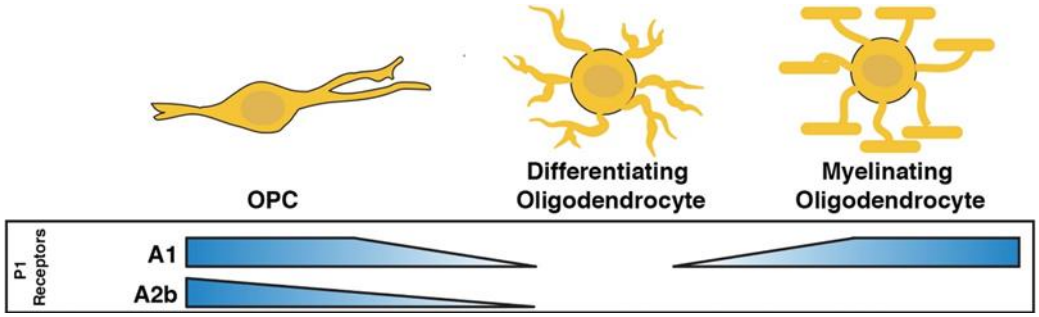

Figure 9: Developmentally regulated expression of A_1 and A_{2B} receptors in the OLG lineage. (Taken from: Welsh and Kucenas, 2018).

Testing the hypothesis that axonally released adenosine mediated OPC proliferation and calcium signaling, Stevens (Stevens *et al.,* 2002) demonstrated calcium responses in OPCs either via electrical stimulation of co- cultured neurons, or by directly applying the P1 agonist 5'- (N-ethylcarboxamido)adenosine (NECA) to OPC monocultures. Additionally, P1 antagonists blocked the activity- dependent calcium response; supporting the conclusion, that adenosine released from firing neurons stimulates calcium signaling in OPCs. Adenosine and the P1 agonist NECA also inhibited proliferation and promoted differentiation and myelin production. The conclusions from cell culture are supported by evidence in cerebellar slices that adenosine inhibits proliferation and increases differentiation of OPCs (Stevens *et al.,* 2002). More recently, *in vitro* pharmacology experiments tested the roles of specific P1 agonists, but with some conflicting results. For example, multiple studies have reported that adenosine inhibits OPC proliferation (Stevens *et al.,* 2002; Agresti *et al.,* 2005). However, selective agonists for A_1 and $A_{2A}AR_S$ did not have any effect on OPC proliferation (Othman *et al.,* 2003; Coppi *et al.,* 2013). In another example of conflicting results, one study found that the A_1 agonist N6- cyclopentyladenosine (CPA) promoted OPC migration in a dose- dependent manner, whereas another study reported that neither adenosine nor CPA had any effect on OPC migration (Agresti *et al.,* 2005; Othman *et al.,* 2003).

Stevens (Stevens *et al.,* 2002) observed that adenosine promotes differentiation of OPCs and myelination. However, the A_{2A} agonist CGS21680 was reported to inhibit differentiation, and the A_1 agonist CPA had no effect on OPC differentiation (Coppi *et al.,* 2013a; Othman *et al.,* 2003).

Table 2. P1 receptor expression and function in OLG lineage cells

	Expression-OPCs	**Expression-mature OLs**	**Migration**	**Proliferation**	**Differentiation**
A_1	Y (RTPCR)1 Y (IHC)2 Y (RNAseq)15	Y (RTPCR)11 Y (IHC)2 Y (RNAseq)15	(+)2 no effect4	No effect2	No effect2
A_{2A}	Y (RTPCR)1 N (RNAseq)15	Y (RTPCR)11 N (RNAseq)15		No effect5	(-) 5
A_{2B}	Y (RTPCR)1 Y (RNAseq)15	Y (RTPCR)11 N (RNAseq)15			
A_3	Y (RTPCR)1 N (RNAseq)15	Y (RTPCR)11 N (RNAseq)15			
P1 (unspecified)	n/a	n/a	No effect4	(-) 1,4	(+) 1

Table 2. OPCs, oligodendrocyte progenitor cells. Y, expression detected; N, expression examined and not detected; (+) increased, (-) decreased. (Taken from: Welsh and Kucenas, 2018).

6. Fingolimod

6.1 Historic development of fingolimod

Fingolimod, GilenyaR, 2-amino-2[2-(4-octylphenyl)ethyl]-1,3-propanediol) was originally synthesized by the Japanese chemist Tetsuro Fujita from Yoshitomi Pharmaceutical Industries Ltd. (present: Mitsubishi Tanabe Pharma Corporation, Japan) (Adachi *et al.*, 1995) using the natural compound myriocin (ISP-1) as a lead. Myriocin was previously isolated by the same group from the culture broth of *Isaria sinclairii*, the imperfect or asexual stage of the genus *Cordyceps sinclarii* (cordycipitaceae), a subfamily of parasitic fungi. It was described as an immunosuppressant 10–100 times more potent than cyclosporine A (CSA) (Chiba *et al.*, 1998; Fujita *et al.*, 1996). Remarkably, extract and powder from the near relative *Cordyceps sinensis* has been widely used in Traditional Chinese Medicine for its energy boosting effect and to grant eternal youth. Based on the chemical structure of myriocin, a series of derivatives were synthesized from which Fingolimod turned out to be an even more potent immunosuppressant when tested *in vitro* in a mouse allogenic mixed lymphocyte reaction assay, and *in vivo* in rat and dog transplantation models where allograft survival was prolonged for several weeks (Chiba *et al.*, 1998; Fujita *et al.*, 1996; Suzuki *et al.*, 1996).

6.2 Mechanism of action of fingolimod

The main immunomodulatory mechanism of action of fingolimod is based on its effect on lymphocyte homing. It reversibly redistributes T and B cells from the circulation to secondary lymphoid organs like peripheral and mesenteric lymph nodes and Peyer's patches, thereby causing a state of peripheral lymphopenia (Chiba *et al.,* 1998). Since fingolimod resembles in chemical structure the sphingolipid molecule sphingosine, it can serve as a substrate for sphingosine kinase (SphK) to become phosphorylated to the active metabolite fingolimod-P (Brinkmann *et al.,* 2002). Thus, fingolimod is a pro-drug which requires SphK to become active. Two subtypes of SphK, SphK1 and SphK2, exist and in principle both enzymes can phosphorylate fingolimod *in vitro* (Billich *et al.,* 2003). However, SphK2 is 30-fold more efficient due to a lower Km value of fingolimod for SphK2 compared to SphK1 (Billich *et al.,* 2003). Furthermore, SphK2 is the only enzyme which activates fingolimod *in vivo*, since only Sphk2 knockout mice are resistant to fingolimod-induced lymphopenia (Zemann *et al.,* 2006) and lack fingolimod-mediated protection from disease symptoms in experimental autoimmune encephalomyelitis (EAE), a widely used animal model for multiple sclerosis (Imeri *et al.,* 2016).

Fingolimod-P mimics sphingosine 1-phosphate (S1P) in structure and thus, not surprisingly, also binds to S1P receptors (Brinkmann *et al.,* 2002; Mandala *et al.,* 2002). S1P receptors were originally described as endothelial differentiation genes (edg) and build a subclass of G protein-coupled lipid receptors, which are most homologous to the lysophosphatidic acid (LPA) receptors. So far, 5 subtypes of S1P receptors have been identified, denoted $S1P_{1–5}$. They have all been determined to bind S1P with high affinity (Kihara *et al.,* 2014) with binding constants ranging from 1 to 10 nM, except for $S1P_4$, which has a ten-fold lower affinity (Mandala *et al.,* 2002). Fingolimod-P binds with similar affinity as S1P to $S1P_1$, $S1P_3$, and $S1P_5$, but shows much better binding to $S1P_4$ than S1P (6 nM *vs* 90 nM) (Mandala *et al.,* 2002). Fingolimod is not a ligand for $S1P_2$. Due to the diversity of S1P receptor subtypes with their distinct function and ubiquitous expression in the body (Kihara *et al.,* 2014; O'Sullivan, 2017), in theory multiple effects can be expected from using fingolimod, which may either have therapeutic benefit or cause adverse events.

6.3 Specific fingolimod targets

6.3.1 The S1P receptor family: The $S1P_1$ receptor

As outlined above and because of its binding to and activation of the various S1P receptor subtypes, except for $S1P_2$, "active" fingolimod is pharmacologically considered an unselective S1P receptor agonist (Brinkmann, 2007; Brinkmann *et al.,* 2002, Mandala *et al.,* 2002). Moreover, it causes sustained desensitization of the $S1P_1$-mediated signalling pathway by inducing receptor internalization and degradation, which on the cellular level results in functional antagonism. This effect of fingolimod on $S1P_1$ is unique and not seen with the endogenous ligand S1P, which also internalizes $S1P_1$ upon binding but then dissociates in endosomes and the receptor recycles back to the plasma membrane. Similarly, $S1P_{3\text{-}4}$, and $S1P_5$ are also internalized upon fingolimod-P binding

and then redistribute back to the cell surface. Particularly, downregulation of $S1P_1$ on T cells is supposed to account for the immunosuppressive effect of fingolimod, whereas downregulation of $S1P_1$ in other cell types, notably in endothelial cells, is likely responsible for the adverse events observed under long-term fingolimod treatment (Brinkmann, 2007). The agonistic effect of fingolimod on $S1P_{3\text{-}4}$, and $S1P_5$ may account for additional biological effects with unknown consequences as outlined below (Figure 10).

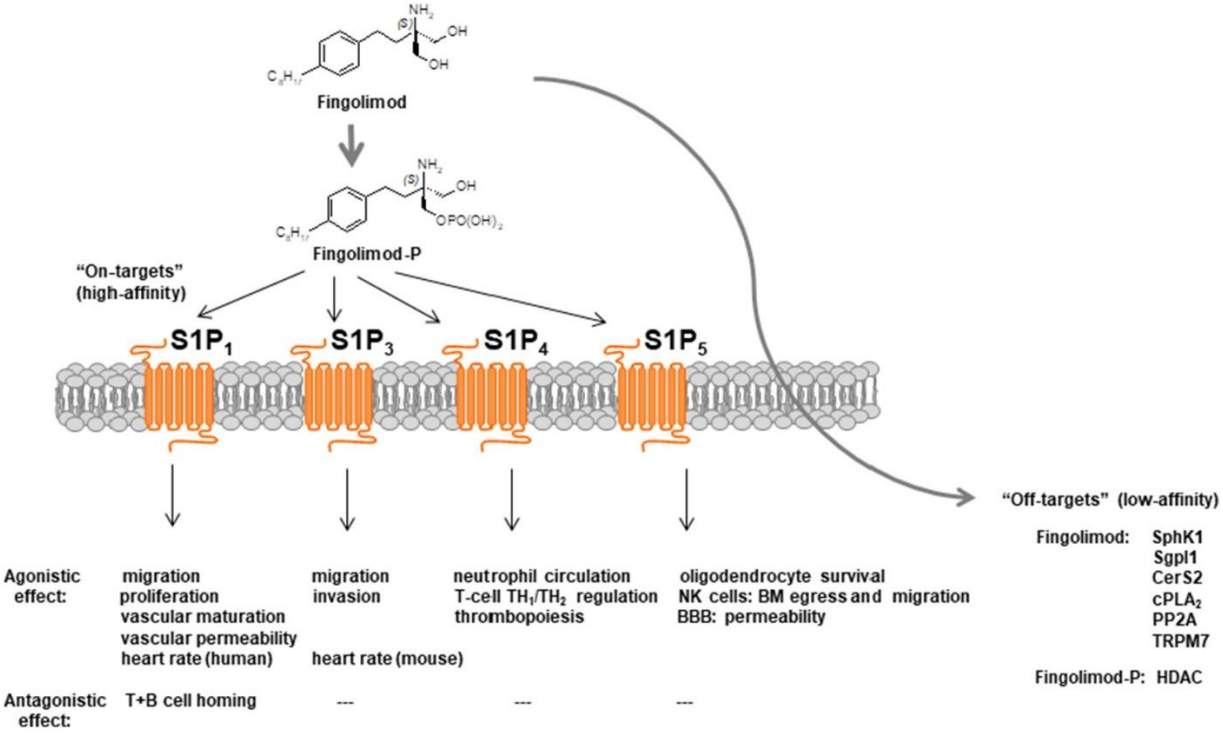

Figure 10: Schematic view of cellular on-targets and off-targets of fingolimod and possible functions. (Taken from: (Huwiler and Zangemeister-Wittke, 2018).

These early pioneering studies have fuelled research on $S1P_1$ receptor biology to better understand its role in human diseases. Since $S1P_1$ is ubiquitously expressed in almost every cell type, its downregulation by prolonged fingolimod treatment is expected to have multiple consequences on cellular responses and tissue homeostasis. The generation of systemic S1pr1 knockout mice corroborated the vital biological function of $S1P_1$, since embryos die in the developmental stage of day E12.5–E14.5, due to impaired vessel maturation and hemorrhagic bleedings.

Besides its role in immune cell trafficking and vascular development, $S1P_1$ is implicated in the regulation of vascular integrity. Increased vascular permeability is a typical feature of inflammation and allergy, and therefore a possible barrier protective effect of S1P signaling is of therapeutic interest. Various *in vitro* and *in vivo* studies have investigated the effect of S1P and fingolimod on the endothelial barrier function. It was shown that endotoxin-induced microvascular permeability and inflammation leading to acute lung and kidney injury in mice can be reduced by direct application of either S1P or fingolimod (Peng *et al.*, 2004). On the contrary, application of a $S1P_1$ receptor antagonist (W146) induced loss of capillary integrity in mouse skin and lung (Sanna *et al.*, 2006),

and the most recently developed potent $S1P_1$ selective antagonist NIBR-0213 induced transient lung and heart permeability defects in rats, which promoted chronic inflammatory remodeling (Bigaud *et al.,* 2016). Furthermore, a conditional gene deletion approach was used to demonstrate that plasma S1P is crucial for vascular integrity. Since Sphk1/Sphk2 double knockout mice are embryonically lethal, a conditional double knockout (KO) mouse was generated, which contains one conditional Sphk1 allele and one null Sphk1 allele in a Sphk2 null background (Sphkf/−Sphk2−/−) and carries a Cre transgene. By inducing Cre, plasma S1P levels became undetectable. These "pS1Pless" mice showed a several-fold increased vascular leakage and reduced survival compared to wildtype mice upon administration of platelet activating factor (PAF), and the symptoms could be relieved by injection of a selective $S1P_1$ agonist (AUY954) (Camerer *et al.,* 2009).

Improved endothelial barrier function resulting from $S1P_1$ activation by S1P and fingolimod was also demonstrated in cultures of human endothelial cells *in vitro* (Dudek *et al.,* 2007).

The molecular mechanisms underlying the barrier enhancing effect are not yet fully understood, but the role of adherents junction molecules, such as VE-cadherin and platelet-endothelial cell adhesion molecule (PECAM-1), appears to be crucial. In this regard, it was shown that S1P and fingolimod-P can stimulate the translocation of VE-cadherin to cell-cell contact sites of endothelial cells in cultures (Sanchez *et al.,* 2003), and *in vivo* in S1pr1 knockout mice the retinal vasculature lost VE-cadherin staining (Gaengel *et al.,* 2012). For PECAM-1, upregulation was detected in endothelial cells overexpressing SphK-1, which is supposed to increase S1P levels (Limaye *et al.,* 2005).

Furthermore, $S1P_1$ silencing was shown to reduce expression of PECAM-1 and VE-cadherin (Krump-Konvalinkova *et al.,* 2005), and deregulation of these adherents junction molecules by fingolimod was also seen in a mouse model of multiple sclerosis, i.e. EAE (Imeri *et al.,* 2016).

On the other hand, the barrier enhancing effect of fingolimod seems to be dose-dependent, since higher concentrations in the range of 10 to 100 μM in cultures of human umbilical vein endothelial cells rather compromised the barrier function, and *in vivo* in mechanically ventilated mice even aggravated lung injury (Müller and Jacobson, 2011). Similarly, in a bleomycin-induced lung injury model in mice, prolonged exposure to fingolimod resulted in vascular leak, fibrosis and increased mortality (Shea *et al.,* 2010). Altogether, these studies suggest that $S1P_1$ activation improves the endothelial barrier function, whereas $S1P_1$ antagonism, notably also by prolonged fingolimod treatment, disrupts it, thereby increasing permeability and vascular leakage.

6.3.2 The $S1P_3$ receptor

A more detailed characterization of $S1P_3$ activation by fingolimod-P showed that it has an EC_{50} value of 7 to 10 nM for $S1P_3$, which is comparable to the endogenous ligand S1P. However, its efficacy reached only 50% of S1P, suggesting a partial agonistic effect (Riddy *et al.,* 2012). By definition, a partial agonist in the presence of a full agonist produces an antagonistic output. This could mean that *in vivo*, fingolimod can also antagonize $S1P_3$ signaling rather than stimulate it, depending on the local S1P concentration.

In this context it is noteworthy that $S1P_3$ was recently shown to have prometastatic properties in breast and lung carcinoma cells (Filipenko *et al.,* 2016; Zhang *et al.,* 2013b), and high expression is frequently found in tumors from breast cancer patients where it correlates with poor prognosis (Watson *et al.,* 2010). Since plasma S1P levels are often elevated in cancer patients (Alberg *et al.,* 2013; Sutphen *et al.,* 2004; Zhang *et al.,* 2015), the requirements for fingolimod to act as a partial $S1P_3$ agonist and thus impede metastatic growth might be fulfilled.

6.3.3 The $S1P_4$ receptor

The role of $S1P_4$ in physiological processes is still poorly understood and therefore the effects of fingolimod mediated by $S1P_4$ are unclear. S1P and fingolimod-P associate with $S1P_4$ with binding constants of 95 nM and 6 nM, respectively, which means that fingolimod is a much better ligand for this receptor than the endogenous ligand (Mandala *et al.,* 2002). $S1P_4$ expression is restricted in the body and mainly found in lymphocytes and tissues of the immune and hematopoietic system (Gräler *et al.,* 1998).

Knockout of S1pr4 in mice and zebrafish consistently revealed a reduction of the number of circulating neutrophils, suggesting a role for $S1P_4$ in immunity and infection (Allende *et al.,* 2011; Pankratz *et al.,* 2016). S1pr4 deficient mice also show differential reactions to inflammation with exacerbated T helper (Th)2 cell responses and decreased responses of Th1 cells (Allende *et al.,* 2011). Moreover, megakaryocytes generated from S1pr4 deficient mice showed atypical and reduced formation of proplatelets *in vitro,* and the recovery of platelet numbers after experimental thrombocytopenia was significantly delayed, suggesting a role for $S1P_4$ in thrombopoiesis (Golfier *et al.,* 2010). Of note, in humans, a rare missense variant of $S1P_4$ (Arg365Leu) was reported, which generates a loss-of-function receptor and is associated with reduced white blood cells and neutrophil counts (Pankratz, 2016), thus corroborating the preclinical data from mice (Allende *et al.,* 2011).

6.3.4 The $S1P_5$ receptor

The $S1P_5$ receptor was originally cloned as rat nerve growth factor-regulated G protein-coupled receptor Nrg-1 (Glickman *et al.,* 1999) and later found to be identical to $S1P_5$/edg8. It is predominantly expressed in the brain and spleen (Im *et al.,* 2000; Malek *et al.,* 2001) and in these tissues, it is further concentrated in oligodendrocytes and natural killer (NK) cells (O'Sullivan, 2017). Fingolimod-P and S1P bind to $S1P_5$ with equally high affinity. In oligodendrocytes this triggers two distinct functional responses depending on the developmental stage of the cells. It leads to retraction in pre-oligodendrocytes, whereas it increases the survival of mature cells (Jaillard *et al.,* 2005).

In addition, migration of OPCs, which normally migrate over considerable distances during brain development, is inhibited by $S1P_5$ activation (Novgorodov *et al.,* 2007).

Fingolimod was also shown to protect human oligodendrocytes from apoptosis induced by serum and glucose deprivation, suggesting a neuroprotective effect by activating $S1P_5$ (Miron *et al.,* 2008). Moreover, $S1P_5$ is also expressed on brain microcapillary endothelial cells where it contributes to the

blood-brain barrier function and maintains the immunoquiescent state of brain endothelial cells (van Doorn *et al.*, 2012).

In S1pr5 knockout mice the number of circulating NK cells is decreased (Walzer *et al.*, 2007), proposing a function of $S1P_5$ in promoting NK cell egress from bone marrow and lymph nodes into the blood and recruiting them to sites of inflammation (Jenne *et al.*, 2009; Walzer *et al.*, 2007).

S1pr5 knockout mice also lack circulating Ly6C-negative peripheral monocytes, but maintain normal levels in the bone marrow (Debien *et al.*, 2013).

6.3.5 SphK1

As determined *in vitro*, fingolimod is a substrate of SphK2 and is also phosphorylated by SphK1, but with much lower efficiency (Billich *et al.*, 2003). *In vivo*, however, SphK2 is the only kinase which activates fingolimod as demonstrated in Sphk1- and Sphk2-deficient mice. Fingolimod, but not fingolimod-P, acts also as a direct inhibitor of SphK1, but very high concentrations of 50 μM are needed to achieve 50% inhibition (Tonelli *et al.*, 2010; Vessey *et al.*, 2007). As a pharmacological target with oncogenic potential, SphK1 is of interest for cancer therapy. Considering the toxicity profile of fingolimod at 0.5 mg per day in patients, however, it is unrealistic to believe that such high doses can be tolerated. Nevertheless, numerous preclinical studies have shown pro-apoptotic and anti-tumor effects of fingolimod with tumor cell lines *in vitro* and in tumor models in mice, which could be partly attributed to inhibition of SphK1 (Pchejetski *et al.*, 2010).

6.4 S1P receptor signalling within the CNS

We have already mentioned that S1P levels are primarily regulated by SphK1and SphK2 (EC: 2.7.1.91), and S1P-degrading enzymes, such as S1P phosphatases (SPPs) that convert S1P to sphingosine and S1P lyase (SPL), which terminally cleaves this sphingolipid (Figure 11). SphK1 and SphK2 sequence differences arise from alternate splicing, which affects their differential subcellular localization and biochemical properties. As a consequence, the S1P pools synthesized by individual kinases could play a different roles in cells. S1P synthesized by SphK1 localised in the cytoplasm and endoplasmic reticulum can be transported out of the cell and exert mitogenic and anti-apoptotic effects in an autocrine, i.e 'Inside-Out signalling', or paracrine manner, affecting other cell types. Transport of these bioactive sphingolipids is carried out by spinster protein 2 (Spns2) and the ATP-binding cassette (ABC) family of transport proteins (ABC1, ABCG2, ABCA1). S1P is a ligand of five S1P-specific G protein-coupled cell plasma membrane receptors, called $S1P_{1\text{-}5}R$ (O'Sullivan S *et al.*, 2017).

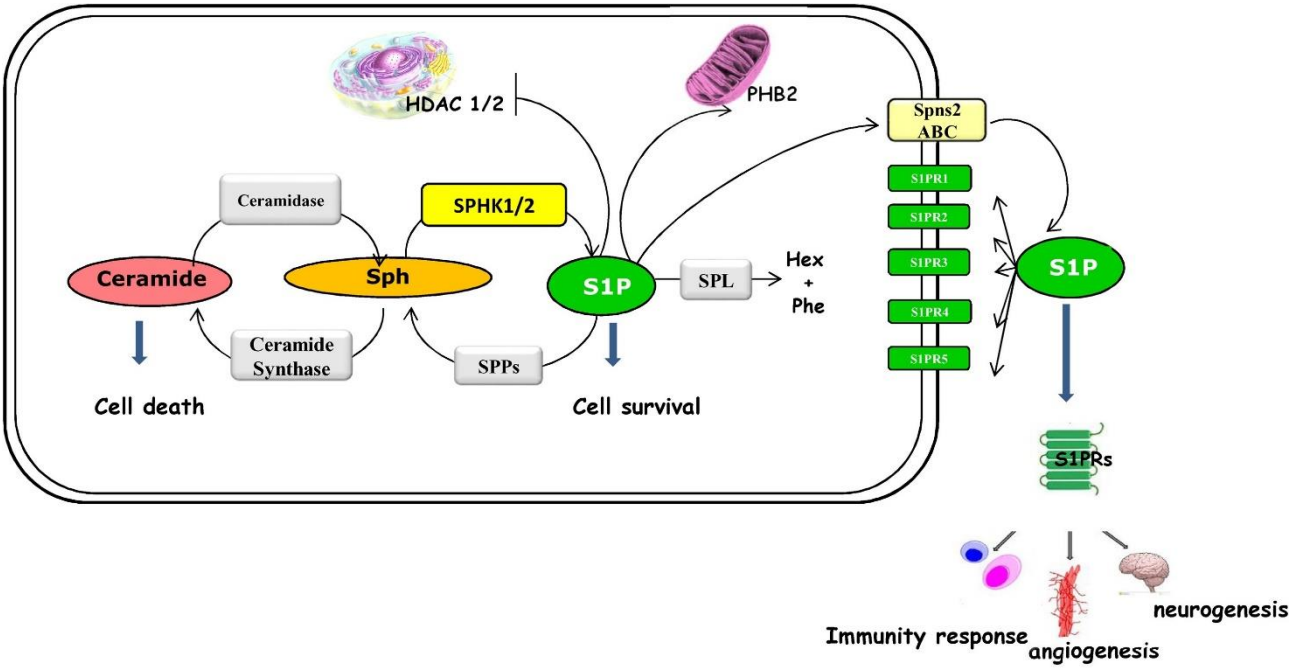

Figure 11: Metabolism and mechanism of S1P action. (Taken from: Motyl and Strosznajder, 2018).

Four of the five S1P receptors ($S1PR_S$), ($S1PR_1$, $S1P_2R$, $S1P_3R$, and $S1P_5R$) are located in both neurons and glial cells within the CNS. S1PR-mediated signalling is essential for development of the neural tube and vascular system during embryogenesis (Mizugishi *et al.*, 2005). In the mature CNS, S1P regulates the activation of neuronal progenitor cells and their migration to affected regions. S1P-dependent signalling influences the synthesis of neurotrophic factors and pro-inflammatory cytokines, as well as cellular communication. $S1P_1R$ is the most abundant S1PR in the CNS. The level of expression of $S1P_1R$ and $S1P_3R$ changes over a lifespan, under pathological conditions, and depends on the environmental milieu. The key effector protein of $S1P_1R$ and $S1P_3R$ is phosphatidylinositol-3 kinase (PI3 K) conjugated to Akt kinase, which is responsible for phosphorylation of proteins associated with regulation of cell proliferation, migration, and survival. Mice with a $S1P_1R$ receptor deletion are characterized by abnormal formation of the neural tube and blood vessel failure that leads to embryonic death. Mortality at the embryonic stage is not observed upon deletion of the other four S1PRs (Mizugishi *et al.*, 2005). This supports $S1P_1R$ as a valuable pharmacological target in neuroprotective strategies.

6.5 Significance of SphK1/S1P/S1PRs signalling in neurodegenerative diseases

A disrupted balance between S1P and ceramide has been documented in AD patients and reported in other neurodegenerative diseases. Activity of SphK1s and level of S1P decline, according to the Braak pathology scale, in brain regions that are affected relatively early in AD (Couttas *et al.*, 2014; He *et al.*, 2010) increase in ceramide concentration in the cerebrospinal fluid and serum is suggested to be an appropriate biomarker of AD (He *et al.*, 2010; Satoi *et al.*, 2005). It was also reported that S1P concentration exhibits a strong inverse correlation with tissue Aβ levels and

hyperphosphorylation of tau protein in postmortem brain from AD patients (He *et al.,* 2010). The close relationship between S1P levels and Aβ peptide was recently demonstrated. Endogenously released Aβ peptides induced significant inhibition of both expression and activity of SphKs in PC12 cells transfected with the human gene for Aβ precursor protein (Gassowska *et al.,* 2014), moreover, another study demonstrated decreased SphK1 expression under Aβ peptide toxicity in PC12 cells (Cieślik *et al.,* 2015). Importantly, small interfering RNA knockdown of SPHK1 increases Aβ accumulation and decreases learning and memory function in an AD mouse model, revealing SphK1 modulation as a potential target for AD treatment (Zhang *et al.,* 2013c)

Patients with MS undergoing long-term treatment with Fingolimod (FTY720) showed reduced brain volume loss, reduced number of relapses, and a significantly slower progression of disability. These results suggest that, in addition to an immunosuppressive effect, FTY720 has neuroprotective properties (Brunkhorst, 2014).

Patients treated with FTY720, might be more susceptible to serious infections, such as disseminated or CNS herpetic infection, because of reduced number of circulating lymphocytes. The above side effects determine some limitations with FTY720 therapy to patients with cardiovascular and immune risk factor, especially in patients with diagnosed immunodeficiency syndrome. FTY720 treatment can induce also hepatobiliary disorders and macular oedema, which the last one is connected with internalization of $S1P_1$ (Yoshii *et al.,* 2017). In the last few years, several second-generation compounds with structural similarity to the FTY720 prodrug backbone, such as Siponimod, KRP-203, CS-0777, and RPC-1063, were synthesized and used in clinical trials. These S1PR modulators show higher selectivity for $S1P_1R$ than $S1P_3R$ (O'Sullivan *et al.,* 2017).

The mechanisms underlying neuroprotective effects elicited by FTY720 are not fully understood. However, a recent study indicated an important role for synthesis of neurotrophic factors like brain-derived neurotrophic factor (BDNF), prevention of astrogliosis and over-activation of transcription factor NF-κB in a Huntington's disease model, and decreasing TNFα and induced nitric oxide synthase (iNOS) levels. FTY720 has reached clinical trials for other nervous system diseases, like amyotrophic lateral sclerosis (ALS), acute stroke, Rett syndrome, glioblastoma, and schizophrenia. Its potential utility has also been demonstrated in numerous *in vitro* and *in vivo* models of neurological disorders, like spinal cord injury, Huntington's disease, epilepsy, and toxicity of Aβ (O'Sullivan *et al.,* 2017).

6.5.1 Role of S1PR modulation in MS

S1PR modulation has emerged as an effective disease modifying therapeutic strategy in MS. The therapeutic effect of FTY720 in MS and its animal model experimental autoimmune encephalomyelitis (EAE) is attributed to the downregulation of $S1P_1$ on lymphocytes resulting in their retention within lymph nodes (Balatoni *et al.,* 2007; Brinkmann, 2007; Brinkmann *et al.,* 2002; Mandala *et al.,* 2002; Matloubian *et al.,* 2004).

In addition, there is also evidence supporting the concept of anti- inflammatory, glioprotective and neuroprotective actions of S1PR modulators in the CNS (Choi *et al.,* 2011; Kim *et al.,* 2011; Soliven *et al.,* 2011). *In vitro* studies have demonstrated that Fingolimod-phosphate (FTY720- P) regulates the survival, differentiation and process dynamics of cultured rodent and human OLG lineage cells (Coelho *et al.,* 2007; Jung *et al.,* 2007; Miron *et al.,* 2008). Furthermore, we found that treatment of mice with fingolimod protects against acute cuprizone (cupr)- induced OLG injury, demyelination and axonal loss but does not promote remyelination in this model. The protective effect of fingolimod in the cuprizone model may be mediated not only by direct actions on S1PR on OLGs, but also by indirect or anti- inflammatory actions on astrocytes and microglia (Kim *et al.,* 2011).

6.6 Role of $S1PR_S$ in Oligodendrogenesis

$S1P_{1\text{-}5}$ are found in oligodendroglial cells, where they regulate a number of processes, ranging from cell proliferation and maturation to dendrite elongation (Jaillard *et al.,* 2005; Jung *et al.,* 2007; Miron *et al.,* 2008).

In particular, mature OLG express $S1P_5$ and at lesser extent $S1P_1$ $S1P_2$ and $S1P_3$, whereas OPC express at a higher level $S1P_1$ than $S1P_2$, $S1P_3$ and $S1P_5$. (Jung *et al.,* 2007; Novgorodov *et al.,* 2007; Yu *et al.,* 2004).

In vitro studies demonstrated that FTY720-P differently modulates differentiation, proliferation migration and availability of OPCs and/or OLGs relying on the activation of different S1PR subtypes whose expression depends upon the developmental stage of OPC_S (Jung *et al.,* 2007). Furthermore, it protects from myelin damage in EAE model and chronic progressive CNS inflammation (Kataoka *et al.,* 2005; Rothhammer *et al.,* 2017).

7. Neuropathic pain

Pain is the most common reason for people to seek medical attention (Salter, 2014). Despite this, nociceptive pain is a vital physiologic process that signals actual or potential tissue damage (Iadarola and Caudle, 1997). By so doing, it protects the individual from injury and secures the survival of the species. By contrast, direct injury to neural tissue can produce nerve or neuropathic pain that lasts for months or years after any injury has healed (Costigan *et al.,* 2009; Moulin *et al.,* 2014).

Exact prevalence of neuropathic pain within the global population is unknown, but most studies put estimates at between 1.5% and 8%, equating to between 100 million and 560 million people worldwide (Bouhassira and Attal, 2016; Gilron *et al.,* 2006; Salter, 2014; Torrance *et al.,* 2013, 2006).

Neuropathic pain is defined formally as “pain caused by a lesion or disease of the somatosensory system” (Jensen *et al.,* 2011). It can be caused by traumatic nerve, spinal cord, or brain injury (including stroke) or can be associated with diabetic, human immunodeficiency virus/AIDS, and postherpetic neuropathies, or with multiple sclerosis (Treede *et al.,* 2008) or cancer, and/or the toxic effects of chemotherapeutic agents (Xiao *et al.,* 2007; Schmidt *et al.,* 2010).

Tissue damage or perturbation capable of causing pain is detected by free nerve endings in peripheral and visceral structures and relayed by first-order sensory neurons (primary afferents) to second-order sensory neurons in the dorsal horn of the spinal cord. Glutamate and neuropeptides such as substance P and calcitonin gene-related peptide mediate neurotransmission between primary afferent and second-order sensory neurons. Glutamate interacts with Ca^{2+}-permeable and Ca^{2+}-impermeable α-amino-3-hydroxy-5-methyl-4-isoxazolepropionic acid (AMPA) and with N-methyl D-aspartate (NMDA) receptors, but not with kainate receptors (Tong and MacDermott, 2006). The cell bodies of first-order sensory neurons reside in the dorsal root ganglia (DRG).

Although all primary afferent neurons are widely believed to be glutamatergic (West *et al.*, 2015), it has been suggested that GABA-mediated inhibitory interactions may play a role in nociceptive processing at the level of the DRG (Du *et al.*, 2017). If these findings are verified, they will provoke considerable debate and reassessment of current ideas of sensory and nociceptive processing. It is possible that primary afferent neurons release GABA from their cell bodies in DRG, yet release glutamate from their terminals in the spinal cord.

The gray matter of the spinal cord is divided into the 10 laminae of Rexed (Figure 12A) (Rexed, 1952). Nociceptive information is received in lamina I, lamina II (substantia gelatinosa; Figure 12, A and B), and, to a lesser extent, lamina V (Peirs and Seal, 2016; Todd, 2010; West *et al.*, 2015; Zeilhofer *et al.*, 2012). Although lamina I contains interneurons for modulation and projection neurons for transmission of nociceptive information, lamina II contains mainly interneurons that project to lamina I. In spite of its importance, there is still very much that is unknown about dorsal horn circuitry and how it relates to the pathophysiology of chronic pain (Peirs and Seal, 2016; Prescott *et al.*, 2014; Sandkühler, 2009; Todd, 2010).

Current treatments (opioids, non-steroidal anti-inflammatory drugs, antidepressants or anticonvulsants) are frequently inadequate or associated with adverse side (Di Cesare Mannelli *et al.*, 2015; Goldberg and McGee, 2011; Pizzo and Clark, 2012). Therefore, new therapeutics for managing patient pain are being developed.

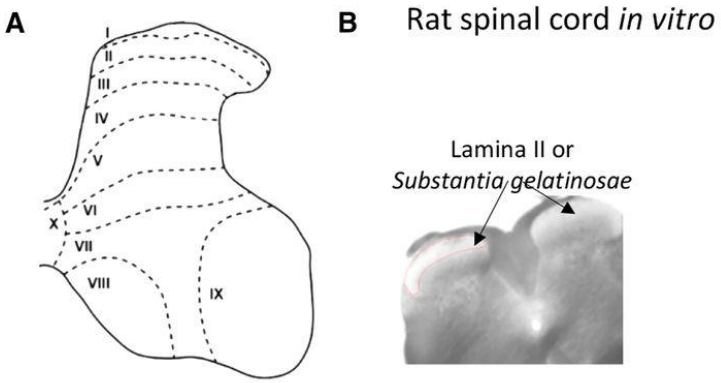

Figure 12: (A) Rexed laminae of the spinal cord. Laminae I and II form the marginal zone and substantia gelatinosa, respectively, and together these make up the superficial dorsal horn. Within the dorsal horn, Aβ tactile and hair afferents end mainly in laminae III–VI with some extension into lamina IIi with distribution dependent on function. Aδ hair-follicle afferents extend across the lamina II/III border. Aδ nociceptors end

mainly in lamina I, occasionally branching to laminae V and X. Peptidergic, nociceptive C fiber afferents synapse mainly in lamina I and IIo. Nonpeptidergic C fibers occupy the inner part of lamina II. (B) Acutely isolated spinal cord slice from a 30-day-old rat. The substantia gelatinosa is clearly visible as a translucent band under infrared differential interference contrast optics (Taken from: Peirs and Seal, 2016).

7.1 Role of Calcium and Potassium Channels

Voltage-operated Ca^{2+} channels (VOCCs) are crucial mediators of neuropathic pain, as confirmed by the fact that α2δ ligands, i.e. gabapentinoids, are a first-line treatment in this pathology (Field *et al.,* 2007; Vink and Alewood, 2012). Activation of VOCCs at a pre-synaptic level induces neurotransmitter release through the peripheral and CNS, including sensory neurons in dorsal root ganglia (DRG), which are considered the primary station of nociceptive transmission. It is noteworthy that dorsal root stimulus-evoked excitatory post-synaptic currents in lamina I dorsal horn neurons are inhibited by 60% by the selective N-type VOCC blocker ω-conotoxin GIVA (ω-CTX) (Heinke *et al.,* 2004) suggesting that these channels express a primary role in mediating neurotransmitter release during nociception. Furthermore, aberrant expression and/or activity of N-type VOCCs is associated with neuropathic pain (Hannon and Atchison, 2013) and ziconotide, a derivative of ω-CTX, was FDA approved in 2000 (Prialt™) for intrathecal treatment of severe and refractory chronic pain (Brookes *et al.,* 2017; Jain, 2000; McDowell and Pope, 2016). However, severe adverse effects are associated with direct Ca^{2+} channel block; so a milder modulation of Ca^{2+} influx is needed.

Attenuation of various types of K^+ channel conductance also contributes to the increased excitability of DRG neurons that follows injury or exposure to inflammatory cytokines such as IL-1β (Abdulla and Smith, 2001; Cao *et al.,* 2012; Gonzalez and Rodríguez, 2017; Kim *et al.,* 2002; Stemkowski *et al.,* 2015; Stemkowski and Smith, 2012; Tan *et al.,* 2006; Tsantoulas *et al.,* 2012; Waxman and Zamponi, 2014).

Changes in K^+ channel currents may also contribute to pain associated with diabetic neuropathy (Cao *et al.,* 2010). This prompted the suggestion that the anticonvulsant retigabine (Passmore *et al.,* 2003) and related Kv7.2–Kv7.3 channel openers (Busserolles *et al.,* 2016; Q. Zhang *et al.,* 2013), as well as facilitators of Na^+ activated K^+ channel currents (Huang *et al.,* 2013) or two pore K^+ channels or KV2 or Kv9.1 channels, may be useful in pain management (Tsantoulas *et al.,* 2012; Yekkirala *et al.,* 2017). Unfortunately, a clinical trial with retigabine failed to meet its primary efficacy end point (Yekkirala *et al.,* 2017). The retigabine analog N-(6-chloro-pyridin-3-yl)-3,4-difluoro-benzamide (ICA-27243) has been reported to attenuate inflammatory pain in animal models (Hayashi *et al.,* 2014), but we are unaware of any clinical trials with this substance. Beyond neuropathic pain arising from peripheral nerve injury, it has been reported that injury to the spinal cord *per se* can impede K^+ channel function in DRG (Ritter *et al.,* 2015), and this may contribute to mechanical allodynia. Altered K^+ channel function in DRG may reflect the diffusion of inflammatory mediators from the site of injury within the spinal cord (Carlton *et al.,* 2009).

Changes in K^+ channel function may not always involve changes in expression or properties of pore-forming α subunits themselves but may rather result from changes in regulatory subunits. For

example, it was recently shown that K^+ channel modulatory subunits KChIP1, KChIP2, and DPP10 are coexpressed with Kv4.3 in nonpeptidergic small neurons of the rat DRG. Spinal nerve ligation downregulated all three modulatory subunits, and their knockdown by intrathecal injection of a gene-specific antisense oligodeoxynucleotides evoked mechanical hypersensitivity. Rescue of the downregulated subunits by injection of appropriate cDNA constructs attenuated injury-induced hypersensitivity (Kuo *et al.*, 2017). These findings imply that targeting of regulatory subunits rather than pore-forming subunits of K^+ channels may lead the way to new therapeutic approaches. This is in fact analogous to targeting the α2δ-1 subunit of Ca^{2+} channels by gabapentin to control α subunit function (Dolphin, 2016) and to the suggested targeting of nonconducting β subunits of Na^+ channels (O'Malley and Isom, 2015).

7.2 Pain and Adenosine

Adenosine plays an integral role in CNS processing of pain through its regulation of excitatory neurotransmission, persistent neuronal signalling and regulation of glial activation and proliferation. Accordingly, the ability of adenosine and its analogues to inhibit pain behaviour has been documented in models of various aetiologies, including neuropathic pain associated with spinal cord injury, spinal nerve ligation and in the mustard oil, formalin and carrageenan pain models (Carpenter *et al.*, 2000). Indeed, in the clinical setting, i.t. adenosine administration has been shown to provide sustained relief of chronic neuropathic pain lasting for several h up to months in some patients (Hayashida *et al.*, 2005). Adenosine therapy has also been employed for the prevention of post-operative pain with mixed results: prophylactic i.v. administration of adenosine prior to surgical procedures conferred persistent pain relief in several studies (Gan and Habib, 2007; Hayashida *et al.*, 2005). while another similar clinical trial did not observe a prophylactic effect (Habib *et al.*, 2008). Unfortunately, the i.v. administration of adenosine is associated with undesirable cardiac side effects (Zylka, 2011) that limit its utility and route of administration (e.g. i.t.) in patients. Thus, isolating the antinociceptive qualities of adenosine from its cardiovascular side effects by evaluating receptor involvement has become an important focus for the development of adenosine- based therapeutics in pain.

7.2.1 Role of A_3AR

Adenosine is an endogenous neuromodulator acting on four metabotropic receptors: the Gi-coupled A_1 and A_3ARs and the Gs-coupled A_{2A} and A_{2B} subtypes (Fredholm *et al.*, 2011).

A_1AR activation inhibits pain behaviours in different models of acute or chronic pain (Dib-Hajj *et al.*, 2009). Unfortunately, the therapeutic utility of A_1AR agonists is limited by their adverse cardiovascular effects. Of note, exciting preclinical observations designate the A_3AR as a powerful analgesic mediator in different *in vivo* rodent models of experimental neuropathic pain (Janes *et al.*, 2016; Little *et al.*, 2015), suggesting A_3AR agonists can be used for analgesia treatment without cardiovascular implications.

The idea that the most effective agents in neuropathic pain management likely exert actions through multiple targets has already been alluded to. Adenosine A_3AR agonists represent one such class of agents as they interact with several of the pathophysiological mechanisms outlined above (Janes *et al.,* 2016). A_3AR_S are found on immune cells, astrocytes (Björklund *et al.*, 2008; Janes *et al.,* 2015), microglia (Hammarberg *et al.,* 2003), and both peripheral and central neurons (Janes *et al.,* 2016). The cellular mechanisms mediating pain relief on A_3AR activation remain largely unexplored.

The first definitive characterizations of the A_3AR as antinociceptive resulted from the use of a more specific A_3AR agonist, IB- MECA (N 6- (3- iodobenzyl)- adenosine- 5′- N- methyluronamide): IB- MECA is 50- fold selective for the A_3AR over the A_1 or A_{2A}AR, as compared with the 14- fold selectivity of N 6- benzyl–NECA (Gallo-Rodriguez *et al.,* 1994; Jacobson, 1998).

In 2005, a study demonstrated that systemically administered IB- MECA exerts a significant antinociceptive effect during the second phase of the formalin test without altering protective nociceptive responses (i.e. response to noxious thermal or mechanical stimuli) (Yoon *et al.,* 2005). i.t. administration of an A_3AR antagonist (MRS1220) prevented the antinociceptive actions of adenosine in the second phase of the formalin test, supporting a role for spinal A_3AR_S in the effect of adenosine (Yoon *et al.,* 2006).

A_3AR-selective ligands available nowadays allow for the dissection of A_3AR-based molecular effects on DRG neuronal excitability (Janes *et al.,* 2016); The recently synthetized and highly selective A_3AR agonists MRS5698, and the more water-soluble congener MRS5980, proved reverse allodynia and hyperalgesia associated with traumatic nerve injury, chemotherapy and bone cancer in rodents (Ford *et al.,* 2015; Janes *et al.,* 2014; Little *et al.,* 2015). These second generation, highly selective A_3AR agonists are at least several orders of magnitude more selective than the early generation exemplified by IB-MECA and Cl-IB-MECA (Janes *et al.,* 2014; Little *et al.,* 2015; Tosh *et al.,* 2014).

In addition, the A_3AR agonist MRS5698 attenuates KCC2 downregulation and restores Cl^- gradients in rodent CCI models (Ford *et al.,* 2015), a process that may involve attenuation of BDNF signaling (Janes *et al.,* 2016). A_3AR activation also attenuates neuroinflammatory responses, astrocyte reactivity, and cytokine release (Janes *et al.,* 2016, 2015). Because cardiovascular actions of adenosine are mediated via A_1 and A_2 adrenoceptors (Sawynok, 2016), A_3 agonists show considerable promise as therapeutic agents (Janes *et al.,* 2016).

Due to the recent emergence of the A_3AR as a valid target for pain relief, much remains to be explored regarding the specific mechanisms of action downstream of receptor activation. To date, it is known that in the CCI model of neuropathic pain, the effects of A_3AR agonists are mediated independently of the opioidergic and cannabinoid systems, but do act supraspinally to recruit the activation of 5-hydroxytryptaminergic and noradrenergic bulbospinal circuits, and reduce the excitability of wide dynamic range spinal neurons (Little *et al.,* 2015). The A_3AR activation in other disease states alters processes involved in the development of central sensitization and pain, including protein kinase activity, glutamatergic neurotransmission, ion conductance and neuroinflammation (Figure 13).

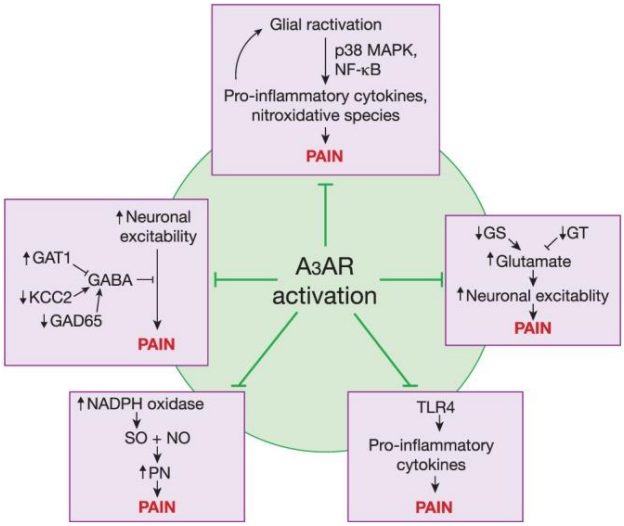

Figure 13: Potential mechanisms of A_3AR- mediated antinociception. Several pathways are known to be important in the establishment of pain states including impairment of GABAergic neurotransmission, enhanced neuroinflammation characterized by increased glial hyperactivation and TLR4 signalling, increased glutamatergic signalling and heightened production of nitroxidative species. The A_3AR has been shown to modulate these pathways through the use of selective agonists, potentially explaining A_3AR antinociceptive actions**.** (Taken from: Janes *et al.*, 2016).

AIM OF THE STUDY

AIM OF THE STUDY

Chapter 1

1. Role of A_{2B}AR under oxygen and glucose deprivation

We investigated the role of A_{2B}AR during OGD in the CA1 region of rat hippocampus, the most susceptible hippocampal area to an ischemic insult. For this purpose two selective A_{2B}AR antagonists were used: PSB603 and MRS1754. In order to characterize the OGD-induced cell injury and putative pharmacological protection, we conducted extracellular recordings of CA1 field excitatory post-synaptic potentials (fEPSPs) before, during and after a severe (7 min or 30 min) simil ischemic insult in the absence or presence of these compounds.

A severe OGD episode bring about irreversible depression of neurotransmission and the appearance of anoxic depolarization (AD) (Frenguelli *et al.*, 2007; Pugliese *et al.*, 2007). AD is a severe neuronal depolarization, which triggers a variety of molecular events and represents an unequivocal sign of neuronal injury (Somjen, 2001). In the present research, we investigated the role of A_{2B}ARs in AD appearance and irreversible synaptic failure during severe OGD in the CA1 hippocampus *in vitro*.

Chapter 2

2. *Role of A_{2B}AR on CA1 hippocampal transmission and paired pulse facilitation*

Little is known about A_{2B}AR effects in the CNS, where they are uniformly, although scarcely, expressed (Dixon *et al.*, 1996; Perez-Buira *et al.*, 2007). Gonçalves and co-workers (2015) provided direct evidence for the presence of A_{2B}AR in presynaptic glutamatergic terminals of the hippocampus. In this brain area, the A_{2B}AR subtype decreases the phenomenon of PPF by reducing A_1AR activation as proved by the blockade of this effect in the presence of the A_1AR antagonist DPCPX (Gonçalves *et al.*, 2015). The A_{2B}AR decrease of PPF is shared by A_{2A}AR, which, facilitating glutamate release, decreases CA1 PPF (Lopes *et al.*, 2002). PPF is a model of short-term synaptic plasticity which allows investigation into the site of action for a given compound (Regehr, 2012). Most of PPF works have been performed in the hippocampus, in particular at Schaffer collateral-CA1 synapses, where it is known that a reduction in PPF reflects an increase of pre-synaptic glutamate release and vice versa. In accordance, adenosine potently increases PPF through the activation of A_1AR, known to inhibit glutamate release (Fernández-Fernández *et al.*, 2015). In the present research we confirmed the effect of the prototypical A_{2B}AR agonist BAY606583 and we provide the first characterization of the effects of two newly synthesized A_{2B}AR agonists, P453 and P517, on PPF in the CA1 area of the rat hippocampus. Our results confirm that A_{2B}AR activation reduces PPF in an A_1AR-dependent manner, thus corroborating the facilitatory role of A_{2B}AR stimulation in glutamate release at presynaptic level in this brain area.

Chapter 3

3. Role of A_{2B}AR on cell differentiation in cultured OPC_S by modulating SphK1 signaling pathway.

In vitro studies on OPC cultures demonstrate that adenosine, by stimulating A_1AR, promotes OPC maturation (Stevens *et al.,* 2002) and migration (Othman *et al.,* 2003). Our group contributed to depict the role of purinergic signaling in oligodendrogliogenesis by demonstrating that selective A_{2A}AR activation in cultured OPCs prevents oligodendrocyte maturation by inhibiting I_K currents (Coppi *et al.,* 2013a), whereas the activation of the Gi coupled purinergic P2Y-like receptor GPR17 by its agonist UDP-glucose increases I_K currents and, hence, promotes OPC differentiation (Coppi *et al.,* 2013b). To date, no evidence exists concerning the functional role of A_{2B}AR in OPC cells. The bioactive lipid mediator S1P has recently gained attention in myelination within the CNS since its receptors ($S1P_{1-5}$) are found in oligodendroglial cells, where they regulate a number of processes, ranging from cell proliferation and maturation to dendrite elongation (Yu *et al.* 2004; Jaillard *et al.,* 2005; Jung *et al.,* 2007; Miron *et al.,* 2008). In particular, mature OLG express $S1P_5$ and at lesser extent $S1P_1$, $S1P_2$ and $S1P_3$, whereas OPC express at a higher level $S1P_1$ than $S1P_2$, $S1P_3$ and $S1P_5$. From these evidences, it appears that both adenosine receptors and SphK/S1P signaling are key regulators of oligodendrocyte development. Since these two signaling pathways have been shown to interact in a different cell system (i.e. human erythrocytes) (Sun *et al*., 2015) we hypothesized that this could be the case also in oligodendroglial cells. Thus, the aim of the present study was to unveil the still unknown functional role of A_{2B}AR activation in cultured OPCs and a possible cross-talk of this purinergic receptor subtype with the SphK/S1P signaling pathway. We thus investigated the effects of A_{2B}AR ligands and SphK/S1P modulators on: i) outward K^+ currents and ii) myelin basic protein (Mbp) and myelin-associated glycoprotein (MAG) expression at different times in culture.

Chapter 4

4. Role of A_3AR on dorsal root ganglia excitability

Pain control is a vast, unmet medical need with a high societal cost impact (Goldberg *et al.,* 2011). Current treatments (opioids, non-steroidal anti-inflammatory drugs, antidepressants or anticonvulsants) are frequently inadequate or associated with adverse side effects (Mannelli *et al.,* 2015; Pizzo *et al.,* 2012). Therefore, new therapeutics for managing patient pain are being developed. In recent years, there have been further significant developments that enhance an understanding of the role of adenosine in nociception (Sawynok, 2016).

It's known that A_1AR activation inhibits pain behaviours in different models of acute or chronic pain (Dickenson *et al.,* 2000). Unfortunately, the therapeutic utility of A_1AR agonists is limited by their adverse cardiovascular effects. Of note, exciting preclinical observations designate the A_3AR as a

powerful analgesic mediator in different *in vivo* rodent models of experimental neuropathic pain (Janes *et al.*, 2016; Little *et al.*, 2015), suggesting A_3AR agonists can be used for analgesia treatment without cardiovascular implications. The cellular mechanisms mediating pain relief on A_3AR activation remain largely unexplored.

In order to elucidate the cellular mechanisms of A_3AR-mediated analgesic effect, in this study, we investigated the expression and functional effects of A_3AR on the excitability of small-sized, capsaicin-sensitive, dorsal root ganglion (DRG) neurons isolated from 3-4 week-old rats and whether the A_3AR modulates membrane currents and excitability in these cells.

MATERIALS AND METHODS

MATERIALS AND METHODS

Chapters 1 and 2

1. Animals

All animal procedures were conducted according to the Italian Guidelines for Animal Care, DL 116⁄92, application of the European Communities Council Directive (86⁄609⁄EEC) and approved by the Committee for Animal Care and Experimental Use of the University of Florence. Male Wistar rats (150-200 g body weight) were obtained from Harlan Italy.

2. Extracellular recordings

2.1 Acute rat hippocampal slices preparation

Experiments were carried out on acute hippocampal slices (Pugliese *et al.,* 2006), prepared from Male Wistar rats (Harlan Italy; Udine Italy). Animals were killed with a guillotine under anesthesia with ether and their hippocampi were rapidly removed and placed in ice-cold oxygenated (95% O2 - 5% CO2) aCSF of the following composition (mM): NaCl 125, KCl 3, NaH_2PO4 1.25, $MgSO_4$ 1, $CaCl_2$ 2, $NaHCO_3$ 25 and D-glucose 10. Slices of hippocampi (400 μm thick) were cut using a McIlwain tissue chopper (The Mickle Lab. Engineering, Co. Ltd., Gomshall, U.K.) and kept in oxygenated aCSF for at least 1 hour at room temperature. A single slice was then placed on a nylon mesh, completely submerged in a small chamber (0.8 ml) and superfused with oxygenated aCSF (31-32°C) at a constant flow rate of 1.5-1.8 ml min^{-1}. Changes in superfusing solutions (OGD or drugs) reached the preparation in 60 s and this delay was taken into account in our calculations.

2.2 Experimental procedure

Extracellular Recordings: Test pulses (80 ms, 0.066 Hz) were delivered through a bipolar nichrome electrode positioned in the stratum radiatum of the CA1 region of the hippocampus to stimulate the Schaffer collateral-commissural pathway (Figure 14A). Evoked potentials were extracellularly recorded with glass microelectrodes (2–10 MΩ, Harvard Apparatus LTD, United Kingdom) filled with 150 mM NaCl. The recording electrode was placed at the dendritic level of the CA1 region to record field excitatory postsynaptic potentials (fEPSPs) (Figure 14A). Responses were amplified (200, BM 622, Mangoni, Pisa, Italy), digitized (sample rate, 33.33 kHz), and stored for later analysis with LTP (version 2.30D) program (Anderson and Collingridge, 2001).

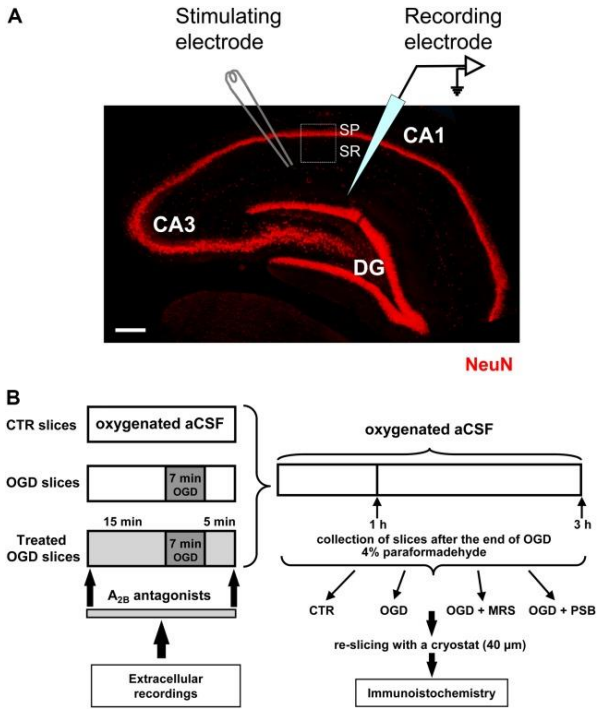

Figure 14: (A) Microphotography of an hippocampal slice showing the three subregions, the localization of the stimulating and recording electrodes and the region of interest (ROI, framed area) for the immunohistochemical analyses. SP, stratum pyramidale; SR, stratum radiatum. Scale bar: 200 µm. (B) Schematic representation of the experimental method.

The amplitude of fEPSP was measured as the difference between the negative peak following the afferent fiber volley and the baseline value preceding the stimulus artifact. In some experiments both the amplitude and the initial slope of fEPSP were quantified, but since no appreciable difference between these two parameters was observed under control conditions, in the presence of drugs or during *in vitro* ischemia, only the measure of the amplitude was expressed in the figures. When a stable baseline of evoked responses was reached, fEPSP amplitudes were routinely measured and expressed as the percentage of the mean value recorded 5 min before the application of any treatment (in particular pre-OGD). Stimulus-response curves were obtained by gradual increase in stimulus strength at the beginning of each experiment. The test stimulus strength was then adjusted to produce a response whose amplitude was 40% of the maximum and was kept constant throughout the experiment. Simultaneously, with fEPSP amplitude, AD was recorded as negative extracellular direct current (d.c.) shifts induced by OGD. The d.c. potential is an extracellular recording considered to provide an index of the polarization of cells surrounding the tip of the glass electrode (Farkas *et al.*, 2008). AD latency, expressed in min, was calculated from the beginning of OGD; AD amplitude, expressed in mV, was calculated at the maximal negativity peak. In the text and bar graphs, AD amplitude values were expressed as positive values. The terms "irreversible synaptic failure" or "irreversible loss of synaptic transmission" used in the present work refer to the maximal time window of cell viability in our experimental model (acutely isolated hippocampal slice preparation) which, according to our previous results is 24 h (Pugliese *et al.*, 2009).

2.2.1 Application of OGD and A_{2B}AR Antagonists

The experimental method is shown in Figure 14B. Conditions of OGD were obtained by superfusing the slice with aCSF without glucose and gassed with nitrogen (95% N_2–5% CO_2) (Pedata *et al.,* 1993). This causes a drop in pO2 in the recording chamber from 500 mmHg (normoxia) to a range of 35–75 mmHg (after 7 min OGD) (Pugliese *et al.,* 2003). At the end of the ischemic period, the slice was again superfused with normal, glucose-containing, oxygenated aCSF. The terms 'OGD slices' or 'treated OGD slices' refer to hippocampal slices in which OGD was applied in the absence or in the presence of A_{2B}AR antagonists, respectively. Control slices were not subjected to OGD or treatment with A_{2B}AR antagonists but were incubated in oxygenated aCSF for identical time intervals. All the selective A_{2B}AR antagonists were applied 15 min before, during and 5 min after OGD. In a typical experimental day, first a control slice was subjected to 7 min of OGD. If the recovery of fEPSP amplitude after 60 min of reperfusion with glucose containing and normally oxygenated aCSF was 15% of the pre-OGD value, and AD developed into 7 min OGD, a second slice from the same rat was subjected to an OGD insult in the presence of the A_{2B}AR antagonist under investigation. To confirm the result obtained in the treated group, a third slice was taken from the same rat and another 7 min OGD was performed under control conditions to verify that no difference between slices was caused by the time gap between the experiments. In some slices the OGD period was prolonged to 30 min and the A_{2B}AR antagonists were applied 15 min before and during OGD application. After the extracellular recordings, slices were maintained in separate chambers for 1 or 3 h from the end of OGD in oxygenated aCSF at room temperature (RT). At the end, slices were harvested and fixed overnight at 4 C in 4% paraformaldehyde in PBS, cryopreserved in 18% sucrose for 48 h, and resliced as written below.

2.2.2 OGD conditions

Conditions of OGD were obtained by superfusing the slice with aCSF without glucose and gassed with nitrogen (95% N_2–5% CO_2) (Pedata *et al.,* 1993). This caused a drop in pO_2 in the recording chamber from ~500 mmHg (normoxia) to a range of 35–75 mmHg (after 7 min OGD) (Pugliese *et al.,* 2003). At the end of the ischemic period, the slice was again superfused with normal, glucose-containing, oxygenated aCSF. Throughout this thesis, the terms 'untreated OGD slices' or 'treated OGD slices' refer to hippocampal slices in which OGD episodes of different duration were applied in the absence or in the presence of drugs, respectively. Control slices were not subjected to OGD or drug treatment, but were superfused in oxygenated aCSF for identical time intervals.

2.2.3 Paired pulse facilitation protocols

To elicit PPF of fEPSP, we stimulated the Schaffer collateral-commissural fibers twice with a 40-ms interpulse interval. Double stimulation was evoked once every 15 s. The synaptic facilitation was quantified as the ratio (P2/P1) between the slope of the fEPSP elicited by the second (P2) and the first (P1) stimuli.

Test pulses (80 µs, 0.066 Hz) were delivered through a bipolar nichrome electrode positioned in the stratum radiatum of the CA1 region of the hippocampus to stimulate the Schaffer collateral-commissural pathway (Figure 15A). Evoked potentials were extracellularly recorded with glass microelectrodes (2–10 MΩ, Harvard Apparatus LTD, United Kingdom) filled with 150 mM NaCl. The recording electrode was placed at the dendritic level of the CA1 region to record field excitatory postsynaptic potentials (fEPSPs) (Figure 15A). Responses were amplified (200×, BM 622, Mangoni, Pisa, Italy), digitized (sample rate, 33.33 kHz), and stored for later analysis with LTP (version 2.30D) program (Anderson and Collingridge, 2001). Responses were quantified as the initial slope (between 20 and 80% of maximal amplitude) of the fEPSP trace. Input-output curves were obtained by gradual increase in stimulus strength at the beginning of each experiment. The test stimulus strength was then adjusted to produce a response of about 40% of the maximum and was kept constant throughout the experiment.

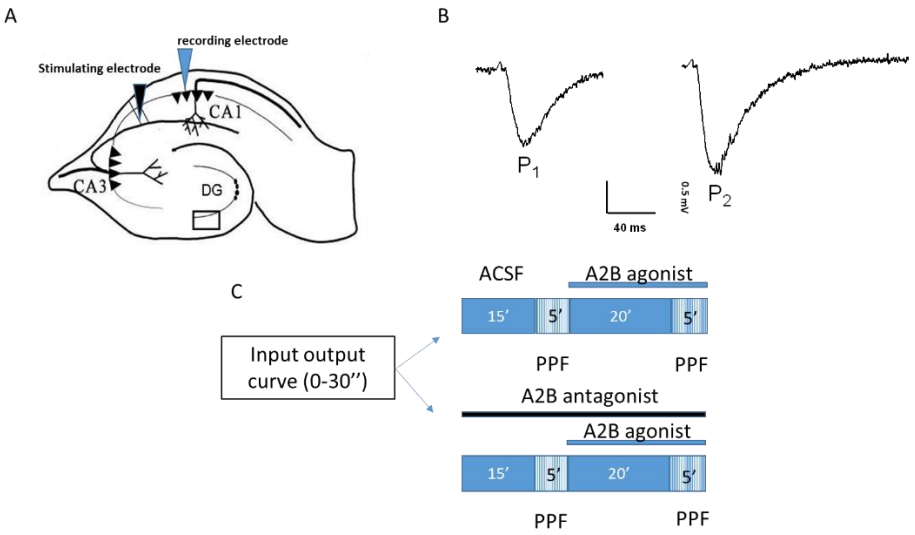

Figure 15: Experimental procedure. (A) Schematic representation of an acute hippocampal slice showing the tri-synaptic circuit and the localization of the stimulating and recording electrodes. (B) Representative trace of fEPSP responses evoked by a paired pulse facilitation (PPF) protocol (40-ms interval) in a typical hippocampal slice. (C) Schematic synthesis of the experimental protocol used to apply the A_{2B}AR agonists alone (upper panel) or in the presence of A_{2B}AR antagonists (lower panel). BSN: basal synaptic neurotransmission.

2.2.4 Treatment of hippocampal slices with glutamate in vitro

Experiments were carried out on acute hippocampal slices, prepared from male Wistar rats as described above. The A_{2B}AR antagonists were dissolved in DMSO to obtain a stock solution suitable for a 1:2000 dilution. Slices, maintained oxygenated throughout the procedure, were incubated according to the following scheme:

- Control slices were incubated for 1 h in aCSF and then for 25 min in aCSF with DMSO (1:2000; 0.05%);

-Glutamate (GLU) treated slices were incubated 1 h in aCSF and then for 10 min with 100 mM glutamate in aCSF;

- MRS+GLU treated slices were incubated for 1 hour in aCSF, then for 15 min with 500 nM MRS1754 and for further 10 min with 500 nM MRS1754 plus 100 mM glutamate, in aCSF;
- PSB+GLU treated slices were incubated for 1 hour in aCSF, then for 15 min with 50 nM PSB603, and for further 15 min with 50 nM PSB603 plus 100 mM glutamate in aCSF; After the incubation with glutamate and A_{2B}AR antagonists, slices were further incubated for 3 h in aCSF, and then harvested and fixed overnight at 4 C in 4% paraformaldehyde in PBS, cryopreserved in 18% sucrose for 48 h, and resliced as written below.

2.2.5 Immunohistochemistry

One hour or 3 hour after OGD, or after the incubation with glutamate and A_{2B}AR antagonists, the 400 µm thick slices fixed in paraformaldehyde were placed on an agar support (6% agar in normal saline), included in an embedding matrix and re-sliced with a cryostat to obtain 40 µm thick slices. The more superficial sections were eliminated, while those obtained from the inner part of the slice were collected and stored in vials with 1 ml of antifreeze solution at -20 C until immunohistochemical analyses. From the 400 µm thick slices on average only a maximum of 2–3 complete 40 µm thick slices were obtained, which were then randomly allocated to the fluorescent immunohistochemical staining groups.

2.2.6 Antibodies Used – Primary Antibodies

Neurons were immunostained with a mouse monoclonal anti-NeuN antibody (1:200, MilliporeSigma, Carlsbad, CA, United States), astrocytes were detected by means of a polyclonal rabbit antibody anti-Glial Fibrillary Acidic Protein (GFAP, 1:500, DakoCytomation, Glostrup, Denmark), Cytochrome C with a mouse monoclonal antibody (1:200, Abcam, Cambridge, United Kingdom). Activated mTOR was detected using a polyclonal rabbit primary antibody raised against phospho- (Ser2448)-mTOR (1:100, Abcam, Cambridge, United Kingdom). Fluorescent secondary antibodies: Alexa Fluor 488 donkey anti rabbit (fluorescence in green, 1:400), Alexa Fluor 555 donkey anti mouse (fluorescence in red, 1:400), Alexa Fluor 635 goat anti-rabbit (fluorescence in far red, 1:400) (all from Life Technologies, Carlsbad, CA, United States). All primary and secondary antibodies were dissolved in Blocking Buffer (BB, 10% Normal Goat Serum, 0.05% NaN3 in PBS-TX). All procedures were carried out with the free-floating method in wells of a 24-well plate (Cerbai *et al.*, 2012; Lana *et al.*, 2013).

Day 1: The sections were washed (3 times, 5 min each) in PBS-0.3% Triton X-100 (PBS-TX), blocked with 500 ml BB for 1 h, at RT under slight agitation and then incubated overnight at 4C with the primary antibody under slight agitation.

Day 2: After washing in PBS-TX (3 times, 5 min each), sections were incubated for 2 h at room temperature in the dark with a solution containing one or two (for double immunostaining) fluorescent secondary antibodies, as appropriate. Sections were washed (3 times, 5 min each) with BB and then with 1 ml of distilled H2O at RT in the dark, mounted on gelatinized microscopy slides,

dried and coverslipped with a mounting medium containing DAPI to counterstain nuclei (Vectashield, Hard set mounting medium with DAPI, Vector Laboratories, Burlingame, CA, United States). Sections were kept refrigerated in the dark until microscopy analyses.

Day 3: Qualitative and quantitative analyses of NeuN positive neurons, CytC and phospho-mTOR positive cell bodies were performed in CA1 stratum pyramidale (SP), while astrocytes, phosphomTOR positive dendrites and microglia were performed in CA1 stratum radiatum (SR) as shown in Figure 14A. Epifluorescence microscopy: sections were observed under an Olympus BX63 microscope equipped with an Olympus DP 50 digital camera (Olympus, Milan, Italy). For quantitative analysis images were acquired at 20magnification with the digital camera.

2.2.7 Confocal Microscopy

Scans were taken at 0.3 mm z-step, keeping constant all the parameters (pinhole, contrast, and brightness), using a LEICA TCS SP5 confocal laser scanning microscope (Leica Microsystems CMS GmbH, Mannheim, Germany). Images were converted to green, or red using ImageJ (freeware provided by National Institute of Health1). The region of interest (ROI) in CA1, containing stratum pyramidalis and stratum radiatum was consistently analyzed in all slices, as shown in Figure 14A (Lana *et al.*, 2014). Quantitative analyses of NeuNC neurons, HDN neurons, LDN neurons, GFAPC astrocytes, CytCC apoptotic neurons and phospho-mTOR positive cell bodies and dendrites were performed blind by two experimenters and results were averaged. Areas were expresses as mm2. Digitized images were transformed into TIFF files and thresholded using ImageJ. Care was taken to maintain the same threshold in all sections within the same experiment. In CA1 pyramidal layer, the area labeled above the set threshold with NeuN or phospho-mTOR was calculated in pixels and expressed as NeuNC pixels/mm^2 or phospho-mTORC pixels/mm^2. HDN neurons, LDN neurons, Cytochrome C-positive (CytCC) apoptotic neurons in CA1 stratum pyramidale and GFAPC astrocytes in CA1 stratum radiatum were counted and were expressed as number of cells/mm^2. In order to evaluate mTOR activation in basal dendrites the length of phospho-mTORC dendrites was measured at three fixed locations, equal in all slices and evenly distributed throughout the CA1 stratum radiatum ROI, and results were averaged.

2.3. Drugs

Two selective A_{2B}AR antagonists, N-(4- Cyanophenyl)-2-[4-(2,3,6,7-tetrahydro-2,6-dioxo-1,3-dip-ropyl- 1H-purin-8-yl)phenoxy]-acetamide) (MRS1754, Figure 21) and 8-[4-[4-(4-Chlorophenzyl) piperazide-1-sulfonyl) phenyl]]-1-propyl xanthine (PSB603, Figure 20) were used. D-2-amino-5-phosphonovalerate, a selective NMDA receptor antagonist was used. All these compounds were purchased from Tocris (Bristol, United Kingdom). The A_1AR antagonist DPCPX (8- cyclopentyl-1,3-dipropylxanthine, Figure 25) was purchased from Sigma-Aldrich (https://www.sigmaaldrich.com). The new A_{2B}AR agonist, P453 was synthetized by the pharmaceutical chemists of our team at the University of Florence (compounds 15 and 9 respectively,

in (Betti *et al.*, 2018) and the chemical structure are shown in Figure 17. We used the prototypical A_{2B}AR agonist 2-[[6-amino-3,5-dicyano-4-[4-(cyclopropylmethoxy)phenyl]-2-pyridinyl]thio]-acetamide (BAY606583, Figure 18), which was purchased by Tocris (Bristol, United Kingdom), as a reference compound for the functional effects of A_{2B}AR activation in our experimental protocol. All drugs were dissolved in dimethyl sulphoxide (DMSO). Stock solutions, of 1000–10.000 times the desired final concentration, were stored at -20 C. The final concentration of DMSO (0.05% and 0.1% in aCSF) used in our experiments did not affect either fEPSP amplitude or the depression of synaptic potentials induced by OGD (data not shown).

2.4 Statistical analysis

Statistical significance was evaluated by Student's paired or unpaired t-tests. Analysis of variance (one-way ANOVA), followed by Newman–Keuls multiple comparison post hoc test was used, as appropriate. *P*-values from both Student's paired and unpaired t-tests are two-tailed.Data were analyzed using software package GraphPad Prism (version 7.0; GraphPad Software, San Diego, CA, United States). All numerical data are expressed as the mean±standard error of the mean (SEM). A value of $P < 0.05$ was considered significant.

MATERIALS AND METHODS

Chapter 3

3. Experimental procedure

3.1 Patch clamp recordings

3.1.1 Cell cultures preparation

Animal experiments were performed according to Directive 2010/63/EU of the European Parliament and of the European Union Council (22 September 2010) and to the Italian Law on Animal Welfare (DL 26/2014). The protocol was approved by the Institutional Animal Care and Use Committee of the University of Florence and by the Italian Ministry of Health. All efforts were made to minimize animal suffering and to use a minimal number of animals needed to produce reliable scientific data. Purified cortical OPC cultures were prepared as described elsewhere (Coppi *et al.*, 2013b). Wistar rat pups (postnatal day 1-2) were killed and cortices removed, mechanically and enzymatically dissociated, suspended in DMEM medium containing 20% fetal bovine serum (FBS), 4 mM L-glutamine, 1 mM Na-pyruvate, 100 U/ml penicillin, 100 U/ml streptomycin (all products are from EuroClone, Milan, Italy), and plated in poly-D-lysin coated T75 flasks (1 flask per animal). After 2-3 days in culture, OPCs growing on top of a confluent monolayer of astrocytes were detached by 5

h of horizontal shaking. Contaminating microglial cells were eliminated by a 1 h pre-shake and by further plating of detached cells on plastic culture dishes for 1 h. OPCs, which do not attach to plastic, were collected by gently washing the dishes and replated onto poly-DL-ornithine-coated (final concentration: 50 µg/ml, Sigma-Aldrich) 13 mm-diameter glass coverslips laid in 24 multi well chambers (l04 cells/well: electrophysiological and immunocytochemical experiments), poly-DL-ornithine-coated 25 mm-diameter glass coverslips laid in 6 multi well chambers (2 x l04 cells/well: Ca^{2+} imaging experiments) or poly-DL-ornithine-coated 6 cm tissue culture dishes (3.5 x 105 cells/dish: western-blot experiments). OPC cultures were maintained in Neurobasal medium (Thermo Fisher Scientific) containing 2% B27, 4 mM L-glutamine, 1 mM Na-pyruvate, 100 U/ml penicillin, 100 U/ml streptomycin, 10 ng/ml platelet derived growth factor (PDGF-BB) and 10 ng/ml basic fibroblast growth factor (bFGF; both grow factors were from PeproTech EC Ltd, London, UK) to promote cell proliferation (proliferating medium: PM).

3.1.2 OPC differentiation

OPCs show a bipolar or tripolar morfology, when grown in a proliferating medium (PM); they were allowed to differentiate to mature oligodendrocytes, by switching to a Neurobasal medium lacking growth factors (differentiating medium: DM) (Figure 16). The day at which cells were switched from PM to DM is indicated as t_0. According to our previous results (Coppi *et al.*, 2013a; Coppi *et al.*, 2013b), cells cultured in DM undergo gradual maturation as demonstrated by the decrease on NG2 expression and the parallel increase in myelin-related proteins such as MAG, Mbp1 and Mbp3 antigens. After 7 days in DM (t_7) the expression of myelin-related proteins reaches steady state levels (no further increase at t_{10} was observed) so the culture is considered to be composed of mature OLs. In order to study the effect of $A_{2B}AR$ and/or SphK/S1P signalling pathway on oligodendroglial maturation, OPCs were grown in DM in the absence or presence of different pharmacological treatments for 7 days (from t_0 to t_7).

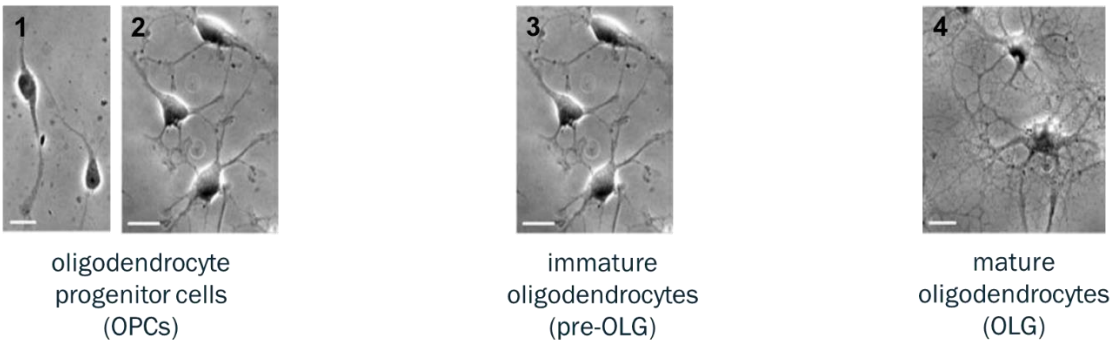

Figure 16: Oligodendrocyte maturation involves a sequences of distinct phases with distinct morphological charateristics. (Taken from: Coppi *et al.*, 2013)

3.1.3 Electrophysiology

Whole-cell patch-clamp recordings were performed on purified primary OPC cultures as described (Coppi *et al.*, 2013a). Cells grown on a poly-DL-ornithine-coated 13 mm-diameter glass coverslip were transferred to a small chamber (1 ml volume) mounted on the platform of an inverted microscope (Olympus CKX41, Milan, Italy) and superfused at a flow rate of 2 ml/min with a standard extracellular solution containing (mM): HEPES 5, D-glucose 10, NaCl 140, KCl 5.4, $MgCl_2$ 1.2, and $CaCl_2$ 1.8 (pH adjusted to 7.3 with NaOH, see Table 3). In all electrophysiological experiments, the following adenosine receptor antagonists were added to the extracellular solution in order to prevent non-specific adenosine receptor activation upon the superfusion with various A_{2B}AR agonists: DPCPX, SCH58261 and MRS1523, all at 100 nM concentration, in order to block A_1, A_{2A} and A_3AR respectively. Borosilicate glass electrodes (Harvard Apparatus, Holliston, Massachusetts USA) were pulled with a Sutter Instruments puller (model P-87) to a final tip resistance of 4–7 MΩ. Standard pipette solution contained (in mM): K-gluconate 130, NaCl 6, $MgCl_2$ 2, Na_2-ATP 2, Na_2-GTP 0.3, EGTA 0.6, HEPES 10 (pH adjusted to 7.4 with KOH). For K^+-replacement experiments a Cs^+-based pipette solution was used (in mM): CsCl 130, NaCl 6, $MgCl_2$ 2, Na_2-ATP 2, Na_2-GTP 0.3, EGTA 0.6, HEPES 10 (pH adjusted to 7.4 with CsOH, see Table 4).

Data were acquired with an Axopatch 200B amplifier (Axon Instruments, CA, USA), low-pass filtered at 10 kHz, stored and analyzed with pClamp 9.2 software (Axon Instruments, CA, USA). All the experiments were carried out at room temperature (RT: 20 –22°C).

Table 3: Extracellular solution

salts	**Concentration (mM)**
HEPES	5
D-glucose	10
NaCl	140
KCl	5.4
$MgCl_2$	1.2
$CaCl_2$	1.8

Table 4: Pipette solutions

Standard pipette solution	**Salts**	**Concentration (mM)**
	K-gluconate	130
	NaCl	6
	$MgCl_2$	2
	Na_2-ATP	2

	Na_2-GTP	0.3
	EGTA	0.6
	HEPES	10
Cs^+-based pipette solution		
	CsCl	130
	NaCl	6
	$MgCl_2$	2
	Na_2-ATP	2
	Na_2-GTP	0.3
	EGTA	0.6
	HEPES	10

3.1.4 Protocols

Unless otherwise stated, cells were voltage-clamped at –70 mV. Series resistance (Rs), membrane resistance (Rm) and membrane capacitance (Cm) were routinely measured by fast hyperpolarizing voltage pulses (from -70 to -75 mV, 40 ms duration). Only cells showing a stable Cm and Rs before, during, and after drug application were included in the analysis. Immediately after breakthrough into whole-cell configuration, cell resting membrane potential (Vrest) was determined by switching to the current-clamp mode. A voltage ramp protocol (800 ms depolarization from -120 to +80 mV) was recorded every 15 s to evoke a wide range of overall voltage-dependent membrane currents before, during and after drug treatments. Variations in membrane potential (Vm) induced by drug treatments were measured by calculating the reversal potential (the "zero current" potential) of ramp-evoked currents before, during and after drug application. Outward K^+ currents were evoked by two different depolarizing voltage-step protocols in order to separate delayed rectifier outward K^+ currents (I_K) from transient outward (I_A) conductances. A first protocol was applied in which 10 depolarizing voltage steps (10 mV steps from –40 to +80 mV, 200 ms each) were preceded by a 60 ms pre-step potential (Vpre) at –80 mV. This protocol activates a mixture of outward I_K and I_A currents in cultured OPCs. Since transient I_A currents present a voltage-dependent inactivation at potential positive to -80 mV, a second protocol was applied in the same cell with a Vpre at -40 mV which selectively inactivates I_A leaving the I_K component unchanged. Net I_A current expressed in each cell was then obtained by digital subtraction of the two traces. Current-to-voltage relationships (I-V plots) of I_K or I_A currents were obtained by measuring current amplitude at the steady state (200-250 ms after step onset) or as a peak (1-20 ms after step onset), respectively.

Current amplitude (measured as pA) was normalized to respective cell capacitance (Cm, measured in pF) and expressed as current density (pA/pF) in averaged results. All drugs were applied by superfusion with a three-way perfusion valve controller (Harvard Apparatus, Holliston, MA USA)

after a stable baseline of ramp-evoked currents was obtained. A complete exchange of bath solution in the recording chamber was achieved within 28 s.

PCR, Western Blot and electrophysiological experiments were run in parallel in order to correlate the current profile with maturation stages of cultured cells.

3.2 Real-Time PCR

Gene expression analysis was performed by Real-Time PCR, using 2^ (-ΔΔCT) comparative method of quantification (Livak et al. 2001). Briefly, total RNA (500 ng), extracted with GenElute™ Mammalian Total RNA Miniprep (Sigma-Aldrich s.r.l. Milan, Italy at http://www.sigma-aldrich.com) was reverse transcribed using iScript™ Advanced cDNA Synthesis Kit for RT-qPCR (Bio-Rad Laboratories S.r.l., Segrate (MI), Italy, at http://www.bio-rad.com/) according to the manufacturer's instructions. The design of MAG, Mbp and A_{2B} probes was performed employing Primer Express® Software v3.0.1 (Thermo Fisher Scientific INC. Monza (MB), Italy, at https://www.thermofisher.com/) that provides customized application-specific documents for absolute and relative quantitation. Rat oligonucleotide primers employed in gene expression studies are listed in Table 5. The quantification of target gene mRNA levels was performed employing PowerUp™ SYBR™ Green Master Mix (Bio-Rad Laboratories S.r.l). Each measurement was carried out in triplicate, using the automated ABI Prism 7500 Sequence Detector System (Thermo Fisher Scientific, INC) as previously described (Donati *et al.*, 2007), by simultaneous amplification of the target gene together with the housekeeping gene (beta-actin and GAPDH) in order to normalize expression data. Results were analysed by ABI Prism Sequence Detection Systems software, version 1.7 (Applied Biosystems, Foster City, CA). The 2^(−ΔΔCT) method was applied as a comparative method of quantification (2) and data were normalized to beta-actin expression.

Table 5. Sequences of rat oligonucleotide primers employed in gene expression studies.

Oligo Name	**Sequence 5' to 3' (include modification codes if applicable)**
Mag-FW	TTCCGAATCTCTGGAGCACCTGATAAG
Mag-RV	TCCTCACTTGACTCGGATTTCTGCGT
Actb-FW	GAACACGGCATTGTCACCAACTGGGA
Actb-RV	GCCTGGATGGCTACGTACATGGCT
Mbp1-FW	GCCCTCTGCCTTCTCATGCCC
Mbp1-RV	CCTCGGCCCCCCAGCTAAATCT
ADORA2B-FW	GTGGGAGCCTCGAGTGCTTTACAG
ADORA2B-RV	GCCAAGAGGCTAAAGATGGAGCTCTG

3.3 Western blot analysis

Primary rat cortical OPC culture were collected after 10 µM BAY606583 challenge for 10 min and lysed in a buffer containing 50 mM Tris, pH 7.5, 120 mM NaCl, 1mM EDTA, 6 mM EGTA, 15 mM

$Na_4P_2O_7$, 20 mM NaF, 1% Nonidet and protease inhibitor cocktail for 30 min at 4°C. Then lysates were centrifuged at 10.000xg, 15 min 4°C, supernatant collected for protein quantification and 15 µg of protein from total cell lysates were used to perform a SDS-polyacrylamide gel electrophoresis and Western blot (WB) analysis. The rate of phosphorylation of SphK1 and SphK2 was measured using the Sphingosine kinase activation antibody sampler kit (ECM Biosiences ECM Biosciences, Versailles, KY USA at https://www.ecmbiosciences.com/index.php?content=Contact. PDVF membranes were incubated overnight with the primary antibodies at 4°C and then with specific secondary antibodies for 1 h at room temperature. Binding of the antibodies with the specific proteins has been detected by chemiluminescence, employing Amersham imager 600.

3.4 Drugs

2-[[6-Amino-3,5-dicyano-4-[4-(cyclopropylmethoxy)phenyl]-2-pyridinyl]thio]-acetamide (BAY606583, Figure 18); 8-cyclopentyl-1,3-dipropylxanthine (DPCPX, Figure 25); 3-propyl-6-ethyl-5-[(ethylthio)carbonyl]-2 phenyl-4-propyl-3-pyridine carboxylate (MRS1523, Figure 23); 2-(2-furanyl)-7-(2-phenylethyl)-7H-pyrazolo[4,3-e][1,2,4]triazolo[1,5-c]pyrimidin-5-amine (SCH58261, Figure 24); 8-(4-(4-(4-chlorophenyl)piperazide-1-sulfonyl)phenyl)-1-propylxanthine, 8-[4-[[4-(4-Chlorophenyl)-1-piperazinyl]sulfonyl]phenyl]-3,9-dihydro-1-propyl-1H-purine-2,6-dione (PSB603, Figure 20); N-(4-cyanophenyl)-2-[4-(2,3,6,7-tetrahydro-2,6-dioxo-1,3-dipropyl-1H-purin-8-yl)phenoxy]-acetamide (MRS1754, Figure 21); amidine analogues that inhibits sphingosine kinase, VPC96047 and VPC96091 (Figures 27, 28), were kindly provided by Prof. K. Lynch (University of Virginia); FTY720 (S)-Phosphate (Figure 26) was provided by Cayman Chemical, (Michigan USAhttps://www.caymanchem.com/); tetraethyl ammonium (TEA, Figure 35) and 4-amino-pyridine (4-AP) were purchased from Sigma-Aldrich (www.sigmaaldrich.com). N-(4-cyanophenyl)-2-[4-(2,3,6,7-tetrahydro-2,6-dioxo-1,3-dipropyl-1H-purin-8-yl)phenoxy]-acetamide (MRS1754, Figure 21) and N-(4-acetylphenyl)-2-[4-(2,3,6,7-tetrahydro-2,6-dioxo-1,3-dipropyl-1H-purin-8-yl)phenoxy]acetamide (MRS1706, Figure 22) were purchased from Tocris (www.tocris.com). Tetrodotoxin (TTX, Figure 33) was purchased from Alomone labs. The new, highly selective, A_{2B}AR agonists P453 (2-{[(1H-imidazol-2-yl)methyl]thio}-6-amino-4-[4-(cyclopropylmethoxy)phenyl]pyridine-3,5-dicarbonitrile) and P517 (2-{[6-amino-3,5-dicyano-4-(4-(cyclopropylmethoxy)phenyl)pyridin-2-yl]thio}-N-methylacetamide). were synthesized are previously reported and showed in Figure 17 (Betti *et al.*, 2018). All drugs were stored at -20°C as 10^3 to 10^4 times more concentrated stock solutions and dissolved daily in the extracellular solution to the final concentration and applied by bath superfusion. TTX, apamin and TEA stock solutions were prepared in distilled water. All other compounds were dissolved in dimethylsulphoxide (DMSO). Control experiments performed in the present research demonstrated that the maximal DMSO concentration used in the present work (0.1%) was inactive in modulating membrane currents (see Figure 61C) in our experimental conditions in DRG neurons.

3.4.1 Chemical structure of drugs

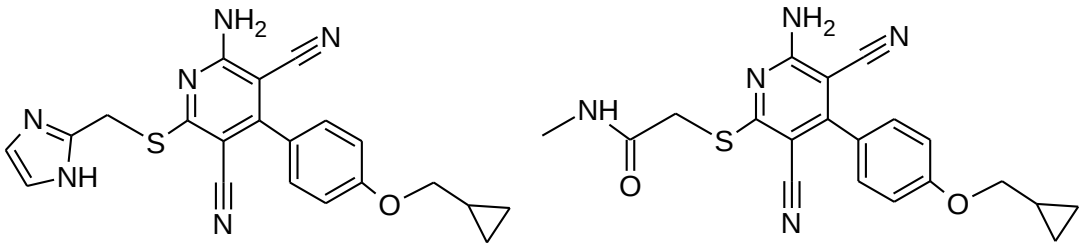

Figure 17: the non-adenosine like A_{2B}AR agonists, **P453:** (2-{[(1H-imidazol-2-yl)methyl]thio}-6-amino-4-[4-(cyclopropylmethoxy)phenyl]pyridine-3,5-dicarbonitrile) and **P517:** (2-{[6-amino-3,5-dicyano-4-(4-(cyclopropylmethoxy)phenyl)pyridin-2-yl]thio}-N-methylacetamide).

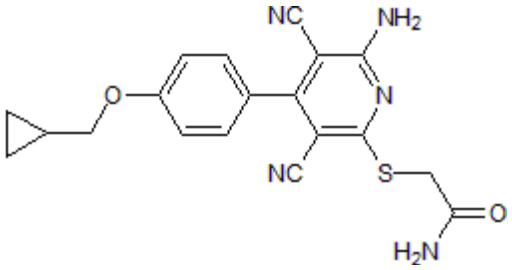

Figure 18: BAY606583: 2- [[6- Amino- 3,5- dicyano- 4- [4- (cyclopropylmethoxy) phenyl] - 2- pyridinyl] thio] – acetamide. Potent A_{2B}AR agonist (Tocris Biosciences, Bristol, UK).

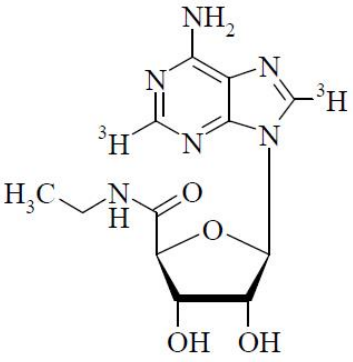

Figure 19: NECA: 5′-(N-Ethylcarboxamido)adenosine. An unselective AR_S agonist (Sigma-Aldrich).

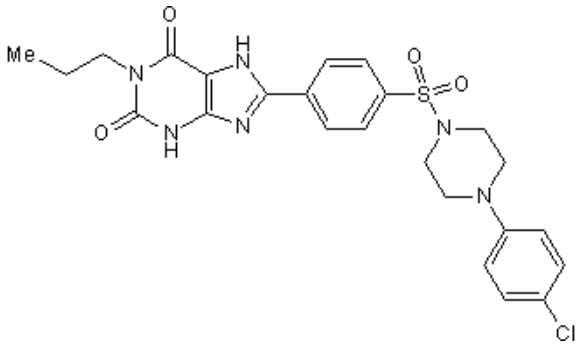

Figure 20: PSB603: 8-[4-[4-(4-Chlorophenzyl) piperazide-1-sulfonyl) phenyl]] -1-propylxanthine. Selective A_{2B}AR antagonist (Tocris Biosciences, Bristol, UK).

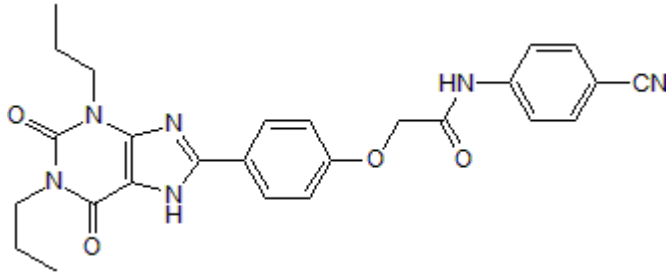

Figure 21: MRS1754: N-(4-Cyanophenyl) -2-[4-(2,3,6,7-tetrahydro-2,6-dioxo- 1,3-dipropyl-1H-purin-8-yl) phenoxy] -acetamide. Selective A_{2B}AR antagonist (Tocris Biosciences, Bristol, UK).

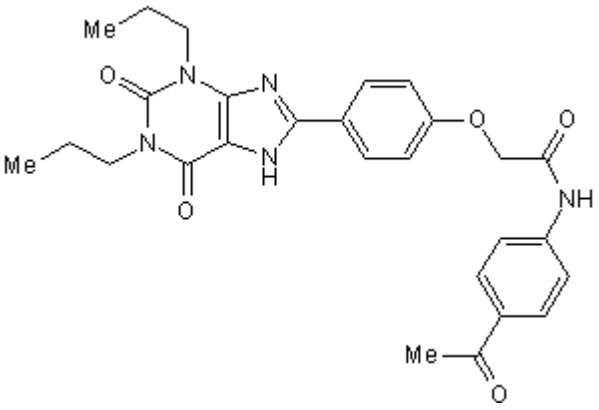

Figure 22: MRS1706: N-(4-Acetylphenyl)-2-[4-(2,3,6,7-tetrahydro-2,6-dioxo-1,3-dipropyl-1H-purin-8-yl)phenoxy]acetamide. Potent and selective A_{2B}AR agonist (Tocris Biosciences, Bristol, UK).

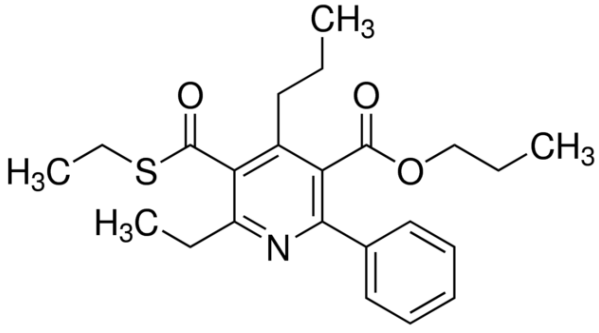

Figure 23: MRS1523: 3-Propyl-6-ethyl-5-[(ethylthio)carbonyl]-2 phenyl-4-propyl-3-pyridine carboxylate. Selective A_3AR antagonist (Sigma-Aldrich).

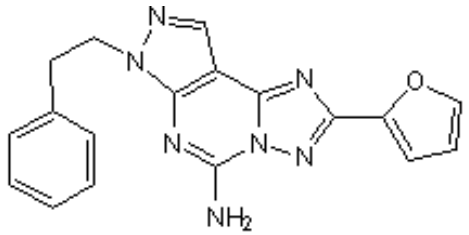

Figure 24: SCH58261: 2-(2-Furanyl) -7-(2-phenylethyl) -7H-pyrazolo [4,3e] [1,2,4] triazolo[1,5-c] pyrimidin-5-amine. Selective A_{2A}AR antagonist (Tocris Biosciences, Bristol, UK).

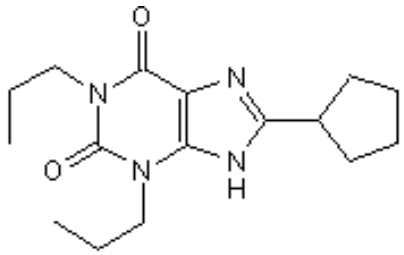

Figure 25: DPCPX: 8-Cyclopentyl-1,3-dipropylxanthine. Selective A_1AR antagonist (Tocris Biosciences, Bristol, UK).

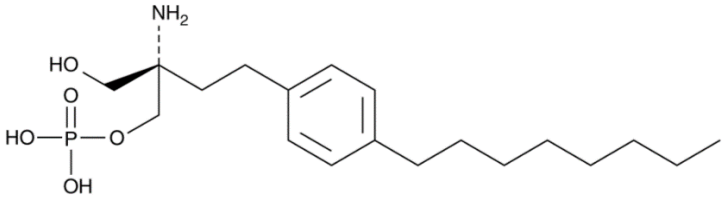

Figure 26: FTY720-P: (2S)-amino-2-[2-(4-octylphenyl)ethyl]-1-(dihydrogen phosphate)-1,3-propanediol. (Cayman Chemical, Michigan, USA).

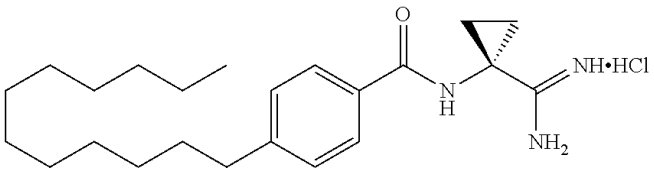

Figure 27: VPC96047: an aspecific inhibitor of the two isoforms SphK1 e SphK2.

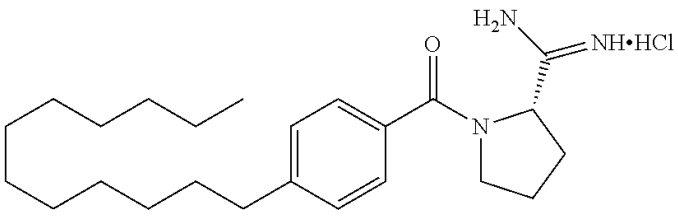

Figure 28: VPC96091: a selective inhibitor of SphK1.

3.5 Statistical analysis

Data are expressed as mean ± SEM (standard error of the mean). Student's paired or unpaired t-tests or One-way ANOVA followed by Bonferroni's post-hoc test analysis were performed, as appropriate, in order to determine statistical significance (set at $P<0.05$). Data were analysed using software package GRAPHPAD PRISM (GraphPad Software, San Diego, CA, USA).

MATERIALS AND METHODS

Chapter 4

4. Experimental procedure

4.1 Patch Clamp recordings

4.1.1 Cell cultures

Animal experiments were performed according to Directive 2010/63/EU of the European Parliament and of the European Union Council (22 September 2010) and to the Italian Law on Animal Welfare (DL 26/2014). The protocol was approved by the Institutional Animal Care and Use Committee of the University of Florence and by the Italian Ministry of Health. All efforts were made to minimize animal suffering and to use a minimal number of animals needed to produce reliable scientific data. Sprague Dawley rats (3-4 weeks old, Envigo, Italy) of both sexes were housed in a temperature- and humidity-controlled plastic cages (12 h dark/light cycle, free access to food and water) and sacrified by cervical dislocation. Primary DRG neurons were isolated and cultured as described (Fusi *et al.*, 2014; Nassini *et al.*, 2015). Briefly, ganglia were bilaterally excised and enzymatically digested using 2 mg/ml of collagenase type 1A and 1 mg/ml of trypsin (both compounds from Sigma-Aldrich) in Hank's Balanced Salt Solution (HBSS) (25–35 min at 37 °C). Cells were then pelleted and resuspended in Dulbecco's Modified Eagle's Medium (DMEM) supplemented by 10% heat inactivated horse serum containing 10% heat-inactivated fetal bovine serum (FBS), 100 U/ml penicillin, 0.1 mg/ml streptomycin and 2 mM L-glutamine for mechanical digestion. After centrifugation (1200 x g, 5 min), neurons were suspended in the above medium, enriched with 100 ng/ml mouse-NGF and 2.5 mM cytosine-β-D-arabino-furanoside free base, and then plated on 13 mm glass coverslips coated by poly-L-lysine (8.3 mM) and laminin (5 mM). DRG neurons were cultured for 1–2 days before being used for experiments.

4.1.2 Electrophysiology

Whole-cell patch-clamp recordings were performed in -60 mV clamped-cells as previously described (Coppi *et al.*, 2013; Coppi *et al.*, 2012). The following solutions were used: standard K^+-based extracellular solution (mM): NaCl 147; KCl 4; $MgCl_2$ 1; $CaCl_2$ 2; HEPES (4-(2-hydroxyethyl)-1-piperazineethanesulfonic acid) 10; D-glucose 10 (pH 7.4 with NaOH). Standard K^+-based pipette

solution (mM): K-gluconate 130; NaCl 4.8; KCl 10; $MgCl_2$ 2; $CaCl_2$ 1; Na_2-ATP 2; Na_2-GTP 0.3; EGTA 3; HEPES 10 (pH 7.4 with KOH). For K^+-replacement experiments, extracellular K^+ was substituted by equimolar Cs^+ and the pipette solution used was (mM): CsCl 120; Mg_2-ATP 3; EGTA 10; HEPES 10 (pH adjusted to 7.4 with CsOH). Ca^{2+} currents were isolated by using Cs^+-based pipette solution and by adding 1 µM tetrodotoxin (TTX), 200 nM A887826 to a 5 mM Ca^{2+}-containing extracellular solution in order to block TTX-sensitive and TTX-insensitive Na^+ channels, respectively. As reported in Results and in Figure 4E-F, ramp experiments in Cs^+-replacement conditions revealed that Cl-IB-MECA-inhibited Ca^{2+} currents in DRG neurons are completely prevented in the presence of extracellular Cd^{2+}. So, when studying the effect of this compound on Ca^{2+} currents evoked in isolation, 100 µM Ni^{2+} was added to the extracellular solution in order to exclude T-type Ca^{2+} channels, which do not seem to be involved in A_3AR-mediated effect. For this reason, the hypothetical, additional, involvement of T-type Ca^{2+} channels in A_3AR-mediated Ca^{2+} channel modulation is not investigated in the present research and will be addressed in a separate work.

Cells were transferred to a 1 ml recording chamber mounted on the platform of an inverted microscope (Olympus CKX41, Milan, Italy) and superfused at a flow rate of 2 ml/min by a three-way perfusion valve controller (Harvard Apparatus). Borosilicate glass electrodes (Harvard Apparatus, Holliston, MA) were pulled with a Sutter Instruments puller (model P-87) to a final tip resistance of 1–3 MΩ. Data were acquired with an Axopatch 200B amplifier (Axon Instruments, CA), low-pass filtered at 10 kHz, stored and analysed with pClamp 9.2 software (Axon Instruments, CA). All the experiments were carried out at room temperature (RT: 20–22°C). Series resistance (Rs), membrane resistance (Rm), and membrane capacitance (Cm) were routinely measured by fast hyperpolarizing voltage pulses (from -60 to -70 mV, 40 ms duration). Only cells showing a stable Cm and Rs before, during, and after drug application were included in the analysis. Immediately after seal breaking-through, cell resting membrane potential was determined by switching the amplifier to the current-clamp mode. A voltage ramp protocol (800 ms depolarization from -120 to +80 mV) was used to evoke a wide range of overall voltage-dependent currents before, during, and after drug treatments. VOCCs currents were evoked in Cs^+-replacement conditions by a 0 mV step depolarization (200 ms) once every 30 s to minimize Ca^{2+} current run down. The current-to-voltage relationship of the Ca^{2+} currents was obtained by eliciting 10 depolarizing voltage steps (200 ms duration, 10 mV increments, 5 s interval) from -50 to +50 mV starting from a holding potential (Vh) of -65 mV. Averaged currents were normalized to cell capacitance and expressed as pA/pF. Cell capacitance was used to estimate neuronal diameter by assuming an approximated spherical cell shape accordingly to Hille (Hille, 2001).

Current-clamp recordings were performed as described (Coppi *et al.*, 2012). A ramp current protocol consisting in 1 s injection of 30 pA positive current from the resting membrane potential (only cells showing a Vm of at least -50 mV were chosen) was used to evoke action potential (AP) firing in a

typical DRG neuron once every 15 sec. After at least 3 min recording of a stable baseline, Cl-IB-MECA (100 nM) was applied for at least 5 min.

AP firing was quantified by counting the number of APs evoked by a ramp current (1s) and expressed as AP frequency (Hz). When the Cl-IB-MECA was applied in the presence of MRS1523 (100 nM) or PD173232 (1 μM), the A_3AR antagonist or the N-type VOCC blocker were added at least 10 min before the agonist. Current-clamp recordings were filtered at 10 kHz and digitized at 1 kHz. The rate of AP depolarization and hyperpolarization was measured as the first derivative of membrane potential over time (mV/ms). AP threshold was defined as the point at which the derivative first exceeded 30 mV/ms. AP amplitude was calculated as the difference between the peak reached by the overshoot and the threshold. AP time to peak was measured as the time between the threshold and the voltage peak reached by the AP. AP half-width was measured at half the AP amplitude, (see Table 6).

Table 6

	Resting Vm (mV)	**Time to peak (ms)**	**Half width (ms)**	**Peak amplitude (mV)**
ctrl	-48.3 ± 5.3	737.1±91.6	1.5±1.0	119.1±23.5
Cl-IB-MECA	-47.9 ± 5.1	934.0±131.4	2.6±3.7	132.1±28.2
1523	-49.6±2.9	839.4±103.2	3.3±1.7	117.7±41.0
1523+Cl-IB-MECA	-48.6±3.3	885.3±201.5	4.1±1.9	119.5±48.0
PD	-51.1 ± 5.4	348.3 ± 45.1	3.6 ± 1.8	99.0 ± 12.8
PD+Cl-IB-MECA	-51.3 ± 5.5	448.6 ± 52.9	4.2 ± 2.0	101.5 ± 28.4

Table 6. Action potential parameters measured in DRG neurons under current clamp mode before (control: Ctrl) or after Cl-IB-MECA (Cl-IBM, 100 nM) application in the absence (n=6) or presence (n=5) of the A_3AR selective antagonist MRS1523 (1523, 100 nM) or in the presence (n=4) of the N-type Ca^{2+} channel blocker PD173212 (PD, 1 μM). No significant difference was found between any of the measured parameters through the different experimental groups, Paired Student's t-test.

4.2 Quantitative RT-PCR Analysis

Total RNA was isolated using Nucleospin®RNA (Macherey–Nagel Duren, Germany) with DNAse treatment according to the manufacturer's instructions. The expression of A_3AR was evaluated by Real-Time quantitative polymerase chain reaction (RT-PCR) using gene-specific flourescently labeled TaqMan MGB probe (minor groove binder). For the RT-PCR of A_3AR a pre-developed assay was used: Adora3 Rn_00563680_m1. The amount of target mRNA was normalized to the endogenous reference, Gadph Rn 01749022_g1 and to a homogenate of rat brain taken as a positive,

according to the 2−ΔΔCt method. The results were expressed as fold changes compared to control. Data are the result of three independent experiments performed in triplicate.

4.3 Immunocytochemical analysis

Primary DRG cultures grown on 13 mm diameter coverslips were fixed with 4% paraformaldehyde in 0.1 M phosphate buffered saline (PBS) for 20 min at RT. Rabbit polyclonal A_3AR-selective primary antibody (Alomone labs, Jerusalem, Israel; https://www.alomone.com) was diluted 1:200 in bovine serum dilution buffer (BSDB: 450 mM NaCl, 20 mM sodium phosphate buffer, pH 7.4, 15% FBS, 0.3% Triton X-100) and incubated for 2.5 h at RT. Cells were then washed three times with PBS and incubated for 1 h at RT with a donkey anti-rabbit secondary antibody (diluted 1:500 in BSDB) conjugated to AlexaFluor 488 (Life Techologies, Invitrogen, Milan, Italy). Coverslips were mounted with Vectashield mounting medium (Vector Laboratories, Burlingame, CA) containing 40,6-diamidino-2-phenylindole (DAPI) to visualize cell nuclei, digitized and acquired by using an Olympus BX40 microscope equipped with CellSens Dimention software (Olympus, Germany).

4.4 Intracellular Ca^{2+} measurement

Intracellular cytosolic Ca^{2+} dynamic ($[Ca^{2+}]i$) was evaluated in fura-2 loaded DRG neurons as described (Di Cesare Mannelli *et al.,* 2016). Briefly, l04 cells were plated on round glass coverslips (25 mm diameter) and seeded for 1-2 days in complete medium. Cells were loaded with 4 µM fura-2AM (Molecular Probes-Invitrogen Life technologies, San Giuliano Milanese, Italy) for 45 min at 37°C and then washed with the K^+-based standard extracellular solution described above. Coverslips were mounted in a perfusion chamber and placed on the stage of an inverted reflected light fluorescence microscope (Zeiss Axio Vert. A_1 FL-LED) equipped with fluorescence excitation (385 nm) based on LED. Before electrical field stimulation, cells were incubated for at least 5 min with different solutions containing the following molecules: control (standard extracellular solution), 1 µM TTX + 200 nM A887826, 30 nM Cl-IB-MECA, 1 µM Verapamil + 500 nM PD173212. Fura-2 fluorescence was recorded with a Tucsen Dhyana 400D CMOS camera (Tucsen Photonics Co., Ltd., Fuzhou, China) with a frame rate of 40 Hz and a resolution of 1024X1020 pixels2. Ca^{2+} dynamic was measured by single cell imaging analysis at 35°C (Di Cesare Mannelli *et al.,* 2016). Images were recorded using Dhyana software SamplePro and dynamically analyzed with the open source community software for bio-imaging Icy (Institut Pasteur, Paris, France). Ca^{2+} transients were induced by electrical field stimulation at 0.1 Hz frequency, 100 mV voltage and 50 ms width duration. A signal-to-noise ratio of at least 5 A.U. (fluorescence arbitrary units) was considered as Ca^{2+} transient. "Responder" DRG neurons were identified as cells showing at least 5 Ca^{2+} transients in 1 min. In responder cells, the following parameters were evaluated as the mean of at least three different Ca^{2+} transients: the ratio between the fluorescence maximal variation induced by electrical-field stimulation and basal fluorescence (ΔF/F, measured as arbitrary units) and the area under the curve calibrated on basal fluorescence (AUC/F, evaluated as arbitrary units). The cell diameter of

analyzed DRG neurons was measured in pixels using ImageJ software and transformed in µM by a specific calibration scale. Experiments were repeated in 4 different neuronal preparations. All DRG neurons (identified by transmitted light microscopy) found in an optical field (using 40X magnification objective) were analyzed. From 16 to 22 cells were evaluated blindly every experimental day for each experimental treatment.

4.5 Drugs

2-Chloro-N6-(3-iodobenzyl)-adenosine-5′-N-methyluronamide (Cl-IB-MECA, Figure 29), 5-(4-butoxy-3-chlorophenyl)-N-[[2-(4-morpholinyl)-3-pyridinyl]methyl]-3-pyridinecarboxamide (A887826, Figure 30), 3-propyl-6-ethyl-5-[(ethylthio)carbonyl]-2 phenyl-4-propyl-3-pyridine carboxylate (MRS1523, Figure 23), N-(2-methoxyphenyl)-N′-[2-(3-pyridinyl)-4-quinazolinyl]-urea (VUF5574, Figure 31), 8-Cyclopentyl-1,3-dipropylxanthine (DPCPX, Figure 25), N^6-cyclopentyladenosine (CPA, Figure 34), apamin and tetraethylammonium (TEA,Figure 35) were purchased from Sigma-Aldrich (www.sigmaaldrich.com). Tetrodotoxin (TTX, Figure 33) and 4-t-butyl-N-methyl-N-aralkyl-peptidylamine (PD173212, Figure 32) were purchased from Alomone Lab. Verapamil was purchased from Calbiochem (Merck; Darmstadt, Germany). The new, highly selective, A_3AR agonist (1S,2R,3S,4R,5S)-4-(2-((5-chlorothiophen-2-yl)ethynyl)-6-(methylamino)-9H-purin-9-yl)-2,3 dihydroxy-N-methylbicyclo[3.1.0]hexane-1-carboxamide (MRS5980) was synthesized as reported previously (Fang *et al.*, 2015; Tosh *et al.*, 2014). All drugs were stored at -20°C as 10^3 to 10^4 times more concentrated stock solutions and dissolved daily in the extracellular solution to the final concentration and applied by bath superfusion. TTX, apamin and TEA stock solutions were prepared in distilled water. All other compounds were dissolved in dimethyl sulphoxide (DMSO). Control experiments performed in the present research demonstrated that the maximal DMSO concentration used in the present work (0.1%) was inactive in modulating membrane currents (see Figure 61C) in our experimental conditions in DRG neurons.

4.5.1 Chemical structure of drugs

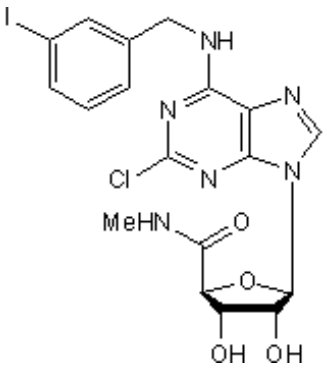

Figure 29: Cl-IB-MECA: 2-Chloro-N6-(3-iodobenzyl)-adenosine-5′-N-methyluronamide. Highly selective A_3AR agonist. (Tocris Biosciences, Bristol, UK).

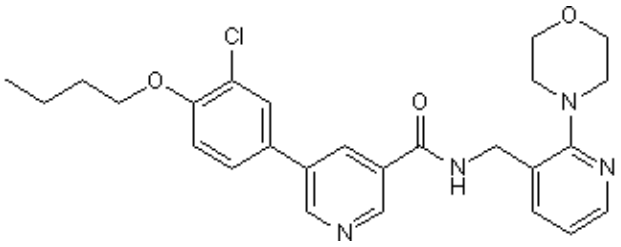

Figure 30: A887826: 5-(4-butoxy-3-chlorophenyl)-N-[[2-(4-morpholinyl)-3-pyridinyl]methyl]-3-pyridinecarboxamide. Potent voltage-dependent NaV1.8 channel blocker. (Tocris Biosciences, Bristol, UK).

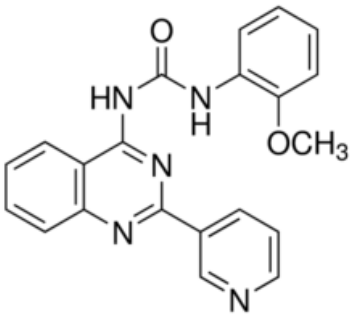

Figure 31: VUF5574: N-(2-methoxyphenyl)-N′-[2-(3-pyridinyl)-4-quinazolinyl]-urea. Selective, competitive and potent antagonist for the human A_3AR (Sigma-Aldrich).

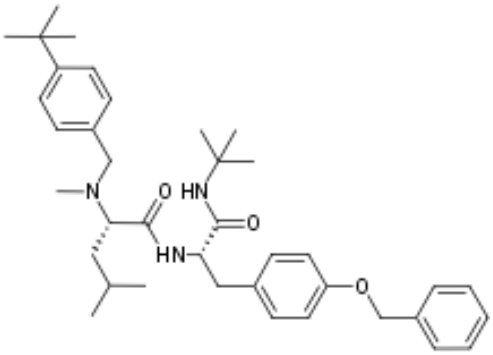

Figure 32: PD173212: 4-t-butyl-N-methyl-N-aralkyl-peptidylamine. A novel blocker of N-type CaV channels (Alomone Lab.).

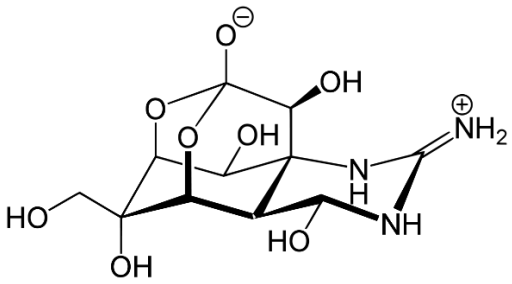

Figure 33: Tetrodotoxin (TTX): A classic blocker of a subset of NaV Channels (Alomone Lab.).

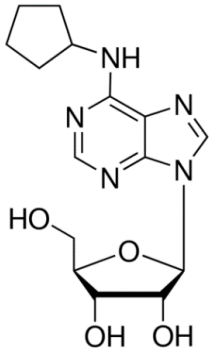

Figure 34: CPA: N^6-cyclopentyladenosine**.** Selective A_1AR agonist (Sigma-Aldrich).

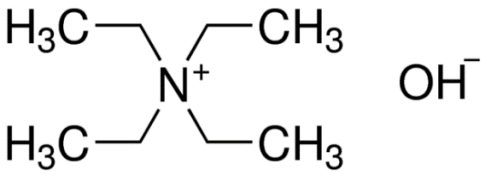

Figure 35: TEA: tetraethylammonium. Voltage-dependent K^+ channels blocker (Sigma-Aldrich).

4.6 Statistical analysis

Data are expressed as mean ± SEM (standard error of the mean). Student's paired or unpaired t-tests or One-way ANOVA followed by Bonferroni post-test analysis were performed, as appropriated, in order to determine statistical significance (set at $P<0.05$). In experiments of intracellular Ca^{2+} measurement, three different parameters were measured: 1) the ratio between DRG neurons defined as "responders" (Ca^{2+} transient) and "not responders" in each experimental condition; 2) $\Delta F/F$ and 3) AUC/F of Ca^{2+} transient evoked in "responder" cells. The effect of each treatment in changing the ratio between "responders" and "not responders" was evaluated by using χ^2 test (PRIMER^{TM}). Data were analysed using "Origin® 10" or "GRAPHPAD PRISM" (GraphPad Software, San Diego, CA, USA) software.

RESULTS AND DISCUSSIONS

Chapter 1: *Role of A_{2B}AR under oxygen and glucose deprivation*

The selective antagonism of $A_{2B}AR_S$ reduces the synaptic failure and neuronal death induced by oxygen and glucose deprivation in rat CA1 hippocampus *in vitro*

1. Results

1.1 Electrophysiological experiments

It has been established that 7 min OGD episodes bring about irreversible depression of neurotransmission and the appearance of a severe neuronal anoxic depolarization or AD (Pugliese *et al.*, 2006, 2007, 2009), a critical event that has been demonstrated both *in vivo* (Somjen, 2001) and *in vitro* (Fowler, 1992; Frenguelli *et al.*, 2007; Pearson *et al.*, 2006; Pugliese *et al.*, 2009, 2007, 2006). Therefore, we studied the effects of two selective A_{2B}AR antagonists, MRS1754 and PSB603, on AD development and synaptic responses in the CA1 region of acute rat hippocampal slices under severe OGD episodes by extracellular recording of fEPSPs performed on 133 hippocampal slices taken from 42 rats.

1.2 The selective adenosine A_{2B}AR antagonism prevents or delays AD development and protects from synaptic failure induced by severe OGD in CA1 hippocampus

In agreement with our previous results (Pugliese *et al.*, 2006, 2007, 2009), in untreated OGD slices the d.c. shift presented a mean latency of 6.04 ± 0.2 min (calculated from the beginning of OGD) and a mean peak amplitude of -6.7 ± 0.4 mV (n = 24) (Figure 36A). Seven min OGD exposure induced a rapid and irreversible depression of fEPSPs amplitude evoked by Schaffer-collateral stimulation, since synaptic potentials did not recover their amplitude after return to oxygenated aCSF (Figure 36D, n = 24, 2.5 ± 2.7% of pre-OGD level, calculated 50 min from the end of OGD). Control slices, followed for up to 3 h in oxygenated aCSF, maintained stable fEPSPs for the entire experimental time recording and never developed the d.c. shift (data not shown).

Oxygen and glucose deprivation was then applied in the presence of the selective A_{2B}AR antagonists MRS1754 or PSB603, administered 15 min before, during and 5 min after OGD. The two A_{2B}AR antagonists did not modify basal synaptic transmission measured before OGD. Indeed, MRS1754 (500 nM, n = 17) did not change fEPSPs amplitude under normoxic conditions (from 1.05 ± 0.06 mV immediately before to 1.01 ± 0.08 mV after 15 min drug application, n = 17). Also, PSB603 did not change the amplitude of synaptic potentials under normoxic conditions (from 1.32 ± 0.12 mV before to 1.35 ± 0.14 mV after 15 min drug application, n = 15). These data indicate that the blockade of A_{2B}AR does not modify low-frequency-induced CA1 synaptic transmission under normoxic conditions, in agreement with results reported in mouse hippocampal slices (Gonçalves *et al.*, 2015). Nevertheless, the two A_{2B}AR antagonists were able to prevent or delay the appearance of AD and to modify synaptic responses after OGD.

During 7 min OGD, MRS1754 prevented the appearance of AD in 13 out of 17 slices tested (Figure 36B). In these 13 slices a complete recovery of fEPSPs was recorded (111.9 ± 7.4%, calculated 50 min from the end of OGD, Figure 36D). In the remaining 4 slices, AD developed, although at later times (Figure 36F, mean AD latency: 7.37 ± 0.41 min; mean peak amplitude: -5.8 ± 1.1 mV, n = 4), and, unexpectedly, was followed by a consistent fEPSP recovery (85.2 ± 15.3%, n = 4, Figure 36D). During 7 min OGD, PSB603 prevented the appearance of AD in 11 out of 15 slices tested (Figure 36C). In these 11 slices a complete recovery of fEPSPs was found (110.4 ± 10.2%, n = 11, Figure 36E). In the remaining four slices in which AD appeared, a delay in AD latency was recorded (Figure 36F, mean AD latency: 7.33 ± 0.08 min; mean peak amplitude: -6.8 ± 1.9 mV, n = 4). Moreover, in these four PSB603-treated slices, a significant recovery of fEPSP (36.2 ± 19.7%, n = 4, Figure 36E) was found. In the slices in which AD appeared in the presence of MRS1754 or PSB603, we compared the time of AD appearance in the absence and in the presence of drugs. As illustrated in Figure 36F, during 7 min OGD, AD appeared in OGD slices with a mean latency of 6.04 ± 0.2 min (Left panel) and a mean peak amplitude of 6.7 ± 0.4 mV (n = 24, Right panel). When 7 min OGD was applied in the presence of 500 nM MRS1754 or 50 nM PSB603 the d.c. shifts were always delayed (Figure 36F, Left panel), while AD amplitude values were not significantly modified in comparison to OGD slices (Figure 36F, Right panel).

In an experimental group of slices which never developed AD in the presence of PSB603 (50 nM, n = 6) and MRS1754 (500 nM, n = 6), we followed the evolution of the synaptic response for 3 h after the end of the 7 min ischemic like insult in comparison to untreated OGD slices (n = 6). As reported in the representative electrophysiological traces shown in Figure 36G, PSB603 (50 nM) and MRS1754 (500 nM) allowed the recovery of synaptic potentials for at least 3 h after 7 min OGD.

Furthermore, in order to confirm that both the recovery of fEPSP and the irreversible loss of neurotransmission after 7 min OGD observed in the different experimental groups were not transient, we tested slice viability 24 h after the OGD insult in control, untreated, slices and slices treated with A_{2B}AR antagonists. In agreement with our previously published results (Pugliese *et al.*, 2009), we showed that untreated OGD slices, which did not recover any synaptic activity within 1 h after the insult, maintained synaptic impairment when tested 24 h later (Figure 37A shows a representative experiment out of a total of six slices). On the contrary, MRS1754- or PSB603-treated OGD slices, which recovered initial fEPSP amplitude 1 h after OGD, preserved neurotransmission for at least 24 h after the insult (Figure 37B shows a representative experiment out of a total of four slices; Figure 37C shows a representative experiment out of a total of five slices for MRS1754 and PSB603, respectively).

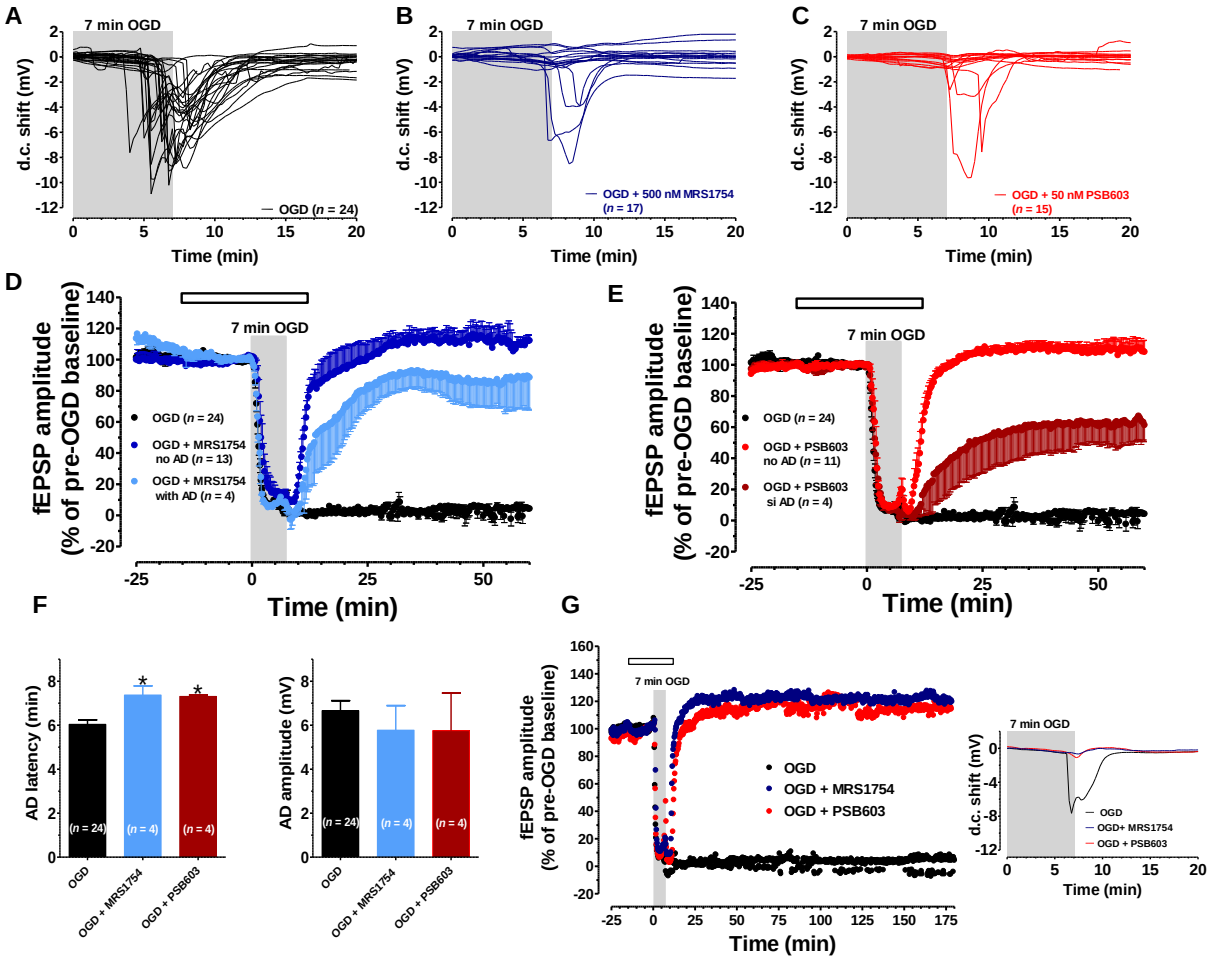

Figure 36: The selective A_{2B}AR antagonists MRS1754 or PSB603 significantly reduced the synaptic failure induced by 7 min oxygen and glucose deprivation (OGD) in the CA1 region of rat hippocampal slices. (A–C) anoxic depolarization (AD) was recorded as a negative direct current (d.c.) shift in response to 7 min OGD in untreated OGD slices (A), in 500 nM MRS1754-treated slices (B) or 50 nM PSB603-treated slices (C). Note that MRS1754 prevented the appearance of AD in 13 out of 17 slices, while PSB603 in 11 out of 15 slices. (D) The graph shows the time-course of the effect of 7 min OGD on field excitatory post-synaptic potential (fEPSP) amplitude, expressed as percentage of pre-OGD baseline in the CA1 hippocampal region in the absence (n = 24) or in the presence of 500 nM MRS1754 (n = 17). Note that, in untreated slices, the ischemic-like insult caused gradual reduction, up to disappearance, of fEPSPs amplitude that did not recover after washing in oxygenated artificial cerebrospinal fluid (aCSF). On the contrary, after reperfusion in oxygenated standard solution, a recovery of fEPSP in all MRS1754 treated OGD slices was found, even in those in which AD developed. (E) The graph shows the time course of the effect of 7 min OGD on fEPSP amplitude in 50 nM PSB603 treated OGD slices. Note that, after reperfusion in normal oxygenated standard solution, a recovery of fEPSP was found in all OGD-treated PSB603 slices, even those in which AD occurred. (F, Left) each column represents the mean ± SEM of AD latency recorded in the CA1 region during 7 min OGD in the absence or in the presence of MRS1754 (500 nM) or PSB603 (50 nM). AD latency was measured from the beginning of OGD insult. Note that when OGD was applied in the presence of MRS1754 or PSB603 the appearance of AD was significantly delayed in comparison to OGD untreated slices. $^{*}P < 0.05$ *vs.* OGD, One-way ANOVA followed by Newman–Keuls Multiple comparison test. (Right) each column represents the mean ± SEM of AD amplitude recorded in the CA1 during 7 min OGD. The number of slices is reported in the columns. (G) The graph shows the time course of the effect of 7 min OGD on fEPSP amplitude in OGD-untreated slices and in 500 nM MRS1754- or 50 nM PSB603-treated slices. The selective antagonism of adenosine A_{2B}AR counteracted the CA1 synaptic damage induced by severe OGD up to 3 h from the end of the insult. Inset: 7 min OGD induced AD was recorded in untreated OGD slices, but not in the presence of 500 nM MRS1754 or 50 nM PSB603. Gray bar: OGD time duration. Open bar: time of drug application. Amplitude of fEPSPs (mean ± SEM) is expressed as percentage of pre-OGD baseline.

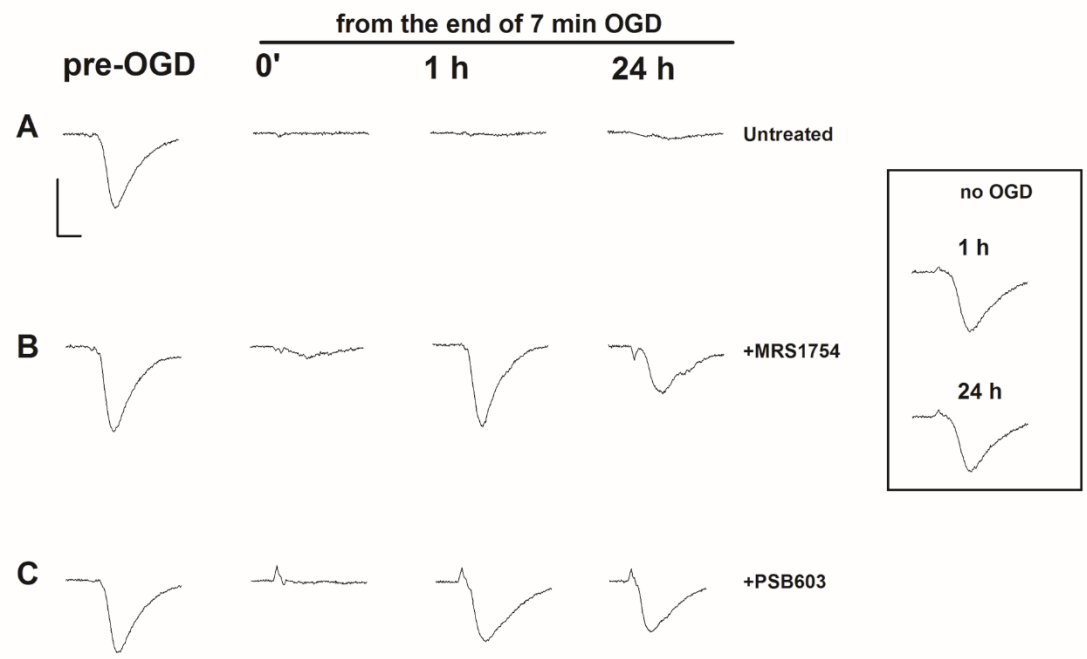

Figure 37: The selective block of $A_{2B}AR$ allowed a recovery of synaptic potentials up to 24 h after the end of 7 min OGD. A-C: fEPSPs were recorded before (pre-OGD) and at different times after the end of OGD in untreated OGD slice (A), in 500 nM MRS1754-treated OGD slice (B) and in 50 nM PSB603-treated OGD slice (C). Each trace, taken from a typical experiment, represents the average of two consecutive fEPSP recorded. Note that after OGD in untreated slice only the afferent volley was recorded. In control conditions (inset: no OGD) a stable fEPSP can be recorded for up to 24 h after slice preparation. Calibration: 1 mV, 5 ms.

In order to characterize the role of adenosine $A_{2B}AR_S$ on AD development, in a next series of experiments we prolonged the OGD duration up to 30 min, in order to allow AD to unavoidably appear in all experimental groups. This longer duration of OGD is invariably associated with tissue damage (Pearson *et al.*, 2006). We compared the latency and the magnitude of depolarizing d.c. shifts recorded in the absence or presence of PSB603 or MRS1754. As illustrated in Figure 38A, 30 min OGD elicited the appearance of AD in all slices, with a mean peak amplitude of -7.5 ± 0.7 mV (n = 8) and a mean latency of 5.8 ± 0.3 min, as shown in Figures 38D,E. When OGD was applied in the presence of 500 nM MRS1754, the d.c. shift was significantly delayed to 9.2 ± 0.7 min (Figures 38B, D; n = 5), although the AD amplitude (-5.7 ± 0.7 mV) was not significantly changed (Figure 38E). Similarly, when OGD was applied in the presence of 50 nM PSB603, the d.c. shift was significantly delayed to 7.7 ± 0.3 min (Figures 38C,D; n = 7) whereas AD amplitude (-7.7 ± 0.7 mV) was unchanged (Figure 38E).

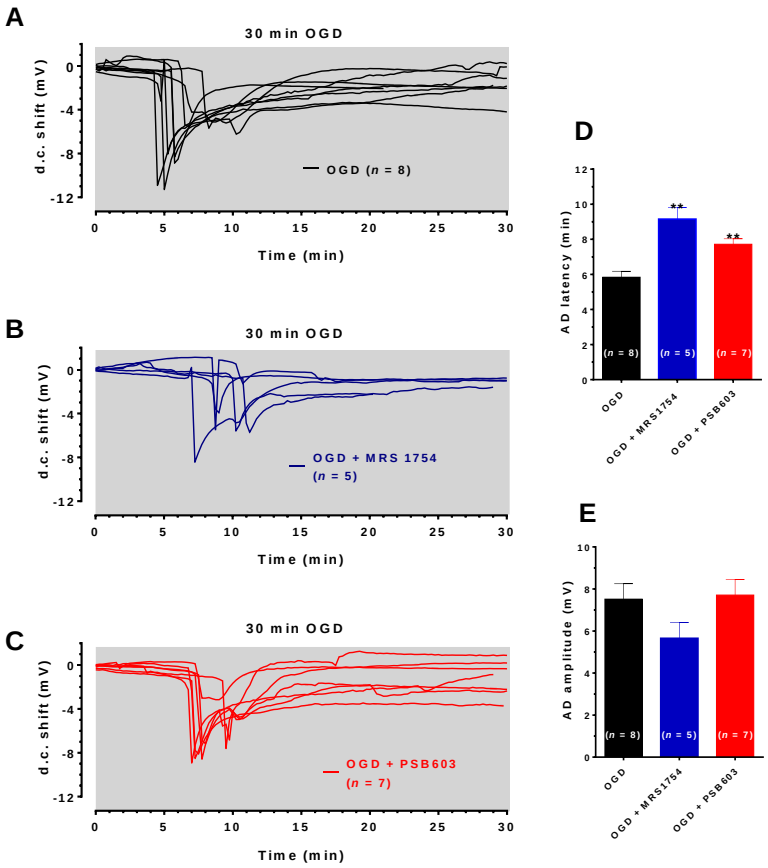

Figure 38: MRS1754 and PSB603 delayed the appearance of AD induced by 30 min OGD in rat hippocampal slices. (A–C) The graphs show the d.c. shift traces during 30 min OGD in untreated OGD slices (A, n = 8), in the presence of 500 nM MRS1754 (B, n = 5), or 50 nM PSB603 (C, n = 7). (D) Each column represents the mean ± SEM of AD latency recorded in hippocampal slices during 30 min OGD in different experimental groups. AD was measured from the beginning of OGD insult. Note that both A_{2B}AR antagonists significantly delayed AD development. $^{**}P < 0.01$ *vs.* OGD, One-way ANOVA followed by Newman–Keuls Multiple comparison test. (E) Each column represents the mean ± SEM of AD amplitude recorded in the CA1 during 30 min OGD. The number of slices is reported in the columns.

Data in the literature demonstrate that A_{2B}AR exert their effects through a control of A_1AR function in the hippocampus under simil-physiological, normoxic, conditions (Gonçalves *et al.*, 2015). In order to test this possibility, we studied whether A_{2B}AR antagonists were still effective in inhibiting OGD-induced alterations of synaptic transmission in the presence of the A_1AR antagonist DPCPX. As shown in Figures 39A–C, we applied DPCPX before, during and after a 7 min OGD and, unexpectedly, we found that 2 out of 6 slices tested did not undergo AD and completely recovered their synaptic activity. This unexpected result was possibly due to the unselective block of A_{2A}AR by DPCPX, as already described in hippocampal slices during OGD (Sperlágh *et al.*, 2007). Therefore, we reduced DPCPX concentration to 100 nM and we prolonged the OGD period up to 30 min (Figure 39D). Under these experimental conditions, DPCPX-exposed slices presented a delayed AD appearance (mean AD peak time = 8.4 ± 0.5 min) in comparison to control, untreated, OGD slices (mean AD peak time = 6.8 ± 0.2 min), thus confirming that DPCPX protects hippocampal

slices from OGD insults (Figure 39E). The time window of A_{2B} or A_1AR-mediated effects found in the present studies overlaps with the delay found treating the slices with glutamate receptor antagonists (Tanaka *et al.*, 1997; Yamamoto *et al.*, 1997), or blocking NMDA receptors that are involved both in initiation and propagation of AD (Herreras and Somjen, 1993; Somjen, 2001). In a further series of experiments, we demonstrated that D-AP5 (50 μM) significantly delayed AD appearance (from 6.8 ± 0.2 min in untreated OGD slices to 9.8 ± 1.0 min in D-AP5-treated OGD slices, Figure 39E). For this reason, in order to assess the involvement of A_1AR in A_{2B}AR-mediated effects, we choose a different protocol. It has been shown that short-term plasticity, measured by PPF, is modified by A_{2B}AR activation in mouse hippocampal slices in a DPCPX-sensitive manner (Gonçalves *et al.*, 2015).

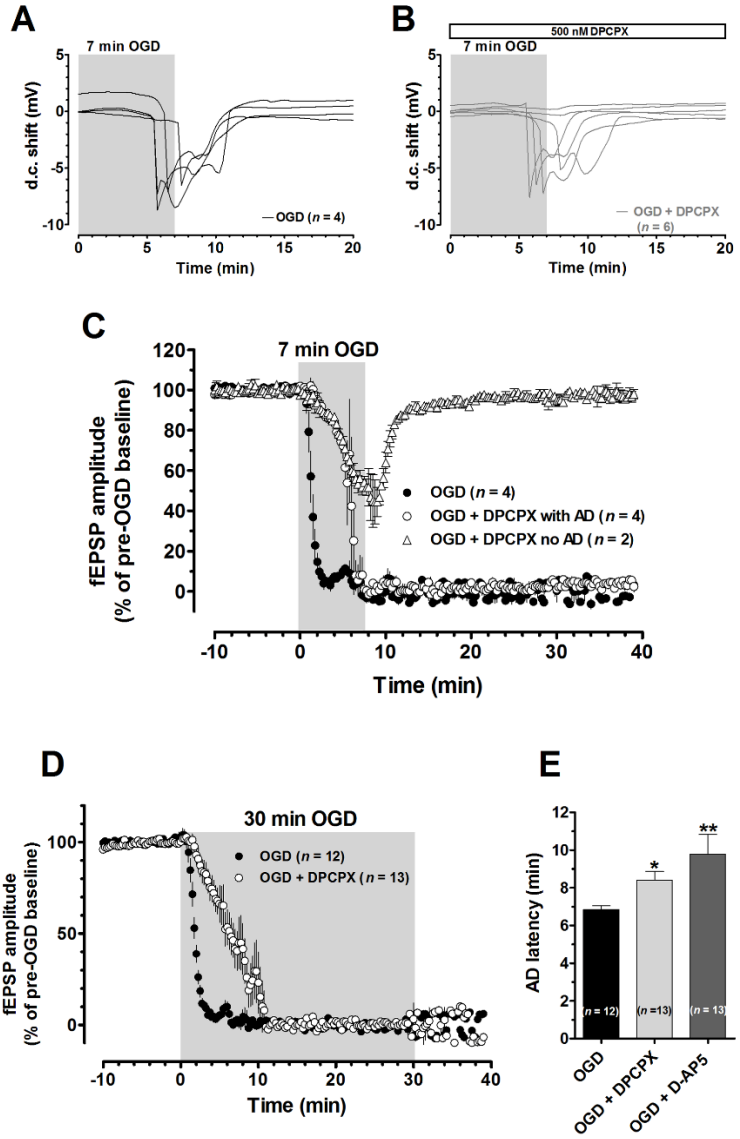

Figure 39: Effects of DPCPX, a selective A_1AR antagonist, on OGD-induced damage in rat hippocampal slices. A-B: AD was recorded as a negative d.c. shift in response to 7 min OGD in the absence (A, n=4) or in the presence (B, n=6) of 500 nM DPCPX. Note that the A_1AR antagonist prevented the appearance of AD in

2 out of 6 slices. C: Graph shows the time course of 7 min OGD effects on fEPSP amplitude (mean±SEM) in untreated (n=4) OGD slices and in 500 nM DPCPX- (n=6) treated OGD slices. Note that, after reperfusion in normal oxygenated standard solution, a recovery of fEPSP was found only in DPCPX -treated OGD slices in which AD did not occur. Note that in the presence of the A_1AR antagonist, the time course of fEPSP depression during OGD was delayed in comparison to corresponding times in the absence of the drug. D: Graph shows the time course of 30 min OGD effects on fEPSP amplitude in OGD-untreated slice (n=12) and 100 nM DPCPX-treated slices (n=13). E: Each column represents the mean±SEM of AD latency recorded in hippocampal slices during 30 min OGD in the absence, in the presence of 100 nM DPCPX or 50 nM D-AP5, a potent, selective NMDA antagonist. AD was measured from the beginning of OGD insult. Note that AD was significantly delayed in the presence of DPCPX or D-AP5. $*P < 0.05$, $**P < 0.01$, One-way ANOVA followed by Newman-Keuls Multiple comparison test, compared to OGD.

We confirmed that the A_{2B}AR agonist BAY606583, at 200 nM concentration, significantly decreased PPF in rat CA1 hippocampus (Figure 40), thus indicating an increase of presynaptic glutamate release upon A_{2B}AR activation. This effect was blocked not only by the A_{2B}AR antagonists PSB603 and MRS1754, but also by the A_1AR antagonist DPCPX (Figure 40B), thus confirming that A_{2B}AR effects are mediated by the inhibition of the A_1 subtype, as already stated by Gonçalves (Gonçalves *et al.*, 2015).

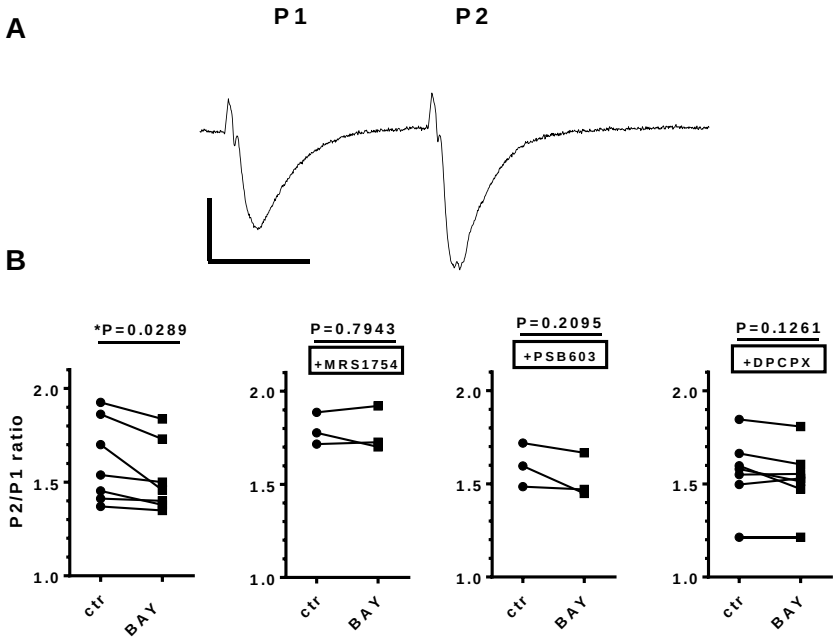

Figure 40: The selective stimulation of $A_{2B}AR_S$ reduced paired-pulse facilitation (PPF) in rat hippocampal slices. (A) Trace of fEPSP responses to PPF protocol (40-ms interval), taken from a typical experiment. Calibration: 0.5 mV, 20 ms. (B) Each graph shows PPF quantified as the ratio (P2/P1) between the slope of the second fEPSP (P2) and the slope first fEPSP (P1). The effect of BAY606583 (BAY, 200 nM) on PPF was investigated in the absence (n = 7) or in the presence of MRS1754 (500 nM, n = 3), PSB603 (50 nM, n = 3), or DPCPX (100 nM, n = 7). $*P < 0.05$ *vs.* ctr, paired Student's t-test.

1.3 Analysis of neuronal damage in CA1 stratum pyramidale 1 and 3 h after the end of 7 min OGD

The extent of neuronal damage caused by 7 min OGD in stratum pyramidale of hippocampal CA1 was assessed by immunohistochemistry using the anti-NeuN antibody in control slices, in slices after 7 min OGD alone, and after 7 min OGD in the presence of 500 nM MRS1754 or 50 nM PSB603, both at 1 and 3 h after the end of OGD. Representative images of NeuN immunostaining in CA1 of slices collected 1 h after the end of OGD are shown in Figures 41A–D.

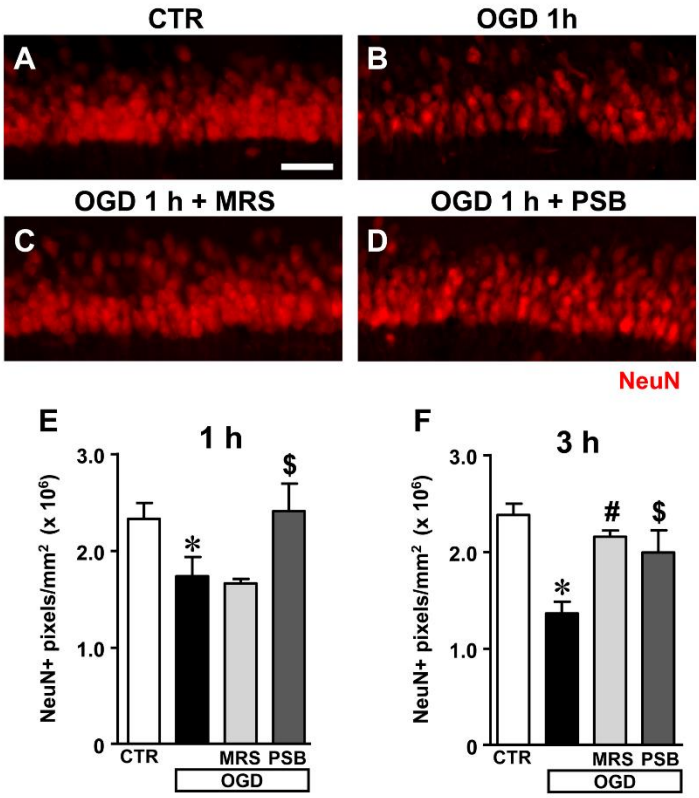

Figure 41: Analysis of NeuN$^+$ immunofluorescence in CA1 stratum pyramidale after the simil-ischemic insult. (A–D) Representative images of NeuN$^+$ immunofluorescence in the ROI of CA1 of a control slice (CTR, A), a slice collected 1 h after 7 min OGD (OGD, B), a slice treated with 500 nM MRS1754 (OGD+MRS, C), and a slice treated with 50 nM PSB603 (OGD+PSB, D), all harvested 1 h after the end of 7 min OGD. Scale bar: 75 µm. (E,F) Quantitative analyses of NeuN$^+$ immunofluorescence in the four experimental groups 1 h (E) and 3 h (F) after the end of 7 min OGD. Each column represents the area, expressed in pixels (×106) above a threshold, maintained constant for all slices investigated. (E) Statistical analysis: One-way ANOVA: $F(3;13) = 6.296$, $P < 0.01$, Newman–Keuls multiple comparison test: $^{*}P < 0.05$, OGD *vs.* CTR; $^{\$}P < 0.05$, OGD+PSB *vs.* OGD. CTR, n = 6; OGD, n = 5; OGD+PSB, n = 3; OGD+MRS, n = 3. (F) Statistical analysis: One-way ANOVA: $F(3,16) = 4.924$, $P < 0.02$; Newman–Keuls multiple comparison test: $^{*}P < 0.05$ OGD *vs.* CTR, $^{\#}P < 0.05$ OGD+MRS *vs.* OGD,$^{\$}P < 0.05$ OGD+PSB *vs.* OGD. CTR, n = 6; OGD, n = 3; OGD+PSB, n = 4; OGD+MRS n = 4. All data in the graphs are expressed as mean ± SEM.

Figures 41E,F show the quantitative analyses of the area of NeuN$^+$ immunofluorescence in CA1, which represents an index of the number of pyramidal neurons, 1 and 3 h after the end of OGD,

respectively. The data demonstrate that $NeuN^+$ CA1 pyramidal neurons significantly decreased both 1 h (Figure 41E) and 3 h (Figure 41F) after the end of 7 min OGD. Statistical analysis showed that 7 min OGD caused a statistically significant reduction of $NeuN^+$ area at 1 h (-29.6%, $^*P < 0.05$ *vs.* control slices) and at 3 h (-41%, $^*P < 0.05$ *vs.* control slices). The time-course of the effect, indicating that the decrease of $NeuN^+$ area was more pronounced at 3 h than at 1 h after the end of OGD, demonstrates that neuronal degeneration is an ongoing process at least at these time points.

The decrease of $NeuN^+$ area in CA1 stratum pyramidale was completely antagonized by treatment with 50 nM PSB603 (-1% at 1 h and -14% at 3 h, ns *vs.* control slices). This effect was statistically significant *vs.* 7 min OGD slices both at 1 and 3 h after the end of OGD ($^\$P < 0.05$ *vs.* respective OGD). Treatment with 500 nM MRS1754 completely blocked the decrease of $NeuN^+$ area in CA1 stratum pyramidale 3 h after the end of OGD (-7% *vs.* control slices, ns; $^\#P < 0.05$ *vs.* OGD). MRS1754 had no effect 1 h after the end of OGD (-31.5% *vs.* control slices; ns *vs.* OGD). Therefore, antagonism of A_{2B}AR blocked the neuronal damage induced by 7 min OGD up to 3 h after the end of the simil-ischemic insult. In the OGD slices treated either with MRS1754 or PSB603 that developed AD we found a partial reduction of neuronal damage at 1 h after the end of OGD (data not shown).

Closer examination of CA1 stratum pyramidale with confocal microscopy indicated the presence of many damaged neurons both 1 and 3 h after the end of 7 min OGD. The representative confocal z stacks in Figures 41B, 42B, each obtained stacking 37 consecutive confocal z-scans (0.3 μm each, total thickness 11.1 μm) through the thickness of CA1, show that 3 h after the end of OGD the layout and morphology of CA1 pyramidal neurons was significantly different from that of the control slice (Figure 42A). Figures 42A1,B1 are magnification of the framed areas in Figures 42A,B, and show stacks of two consecutive z-scans, 0.3 μm each, total thickness 0.6 μm, taken at 2.1 μm depth inside the neurons. It appears evident from panel Figure 42B1 the altered morphology of pyramidal neurons after OGD, in comparison to those of the control slice shown in Figure 42A1. Indeed, in CA1 stratum pyramidale of OGD slices, both at 1 and 3 h after the end of OGD, we observed the presence of many neurons with nuclei that exhibit a highly condensed NeuN-positive nucleus and very faint NeuN cytoplasmic labeling (Figures 42B, B1, open arrows). We defined these neurons as High Density Nucleus neurons, "HDN neurons." Furthermore, we observed many $NeuN^+$ neurons that have lost the $NeuN^+$ nuclear immunofluorescence, an index of damaged nuclei, while $NeuN^+$ immunofluorescence persists in the cytoplasm (Figures 42B, B1, white arrows). We defined these neurons as Low Density Nucleus neurons, "LDN neurons."

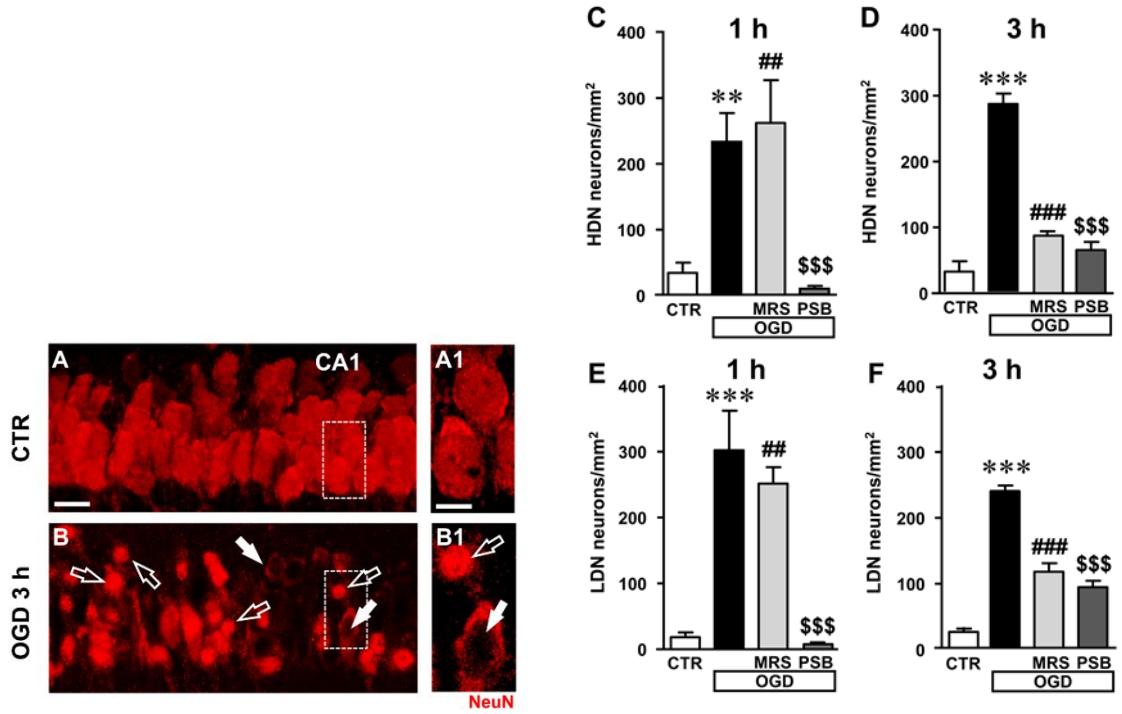

Figure 42: Analysis of damaged neurons in CA1 stratum pyramidale after the simil-ischemic insult. (A–B1) Representative images of NeuN$^+$ immunofluorescence in the CA1 area of a control slice (CTR, A,A$_1$), and of a slice harvested 3 h after the end of 7 min OGD (OGD, B,B1). (A$_1$–B1) magnification of digital subslices of the framed areas in A,B (stacks of two consecutive z-scans taken at 2.1 µm depth inside the neurons, total thickness 0.6 µm). Note the presence of many HDN neurons (open arrows) and LDN neurons (white arrows) in CA1 stratum pyramidale after OGD (B,B1). Scale bars: A,B: 25 µm; A$_1$,B1: 10 µm. (C,D) Quantitative analyses of NeuN$^+$ HDN neurons in CA1 stratum pyramidale 1 h (C) and 3 h (D) after the end of OGD. (C) One-way ANOVA: F(3;12) = 11.32, $P < 0.001$. Newman–Keuls multiple comparison test: $^{**}P < 0.01$, OGD *vs.* CTR; $^{\#\#}P < 0.01$, OGD+MRS *vs.* CTR; $^{\$\$\$}P < 0.001$ OGD+PSB *vs.* OGD. CTR, n = 5; OGD, n = 5; OGD+PSB, n = 3; OGD+MRS, n = 3. (D) One-way ANOVA: F(3;12) = 64.33, $P < 0.001$. Newman–Keuls multiple comparison test: $^{***}P < 0.001$, OGD *vs.* CTR; $^{\#\#\#}P < 0.001$, OGD+MRS *vs.* OGD; $^{\$\$\$}P < 0.001$ OGD+PSB *vs.* OGD. CTR, n = 5; OGD, n = 3; OGD+PSB, n = 4; OGD+MRS, n = 4. (E–F): Quantitative analysis of NeuN+ LDN neurons in CA1 stratum pyramidale 1 h (E) and 3 h (F) after the end of OGD. (E) One-way ANOVA: F(3;14) = 13.80, $P < 0.001$. Newman–Keuls multiple comparison test: $^{***}P < 0.01$, OGD *vs.* CTR; $^{\#\#}P < 0.01$, OGD+MRS *vs.* CTR; $^{\$\$\$}P < 0.001$ OGD+PSB *vs.* OGD. CTR, n = 6; OGD, n = 6; OGD+PSB, n = 3; OGD+MRS, n = 3. (F) One-way ANOVA: F(3;12) = 69.77, $P < 0.001$. Newman–Keuls multiple comparison test: $^{***}P < 0.001$, OGD *vs.* CTR; $^{\#\#\#}P < 0.001$, OGD+MRS *vs.* OGD; $^{\$\$\$}P < 0.001$ OGD+PSB *vs.* OGD. CTR, n = 5; OGD, n = 3; OGD+PSB, n = 4; OGD+MRS, n = 4. All data in the graphs are expressed as mean ± SEM.

In order to better characterize this phenomenon, we performed the quantitative analysis of HDN and LDN neurons in control, 7 min OGD, 7 min OGD plus MRS1754 and 7 min OGD plus PSB603 slices at 1 and 3 h after the end of OGD. The results, presented in Figures 42C,D, show that HDN neurons increased significantly in 7 min OGD slices both at 1 h (+603% *vs.* control slices, $^{**}P < 0.01$) and 3 h (+794% *vs.* control slices, $^{***}P < 0.001$) after the end of OGD. The increase of damaged, HDN neurons in the CA1 area caused by the simil-ischemic insult was significantly blocked by treatment with 50 nM PSB603 at 1 and 3 h after the end of OGD (-97% at 1 h, and -77% at 3 h *vs.* 7 min OGD slices, both $^{\$\$\$}P < 0.001$; ns *vs.* controls). Conversely, treatment with 500 nM MRS1754 significantly blocked the increase of HDN neurons only 3 h after the end of OGD (-70% *vs.* 7 min

OGD slices, $^{###}P < 0.001$; ns *vs.* control slices), but not 1 h after the end of OGD (+12% *vs.* OGD slices, ns; $^{##}P < 0.01$ *vs.* control slices).

Also, as shown by the representative images in Figures 42B,B1, we found many LDN neurons in stratum pyramidale 1 and 3 h after the end of 7 min OGD. As demonstrated by quantitative analysis (Figures 42E,F) LDN neurons in stratum pyramidale were significantly increased both 1 and 3 h after OGD, in comparison to control slices. The increase of LDN neurons, in comparison to control slices, was 1489% at 1 h ($^{***}P < 0.01$ *vs.* control slices) and 1033% at 3 h after the end of 7 min OGD ($^{***}P < 0.01$ *vs.* control slices). The increase of damaged, LDN neurons brought about by the simil-ischemic insult was significantly blocked by treatment with 50 nM PSB603 both at 1 and 3 h after the end of OGD (-98% at 1 h, and -62% at 3 h *vs.* OGD, both $^{$$$}P < 0.001$). Treatment with 500 nM MRS1754 significantly blocked the increase of LDN neurons only 3 h after the end of OGD (-52% *vs.* 7 min OGD,$^{###}P < 0.001$), but not 1 h after the end of OGD (-17% *vs.* 7 min OGD, ns; $^{##}P < 0.01$ *vs.* controls). These data further confirm the efficacy of the two A_{2B}AR antagonists, and particularly of PSB603, in reducing not only the electrophysiological effects but also the morphological modifications that OGD caused on CA1 pyramidal neurons, up to 3 h after the end of the ischemic-like insult.

1.4 Analysis of apoptotic neurons in stratum pyramidale of CA1 1 and 3 h after 7 min OGD

These data demonstrate that 7 min OGD can induce neuronal damage in CA1 stratum pyramidale, as evidenced by immunohistochemical analyses that highlight conformational modifications of pyramidal neurons that may subtend cell death. Therefore, we studied whether all the above-described effects and the decrease of neurons in CA1 stratum pyramidale might be caused by apoptosis. To this end, as an apoptosis marker we used CytC, a protein which, in physiological conditions, is found in mitochondria but in the most advanced stages of apoptosis is intensely and diffusely released in the cytoplasm, where it activates caspases (Jiang and Wang, 2004; Kluck *et al.*, 1997; Suen *et al.*, 2008; Yang *et al.*, 1997) and can be used as a marker of apoptosis using immunohistochemical analysis (Martínez-Fábregas *et al.*, 2014). Using a selective antibody, CytC can be visualized in apoptotic cells as an intense and diffuse cytoplasmic immunostaining, as shown by the white arrows in the representative confocal images of an OGD slice 1 h after the end of OGD (Figures 43A–A2). As shown in the confocal subslice of the framed area of Figure 43A2, obtained stacking 17 consecutive confocal z-scans through the $CytC^+$ neuron (0.3 μm each, total thickness 5.1 μm), it is evident that the $CytC^+$ positive neuron is a LDN neuron (Figures 43B–B2, open arrow), thus demonstrating that LDN neurons are apoptotic.

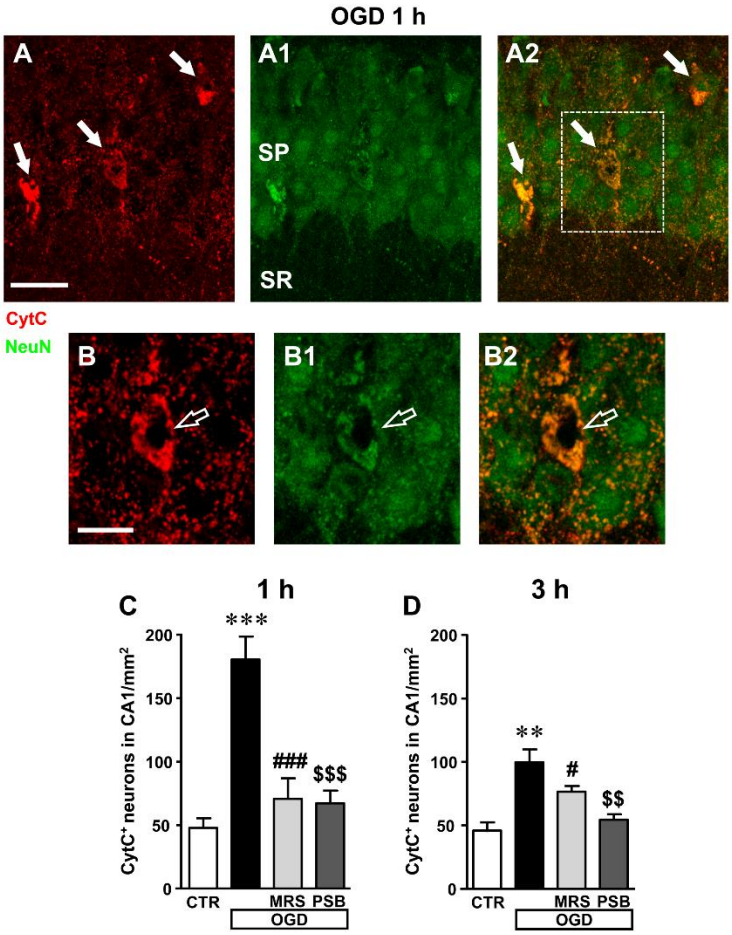

Figure 43: Analysis of CytocromeC$^+$ (CytC$^+$) neurons in CA1 stratum pyramidale after the simil-ischemic insult. (A–A2) Representative microphotographs, taken at the laser scanning confocal microscope, of apoptotic neurons labeled with anti-CytC antibody (A, red), of pyramidal neurons labeled with anti-NeuN antibody (A1, green) and the merge of the two previous images (A2). NeuN$^+$ and CytC$^+$ apoptotic neurons in CA1 stratum pyramidale are indicated by the arrows (yellow-orange color in A2). Scale bar: 25 µm. (B–B2) Subslice of the framed area in A2, obtained stacking 17 consecutive confocal z-scans (5.1 µm total thickness), shown at higher magnification (2×). The open arrow shows an LDN apoptotic pyramidal neuron. Scale bar: 10 µm. (C,D) Quantitative analysis of NeuN$^+$ and CytC$^+$ neurons in CA1 stratum pyramidale at 1 h (C) and 3 h (D) after the end of 7 min OGD. Note the significant increase of CytC$^+$ neurons both 1 and 3 h after the end of OGD. (C) Statistical analysis: One-way ANOVA: F(3;11) = 18.40, $P < 0.001$, Newman–Keuls multiple comparison test: $^{***}P < 0.001$, OGD *vs.* CTR; $^{\#\#\#}P < 0.001$, OGD+MRS *vs.* OGD; $^{\$\$\$}P < 0.001$, OGD+PSB *vs.* OGD. CTR, n = 4; OGD, n = 3; OGD+PSB, n = 4; OGD+MRS, n = 4. (D) Statistical analysis: One-way ANOVA: F(3;11) = 11.41, $P < 0.02$, Newman–Keuls multiple comparison test: $^{**}P < 0.01$, OGD *vs.* CTR; $^{\#}P < 0.05$, OGD+MRS *vs.* OGD; $^{\$\$}P < 0.01$, OGD+PSB *vs.* OGD. CTR, n = 4; OGD, n = 3; OGD+PSB, n = 4; OGD+MRS, n = 4. All data in the graphs are expressed as mean ± SEM.

From the quantitative analysis of CytC$^+$ neurons in CA1 stratum pyramidale, we demonstrated that both 1 and 3 h after the end of 7 min OGD many CA1 pyramidal neurons were apoptotic (Figures 43C,D). The increase was statistically significant in comparison to control slices both at 1 h (+277% *vs.* control slices, $^{***}P < 0.001$) and at 3 h (+107% *vs.* control slices, $^{**}P < 0.01$) after OGD. These data indicate that in CA1 area, already after 1 h from the end of OGD, neurons had clear signs of apoptotic processes. In the presence of MRS1754 or PSB603, there was a significant reduction of CytC immunostaining, both at 1 and 3 h after the end of OGD, showing that antagonism of A_{2B}AR

significantly reduced neuronal death by apoptosis at both times investigated. Indeed, treatment with MRS1754 decreased apoptotic neurons by 61% at 1 h ($^{###}P < 0.001$ *vs.* 7 min OGD; ns *vs.* control slices) and by 33% at 3 h ($^{\#}P < 0.05$ *vs.* 7 min OGD; ns *vs.* control slices), in comparison to OGD slices. Treatment with PSB603 decreased apoptotic neurons by 63% ($^{\$\$\$}P < 0.001$ *vs.* 7 min OGD; ns *vs.* control slices) and by 46% ($^{\$\$}P < 0.001$ *vs.* 7 min OGD; ns *vs.* control slices) in comparison to OGD slices. In the OGD slices treated either with MRS1754 or PSB603 that developed AD the number of HDN and LDN neurons were partially decreased in comparison to OGD slices (data not shown).

These data indicate that in the CA1 area already 1 h after the end of OGD, when there was still no recovery of neurotransmission, neurons showed obvious signs of apoptosis. These data demonstrate that antagonism of A_{2B}AR brought about significant protection against neuron degeneration.

1.5 Analysis of Phospho-mTOR in area CA1 of the hippocampus 1 and 3 h after 7 min OGD

We used a selective antibody for phospho-(Ser244)-mTOR, the activated form of mTOR, to investigate whether mTOR activation might be modified in our experimental conditions (Figures 44A–D1). Representative qualitative images of mTOR activation in cell bodies and dendrites of CA1 pyramidal neurons in a control slice are shown in Figure 44A1 (green). Neurons were also immunolabelled with anti-NeuN antibody (red). The merge of the immunofluorescence (yellow-orange) in a control slice is shown in Figure 44A. It is evident from the images that activated mTOR is present in CA1 pyramidal neurons in basal, control conditions where it is localized both in the cell body and in neuronal apical dendritic tree spanning throughout the stratum radiatum. The simil-ischemic condition caused a significant decrease of mTOR activation 3 h after the end of OGD, as shown in the representative image of Figures 44B,B1. This effect is more evident in Figures 44E,F, that represent digital subslices obtained stacking nine consecutive confocal z-scans throughout the neuronal cell bodies (0.3 μm each, total thickness 2.7 μm) of control and OGD slices. The images clearly show that in control conditions phospho-mTOR was present both in the cell body (Figure 44E, open arrow) and in the dendrites (Figure 44E, white arrows), while 3 h after 7 min OGD activation of mTOR decreased both in cell body and dendrites (Figure 44F). Quantitative analysis showed that in slices harvested 1 h after the end of 7 min OGD, no significant modification of activated mTOR immunostaining was present in the neuronal cell body (Figure 44G) or in the apical dendrites of CA1 pyramidal neurons in any of the groups investigated (Figure 44I). On the contrary, in slices harvested 3 h after the end of 7 min OGD, we found highly significant decrease of activated mTOR immunostaining in the cytoplasm and dendrites of CA1 pyramidal neurons (Figures 44H,J). Indeed, statistical analysis, shown in Figure 44H, demonstrates that 3 h after the end of 7 min OGD there was a statistically significant reduction of activated mTOR immunostaining in the cytoplasm of CA1 pyramidal neurons (-74.8%, $^{***}P < 0.001$ *vs.* control slices, Figure 44H) in comparison to control slices. As shown in Figure 44H, treatment with 50 nM PSB603 blocked this effect (-4% *vs.*

control slices, ns, $^{\$\$\$}P < 0.001$ *vs.* 7 min OGD), while treatment with 500 nM MRS1754 partially, but still significantly attenuated this effect (-31% *vs.* controls, ns, $^{\#\#}P < 0.01$ *vs.* 7 min OGD).

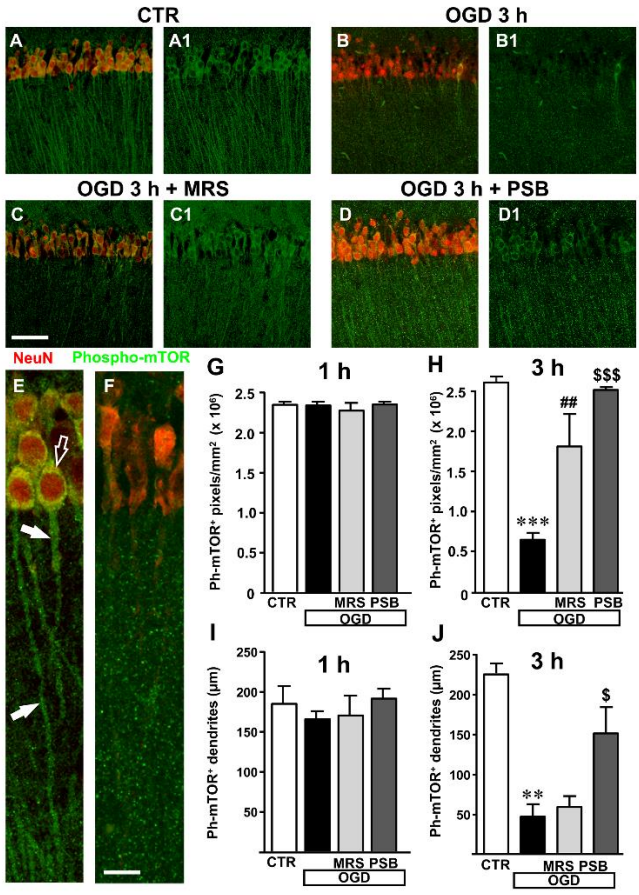

Figure 44: mTOR activation in CA1 stratum pyramidale and stratum radiatum after the simil-ischemic insult. Representative microphotographs, taken at the laser scanning confocal microscope, showing immunolabelling with anti-NeuN antibody (red) and anti-phospho-mTOR antibody (green) of a control slice (A,A_1), a slice harvested 3 h after 7 min OGD (B,B1), a slice treated with MRS1754 and harvested 3 h after 7 min OGD (C,C1), and a slice treated with PSB603 and harvested 3 h after 7 min OGD (D,D1). Scale bar: 75 µm. (E,F) Digital subslices of a control slice (E) and a slice collected 3 h after 7 min OGD (F) immunostained for phospho-mTOR (green) and NeuN (red). The open arrow shows the presence of activated mTOR in the cell body and arrows in the dendrites of pyramidal neurons in the control slice (E). (G,H) Quantitative analysis of activated mTOR in CA1 stratum pyramidale in the different experimental conditions. Each column represents the $mTOR^+$ immunofluorescent area calculated using the ImageJ program (number of pixels above a reference, fixed threshold). (G) No difference among the four experimental groups, was found 1 h after the end of 7 min OGD. Statistical analysis: One-way ANOVA: $F(3;11) = 0.4563$, $P > 0.05$, ns. (H) Slices harvested 3 h after the end of 7 min OGD. Note the significant decrease of activated mTOR in CA1 pyramidal neurons 3 h after the end of OGD. Both MRS1754 and PSB603 significantly blocked this effect. Statistical analysis: One-way ANOVA: $F(3;10) = 26.99$, $P < 0.001$, Newman–Keuls multiple comparison test: $^{***}P < 0.001$, OGD *vs.* CTR; $^{\#\#}P < 0.01$, OGD+MRS *vs.* OGD; $^{\$\$\$}P < 0.001$, OGD +PSB *vs.* OGD. CTR, n = 4; OGD, n = 3; OGD+PSB, n = 3; OGD+MRS, n = 4. All data are expressed as mean ± SEM. (I,J) Quantitative analysis of phospho-$mTOR^+$ dendrites in CA1 stratum radiatum in the different experimental conditions. (I) Length of phospho-$mTOR^+$ dendrites in CA1 stratum radiatum 1 h after the end of 7 min OGD. No difference among the four experimental groups was observed. Statistical analysis: One-way ANOVA: $F(3;11) = 0.7143$, $P > 0.05$, ns. (J) Length of $mTOR^+$ dendrites in CA1 stratum radiatum 3 h after the end of 7 min OGD. Note the significant decrease of activated mTOR in dendrites 3 h after the end of OGD. PSB603 significantly blocked this effect. Statistical analysis: One-way ANOVA: $F(3;9) = 12.38$, $P < 0.02$, Newman–Keuls multiple comparison test: $^{**}P < 0.01$, OGD *vs.* CTR; $^{\$}P < 0.05$, OGD+PSB *vs.* OGD. CTR, n = 3; OGD, n = 3; OGD+PSB, n = 3; OGD+MRS, n = 4. All data in the graphs are expressed as mean ± SEM.

We used, as a determinant of mTOR activation in the dendrites, the analysis of the length of phospho-mTOR positive dendrites, as reported in the methods. The results shown in Figure 44I reveal that mTOR activation was not statistically significant among the four experimental groups 1 h after the end of 7 min OGD. However, in the slices collected 3 h after the end of 7 min OGD we found a significant decrease of mTOR positive dendrites in the stratum radiatum of the CA1 area (Figure 44J). From the statistical analysis we demonstrated a significant decrease of mTOR immunopositive dendrites in CA1 stratum radiatum of 7 min OGD slices 3 h after the end of OGD (-80% *vs.* controls, $^{**}P < 0.01$, Figure 44J). The selective antagonist MRS1754, did not significantly modify this effect, while treatment with PSB603 partially, but significantly, reversed this effect (+226% *vs.* 7 min OGD, $^{\$}P < 0.05$). These data demonstrate that OGD significantly decreased mTOR activation and that the selective antagonism selective antagonism of A_{2B}AR significantly reduced this impairment, a further indication of prevention of neuronal degeneration by blockade of this receptor.

1.6 Analysis of astrocytes in CA1 stratum radiatum after 7 min OGD

Astrocytes were labeled with the anti-GFAP antibody and quantified in the stratum radiatum of CA1 hippocampus in the four experimental conditions: in control slices, in slices after 7 min OGD alone, and after 7 min OGD in the presence of 500 nM MRS1754 or 50 nM PSB603, both at 1 and 3 h after the end of OGD, as shown in the representative microphotographs in Figures 45A–D, taken at 3 h after the end of OGD.

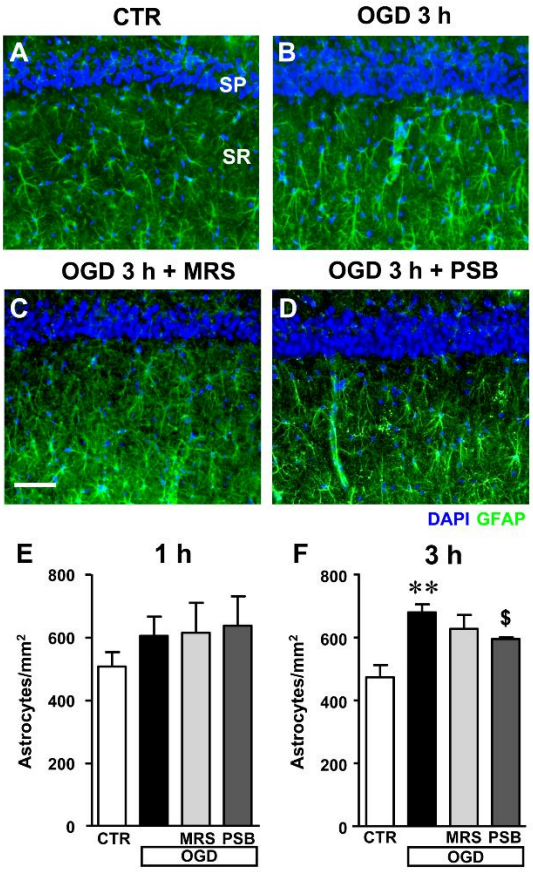

Figure 45: Quantitative analysis of astrocytes in the CA1 area in the different experimental conditions after the simil-ischemic insult. (A–D) Representative microphotographs, taken at the epifluorescence microscope, of astrocytes immunolabelled with anti-GFAP antibodies in the stratum radiatum (green) of a control (A), OGD (B), OGD plus MRS1754 (C), and OGD plus PSB603 (D) slice. Scale bar: 50 µm. (E,F) Quantitative analysis of astrocytes in the stratum radiatum of CA1 in control, OGD, OGD plus MRS1754, and OGD plus PSB603 slices at 1 h (E) and 3 h (F) after 7 min OGD. (E) No significant differences among the four experimental groups analyzed was found. Statistical analysis: One-way ANOVA: $F(3;18) = 0.877$, $P > 0.05$, ns. CTR, n = 8; OGD, n = 7; OGD+PSB, n = 3; OGD+MRS, n = 4. (F) Statistical analysis: One-way ANOVA: $F(3;15) = 6.734$, $P < 0.01$, Newman–Keuls multiple comparison test: $^{**}P < 0.01$, OGD *vs.* CTR; $^{\$}P < 0.05$, OGD+PSB *vs.* OGD. CTR, n = 7; OGD, n = 4; OGD+PSB, n = 4; OGD+MRS, n = 4. All data in the graphs are expressed as mean ± SEM.

In the stratum radiatum of slices harvested 1 h after the end of 7 min OGD we found a slight, not significant increase of astrocytes (Figure 45E, +19%, ns *vs.* controls), which became significant at 3 h after the end of 7 min OGD (Figure 45F, +43% *vs.* control slices, $^{**}P < 0.01$). Both A_{2B}AR antagonists, partially but significantly, reduced the increase of astrocytes caused by the simil-ischemic conditions. MRS1754 decreased the number of astrocytes by 10% (ns *vs.* OGD), while PSB603 by 13% ($^{\$}P < 0.05$ *vs.* OGD). Quantitative analysis of total microglia did not reveal statistically significant modifications in the different experimental conditions both at 1 and 3 h after the end of 7 min OGD (data not shown).

1.7 Neurodegeneration of CA1 pyramidal neurons induced by glutamate was not prevented by A_{2B}AR *antagonists*

In order to have an insight into the mechanism of A_{2B}AR antagonism-induced neuroprotection, we verified whether MRS1754 and PSB603 might protect CA1 pyramidal neurons from the well-known neurodegenerative effects caused by glutamate exposure. We incubated the hippocampal slices *in vitro* with 100 μM glutamate for 10 min and verified the effect of MRS1754 and PSB603 on glutamate-induced cell death (Figures 46A–D).

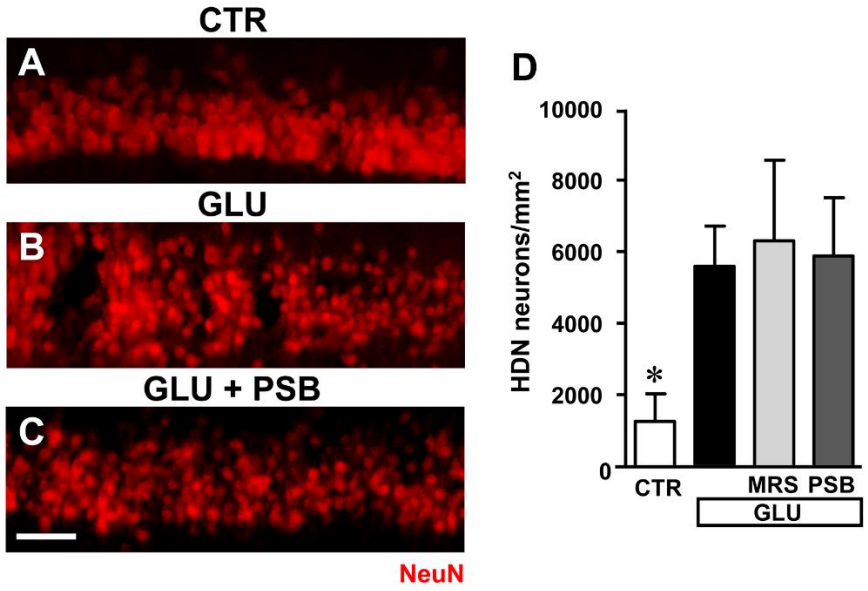

Figure 46: Evaluation of glutamate induced neurotoxicity in CA1 stratum pyramidale in the different experimental conditions. (A–C) Representative microphotographs, taken at the epifluorescence microscope, of CA1 pyramidal neurons immunolabelled with anti-NeuN antibodies in a control slice (A), a slice treated with glutamate (GLU, B), a slice treated with glutamate plus PSB603 (GLU+ PSB, C) slice. Scale bar: 50 μm. (D) Quantitative analyses of $NeuN^+$ HDN neurons in the four experimental groups 3 h after the end of drug incubation. Statistical analysis: One-way ANOVA: $F(3;15) = 3.313$, $P < 0.05$, Newman–Keuls multiple comparison test: $^*P < 0.05$, *vs.* all other groups. CTR, n = 6; GLU, n = 6; GLU+PSB, n = 3; GLU+MRS, n = 4.

Administration of 100 μM glutamate for 10 min caused significant damage to pyramidal neurons at 3 h after the end of incubation, evidenced by the significant increase of HDN neurons in hippocampal CA1, as shown in the representative image presented in Figure 46B. Quantitative analysis (Figure 46D) demonstrated that the increase of HDN neurons was statistically significant in comparison to control slices, and that neither MRS1754 nor PSB603 protected CA1 pyramidal neurons from the excitotoxic effect of glutamate ($^*P < 0.05$ *vs.* all other groups).

1.8 Discussion

The putative protective role of adenosine A_{2B}AR in cerebral ischemia was studied in the CA1 region of hippocampal slices under oxygen-glucose deprivation, an experimental condition that mimics, albeit with the limits of *in vitro* methodology, the most common causes of cerebral ischemia, such as vessel occlusion. *In vitro* slices give a partial view of the physiology of the brain because of the absence of an intact vascular system and the altered tridimensional microenvironment. These alterations involve not only neurons but also glia, and more generally the physiology of the neurovascular unit formed by astrocytes, pericytes, microglia, neurons, and the extracellular matrix (Holloway and Gavins, 2016). Nevertheless, the *in vitro* systems have many benefits such as the opportunity to obtain highly valuable information in terms of the time-course of the electrophysiological events, changes in membrane potential (AD), changes in synaptic transmission and morphological and biochemical changes in neurons and glia. Our results confirm that in the CA1 region of rat hippocampus, the application of a 7 min OGD episode induced the appearance of AD which was followed by irreversible synaptic damage and neurodegeneration of CA1 pyramidal neurons (Coppi *et al.*, 2007; Pugliese *et al.*, 2009, 2006, 2003; Traini *et al.*, 2011).

We now demonstrate that these events are accompanied by neurodegeneration of CA1 pyramidal neurons, with reduction of neuronal density and significant increase of apoptotic neurons. For the first time we demonstrated here that antagonism of $A_{2B}AR_S$ using the selective ligands MRS1754 or PSB603, applied before, during and after OGD, prevented or delayed the appearance of AD, and prevented the irreversible loss of neurotransmission induced by 7 min OGD. Furthermore, we demonstrated that the selective blockade of $A_{2B}AR_S$ during a prolonged (30 min) OGD insult delays the appearance of AD indicating an extension of the time window between the start of the insult and the appearance of excitotoxic damage. Adenosine A_{2B}AR antagonism also counteracted the reduction of neuronal density in CA1 stratum pyramidale and decreased apoptosis mechanisms at least up to 3 h after the end of the insult. Both A_{2B}AR antagonists did not protect CA1 neurons from neurodegeneration induced by glutamate application, indicating that the antagonistic effect is upstream of glutamate release. The hippocampus, and particularly CA1 stratum pyramidale, is one of the most vulnerable brain regions to ischemic damage. We used the acute rat hippocampal slice preparation which allows measurements of synaptic transmission with good spatial and temporal resolution. In the early phases, hypoxia/ischemia is known to induce a massive increase of extracellular glutamate levels which trigger hyperactivation of glutamate receptors, production of reactive oxygen species, pathological increase of intracellular Ca^{2+}, rapid decrease in ATP reserves and activation of various proteolytic enzymes (Al-Majed *et al.*, 2006; Káradóttir *et al.*, 2005; Kovacs *et al.*, 2006). In hippocampal slices, a severe OGD insult as that applied in the present experiments (7 min) elicits the appearance of AD within the OGD period and is invariably followed by irreversible loss of neurotransmission (Frenguelli *et al.*, 2007; Pugliese *et al.*, 2007, 2009), an index of cell suffering, damage to neurons and to the surrounding tissue (Somjen, 2001). AD is caused by the sudden increase of extracellular K^+ and by the contemporary explosive rise in glutamate extracellular

concentration (Somjen, 2001). Contemporarily to the extracellular increase of glutamate, the extracellular concentration of adenosine significantly increases, as demonstrated both in *in vivo* and *in vitro* experiments (Latini and Pedata, 2001). After 5 min OGD, adenosine reaches an extracellular concentration of 30 μM in hippocampal slices (Latini *et al.*, 1999; Pearson *et al.*, 2006). At such high concentration adenosine can stimulate all receptor subtypes, including the A_{2B}AR, which exhibits affinity for adenosine with an EC_{50} in the range of 5–20 μM, lower than all other subtypes (Fredholm *et al.*, 2011). For this reason, it is possible that activation of $A_{2B}AR_S$ occurs mainly during pathological conditions, such as inflammation, hypoxia, trauma, and ischemia (Fredholm *et al.*, 2001).

Our data show that A_{2B}AR antagonists, by preventing or delaying the onset of AD, prevent the irreversible loss of neurotransmission induced by 7 min OGD allowing complete recovery of synaptic potentials. We showed for the first time a partial recovery of neurotransmission was also observed in a group of hippocampal slices, treated with A_{2B}AR antagonists, that developed AD immediately after reoxygenation. This delay of AD appearance might account for the partial recovery of neurotransmission observed in these slices. The occurrence of AD after the end of OGD period is a peculiar characteristic that we observed in our hippocampal preparation. We envisage that when the AD appears during the reoxygenation period, similarly to the phenomenon of spreading depression (Somjen, 2001), neurons are less damaged, and they can partially recover their electrical activity. Thus, even in those slices treated with the A_{2B}AR antagonists in which AD takes place, this event is less harmful to neuronal viability. This is a substantial difference from A_{2A}AR antagonist-mediated neuroprotection during a 7 min OGD insult. Indeed, fEPSP recovery was never observed in those few slices undergoing AD in the presence of the A_{2A}AR blocker ZM241385, as previously published (Pugliese *et al.*, 2009).

As to the mechanism by which A_{2B}AR antagonists protect from hypoxia/ischemia, recent studies (Gonçalves *et al.*, 2015) have demonstrated that in mouse hippocampus A_{2B} AR_S are expressed on glutamatergic terminals anatomically comparable to those from which our recordings were performed. Their selective stimulation counteracts the predominant A_1AR-mediated inhibition of synaptic transmission. We confirmed this assumption by performing PPF experiments in rat hippocampal slices in which the A_{2B}AR agonist BAY606583 was able to reduce PPF ratio, which is known to be caused by increased glutamate release at presynaptic level. This effect is counteracted not only by the A_{2B}AR antagonists MRS1754 and PSB603 but also by the A_1AR antagonist DPCPX. As already hypothesized (Moriyama and Sitkovsky, 2010; Gonçalves *et al.*, 2015), this result may be related to the existence of an A_1/A_{2B}AR heterodimer in the CA1 hippocampal region. On these bases, our purpose was to study the possible involvement of A_1AR_S in the neuroprotective effects elicited by the two A_{2B}AR antagonists during OGD. In accordance to data reported by Canals (Canals *et al.*, 2008) in a model of chemical penumbra produced by a mitochondrial gliotoxin in the hippocampus *in vitro*, we would have expected conservation of synaptic transmission during the first min of OGD and acceleration of AD appearance. In our conditions, a similar response was observed

only in a limited number of slices during 7 min OGD. Instead, in most of the slices we demonstrated that DPCPX induced neuroprotection during OGD, delaying AD appearance. This unexpected result may be due to a different response of A_1AR_S during OGD in our experimental conditions. Our data could also be explained considering the results obtained by Sperlágh (Sperlágh *et al.,* 2007) who demonstrated that DPCPX decreases glutamate release from hippocampal slices subjected to OGD and that this effect is mimicked and occluded by the A_{2A}AR antagonist ZM241385. The same Authors hypothesize that DPCPX, even at low nanomolar concentrations, would directly bind to $A_{2A}AR_S$ during severe ischemia (in accordance with our previously published results, Pugliese *et al.,* 2009). The rational for this assumption is that the A_{2A}AR agonist CGS21680 displays two distinct binding sites in the hippocampus: a "typical" (striatal-like) binding site which is displayed by DPCPX only at high (submicromolar) concentrations, and an "atypical" binding site, which shows high affinity for DPCPX (Cunha *et al.,* 1996; Johansson and Fredholm, 1995).

On these bases, we can hypothesize that, in our OGD experiments, DPCPX binds to this "atypical" binding site (i.e., an A_1–A_{2A}AR heterodimer) thus decreasing glutamate outflow and protecting hippocampal slices from OGD insults. Furthermore, when overstimulated such as during ischemia, A_1AR_S undergo desensitization (Siniscalchi *et al.,* 1999). This phenomenon can be further increased by $A_{2B}AR_S$ activation, triggering a vicious circle in which the beneficial effect of A_1AR stimulation is overcome by the noxious effect of A_{2B}AR activation (Gonçalves *et al.,* 2015) as already suggested for $A_{2A}AR_S$ (Pugliese *et al.,* 2009). Further mechanistic studies suggest that the A_{2A}AR, when stimulated, facilitates A_{2B} receptor externalization from the endoplasmic reticulum to the plasma membrane, possibly increasing the formation of the A_{2A}–A_{2B} dimer (Moriyama and Sitkovsky, 2010). All these results taken together may explain the deleterious activity of adenosine A_{2B}AR stimulation during an ischemic insult, and the protective effect of A_{2B}AR antagonists in this condition. Finally, observation that the A_{2B}AR antagonists did not protect CA1 neurons from neurodegeneration induced by direct glutamate application, confirms that the mechanism underlying their protection against ischemia-induced neurodegeneration is exerted at adenosine receptors that, by the abovementioned mechanisms, regulate extracellular glutamate release. Alternatively, since OGD is above all a problem of efficient energy recovery, the demonstration that $A_{2B}AR_S$ control astrocytic and neuronal glycogen metabolism (Allaman *et al.,* 2003; Magistretti *et al.,* 1986) and glucose utilization by hippocampal slices (Lemos *et al.,* 2015) may suggest an additional effect of these receptors on metabolic activity during OGD.

Severe OGD increased apoptosis and damaged CA1 pyramidal neurons at 1 and 3 h after the end of the ischemic insult. Immunohistochemistry showed that CA1 pyramidal neurons had significant morphological changes, with increased density of nuclei (HDN neurons), karyorrhexis (LDN neurons) and possibly nuclear fragmentation, as evidenced by the significantly higher number of LDN neurons and cell death after OGD. These results are in agreement with those found by Ünal-Çevik (Unal-Cevik *et al.,* 2004) in the cerebral cortex of the rat after mild ischemia. Pyknosis is typical of apoptotic cells (Elmore, 2007) and may precede karyorrhexis. We demonstrated that LDN

neurons, being highly positive for CytC, were undergoing apoptosis. It has been demonstrated that CytC released into the cytosol binds to apoptotic protease activating factor-1, which leads to activation of caspase-9 which is important in neuronal cell death following ischemia (Jiang and Wang, 2004; Kluck *et al.*, 1997; Lana *et al.*, 2017a, 2017b, 2016, 2014; Love, 2003; Suen *et al.*, 2008; Yang *et al.*, 1997).

In turn, caspase-9 is activated by high glutamate levels, as occurs during ischemia (Li *et al.*, 2009). As reported in the literature, activation of mTOR, which has multiple roles in cells among which local protein synthesis at the dendritic and spine level (Frey and Morris, 1997; Thoreen *et al.*, 2012; Tsokas *et al.*, 2007) can be modified in ischemic conditions (Dennis *et al.*, 2001; Laplante and Sabatini, 2012). As already reported (Gegelashvili *et al.*, 2001; Maragakis and Rothstein, 2004), the decrease of mTOR activation may be secondary to the excitotoxic mechanisms evoked by massive increase of glutamate during OGD, which is known to be an important component of neuronal injury *in vitro* (Newell *et al.*, 1995). The participation of decreased mTOR activation in OGD-induced neuronal damage is supported by our results showing decreased activation of mTOR both in the cell body and dendrites of CA1 neurons 3 h after the end of OGD. Within the limits of the *in vitro* model and the alteration of the neurovascular unit and of neuro glia interplay, we found interesting effects on astrocytic responses. Indeed, astrocytes proliferation, possibly caused, among other stimuli, by increased release of glutamate, is one of the early events that takes place after acute focal CNS damage (Burda and Sofroniew, 2014). In accordance to our previous results (Pugliese *et al.*, 2009), we found evidence of significant, although limited, astrocytic proliferation in CA1 stratum radiatum already 3 h after the end of OGD, possibly caused by increased glutamate release. A_{2B}AR antagonism significantly prevented all the above neuronal and astrocytic modifications, sparing neurons from the degenerative effects caused by the simil-ischemic conditions, and reducing astrocytes proliferation. CA1 pyramidal neurons treated with the A_{2B}AR antagonists had a similar morphology to those of control slices, had neither increased nor decreased nuclear density, did not undergo apoptosis, and had activated mTOR levels similar to those of controls.

The similar effects obtained using two different A_{2B}AR antagonists strengthen the hypothesis that the A_{2B} receptor is involved in the mechanisms of cerebral ischemia. Nevertheless, MRS1754 seems to have lower efficiency than PSB603 on some of the parameters investigated. It is possible that the two drugs act with a different time-course or that PSB603 is more efficacious than MRS1754 in this model. In summary, our data demonstrate that antagonists of adenosine A_{2B}AR protect the CA1 area of the hippocampus from an acute damage induced by severe hypoxic/ischemic conditions. The mechanism likely resides in protection from the acute increase of glutamate extracellular concentrations and consequent excitotoxicity. It is worth noticing that since $A_{2B}AR_S$ have low affinity for the endogenous ligand adenosine, they are activated only at high extracellular adenosine concentrations that can be reached under pathological conditions such as ischemia, thus representing a selective target (Popoli and Pepponi, 2012).

Chapter 2: *Role of A_{2B}AR on CA1 hippocampal transmission and paired pulse facilitation*

Functional characterization of a novel adenosine A_{2B}R agonist, P453, by paired pulse facilitation at Schaffer collateral-CA1 synapses.

2. Results

2.1 Adenosine A_{2B}AR stimulation reduced paired-pulse facilitation (PPF) in acute rat hippocampal slices.

Previous work on A_{2B}ARs demonstrated that their activation inhibits PPF evoked at Schaffer collateral synapses in the mouse CA1 hippocampus (Gonçalves *et al.*, 2015). We recently confirmed these data by applying the prototypical A_{2B}AR agonist BAY606583 (200 nM) on rat hippocampal slices. In the present work we functionally characterized the newly synthesized A_{2B}AR agonist P453 (50 nM) (see Betti *et al.*, 2018) by comparing their effects with that of BAY606583 (200 nM) in the same experimental protocol, i.e. PPF in acute rat hippocampal slices. All compounds were applied either under basal Schaffer collateral fibre stimulation (once every 15 s) or during PPF protocol (experimental procedure shown in Figure 15A, see pag. 58 in Materials and methods). As shown in Figure 47, none of the A_{2B}AR agonists affected basal synaptic transmission. At variance, when tested on PPF protocol, all compounds reduced PPF.

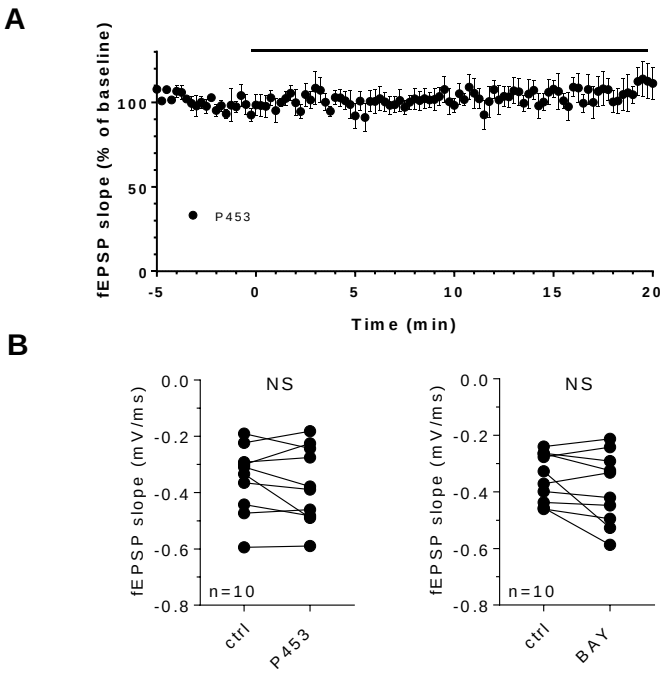

Figure 47: Selective A_{2B}AR activation does not affect basal synaptic neurotransmission in the CA1 hippocampus. (A) Averaged time course of fEPSP slope measured during Schaffer collaterals stimulation in conditions of basal synaptic neurotransmission (BSN), evoked once every 15 s, before and during P453 (50 nM, n=10) application. (B) Pooled data of fEPSP slope, measured 5 min before and during the last 5 min of a 20 min application of the A_{2B}AR agonists P453 (50 nM: left panel) or BAY606583 (200 nM: right panel). No significant difference was found in fEPSP slope measured in the absence or presence of either of the A_{2B}AR agonists when basal synaptic activity was evoked once every 15 s. Paired Student's t-test.

Indeed, 50 nM P453 significantly decreased P2/P1 ratio of fEPSP slope measured at the end of a 20 min application *vs* respective pre-drug, baseline, values in 9 slices tested (Figure 48A1 and 48B2). This effect was prevented when P453 was applied in the presence of either of the two selective A_{2B}R antagonists PSB603 (50 nM: Figure 48A2 and 48B3) or MRS1754 (500 nM: Figure 48B4), thus confirming a receptor mediated effect. Since previous data showed that A_{2B}AR -dependent reduction of PPF at CA1 synapses depends upon inhibition of adenosine A_1AR inhibitory control of glutamate release (Fusco *et al.*, 2018; Gonçalves *et al.*, 2015), we tested whether P453-mediated effect was sensitive to the selective A_1AR antagonist DPCPX. As shown in Figure 48B5, DPCPX (100 nM) blocked the decrease in PPF upon P453 application.

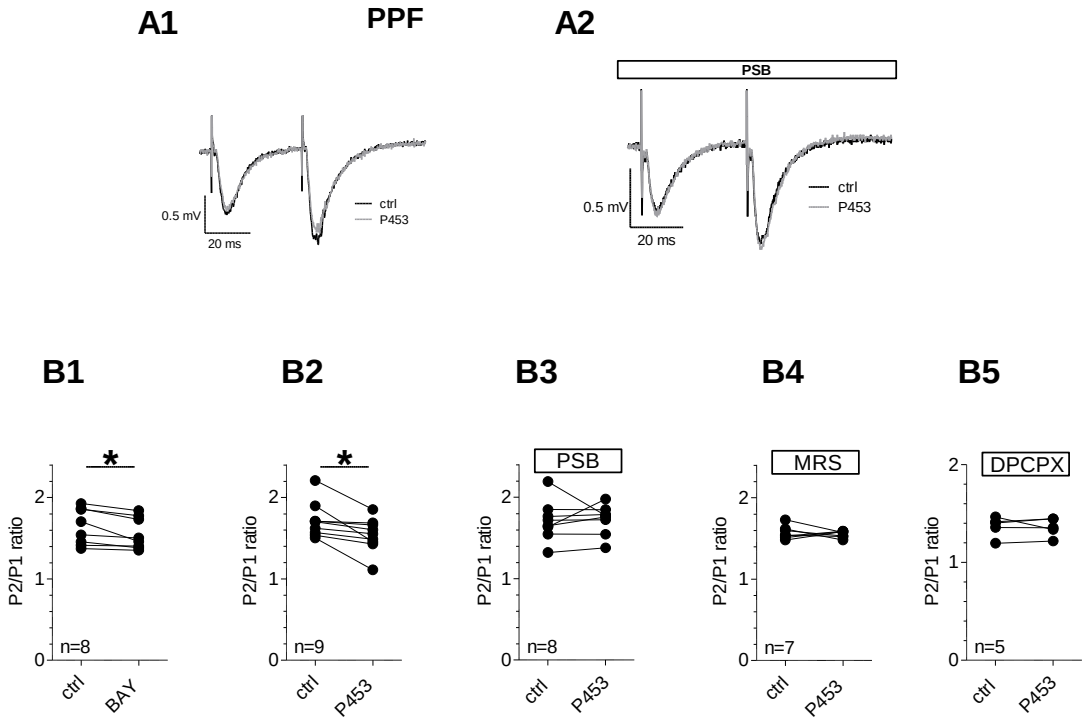

Figure 48: The newly synthesized A_{2B}AR agonist P453 reduces paired-pulse facilitation in acute rat hippocampal slices. (A) Representative traces of fEPSP responses evoked by a paired-pulse facilitation (PPF) protocol (40-ms interval) in two typical hippocampal slice where the A_{2B}AR agonist P453 (50 nM) was applied in the absence (A1) or in the presence (A2) of the A_{2B}AR antagonist PSB603 (PSB: 50 nM). (B) Each graph shows PPF quantified as the ratio (P2/P1) between the slope of the second fEPSP (P2) and the first fEPSP (P1) in different experimental conditions. B1: before (control: ctrl) or after the application of BAY606583 (200 nM: n = 8), **P* = 0.0138, paired Student's t-test. B2: before (control: ctrl) or after P453 (50 nM) application in the absence (n = 9) or in the presence of 50 nM PSB (B3: n = 8), 500 nM MRS1754 (MRS, n=7) or 100 nM DPCPX (B5, n=5). Note that the decrease of P1/P2 ratio induced by P453 (**P* = 0.0121, paired Student's t-test) is prevented in the presence of either of the A_{2B}AR antagonists PSB or MRS and also by the A_1AR antagonist DPCPX.

2.2 Discussion

Present results confirm previous observations (Gonçalves *et al.*, 2015; Fusco *et al.*, 2018) that selective A_{2B}AR stimulation tested in the short term synaptic plasticity paradigm, of PPF, causes a reduction in the P2/P1 ratio of fEPSP slope at mouse Schaffer collateral-CA1 synapses when stimulated by a paired pulse protocol. Furthermore, we provide first evidence about the functional effect of the newly synthesized A_{2B}AR agonist, P453, on PPF, at Schaffer collaterals-CA1 synapses. The compound mimicked BAY606583 in inhibiting PPF at Schaffer collateral-CA1 synapses and the effect was sensitive to the A_{2B}R antagonists PSB603 and MRS1754 and also to the A_1AR antagonist DPCPX, as already described for BAY606583 (Fusco *et al.*, 2018; Gonçalves *et al.*, 2015). It is well known that a reduction in PPF reflects an increase in quantal release of glutamate at presynaptic level (Debanne *et al.*, 1996). Our results are in agreement with evidence demonstrating that Gs-coupled receptors, as the A_{2B}AR subtype, promote glutamatergic neurotransmission at CA1 synapses. As an example, the adenosine A_{2A}AR, also coupled to Gs proteins, shares with A_{2B}ARs the inhibitory effect on PPF at Schaffer collaterals (Lopes *et al.*, 2002). This effect can be explained by Ca^{2+} channel inhibition upon Gs coupled receptor activation (Rosenthal *et al.*, 1988), and in particular upon A_{2B}AR activation. Not surprisingly, none of the A_{2B}AR agonists tested influenced basal synaptic transmission evoked in the CA1 area by Schaffer collateral fibres stimulation, in line with previous works (Gonçalves *et al.*, 2015).

PPF is a model of short-term synaptic plasticity related to pre-synaptic function known to participate to a number of cognitive processes, from information transfer to neural processing. The interaction between facilitation and feed-forward inhibition may play a fundamental role in encoding spatial information in the hippocampus. Facilitation is also proposed to play a critical role in working memory, involving the short-term storage of information for subsequent manipulation and decision-making (Bueno-Junior and Leite, 2018). Our results suggest a fine-tuning role of synaptic A_{2B}AR activation on the short term synaptic plasticity phenomena in the CA1 hippocampus.

Due to their low affinity for the endogenous ligand, A_{2B}ARs are expected to be of relevance during pathological conditions affecting the CNS, such as acute brain trauma, ischemic insults or neurodegeneration when a massive release of adenosine occurs and modulation of glutamate release is relevant in mechanisms of neurodegeneration and cognition.

Chapter 3: *Role of A_{2B}AR on cell differentiation in cultured OPC_S by modulating SphK1 signaling pathway.*

A_{2B}AR activation reduces outward K^+ currents and cell differentiation in cultured OPC_S by modulating SphK1 signaling pathway.

3. Results

3.1 Selective A_{2B}AR stimulation inhibits outward K^+ currents in cultured OPCs.

The electrophysiological study was performed on 165 cells showing, on average, a Vm of 52.8 ± 1.1 mV, a Cm of 6.3 ± 0.2 pF of and a Rm of 845.7 ± 97.2 MΩ. All experiments were performed in the continuous presence of the A_1, A_{2A} and A_3AR antagonists DPCPX, SCH58261 and MRS1523, respectively (all 100 nM).

In a first set of experiments we applied a voltage ramp protocol (from -120 to +80 mV, 800 ms duration: inset of Figure 49A) in cultured OPCs, in the absence or presence of the selective A_{2B}AR agonist BAY606583 (10 μM), in order to investigate whether this receptor modulates voltage-dependent currents in cultured OPC cells. As shown in Figure 49A, the compound reversibly inhibited ramp-evoked outward currents in a typical OPC cell. BAY606583-sensitive current, obtained in the same cell by subtraction of the ramp recorded in the presence of the A_{2B}AR agonist from the control ramp, is a voltage-dependent outward conductance with an activation voltage around -20 mV (Figure 49B). The maximal effect of BAY606583 was reached within 5 min of application (inset of Figure 49A) and was statistically significant in 51 cells investigated (Figure 49C inset: from 227.8 ± 28.1 pA/pF in control to 135.2 ± 22.2 pA/pF in 10 μM BAY606583 at +80 mV, ***P<0.001, paired Student's t-test, 41.9 ± 2.8% current inhibition in BAY606583).

Outward currents evoked by the voltage ramp protocol were absent when extra- and intra-cellular K^+ ions were replaced by equimolar Cs^+ (Figure 49D). Furthermore, under these experimental condition, the effect of BAY606583 was blocked (Figure 49D: current amplitude at +80 mV was 27.3 ± 2.4 pA/pF in control and 24.5 ± 3.1 pA/pF in 10 μM BAY606583, P>0.05, paired Student's t-test, n=3) demonstrating that ramp-evoked outward currents inhibited by BAY606583 are carried by K^+ ions.

In accordance with K^+ current inhibition, OPCs depolarized by 9.8 ± 1.8 mV in the presence of 10 μM BAY606583, as reported in Table 7. This membrane potential depolarization (from -53.8 ± 1.8 to -44.0 ± 2.3 mV) was statistically significant in the 51 cells investigated (from -53.8 ± 1.8 to -44.0 ± 2.3 mV, P<0.0001, paired Student's t-test).

The effect of BAY606583 on outward K^+ currents was concentration-dependent, with an EC_{50} = 0.6 μM (Figure 49E: confidence limits: 0.04 – 9.4 μM), and prevented by the selective A_{2B}AR antagonist MRS1706 (Figure 49F). In accordance, BAY606583-mediated Vm depolarization was prevented in the presence of MRS1706 (Table 7).

Table 7.

	Vm (mV)	n
Ctrl	-53.8 ± 1.8	51
10 µM BAY	-44.0 ± 2.3 ****	51
Ctrl	-54.9 ± 2.9	23
50 nM P453	-43.0 ± 4.1 **	23
1706	-51.7 ± 8.3	7
1706 + 10 µM BAY	-50.3 ± 6.7 **	7

Table 7. Effect of selective A_{2B}AR stimulation on membrane potential (Vm) in cultured OPCs. ctrl: control; BAY: BAY606583 (10 µM); P453 (50 nM); 1706: MRS1706 (10 µM). Vm was calculated as the "zero current potential" during each ramp episode before and after drug application. Ctrl Vm value was measured as the "zero current potential" or ramps recorded during the last min preceding drug application. Vm values in the presence of A_{2B}AR agonists were the measured between 4 and 5 min of drug application. $^{**}P$=0.0011; $^{****}P$<0.0001 vs ctrl, paired Student's t-test.

Surprisingly, other two highly selective and widely used A_{2B}AR antagonists, PSB603 and MRS1754, were ineffective in preventing BAY606583-induced inhibition of outward K^+ currents in OPCs up to supramaximal concentration (10 µM: see Table 8).

Table 8.

	n	current at +80 mV (pA/pF) in control	current at +80 mV (pA/pF) in BAY	BAY-inhibited current at +80 mV (pA/pF)	% inhibited current at +80 mV
1 µM BAY	16	227.0 ± 34.7	161.1 ± 24.8**	65.9 ± 20.5	25.8 ± 4.1
+ 1 µM PSB	3	367.7 ± 19.6	257.3 ± 6.7*	110.5 ± 26.3	35.5 ± 5.7
+ 500 nM 1754	3	352.5± 98.5	166.5 ± 57.9*	186.0 ± 52.0	35.5 ± 8.1
10 µM BAY	51	227.8 ± 28.1	135.2 ± 22.2***	92.6 ± 10.3	41.9 ± 2.8
+ 10 µM PSB	6	217.8 ± 26.2	154.6 ± 34.2*	63.2 ± 26.5	30.4 ± 10.8
+ 10 µM 1754	7	228.5 ± 39.1	152.3 ± 33.3*	76.2 ± 25.6	32.0 ± 10.8
+ 1 µM 1706	5	206.6 ± 39.6	166.2 ± 52.6	40.4 ± 19.5	24.7 ± 12.9
+ 10 µM 1706	5	200.8 ± 11.7	204.2 ± 19.1	-3.4 ± 17.7 #	-0.1 ± 7.3 #

Table 8. Effect of different A_{2B}AR antagonists on BAY606583-mediated inhibition of ramp K^+ currents in cultured OPCs. BAY: BAY606583; PSB: PSB603; 1754: MRS1754; 1706: MRS1706. BAY-inhibited current at +80 mV was measured as the subtraction of current density value recorded at +80 mV in each cell in the presence of BAY from the control value at +80 mV. $^{*}P$<0.05; $^{**}P$<0.01 $^{***}P$<0.001 vs current at +80 mV (pA/pF) in control, Paired Student's t-test; $^{\#}P$<0.05 vs BAY 10 µM alone, One-way ANOVA, Bonferroni post-test.

We further investigated which subtype of K^+ currents were targeted by $A_{2B}AR$ modulation. OPCs are known to express different kinds of K^+ currents, depending upon the step of differentiation. When studied in t_0-t_6 OPCs, two distinct types of K^+ currents were observed: sustained, delayed rectifying, I_K currents and transient, rapidly inactivating, I_A conductances (Knutson *et al.*, 1997; Sontheimer and Kettenmann, 1988). We applied a voltage-step protocol (from -40 to +80 mV, 200 ms step duration, Vh=-80 mV: inset of Figure 49G) in order to activate either peak I_A or steady-state I_K currents, in the absence or presence of 10 μM BAY606583. As shown in Figure 49G, both subtypes of K^+ currents were inhibited in the presence of the $A_{2B}AR$ agonist, with a significant decrease of current density observed starting from the 0 mV step ($P<0.05$, paired Student's t-test) in 16 cells investigated.

Above data were obtained in OPC cultures from t0 to t6, which correspond to the period in which most cells are immature $NG2^+$ OPCs mainly expressing outward rectifying K^+ channels (Coppi *et al.*, 2013a, 2013b). We also tested BAY606583 effects in mature OLGs, grown in differentiating medium up to 15 days (from t_{12} to t_{15}). At this stage, as we previously shown (Coppi *et al.*, 2013a, 2013b), oligodendroglial cultures are mostly composed by highly ramified, Mbp^+ and MAG^+ oligodendrocytes characterized by the appearance, at electrophysiological level, of inwardly rectifying Kir channels, in accordance with previous data (Attali *et al.*, 1997; Gallo *et al.*, 1996; Knutson *et al.*, 1997; Sontheimer and Kettenmann, 1988).

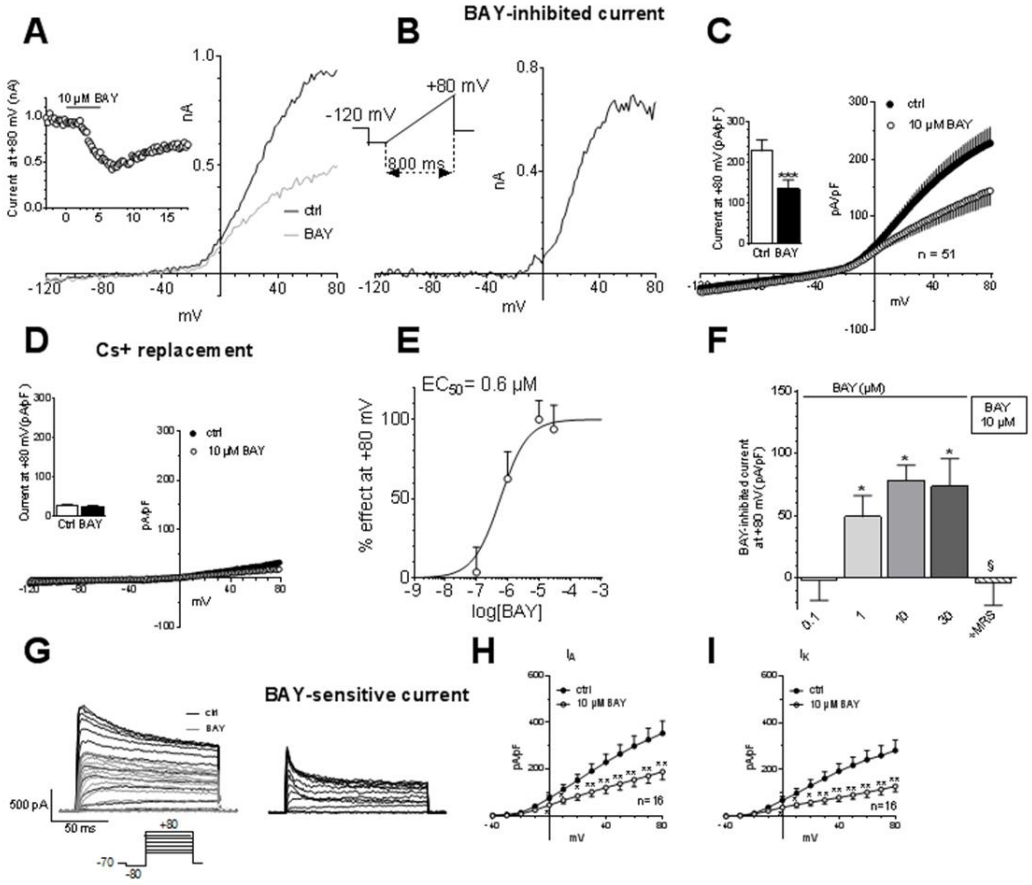

Figure 49: The $A_{2B}AR$ agonist BAY606583 inhibits I_K and I_A outward K^+ currents in cultured OPCs. A. Original whole-cell patch clamp current traces activated by a voltage ramp protocol (from -120 to +80 mV, 800 ms) in a typical OPC before (ctrl) and after BAY606583 (BAY: 10 µM) application (3 min). Inset: time course of ramp-evoked currents at +80 mV in same cell. B. Net BAY606583 inhibited current, obtained by subtraction of the trace recorded in BAY from the control ramp, in the same cell. C. Averaged ramp-evoked currents, and pooled data at +80 mV, recorded in the absence (filled circles and columns) or presence (open circles and columns) of 10 µM BAY in 51 cells investigated. ***P<0.001, paired Student's t-test. D. Averaged ramp-evoked currents and pooled data at +80 mV, recorded in the absence (filled circles and columns) or presence (open circles and columns) of 10 µM BAY in Cs^+-replacement experiments (n=3). E. Concentration-response curve of BAY-mediated inhibition of ramp-evoked outward K^+ currents measured at +80 mV in cultured OPCs. EC_{50} = 0.6 µM, confidence limits = 0.04 – 9.4 µM. At least n=5 for each experimental group. F. Pooled data of BAY606583-sensitive currents measured at +80 mV in the presence of different agonist concentrations or during co-application with the $A_{2B}AR$ antagonist MRS1706 (MRS: 10 µM). *P<0.05 *vs* 0.1 µM BAY606583; §P<0.01 *vs* 10 µM BAY606583, One-way ANOVA, Bonferroni post-hoc test . G. Left panel: original current traces evoked by a voltage-step protocol (from -40 to +80 mV, pre-step -80 mV; 200 ms: upper panel) in a representative cell before (black trace) or after (grey trace) the application of 10 µM BAY606583. Right panel: net BAY-sensitive current, obtained by subtraction of the trace recorded in BAY from the control ramp in the same cell. H-I: Averaged current-to-voltage relationship (I-V plot) of peak, transient, I_A currents (H) or steady-state, sustained, I_K currents (I) recorded in the absence (filled circles) or in the presence (open circles) of 10 µM BAY606583 in 16 cells investigated. *P<0.05; **P<0.01 paired Student's t-test.

As shown in Figure 49A,B, BAY606583 still inhibited outward K^+ currents in mature OLGs at t12 - t15. The effect was significant in 5 cells tested (Figure 50C: from 208.3 ± 15.9 to 98.4 ± 14.2 pA/pF, P=0.0278 paired Student's t-test) and presented a concentration-dependence similar to what observed in immature OPCs (Figure 50D-F: EC_{50}= 2.1 µM, confidence limits: 0.2 – 2.4 µM).

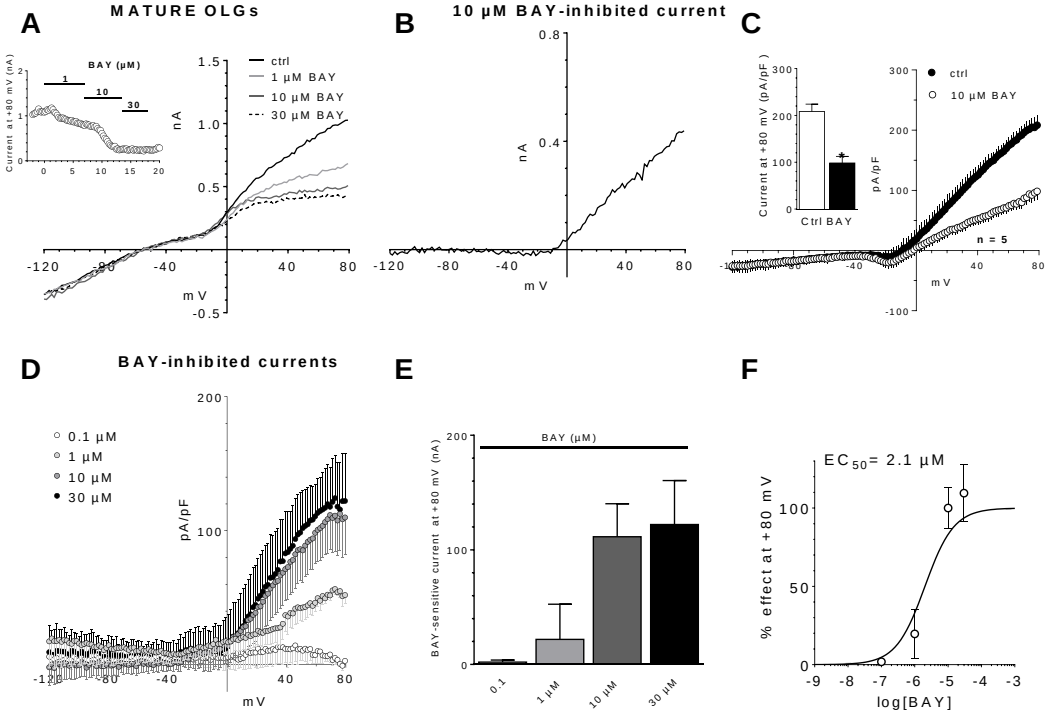

Figure 50: The A_{2B} agonist BAY606583 inhibits I_K and I_A outward K^+ currents in mature OLGs. All experiments were performed in the presence of the A_1, A_{2A} and A_3AR antagonists DPCPX, SCH58261 and MRS1523, respectively (all 100 nM). A. Original whole-cell patch clamp current traces activated by a voltage ramp protocol (from -120 to +80 mV, 800 ms) in a typical OLG before (ctrl) and after BAY606583 (BAY: 1-10-30 µM) application (3 min). Inset: time course of ramp-evoked currents at +80 mV in same cell. B. Net

BAY606583-sensitive current, obtained by subtraction of the trace recorded in 10 µM BAY from the control ramp, in the same cell. C. Averaged ramp-evoked currents, and pooled data at +80 mV, recorded in the absence (filled circles and columns) or presence (open circles and columns) of 10 µM BAY in 5 cells investigated. **P*<0.05, paired Student's t-test. D. Averaged BAY606583-inhibited currents, recorded in the presence of distinct agonist concentrations, in mature OLGs. At least n=4 in each experimental group. E. Pooled data of BAY606583-sensitive currents measured at +80 mV in the presence of different agonist concentrations. F. Concentration-response curve of BAY-mediated inhibition of ramp-evoked outward K^+ currents measured at +80 mV in mature OLGs. EC_{50} = 2.1 µM, confidence limits = 0.02 – 2.4 µM.

The same inhibition of outward K^+ currents observed in the presence of the prototypical A_{2B}AR agonist BAY606583 was observed in the presence of two newly synthesized, highly selective, A_{2B}AR agonists: P453 and P517 (Betti *et al.*, 2018). As shown in Figure 51A, P453 at a concentration of 50 nM significantly inhibited total outward currents evoked by the ramp protocol in 23 OPCs tested. According to BAY606583, also P453 significantly depolarized cell membrane, as reported in Table 7 (11.7 ± 3.0 mV depolarization in 50 nM P453, n=23). The effect was concentration dependent (Figure 51B), blocked by the A_{2B}AR antagonist MRS1706 (Figure 51B) and prevented by Cs^+-replacement of K^+ ions (Figure 51C), thus confirming that A_{2B}AR activation inhibits outward K^+ currents in isolated OPCs. Similarly, P517 inhibited ramp-evoked outward K^+ currents (Figure 51D) and the effect was maximal at 10 µM concentration (Figure 51E). Of note, the current-to voltage (I-V) relationship of A_{2B}AR -inhibited currents (Figure 51F) and the time course of K^+ current inhibition at +80 mV (Figure 51H) were very similar among all the three agonists (BAY606583, P453 and P517) suggesting that the compounds, were able to activate the same receptor subtype. Furthermore, according to BAY606583, both P453 and P517 inhibited either I_A or I_K currents (Figure 51G and 51H).

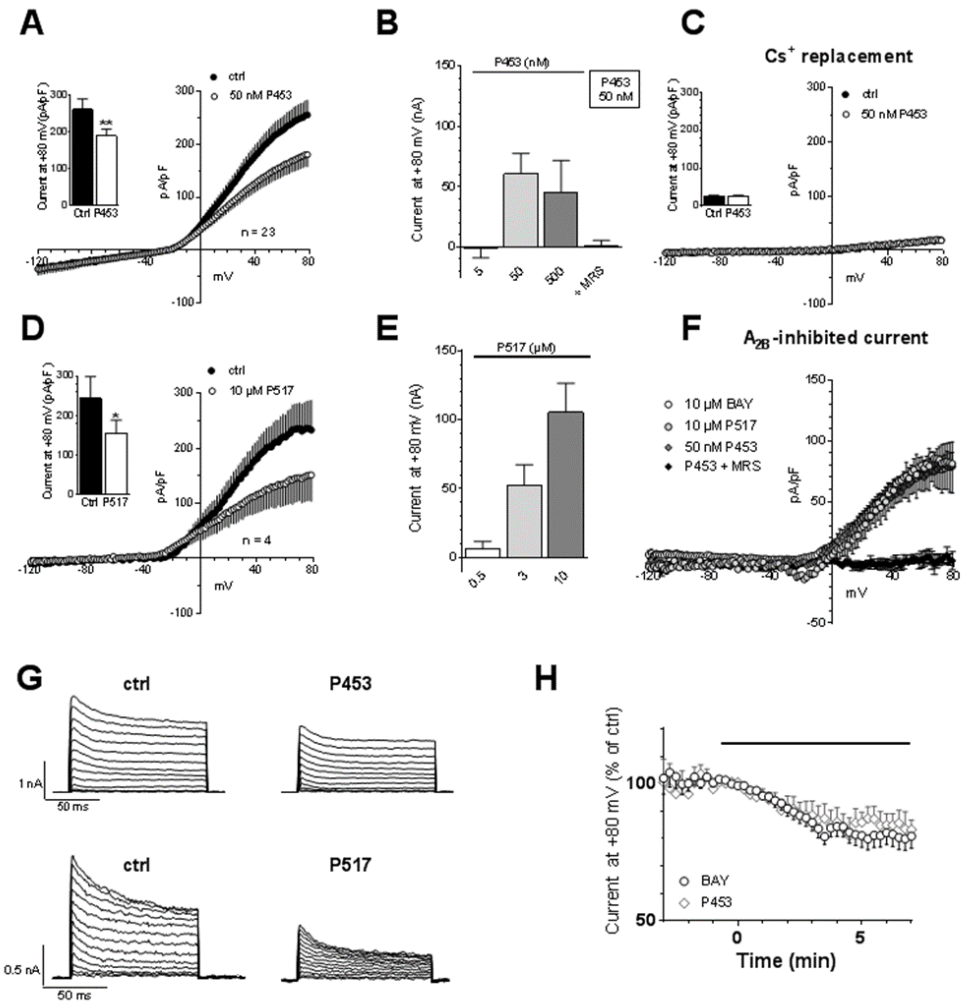

Figure 51: The effect of the prototypical, A_{2B}AR agonist BAY606583 on I_K and I_A currents is mimicked by other two, newly synthetized, A_{2B}AR agonists P453 and P517. All experiments were performed in the presence of the A_1, A_{2A} and A_3AR antagonists DPCPX, SCH58261 and MRS1523, respectively (all 100 nM). A and D. Averaged ramp-evoked currents recorded in the absence (filled circles and columns) or presence (open circles and columns) of the newly synthetized , A_{2B}AR agonists P453 (50 nM: A) or P517 (10 µM: D) in cultured OPCs. **P*<0.05; ***P*<0.01 paired Student's t-test. B and E. Pooled data of P453- (B) or P517- (E) sensitive currents evoked by the voltage ramp and measured at +80 mV in different experimental groups. C. Averaged ramp-evoked currents, and pooled data at +80 mV, recorded in the absence (filled circles and columns) or presence (open circles and columns) of the A_{2B}AR agonist P453 in Cs^+-replacement experiments (n=3). F. Net A_{2B}-sensitive currents, obtained by subtraction of the trace recorded in the presence of agonist from the respective control ramp, in different experimental groups. Note that no A_{2B}-sensitive current is recorded when P453 is co-applied with the A_{2B}AR antagonist MRS1706 (MRS: 10 µM). G. Left panels: original current traces evoked by a voltage-step protocol (from -40 to +80 mV, pre-step -80 mV; 200 ms) in a representative cell before (left panels) and after (right panels) the application of P453 (50 nM) or P517 (10 µM). H. Averaged time course of ramp-evoked current at +80 mV recorded in the absence or presence of different A_{2B}AR antagonists.

As a final proof of A_{2B}AR -mediated functional role on cultured OPCs, we tested the effects on outward K^+ currents of the unselective P1 adenosine receptor agonist NECA, applied, as in the case of all other A_{2B}AR agonists, in the continuous presence of the A_1, A_{2A} and A_3AR antagonists DPCPX, SCH58261 and MRS1523, respectively (as in all other experimental groups). As shown in Figure 52 (panels A and B), in a representative cell, NECA (100 µM) mimicked BAY606583-mediated inhibition of outward ramp-evoked K^+ currents. The effect was significant in 5 cells tested (Figure

52C: ***P*<0.01, paired Student's t-test), it was prevented by the selective A_{2B}AR agonist PSB603 (10 µM: Figure 52D,E) and was concentration-dependent, with an EC_{50}=1.9 µM (confidence limits: 0.4 – 9.0 µM).

In order to confirm the involvement of I_A and I_K current in the A_{2B}AR -mediated effect, we applied BAY606583 in the presence of a combination of the K^+ channel blockers 4-AP (500 µM) and TEA (3 mM), respectively (Gutman *et al.*, 2005). We have previously shown that, in cultured OPCs, 3 mM TEA primarily inhibits delayed rectifier I_K currents whereas 500 µM 4-AP is a selective blocker of transient I_A conductances (Coppi *et al.*, 2013a, 2013b). As shown in Figure 52, only a co-application of both compounds was able to counteract BAY606583-mediated effect (Figure 53C), thus confirming an A_{2B}-mediated inhibition of I_K plus I_A conductances.

Concerning the intracellular mechanism by which the Gs-coupled A_{2B}AR mediates outward K^+ current inhibition, we tested the hypothesis of intracellular cAMP being involved, in accordance with previous data showing that increased levels of this intracellular metabolite decreases steady-state outward K^+ conductances in ovine OPCs (Soliven *et al.*, 1988).

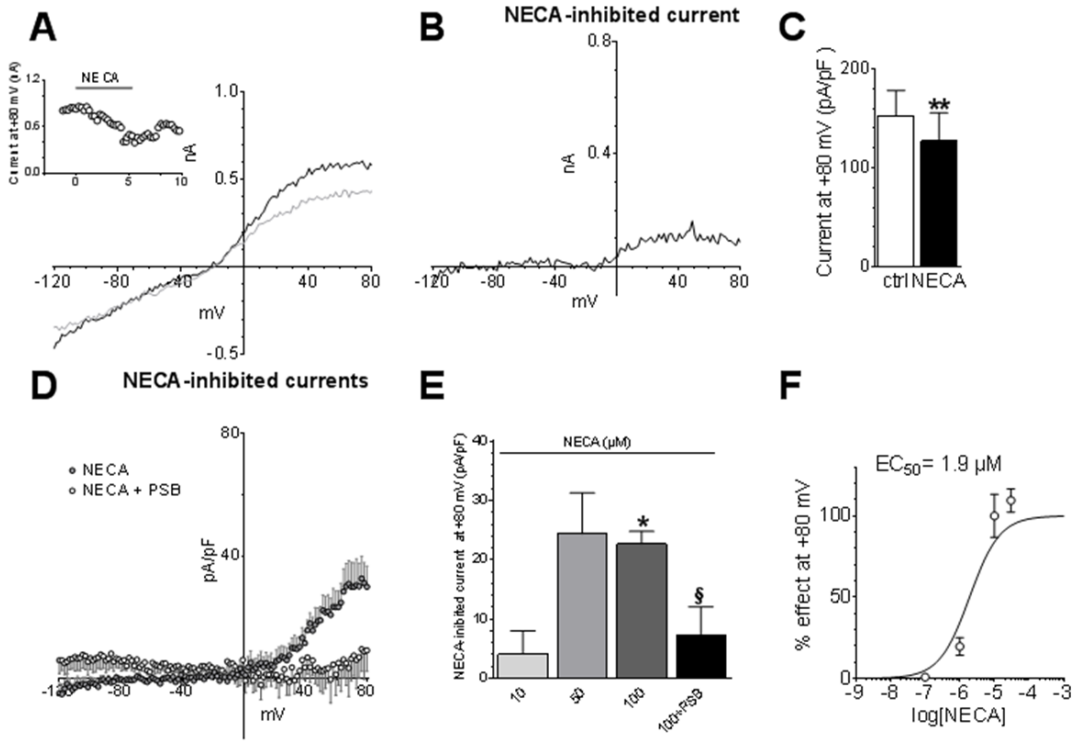

Figure 52: The effect of BAY606583 on I_K and I_A currents is mimicked by the unselective adenosine receptor agonist NECA. All experiments were performed in the presence of the A_1, A_{2A} and A_3AR antagonists DPCPX, SCH58261 and MRS1523, respectively (all 100 nM). A. Original whole-cell patch clamp current traces activated by a voltage ramp protocol (from -120 to +80 mV, 800 ms) in a typical OPC before (ctrl) and after NECA (100 µM) application (5 min). Inset: time course of ramp-evoked currents at +80 mV in same cell. B. Net NECA-inhibited current, obtained by subtraction of the trace recorded in NECA from the control ramp, in the same cell. C. Pooled data of ramp current evoked at +80 mV in the absence (open bar) or presence (filled bar) of 100 µM NECA in 5 cells tested. ***P*<0.01, paired Student's t-test. D. Averaged NECA-inhibited currents recorded in the absence (filled circles) or presence (open circles) of the A_{2B}AR antagonist PSB603 (PSB, 10 µM) in 5 and 3 cells tested, respectively. E. Pooled data of NECA-inhibited currents measured at +80

mV in different experimental groups. **P*<0.05 *vs* 10 µM NECA; §*P*<0.05 *vs* 100 µM NECA, One-way ANOVA, Bonferroni post-hoc test . At least n=3 for each experimental group. F. Concentration-response curve of NECA-mediated inhibition of ramp-evoked outward K^+ currents measured at +80 mV in cultured OPCs. EC_{50} = 1.9 µM, confidence limits = 0.4 – 9.0 µM.

Similarly to what observed in the presence of the A_{2B}AR agonist BAY606583, the adenylyl cyclase activator forskolin (FSK) concentration-dependently inhibited outward ramp-evoked K^+ currents in cultured OPCs (Figure 53, D-F) with a 45.6 ± 6.6% inhibition of ramp-evoked K^+ currents at the maximal concentration tested (100 µM: Figure 53F). The effect was rapidly reversed after a few min of drug washout (inset in Figure 53D).

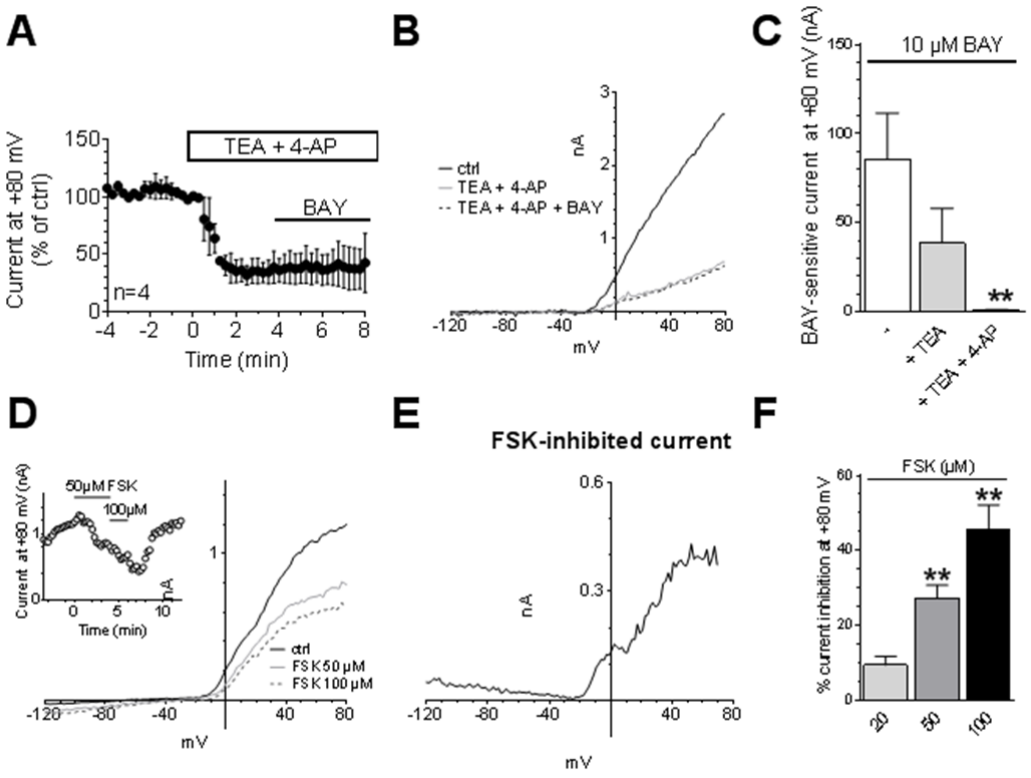

Figure 53: The effect of BAY606583 on I_K and I_A currents in OPCs is prevented by a combination of the K^+ channel blockers TEA and 4-AP. All experiments were performed in the presence of the A_1, A_{2A} and A_3AR antagonists DPCPX, SCH58261 and MRS1523, respectively (all 100 nM). A. Averaged time course of ramp-evoked currents measured at +80 mV before and after the co-application of the K^+ channel blockers tetraethyl ammonium (TEA: 3 mM) and 4-aminopyridine (4-AP: 500 µM) and during the subsequent application of 10 µM BAY606583 (BAY). B. Representative ramp current traces recorded in a typical OPC at significant time points. C. Pooled data of BAY-sensitive currents measured at +80 mV in control conditions, in the presence of TEA alone or in TEA + 4-AP. ***P*<0.01, One-way ANOVA, Bonferroni post-hoc test; at least n=4 in each experimental group. D. Original ramp current traces recorded in a typical OPC before (ctrl) and after forskolin (FSK: 50-100 µM) application (6 min). Inset: time course of ramp-evoked currents at +80 mV in same cell. E. Net 100 µM FSK- inhibited current, obtained by subtraction of the trace recorded in FSK from the control ramp, in the same cell. F. Pooled data of averaged ramp-evoked current at +80 mV recorded in the absence or presence of FSK in 4 cells tested. ***P*<0.01, One-way ANOVA, Bonferroni post-test.

3.2 The A_{2B}AR activation stimulates SphK1 phosphorylation in cultured OPCs.

In the attempt to identify a putative cross-talk between A_{2B}AR and SphK/S1P signalling pathway, we studied whether an acute, 10 min, BAY606583 application in purified OPC cultures, at the same concentration found to inhibit K^+ currents (10 µM), could possibly affect the activation state of one or both isoforms of SphK, SphK1 and SphK2, known to be expressed in oligodendroglial cells (Saini *et al.*, 2005). Since it has been previously demonstrated that SphK1 and 2 activation require phosphorylation and then translocation to the plasma membrane, where the substrate is located (Hait *et al.*, 2007; Pitson *et al.*, 2003), we analysed the phosphorylation of both enzymes after 10 BAY606583 challenge. Results presented here clearly show a significant increase in the phosphorylation of SphK1, but not SphK2, as reported in Figure 54 (A and B), in cells exposed for 10 min to 10 µM BAY606583. Of note, the selective $S1P_1$ receptor agonist SEW2871 was without effect no ramp-evoked K^+ currents, thus excluding the involvement of $S1P_1$ receptors in this effect (data not show).

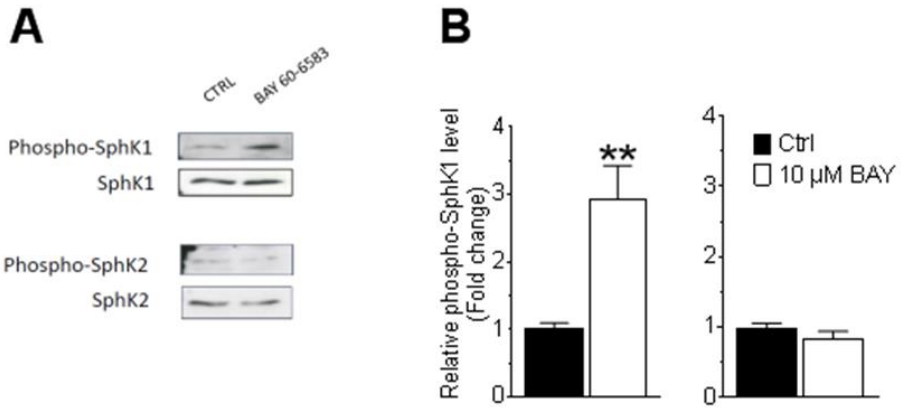

Figure 54: The A_{2B}AR agonist BAY606583 stimulates SphK1 phosphorilation in cultured OPCs. A. Western Blot analysis of phospho-SphK1 (upper panel) and phospho-SphK2 (lower panel) in total cell lysates of OPC cultures demonstrates that 10 min application of 10 µM BAY606583 in cultured OPCs enhances SphK1 phosphorylation. B. In the histogram, band intensity corresponds to the phosphorylated form of SphK1 or SphK2 and is normalized to SphK1 or SphK2 total content. Data are mean ± SEM of three independent experiments, -fold change over control, set as 1. Densitometric analyses are reported as fold change above control (Ctrl).

3.3 SphK/S1P pathway interferes with A_{2B}AR in modulating outward K^+ currents in cultured OPCs.

Based on the latest result, we next tested the hypothesis of a possible involvement of SphK1/S1P pathway in A_{2B}AR -mediated K^+ current inhibition. As shown in Figure 55A-C, the S1P analogue

FTY720-P at a concentration of 1 µM, mimicked the A_{2B}AR agonist BAY606583 in inhibiting ramp-evoked K^+ currents. The effect was significant in 8 cells tested (Figure 55C: from 210.8 ± 57.3 to 136.3 ± 38.3 pA/pF, *P*=0.0014, paired Student's t-test). Of note, when BAY606583 was challenged in the presence of 1 µM FTY720-P, the effect of the A_{2B}AR agonist was partially occluded (Figure 55A-C) as demonstrated by the fact that BAY606583-inhibited outward K^+ current was significantly smaller in the presence of FTY720-P as compared to control (Figure 55J: BAY606583-inhibited current was 78.4 ± 11.6 pA/pF in control conditions and 20.1 ± 17.7 pA/pF in the presence of 1 µM FTY720-P, *P*=0.0261, unpaired Student's t-test; and Figure 55K).

On the contrary, a submaximal (10 nM) concentration of FTY720-P elicited the opposite effect on ramp currents, i.e. an increase of outward K^+ conductances. Furthermore, it did not affect a subsequent application of BAY606583 (Figure 55D-F). Indeed, BAY606583-mediated K^+ current inhibition was not different in the absence or presence of 10 nM FTY720-P (Figure 55J,K). Finally, the product of SphK activity, S1P, at a concentration of 1 µM significantly inhibited ramp currents in cultured OPCs. However, the compound did not significantly affect BAY606583 -mediated inhibition of K^+ currents (Figure 55G-K)

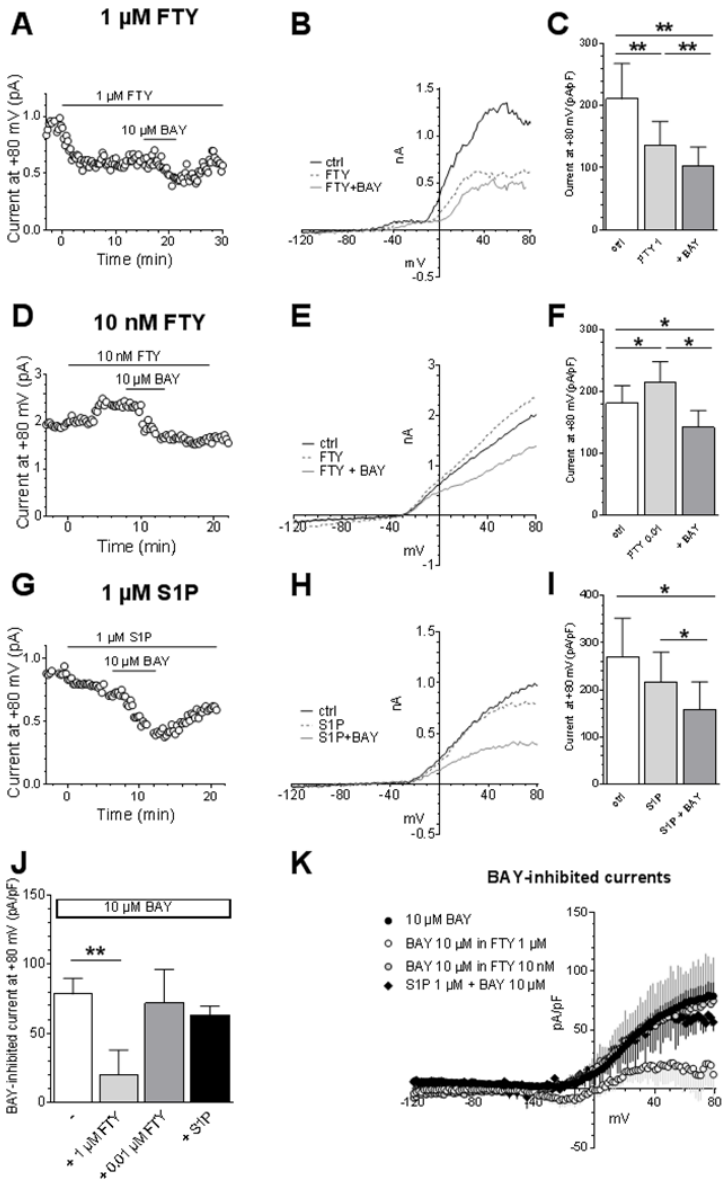

Figure 55: Effects of fingolimod and S1P on A_{2B}AR-mediated inhibition of K^+ currents in cultured OPCs. A. All experiments were performed in the presence of the A_1, A_{2A} and A_3AR antagonists DPCPX, SCH58261 and MRS1523, respectively (all 100 nM). Time course of ramp-evoked currents at +80 mV in a representative cell where FTY720-P (FTY) was applied at high (1 µM) concentration before the superfusion of BAY606583 (BAY: 10 µM). B. Original ramp current traces recorded in the same cell at significant time points. C. Pooled data of ramp-evoked currents measured at +80 mV in 6 cells tested. $^{**}P<0.01$, paired Student's t-test. D. Time course of ramp-evoked currents at +80 mV in a representative cell where fingolimod-P or FTY720-P (FTY) was applied at low (10 nM) concentration before the superfusion of BAY (10 µM). E. Original ramp current traces recorded in the same cell at significant time points. F. Pooled data of ramp evoked currents measured at +80 mV in 4 cells tested. $^{*}P<0.05$, paired Student's t-test. G. Time course of ramp-evoked currents at +80 mV in a representative cell where S1P (1 µM) was applied before the superfusion of BAY (10 µM). E. Original ramp current traces recorded in the same cell at significant time points. F. Pooled data of ramp-evoked currents measured at +80 mV in 3 cells tested. $^{*}P<0.05$, paired Student's t-test. J. Pooled data of BAY-inhibited current in different experimental groups. $^{*}P<0.05$, unpaired Student's t-test. K. Averaged BAY-inhibited currents in different experimental groups.

3.4 A_{2B}AR and SphK activation modulates oligodendrocyte maturation in vitro.

To study oligodendroglial cell maturation *in vitro*, OPC cells were lead to differentiate into mature OLGs by growing for 3, 7 and 10 days in DM. As shown in figure 56A, a significant and time-dependent increase in MAG and Mbp expression was found, compared to OPC (open bar), that was maximal at 7 days (black bar). Moreover, we dissected the time-dependent expression of A_{2B}AR in OLG compared to control OPC and found out that the expression of the receptor increases by the time of incubation with DM (Figure 56B). Interestingly, the expression of A_{2B}AR was not affected by FTY720-P treatment, whereas it was dramatically decreased by VPC96047 for 7 days in respect to control untreated OLGs (7 days in DM, black bar). Since $S1P_5$ displays a time-dependent expression during OLG differentiation, we performed Real-Time PCR to measure $S1P_5$ expression at 3, 7 and 10 days, and confirmed previous results reporting an increase of the receptor during differentiation from OPC towards OLG, turning to be the most expressed S1P receptor in mature OLGs (Jung *et al.,* 2007; Novgordov *et al.,* 2007; Yu *et al.*, 2004). Moreover, $S1P_5$ mRNA levels were not significantly changed after 7 day-treatment with FTY720-P nor VPC96047 (Figure 56C, orange bar, purple bar).

We finally investigated the involvement of A_{2B}AR agonists in oligodendroglial cell maturation *in vitro*, alone or in combination with S1P analogues or SphK inhibitors. According to the results reported in the figure 56, we selected 7 days of DM as the reference time to analyze OPC differentiation under different conditions. The incubation in DM for 7 days in the presence of the A_{2B}AR agonist, BAY606583 (10 μM), dramatically reverted the increase of either MAG or Mbp expression in OLG compared to OPC (Figure 56A, red bar compared to open bar), indicating that A_{2B}AR stimulation counteracts OPC maturation towards OLGs. The opposite effect was observed when OPCs were grown in the presence of the pan SphK-inhibitor VPC96047 or the selective SphK1-inhibitor VPC96091 (both at 500 nM, light grey, light green, respectively). In these two experimental groups, a further increase in MAG and Mbp expression was observed in comparison to 7 day OLGs, thus indicating that SphK inhibition promotes OPC maturation.

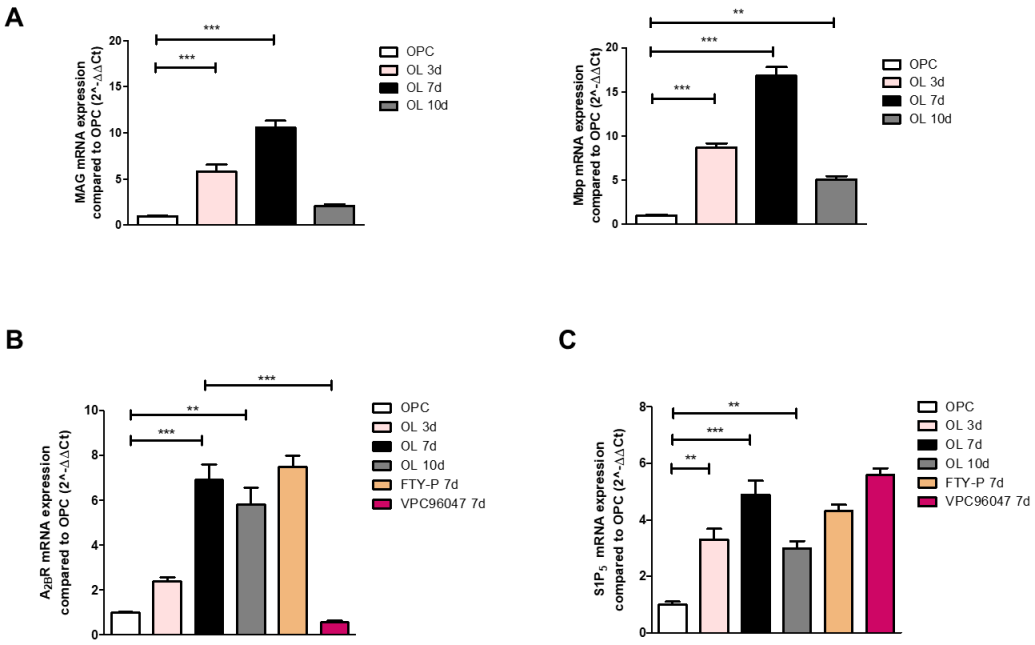

Figure 56: Time course of oligodendrocyte marker expression, $A_{2B}R$ and $S1P_5$ during differentiation from OPC to OL. A. Gene expression analysis of oligodendrocyte differentiation markers MAG and Mbp was performed by Real Time-PCR in OPC and 3, 7 and 10 day-differentiation (OL 3d, 7d, 10d) employing specific rat primers, as reported in Table 3 of materials and methods section, using SYBR green probe. Each measurement was carried out in triplicate. The 2^(−ΔΔCT) method was applied as a comparative method of quantification and data were normalized to β–actin expression. B. $A_{2B}R$ expression, analyzed employing specific rat primers and SYBR Green probe, was reported in OPC and after 3, 7, 10 days (t3, t7, t10) of DM, as 2^(-ΔΔCT) normalized to β–actin and compared to the control OPC. OL 7d were challenge with or without 1 µM FTY720-P and 500 nM VPC96047 (FTY720-P 7d and VPC96047 7d). C. $S1P_5$ receptor expression, analyzed employing specific rat primers, was reported as 2^-ΔΔCT, normalized to β–actin. OL at t7 were challenge with or without 1 µM FTY720-P and 500 nM VPC96047 (FTY720-P t7 and VPC96047 t7). Statistical analysis was performed using One-way ANOVA, followed by Bonferroni post-hoc test, *P<0.05, **P<0.01, ***P<0.001.

The S1P analogue FTY720-P, at a concentration of 1 µM, mimicked the effect of BAY606583 in inhibiting oligodendroglial differentiation (Figure 57A, purple bar). Interestingly, the $A_{2B}AR$ agonist BAY606583 prevented the positive effect on OPC maturation mediated by both SphK inhibitors, VPC96047 and VPC96091.

OLG differentiation was also significantly affected by P453 which significantly decreased both MAG and Mbp expression after 7 day-treatment, even if to a lesser extent in respect to BAY606583, and the effect was not reverted by VPC96047 (Figure 57A).

Data in literature showed that OLGs that hold a targeted deletion of $S1P_1$ did not show an obvious clinical phenotype, but there were subtle abnormalities in myelin (Kim *et al.*, 2011).

Interestingly, recent results demonstrated that $S1P_1$ deficiency caused delayed differentiation of OPCs into OLGs at 3 weeks (Dukala and Soliven, 2016). For this reason, the employment of specific $S1P_1$ agonist and antagonist, SEW2871 and W146, respectively, was exploited to analyze the contribution of $S1P_1$ on BAY606583-induced OLG differentiation. As reported in figure 57B and C, the stimulation with 1 µM SEW2871 did not exert any significant effect of OLG differentiation

marker expression, nor 10 µM W146 treatment. Moreover, in agreement with electrophysiological data, MAG and Mbp expression after BAY606583 stimulation was not significantly affected by W146, ruling out a role for $S1P_1$ in BAY606583 inhibition of oligodendrocyte differentiation.

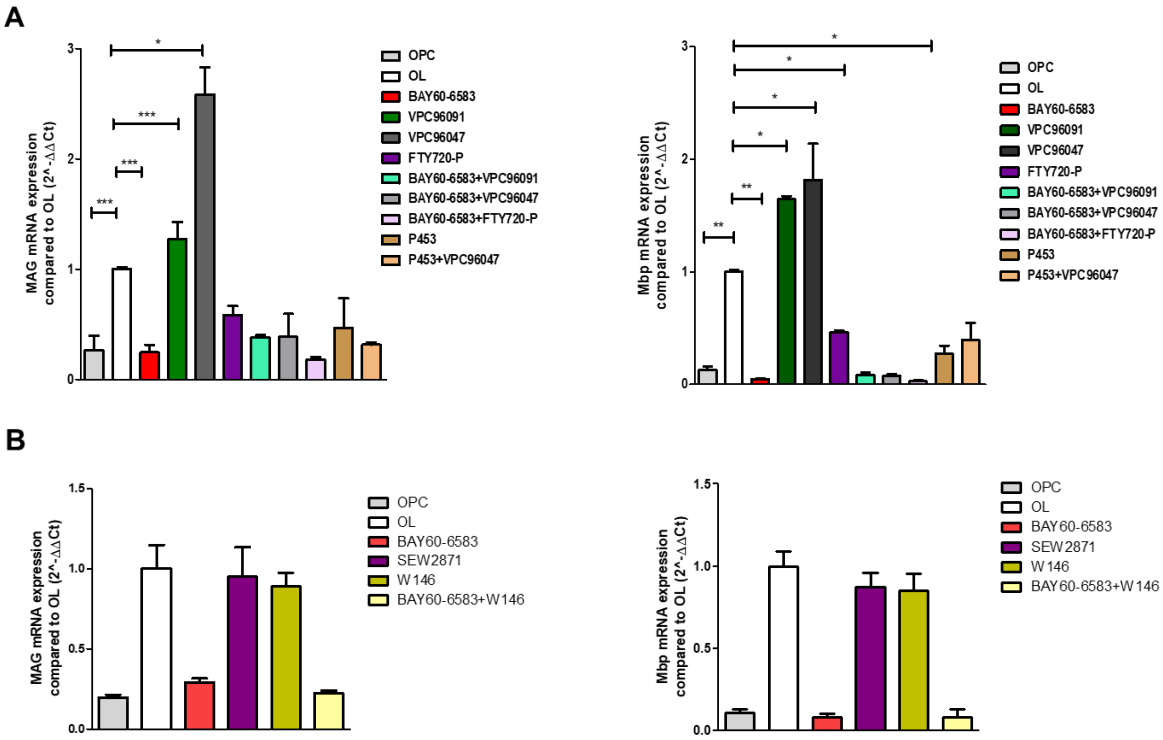

Figure 57: A_{2B}AR- and SphK/S1P mediated effects on oligodendrocyte differentiation *in vitro*. A. A. Gene expression analysis of oligodendrocyte differentiation markers MAG and Mbp by Realtime-PCR in OPC and after 7 days of DM (t7 OL) in the absence or presence of: BAY606583 (10 µM), VPC96047 (500 nM); VPC96091 (500 nM); FTY720-P (1 µM). The quantification of MAG and Mbp mRNA was performed by Real-Time PCR employing specific primers as reported in materials and methods section using SYBR green probe. Each measurement was carried out in triplicate. The 2^(−ΔΔCT) method was applied as a comparative method of quantification and data were normalized to β–actin expression. B. Gene expression analysis of oligodendrocyte differentiation markers MAG and Mbp by Realtime-PCR in OPC and after 7 days of DM (OL 7d) in the absence or presence of: BAY606583 (10 µM), SEW2871 (1 µM), W146 (10 µM). The quantification of MAG and Mbp mRNA was performed by Real-Time PCR as described above.
Statistical analysis was performed by One-way ANOVA followed by Bonferroni post-hoc test, at least n=3 independent experiments.*P<0.05; **P<0.01; ***P<0.001.

3.5 Discussion

The present work provides the first description of a role of A_{2B}ARs in oligodendroglial cell cultures. We demonstrate here that the selective A_{2B}AR activation inhibits outward I_K and I_A currents in cultured OPCs and delays cell differentiation into mature, myelin producing, oligodendrocytes *in vitro.*

Adenosine is known to participate to a number of OPC functions, from cell migration to myelin production (Coppi *et al.,* 2015; Fields and Stevens-Graham, 2002). Our group recently contributed to address this issue by demonstrating that A_{2A}AR stimulation counteracts oligodendriglial cell differentiation *in vitro* by inhibiting outward sustained I_K currents in cultured OPCs, which are known to be necessary to OPC differentiation (Gallo *et al.,* 1996). In the present work, we demonstrate that similar effects are achieved upon selective A_{2B}AR stimulation. However, differently from A_{2A}ARs, A_{2B}AR activation not only inhibits I_K conductances but also I_A transient currents. As we previously shown (Coppi *et al.,* 2013a, 2013b), a close correlation between cell differentiation and the expression of distinct voltage-dependent currents exists in purified primary OPCs, in accordance with various investigators (Attali *et al.,* 1997; Barres *et al.,* 1990; Knutson *et al.,* 1997; Soliven *et al.,* 1989; Sontheimer *et al.,* 1989; Williamson *et al.,* 1997). For these reasons A_{2B}AR, which are found to inhibit I_K and I_A currents in cultured OPC, could potentially modulate OPC differentiation. In line with this hypothesis, and similarly to A_{2A}AR activation, BAY606583 inhibited *in vitro* OPC differentiation when added for 7 days in the culture medium of these cells.

K^+ current inhibition in cultured OPCs was obtained by using four different A_{2B}AR ligands: the prototypical, commercially available, A_{2B}AR -selective agonist BAY606583 (10 µM), two recently synthetized A_{2B}AR -selective agonists (described in Betti *et al.,* 2018): P453 (500 nM) and P517 (10 µM) and, lastly, the unselective P1 agonist NECA. All compounds were applied in the continuous presence of saturating concentrations of A_1, A_{2A} and A_3AR antagonists. On these basis, we claim that the electrophysiological effect observed in the presence of the above mentioned compounds are A_{2B}AR -mediated, even if, surprisingly, only one (MRS1706) out of three A_{2B}AR antagonists tested (PSB603, MRS1754 and MRS1706) was able to counteract BAY06583-or P453-mediated K^+ current inhibition. Of note, the prototypical, highly selective, A_{2B}AR antagonist PSB603 definitely blocked A_{2B}AR -mediated effects only when NECA was used as an agonist, suggesting different sensitivity of A_{2B}ARs to this antagonist (i.e. different receptor conformations) depending upon the agonist used, at least in OPC cells (Welsh and Kucenas, 2018). We argue that a possible explanation for this phenomenon could be due to a species-specific conformation assumed by the rat A_{2B}AR upon binding of BAY606583, or BAY606583-derived compounds, which is insensitive to PSB603 antagonism. In fact, most data in the literature about A_{2B}AR pharmacology were obtained in mouse and/or human cloned A_{2B}AR isoforms. A paucity of knowledge is available to date about rat A_{2B}AR pharmacological profile, in particular in oligodendroglial cells. Another point which is at odds with

previously reported A_{2B}AR–related pharmacology is the unexpectedly high concentration of BAY606583 (10 µM) required in the present work to achieve a maximal inhibition of K^+ currents in OPCs (EC_{50} = 0.6 µM). It is reported in the literature that the affinity of BAY606583 to the A_{2B}AR subtype lays in the low nanomolar range. Nevertheless, this is the first time that this compound was tested in purified rat OPC cultures. So, the discrepancy could be due to species-specific, or cell-specific, differences. We also investigated the intracellular pathway by which A_{2B}ARs modulate K^+ currents in cultured OPCs. In keeping with our previous data showing that the Gs-coupled A_{2A}AR decreases (Coppi *et al.,* 2013a), whereas the Gi-coupled GPR17 receptor increases (Coppi *et al.,* 2013b), outward ramp-evoked K^+ currents in purified OPC cultures, we tested the hypothesis of intracellular cAMP being involved in the effect. As expected, a direct activation of adenylyl cyclase by forskolin decreased ramp-evoked K^+ current amplitude, demonstrating that cAMP is at least one of the intracellular signaling pathways involved in A_{2A}AR -mediated electrophysiological effect in OPCs.

Furthermore, an increase in intracellular cAMP level could be responsible also for the inhibition of oligodendroglial maturation observed in the present work upon A_{2B}AR activation, since previous observations show that forskolin, acting on adenylate cyclase and thereby increasing cAMP, inhibits *in vitro* myelination (Vartanian *et al.,* 1986).

SphK/S1P signaling pathway is known to be a pleiotropic mechanism in modulating a variety of cell functions, also in the oligodendroglial lineage. We provide here the first demonstration of an interplay between SphK and A_{2B}AR activation since an acute application of the A_{2B}AR agonist BAY606583 promotes SphK1 phosphorilation. The effect was specific on this enzyme isoform because no differences were found in the phosphorylated form of SphK2.

In keeping with above data, we focused on elucidating the functional role of SphK1- A_{2B}AR interaction by investigating whether the effects observed upon A_{2B}AR activation in OPCs, i.e. K^+ block and inhibition of cell maturation, were affected by SphK or S1PR ligands. We found that the two SphK inhibitors tested, VPC96047 (which affect both SphK1 and 2) and VPC96091 (that selectively inhibits SphK1), prompted OPC development into myelin-producing cells, because an increase of MAG and Mbp expression in t7 oligodendroglial cultures was observed in the presence of both compounds. Of note, the effect of unselective SphK inhibitor VPC96047, which prevents both SphK1 and SphK2 activation, was much more pronounced that that obtained in the presence of selective SphK1 inhibitor VPC96091, indicating an involvement of both enzyme isoforms in OPC maturation. This result is in accordance with previous works demonstrating that most of the mitogenic effect of PDGF on OPCs is indeed mediated by SphK activity (Soliven *et al.,* 2003). Of note, BAY606583 co-applied with either of the two SphK inhibitors, prevented their pro-differentiating effect, confirming the existence of a cross-talk between the two pathways.

Furthermore, FTY720-P, administered before BAY606583, mimics and partially occludes the effects of subsequent A_{2B}R agonist application. This confirms that the two pathways, SphK1 and A_{2B}ARs, converge on the same intracellular signaling cascade. It is worth noticing that FTY720-P, when

applied at low nanomolar (10 nM) concentration, elicited the opposite effect compared to that observed at higher, 1 µM, concentrations. This is also in accordance with Jung and collaborators who demonstrated that high (1 µM) and low (10 µM) doses of FTY720-P mediate opposite effects in rat OPC cultures (Jung *et al.,* 2007).

Unfortunately, at present, we do not have a valid candidate, among $S1PR_S$, accounting for this interaction. We can only rule out the involvement of $S1P_1$ subtype since neither selective agonism nor antagonism was found to counteract $A_{2B}AR$ agonist effects on K^+ current or cell differentiation. An additional proof that $A_{2B}ARs$ are critical modulators of OPC maturation resides in the fact that this receptor subtype is clearly upregulated during cell differentiation, an effect that is completely prevented when cell differentiation is induced by VPC96047. This data suggests that $A_{2B}AR$ overexpression is necessary to OPC development. $S1P_5$ receptor is also overexpressed during oligodendrogliogenesis but, differently from $A_{2B}AR$, its upregulation is not modified when OPC development is prevented by VPC96047, indicating that $S1P_5$ upregulation is not sufficient to produce OPC differentiation.

FTY720 is the first oral MS disease therapeutic agent and the first human medicine to be approved that targets $S1PR_S$. Emerging evidence from preclinical studies demonstrate that mechanisms independent of peripheral immune effects contribute significantly to the efficacy of FTY720 in models of MS. Indeed, FTY720, which is lipophilic, is able to cross the blood–brain barrier into the CNS and after its conversion by SphK2, FTY720-P has been detected in the cerebrospinal fluid at subnanomolar levels (Foster *et al.,* 2007). In addition, recent data using neural lineages from conditional $S1P_1$ knockout demonstrated a crucial action of FTY720 in reducing the severity of an animal model of MS, EAE. Results from *in vitro* studies have shown that the effects of FTY720-P on cultured oligodendrocyte lineage cells are affected by developmental stage, treatment dose, and duration (Novgorodov *et al.,* 2007; Miron *et al.,* 2008). Cultured rodent OPC treated with FTY720 are protected from apoptosis induced by inflammatory cytokines and microglial activation (Coelho *et al.,* 2007). The differentiation of OPC in our model is reduced after the treatment with high (microM) concentration of FTY720-P in agreement with previous results obtained in rat cultured OPC whose differentiation was stimulated by FTY720 at low nanomolar doses (Jung *et al.,* 2007), but was inhibited at higher concentrations (Miron *et al.,* 2008, Coelho *et al.,* 2007). Similarly, the effects of FTY720 on process dynamics in mature oligodendrocytes depended on both concentration and treatment duration (Miron *et al.,* 2008). Interestingly, SphK inhibition potently reduced A_{2B} mRNA levels in OPC after seven day treatment, claiming a possible positive effect of the sphingolipid on $A_{2B}AR$ expression.

Chapter 4: *Role of A_3AR on dorsal root ganglia excitability*

A_3AR activation inhibits pro-nociceptive N-type Ca^{2+} currents and cell excitability in dorsal root ganglion neurons.

4. Results

4.1 Selective A_3AR activation inhibits Ca^{2+} currents in cultured rat DRG neurons.

The present research was performed on 178 DRG neurons presenting a mean Vm=-54.3 ± 1.5 mV, a Rm=392 ± 40.5 MΩ and a Cm=26.6 ± 0.8 pF, which correspond to a spherical-approximated cell soma of 25 µm (Hille, 2001).

As a first screening of putative A_3AR-mediated effects on voltage-operated currents in DRG neurons, we applied a voltage ramp protocol (from +80 to -120 mV, 800 ms duration: see inset of Figure 58A) before, during and after the superfusion of the selective A_3AR agonist Cl-IB-MECA (100 nM). As shown in Figure 58A, the compound decreased overall outward currents evoked by the voltage ramp protocol: the effect peaked within 5 min of application and was partially reversed after drug wash out. Figure 58B shows that the net Cl-IB-MECA-inhibited current was an outward current activated at potentials positive to -30 mV. Ramp current inhibition measured at +80 mV in the presence of Cl-IB-MECA was statistically significant in 14 cells investigated (Figure 58C,D: from 799.0 ± 111.9 pA/pF in control to 617.2 ± 92.3 pA/pF in 100 nM Cl-IB-MECA, P=0.0005, Paired Student's t-test), whereas no changes in inward ramp currents at -120 mV were detected (Figure 58C-D: from -46.6 ± 10.7 pA/pF in control to -42.8 ± 7.5 pA/pF in 100 nM Cl-IB-MECA, P=0.3734, Paired Student's t-test). The effect of Cl-IB-MECA was observed in all cells tested, in agreement with high levels of A_3AR expression in DRG homogenate as revealed by RT-PCR technique (Figure 58I) and immunocytochemical analysis (Figure 58J,K). The effect was concentration-dependent (Figure 58E), with an EC_{50} of 2.0 nM (confidence limits: from 1.2 to 3.2 nM; Figure 58F), and prevented by two different A_3AR antagonists: VUF5574 (100 nM) and MRS1523 (100 nM) (Figure 58G,H).

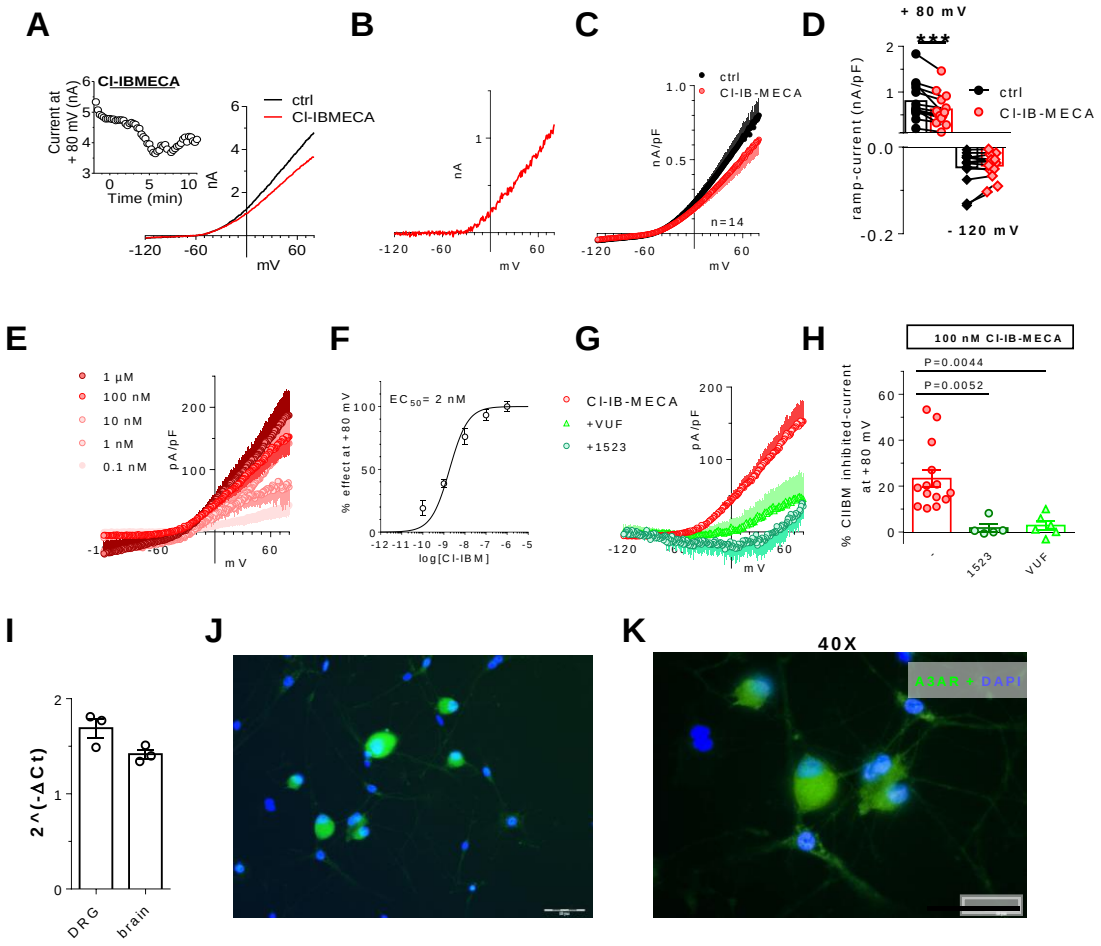

Figure 58: Selective A_3AR activation inhibits ramp-evoked outward currents in cultured rat DRG neurons.

A. Left panel: original patch-clamp current traces recorded in a representative cell where a voltage ramp protocol (+80/-120, 800 ms: right inset) was applied before (ctrl), during and after Cl-IB-MECA (100 nM) superfusion. Left inset: time course of ramp-evoked currents at +80 mV in the same cell. B. net Cl-IB-MECA-inhibited current, obtained by subtraction of the ramp recorded in Cl-IB-MECA from the control ramp, in the same cell. C-D. Averaged ramp traces (C), and pooled data at +80 and -120 mV (D), of ramp-evoked currents measured in the absence or presence of Cl-IB-MECA in 14 cells investigated. ***P=0,0005, Paired Student's t-test. E. Averaged Cl-IB-MECA-inhibited currents in the presence of different agonist concentrations (0.1-1000 nM; at least n=4 in each experimental condition). F. Concentration-response curve of Cl-IB-MECA effect on ramp currents measured at +80 mV (confidence limit: from 1.2 to 3.2 nM). G-H. Net Cl-IB-MECA-(100 nM)-inhibited currents (G), and respective pooled data at + 80 mV (H) recorded in the absence or presence of two different selective A_3AR antagonists: VUF5574 (VUF: 100 nM) and MRS1523 (1523: 100 nM). One-way ANOVA, Bonferroni post-test *vs* CL-IB-MECA. I. RT.PCR experiments demonstrated that A_3AR-coding mRNA is present in rat DRG homogenates. Data were normalized to A_3AR expression in a brain tissue homogenate, taken as positive control, and have been obtained in three independent experiments performed in triplicate. J-K. 20X (J) and 40X (K) magnification of A_3AR immunofluorescent labelling (green) of DRG cultures. Cell nuclei were marked with DAPI (blue). Scale bar: 50 µm.

Another A_3AR agonist that is highly selective was tested: MRS5980, whose EC_{50} is described in the sub-nanomolar range (EC_{50}= 0.7 ± 0.1 nM, Tosh *et al.*, 2014). This compound (100 nM) also concentration-dependently inhibited total outward currents evoked by the ramp protocol at +80 mV in 7 cells investigated (Figure 59A-C), and the effect was prevented by the selective A_3AR antagonist MRS1523 (inset in Figure 59A).

The effect of both A_3AR agonists was shared by the endogenous ligand adenosine (30 µM: Figure 59D), which significantly decreased ramp currents at + 80 mV in 5 cells tested without modifying the inward component (Figure 59E; n=5). Notably, the adenosine effect was significantly inhibited by the A_3AR antagonist VUF5574 (100 nM; n=6: Figure 59F; ***P*=0.0054, unpaired Student's t-test).

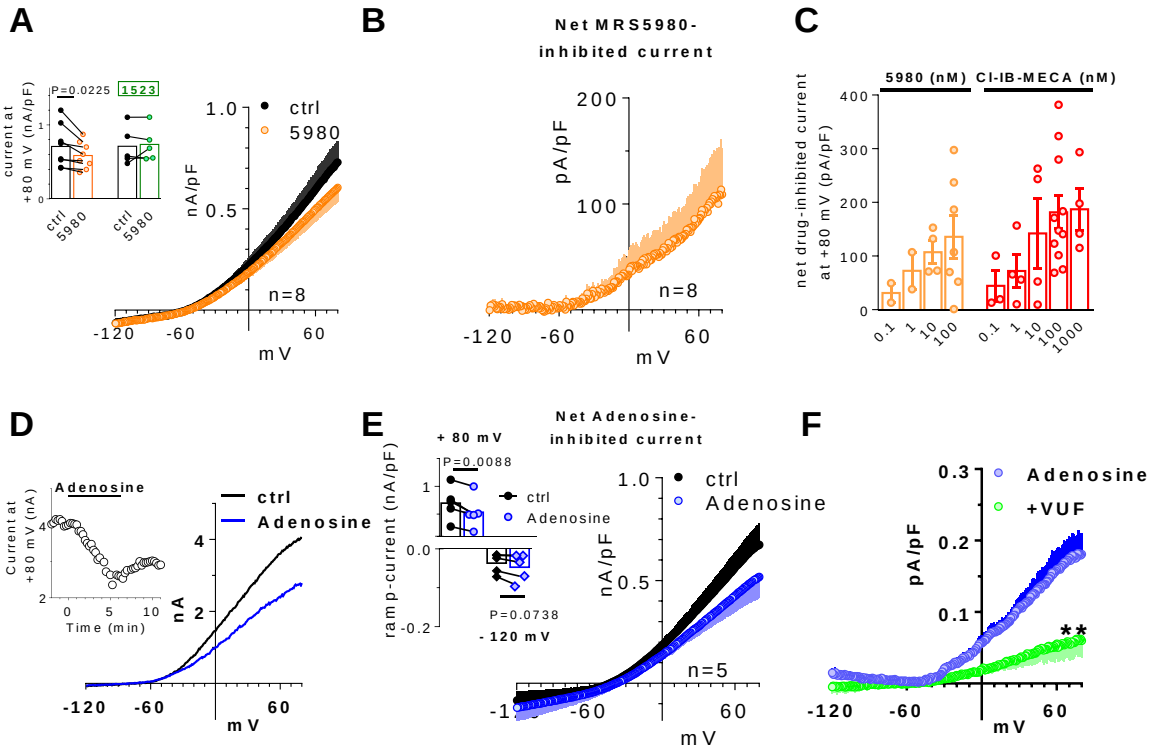

Figure 59: The newly synthetized, highly selective, A_3AR agonist MRS5980 and the endogenous ligand adenosine mimic Cl-IB-MECA effect in inhibiting ramp-evoked outward currents in isolated rat DRG neurons.

A. Averaged traces of ramp-evoked currents measured in the absence or presence of the selective A_3AR agonist MRS5980 (5980; 100 nM) in 7 cells investigated. Inset: pooled data or ramp-evoked current at +80 mV in the presence of MRS5980 alone or during co-application with the A_3AR antagonist MRS1523 (100 nM). Paired Student's t-test. B. Net 5980-inhibited current in 7 cells tested. C. Comparison between net Cl-IB-MECA- or 5980-inhibited ramp currents measured at +80 mV. D. Original ramp current traces recorded in a representative cell before (ctrl), during and after adenosine (30 µM) superfusion. Inset: time course of ramp-evoked currents at +80 mV in the same cell. E. Pooled data of ramp-evoked currents at +80 mV or -120 mV in the absence or presence of Adenosine in 5 cells investigated. Paired Student's t-test. F. Averaged Adenosine-inhibited current obtained by subtraction of the ramp recorded in Adenosine from the control ramp, in the absence (n=5) or presence of the A_3AR antagonist VUF5574 (VUF: 100 nM, n=6). ***P*=0.0054 at + 80 mV, unpaired Student's t-test.

In order to define A_3AR-responding DRG neurons as nociceptors, cells were tested for their responsiveness to the TRPA1 agonist allyl isothiocyanate (AITC) and/or TRPV1 agonist capsaicin (CPS). The TRP agonists were applied consecutively at least 5 min after Cl-IB-MECA removal.

Either CPS or AITC induced an increase in ramp-evoked currents in 11 out of 13 and in 5 out of 7 DRG neurons, respectively, which had previously responded to Cl-IB-MECA (Figure 60A-B). Both TRP agonists also significantly depolarized cell membrane (CPS: from -56.2 ± 3.7 mV to – 38.7 ± 4.6 mV, *P*=0.0064, n=7; AITC: from -51.7 ± 1.7 mV to – 46.7 ± 1.6 mV, *P*=0.0436, n=4; paired Student's t-test, Figure 60C), as expected upon activation of ligand-gated cation channels.

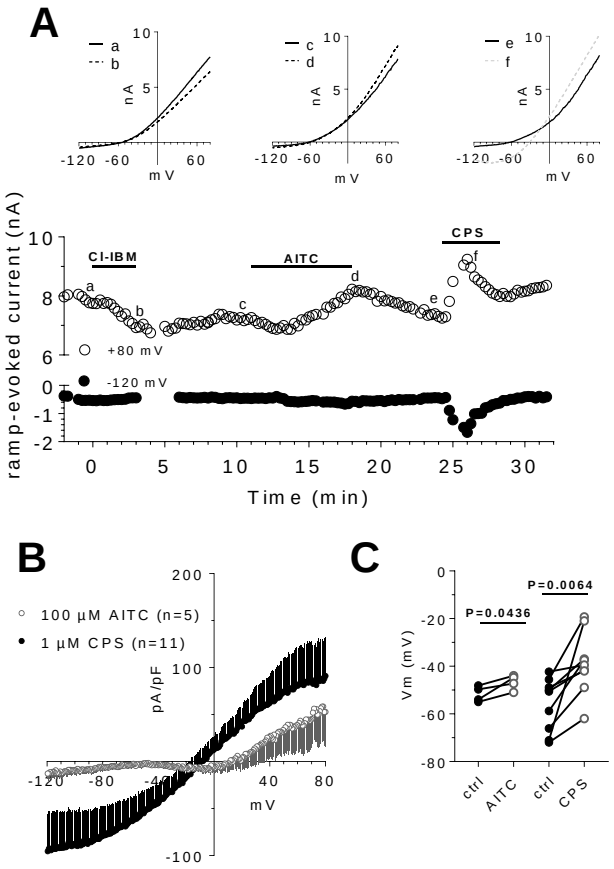

Figure 60: DRG neurons responding to Cl-IB-MECA are nociceptors sensitive to the TRPV1 and TRPA1 agonists capsaicin and allyl isothiocyanate.
A. Time-course, and representative current traces at significant time points (upper panels), of ramp-evoked currents at +80 and -120 mV in a representative DRG neuron where the A_3AR agonist Cl-IB-MECA (Cl-IBM; 100 nM; traces a and b), the TRPA1 agonist allyl isothiocyanate (AITC; 100 µM; traces c and d) and the TRPV1 agonist capsaicin (CPS; 1 µM; traces e and f) and were applied sequentially. B. Averaged CPS- and AITC-activated currents, measured by subtraction of the control ramp from that recorded in the TRP agonist. Note that CPS-sensitive current is an inward and outward rectifying ramp, whereas AITC-sensitive conductance is mostly an outward rectifying current. C. Both TRP agonists significantly depolarized DRG neurons. AITC: n=4; CPS: n=7; paired Student's t-test.

Data in the literature demonstrate that adenosine and its analogues inhibit VOCCs in rat DRG neurons (Dolphin *et al.*, 1986; MacDonald *et al.*, 1986), with no obvious distinction between A_1 *vs* A_3-mediated effects provided to date. For this reason, we tested the hypothesis that the decrease of total outward currents observed in the present work upon A_3AR activation could be dependent upon

a decrease of Ca^{2+} entry from VOCCs and, thus, to reduced activation of Ca^{2+}-activated K^+ conductances (K_{Ca}). Therefore, we applied the A_3AR agonist Cl-IB-MECA in the presence of the non-selective VOCC blocker Cd^{2+}. As shown in Figure 61A-C, 1 mM Cd^{2+} completely prevented the Cl-IB-MECA-induced decrease of outward ramp currents. Data were confirmed by applying two selective blockers of K_{Ca} channels: apamin (APA: 100 nM), which selectively blocks small-conductance K_{Ca} (SK channels), and TEA at low concentrations (200 µM), which selectively inhibits big-conductance K_{Ca} (BK channels). Both compounds, alone or in combination, significantly or completely prevented, respectively, Cl-IB-MECA-mediated inhibition of ramp-evoked outward currents (Figure 61D,E).The above data demonstrate that A_3AR activation inhibits SK and BK channels in rat DRG neurons.

Two possibilities exist to explain this phenomenon: i) A_3AR activation directly inhibits SK and BK channels; or ii) A_3 receptor activation inhibits Ca^{2+} entry from VOCCs which, in turn, decreases SK and BK channel opening. To test the latter hypothesis, we blocked all K^+ currents by replacing intra- and extra-cellular K^+ ions with equimolar Cs^+. In these experimental conditions, an inward component arose in the ramp protocol peaking around 0 mV (Figure 61F). This current was identified as a Ca^{2+} current, since it was abolished by 1 mM Cd^{2+} (Figure 61F,G). When applying Cl-IB-MECA in Cs^+-replacement conditions, a marked decrease of inward peak current was observed (Figure 61H: from –64.3 ± 14.8 pA/pF in control to –41.1 ± 11.4 pA/pF in Cl-IB-MECA, **P*=0.0431, paired Student's t-test; n=5), thus demonstrating that A_3AR activation directly inhibits Ca^{2+} currents.

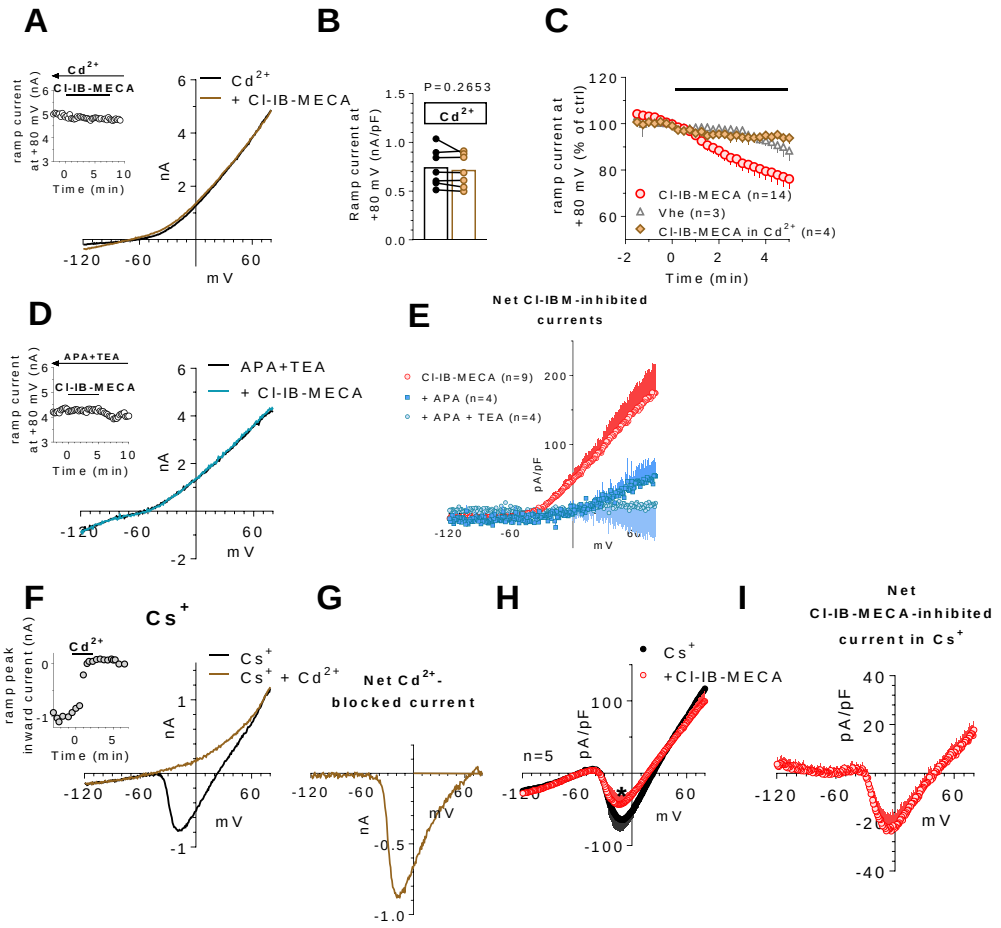

Figure 61: A_3AR activation in DRG neurons inhibits Ca^{2+}-activated K^+ currents by reducing Ca^{2+} influx from voltage-sensitive Ca^{2+} channels.
A. Original ramp current traces recorded in 1 mM Cd^{2+}-containing extracellular solution before (ctrl) and during Cl-IB-MECA (100 nM) application in a representative cell. Inset: time course of ramp-evoked currents at +80 mV in the same cell. B. Pooled data of currents measured at +80 mV in the absence or presence of Cl-IB-MECA in Cd^+-containing extracellular solution in 7 cells investigated. *P*=0.2653, paired Student's t-test. C. Averaged time course of ramp-evoked currents at +80 mV in the presence of Cl-IB-MECA, its vehicle (Vhe: 0.1% DMSO) or Cl-IB-MECA in 1 mM Cd^{2+}. D. Original ramp current traces recorded in apamin (APA, 100 nM) + tetraethylammonium (TEA, 200 µM) before (APA+TEA) or during Cl-IB-MECA (100 nM) application in a representative cell. Inset: time course of ramp-evoked currents at +80 mV in the same cell. E. Averaged Cl-IB-MECA-inhibited currents in the absence or presence of APA alone or during co-application with TEA. F. Original ramp current traces recorded before (ctrl) and during 1 mM Cd^{2+} application in a representative cell where extra- and intracellular K^+ were replaced by equimolar Cs^+. Note that in these experimental conditions a Cd^{2+}-sensitive inward current appears which presents an I-V relationship typical of Ca^{2+} currents. Inset: time course of ramp-evoked current measured at the inward peak in the same cell. G. Net Cd^{2+}-blocked Ca^{2+} current evoked by the ramp protocol in the same cell. H. Averaged ramp-evoked currents recorded in Cs^+-replacement conditions before (ctrl) and during Cl-IB-MECA (100 nM) application in 5 cells tested. **P*=0.0431; paired Student's t-test. I. Averaged Cl-IB-MECA-inhibited Ca^{2+} currents in Cs^+-replacement experiments.

DRG neurons are known to express different subtypes of Ca^{2+} currents (Scroggs and Fox, 1992, 1991; Wilson *et al.*, 2000). In order to identify which of them are inhibited by the A_3AR, we further isolated VOCC-mediated currents by adding, to the Cs^+-based extracellular solution, the Nav1.1, 1.2, 1.3, 1.4, 1.6, 1.7 blocker TTX (1 µM) plus the Nav1.8 inhibitor A887826 (200 nM) to block this TTX-resistant Na^+ channel. Nav1.8 are known to be expressed at high levels in DRG neurons (Dib-Hajj *et al.*, 2009), and we confirmed that because, in the presence of 1 µM extracellular TTX, 200

nM A887826 completely blocked residual, TTX-resistant, Na^+ currents (Figure 62A,B). As shown in Figure 62C, under these experimental conditions, we successfully isolated Ca^{2+} current activated by a 0 mV voltage step depolarization (200 ms duration), which were completely blocked by 500 µM Cd^{2+} (Figure 62C-E). Such Ca^{2+} currents were predominantly N-type currents because, when the selective N-type blocker PD173212 was applied (500 nM: Figure 62C-E), we achieved a >80% block (Hu *et al.*, 1999). Residual, PD-insensitive, Ca^{2+} currents in our experimental conditions were also insensitive to higher PD173212 concentrations (1 µM: Figure 62E) and were attributed to Cd^{2+}-sensitive L-type and, eventually, R and/or P/Q type VOCCs, consistently with a previous report (Wilson *et al.*, 2000).

Current-to-voltage (I-V plot) relationship of Ca^{2+} currents activated by a series of depolarizing voltage steps (from -50 to +50 mV, 10 mV increment, 200 ms duration, Vh=-65 mV: inset in Figure 62F) were consistent with Cd^{2+}-blocked (Figure 62F) and PD173212-sensitive (Figure 62G) and N-type VOCC activation.

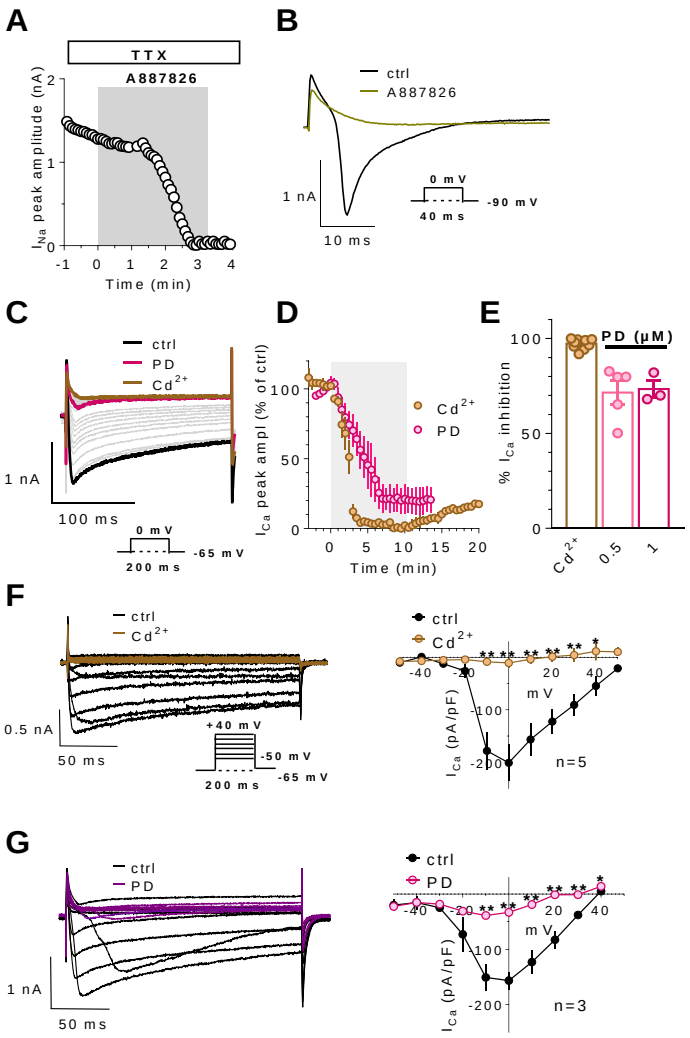

Figure 62: The major component of Ca^{2+} currents recorded in DRG neurons is carried by N-type VOCC opening.

A. Time course of Na^{+} currents recorded in the presence of extracellular TTX (1 µM), Cd^{2+} (0.5 mM) and Ni^{2+} (100 µM) and activated every 5 s by a 0 mV step depolarizazion (40 ms duration, Vh=-90 mV) before and during the application of the Nav1.8 blocker A887826 (200 nM). B. Original current traces recorded before and after 3 min A887826 application. C. Original current traces evoked in a typical DRG neuron by a 0 mV step depolarization (200 ms; Vh=-65 mV) in the presence of extracellular TTX (1 µM), Ni^{2+} (100 µM) and A887826 (200 nM) before (ctrl) or during the application of PD173212 (PD: 500 nM) and, subsequently, Cd^{2+} (no difference was found in the effects of 0.5 or 1 mM Cd^{2+} so data were pooled together). D. Averaged time-courses of Ca^{2+} currents, measured at the inward peak, before and during the application of the nonselective VOCC blocker Cd^{2+} (1 mM; n=7) or the selective N-type Ca^{2+} channel blocker PD (500 nM, n=4). Note that Cd^{2+} rapidly (< 3 min) and reversibly abrogated the totality of Ca^{2+} currents, whereas PD inhibited 70 ± % of VOCCs recorded in DRG neurons under our experimental conditions. E. Pooled data of peak Ca^{2+} current amplitude demonstrating that 500 nM PD maximally inhibited N-type VOCCs. F-G. Original current traces, and respective averaged I-V plots, of Ca^{2+} currents evoked by a series of 10 depolarizing voltage steps (from -50 to + 50 mV, 200 ms duration, Vh=-65 mV: see lower inset) before and during 1 mM Cd^{2+} (F) or 500 nM PD (G) application.

When Cl-IB-MECA was applied in these experimental conditions, a reversible decrease of total Ca^{2+} currents (both in the peak and steady-state component) was observed within 5 min of drug application (Figure 63A). The I-V plot of such Ca^{2+} conductances (Figure 63C) demonstrated that the A_3AR agonist significantly inhibited VOCCs from 0 to +20 mV (paired Student's t-test, n=5). The Cl-IB-MECA effect was significant in 8 cells tested (Figure 63B), either as peak current amplitude (arrow in right panel of Figure 63A, or Figure 63B) or at the steady-state (arrowhead in right panel of Figure 63A: from 57.4 ± 14.5 to 39.8 ± 10.2 pA/pF; *P*=0.0174 paired Student's t-test). However, the A_3AR agonist apparently did not change the Ca^{2+} current kinetics, because the time-to-peak was unaffected (from 15.1 ± 2.2 to 15.7 ± 3.0 ms; *P*=0.5553 paired Student's t-test). Cl-IB-MECA-mediated inhibition of VOCCs was concentration-dependent with a maximal effect observed at 30 nM (Figure 63E), in accordance with ramp experiments, and completely prevented by the A_3AR antagonist MRS1523 (100 nM) and by the selective N-type channel blocker PD173212 (500 nM) but not by the selective, at least at 1 µM concentration (De Paoli *et al.*, 2002), L-type blocker lacidipine (1 µM: Figure 63D,E). The above data demonstrate that A_3AR activation selectively inhibits N-type Ca^{2+} currents in rat DRG neurons.

In the attempt to compare A_3AR *vs* A_1AR-mediated effects on VOCCs, we applied the A_1AR selective agonist CPA. As shown in Figure 63E and F, CPA inhibited Ca^{2+} currents by 24.8 ± 3.2 % (n=9) and by 24.1 ± 3.0 % (n=7) at 1 and 10 µM concentrations. Of note, Ca^{2+} current inhibition measured in the presence of 1 µM CPA was significantly smaller compared to the Cl-IB-MECA-mediated effect (44.1 ± 5.6 % inhibition in the presence of 30 nM Cl-IB-MECA *vs* 24.8 ± 3.2 % inhibition in the presence of 1 µM CPA, *P*=0.0464 One-way ANOVA, Bonferroni post-test, Figure 63E).

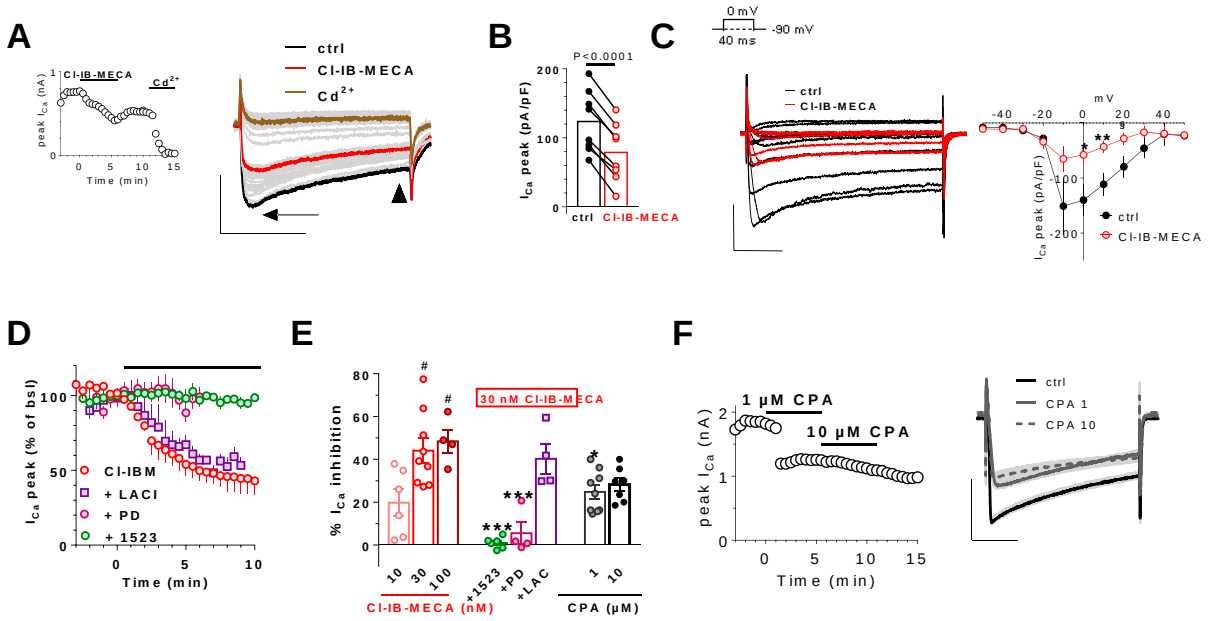

Figure 63: Cl-IB-MECA inhibits N-type Ca^{2+} currents in DRG neurons.

A. Left panel: time course of peak I_{Ca} amplitude evoked by a 0 mV step depolarization in a typical DRG neuron. Note that Cl-IB-MECA (30 nM) inhibits Ca^{2+} currents which were completely abolished by a subsequent 500 μM Cd^{+2} application. Right panel: original current traces recorded in the same cell at significant time points. Scale bars: 0.5 nA, 100 ms. B. Pooled data of Ca^{2+} current peak amplitude measured in the absence or presence of Cl-IB-MECA in 8 cells investigated. Paired Student's t-test. C. Left panel: Original Ca^{2+} current traces evoked by a series of depolarizing voltage steps (inset) before (ctrl) and after Cl-IB-MECA (30 nM) application in a representative cell. Right panel: averaged I-V plot of Ca^{2+} currents measured at the peak in 5 cells tested. **P*=0.0106; ***P*=0.0066; §*P*=0.0105, paired Student's t-test. Scale bars: 0.5 nA, 50 ms. D. Averaged time-courses of peak Ca^{2+} current, expressed as % of baseline values, measured before and after the application of Cl-IB-MECA in different experimental groups. E. Pooled data of Cl-IB-MECA- or CPA-inhibited peak Ca^{2+} currents at different agonist concentrations, or in 30 nM Cl-IB-MECA during co-application with the A_3AR antagonist MRS1523 (1523: 100 nM) or with the selective N-type and L-type Ca^{2+} channels blockers PD173212 (PD: 500 nM) and lacidipine (LACI: 1 μM), respectively. One-Way ANOVA, Bonferroni post-test. **P*<0.05; ****P*<0.0001 *vs* 30 nM Cl-IB-MECA; #*P*<0.05 *vs* 10 nM Cl-IB-MECA, One-way ANOVA, Bonferroni post-test. F. Left panel: time course of peak I_{Ca} amplitude evoked by a 0 mV step depolarization in a typical DRG neuron in the absence or presence of CPA (1-10 μM). Right panel: original current traces recorded in the same cell at significant time points. Scale bars: 1 nA, 100 ms.

The newly synthetized A_3AR agonist MRS5980 mimicked the Cl-IB-MECA effect in inhibiting Ca^{2+} currents (Figure 64A,C) but with higher efficacy, showing a maximal VOCC inhibition at 3 nM concentration (Figure 64B) compared to 30 nM for Cl-IB-MECA. Furthermore, the MRS5980-mediated effect was prevented in the presence of A_3AR antagonist MRS1523 (100 nM; Figure 64B). In order to explore the contribution of A_3AR-mediated inhibition of VOCCs when the endogenous agonist is present in the extracellular space, we applied adenosine (30 μM) in the absence or presence of selective adenosine A_1 or A_3AR antagonists DPCPX and MRS1523, respectively. As expected from published data (Dolphin *et al.*, 1986; MacDonald *et al.*, 1986), adenosine inhibited Cd^{2+}-sensitive Ca^{2+} currents with a maximal effect observed at 30 μM (Figure 64E). Of note, the effect induced by 30 μM adenosine was blocked by 39.1 ± 9.0 % in the presence of the A_1AR antagonist

DPCPX (500 nM) and by 56.6 ± 9.0 % in the presence of the A_3AR antagonist MRS1523 (100 nM, Figure 64E,F). No significant difference was found between DPCPX and MRS1523-mediated inhibition of adenosine effects.

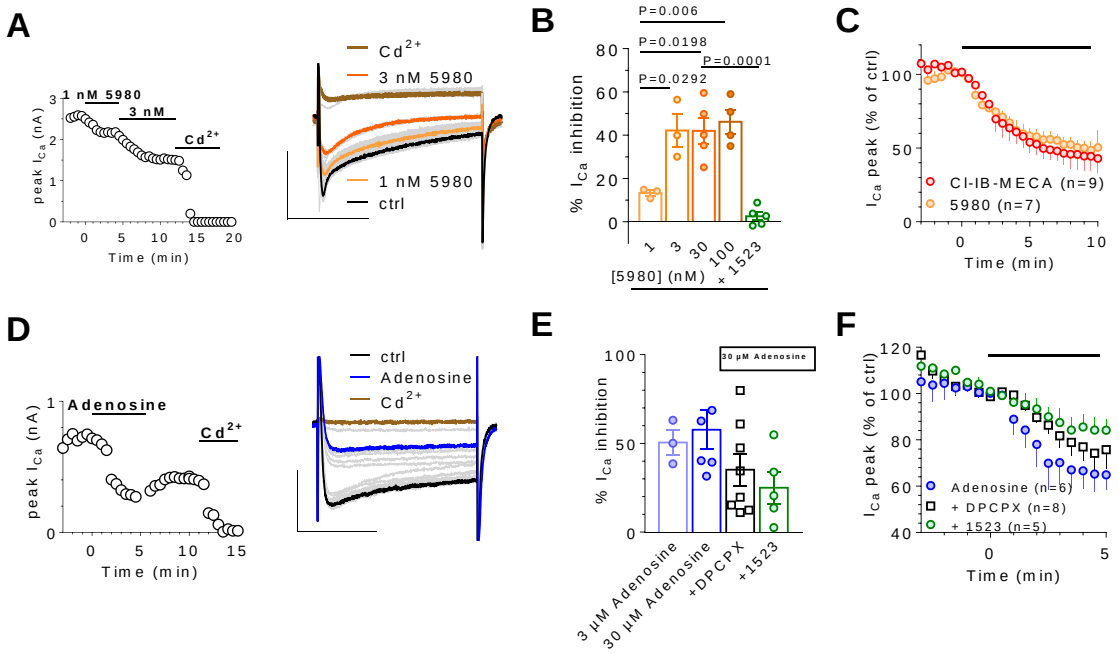

Figure 64: The inhibitory effect of Cl-IB-MECA on N-type Ca^{2+} currents in DRG neurons is mimicked by the newly synthetized A_3AR agonist MRS5980 and by adenosine.
A. Left panel: time course of peak I_{Ca} amplitude in a typical DRG neuron before and after MRS5980 (5980 30 nM) and Cd^{+2} (500 µM) application. Right panel: original current traces recorded in the same cell at significant time points. Scale bars: 2 nA; 100 ms. B. pooled data of 5980-inhibited peak Ca^{2+} current at different agonist concentrations or in the presence of 30 nM 5980 + 100 nM MRS1523 (1523). One-way ANOVA; Bonferroni post-test *vs* 1 nM 5980. C. Averaged time-courses of peak I_{Ca} amplitude before or during Cl-IB-MECA (30 nM) or 5980 (3 or 30 nM) application. D. Left panel: time course of peak I_{Ca} amplitude in a typical DRG neuron before and after adenosine (30 µM) and Cd^{+2} (500 µM) application. Right panel: original current traces recorded in the same cell at significant time points. E. Pooled data of Adenosine-inhibited peak Ca^{2+} currents at different agonist concentrations or in the presence of 30 µM Adenosine + the A_3AR antagonist 1523 (100 nM) or the A_1AR antagonist DPCPX (500 nM). No significant difference was found between any of the experimental groups (One-way ANOVA, Bonferroni post-test). F. Averaged time-courses of peak Ca^{2+} current amplitude before or after adenosine (30 µM) application alone or in the presence of DPCPX (500 nM) or 1523 (100 nM).

Finally, we evaluated the impact of selective A_3AR activation on neuronal excitability. We induced AP firing by injecting a depolarizing ramp current from the resting membrane potential. As shown in Figure 65A, this protocol induced repetitive firing in DRG neurons, which was markedly reduced in the presence of Cl-IB-MECA (Figure 65A,B). The effect was statistically significant in 6 cells tested (Figure 65C) and prevented in the presence of the A_3AR antagonist MRS1523 (100 nM; Figure 65D-F) but not by the N-type VOCC blocker PD173212 (1 µM; Figure 65G-I). Other AP parameters (peak amplitude, time to peak or half width) were not modified by Cl-IB-MECA or by other treatments (Table 6, pag 72 see in Materials and Methods).

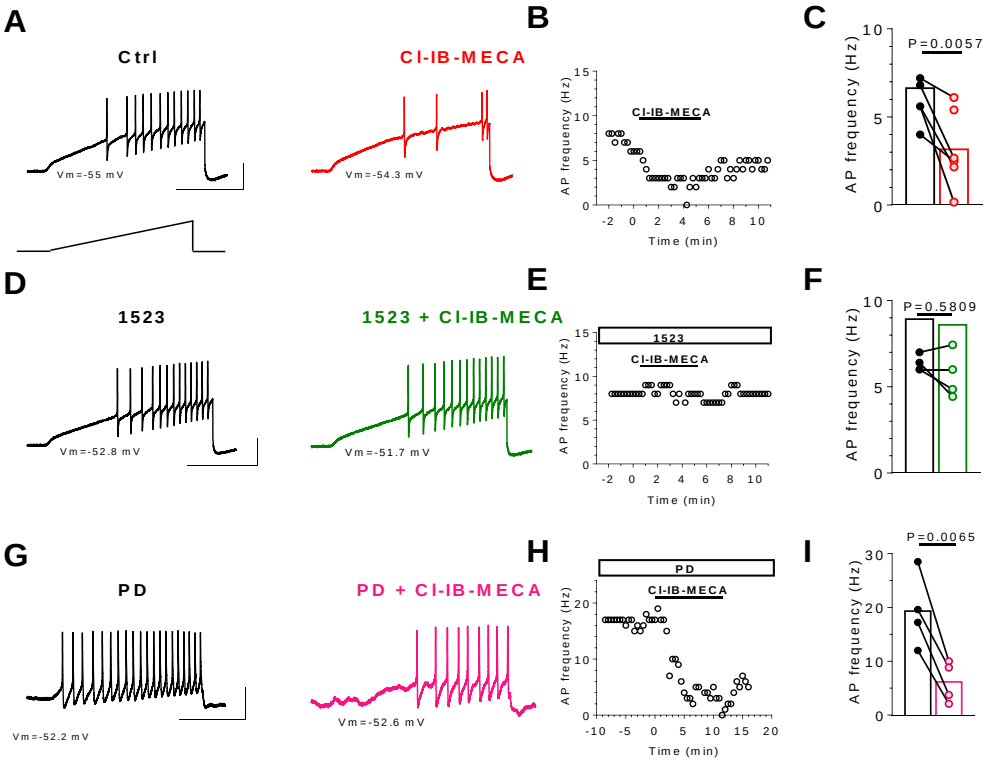

Figure 65: Cl-IB-MECA inhibits AP firing in DRG neurons.

A. Original AP traces evoked in a typical DRG neuron by a 1 s depolarizing ramp current injection (lower inset) recorded before (black trace) or after (red trace) 5 min Cl-IB-MECA (100 nM) application. B. Time course of AP frequency in the same cell. C. Pooled data of AP frequency measured before or after 5 min Cl-IB-MECA application in 6 cells tested. Paired Student's t-test. D. Original traces of AP firing evoked by a 1 s depolarizing ramp current injection recorded before (black trace) or after (green trace) 5 min Cl-IB-MECA (100 nM) applied in the presence of MRS1523 (1523, 100 nM). E. Time course of AP frequency in the same cell. F. Pooled data of AP frequency measured before or after 5 min Cl-IB-MECA application in the presence of 1523 in 5 cells tested. Paired Student's t-test. G. Original traces of AP firing evoked by a 1 s depolarizing ramp current injection recorded before (black trace) or after (purple trace) 5 min Cl-IB-MECA (100 nM) applied in the presence of PD173212 (PD, 1 µM). H. Time course of AP frequency in the same cell. I. Pooled data of AP frequency measured before or after 5 min Cl-IB-MECA application in the presence of PD in 4 cells tested. Paired Student's t-test. Scale bars: 50 mV; 500 ms.

4.2 Intracellular Ca^{2+} measurements confirmed that A_3AR activation inhibits electrical field stimulation-evoked Ca^{2+} transients in isolated DRG neurons.

Fura-2 loaded DRG neurons analysed by transmitted light and fluorescence showed a round morphology with an average diameter of 27.6 ± 0.3 µm (n=318).

In control conditions (standard extracellular solution), 60% (40 out of 68) of the DRG neurons presented electrically-evoked Ca^{2+} transients upon 0.1 Hz field stimulation. The dynamic of cytosolic Ca^{2+} increase presented a rapid onset and a return to basal Ca^{2+} levels following a mono-exponential kinetic. Analysed cells were defined as "responder" when showing at least 5 Ca^{2+} transients in 1 min. Figure 66A shows typical Ca^{2+} transient traces in control condition, in the absence of extracellular Ca^{2+} (0[Ca^{2+}]out) or in the presence of TTX + A887826.

In 0[Ca^{2+}] out, only 4 out of 37 (10.8%) analysed DRG neurons responded to electrical field stimulation (*P*=0.003 *vs* control, χ^2 test, Table 9).

Table 9.

Treatment	n of Responders	ΔF/F (A.U.) (Responders)	AUC/F (A.U.) (Responders)
Ctrl	n=40 out of 68	3.8 ± 0.47	1.6 ± 0.28
0 [Ca^{2+}]out	n=4 out of 37	2.2 ± 0.81	0.9 ± 0.38
TTX + A88	n=12 out of 55	1.6 ± 0.50	0.8 ± 0.31
vera + PD	n=17 out of 37	1.6 ± 0.38*	0.6 ± 0.16
Cl-IB-MECA	n=17 out of 64	5.6 ± 0.77	2.8 ± 0.59

Table 9. ΔF/F and AUC/F measured in DRG neurons induced by electrical field stimulation (responders) according to treatments. n = responders; not responders were not considered to calculate the mean. **P* = 0.03 *vs* Ctrl ΔF/F, One-Way ANOVA Bonferroni's post-test. Control: Ctrl; verapamil: vera; PD173212: PD; A.U.: arbitrary units.

Indeed, as shown in a typical trace in Figure 66A (dotted line), the majority of analysed cells did not show Ca^{2+} transients in the absence of extracellular Ca^{2+}. The insert of Figure 66A depicts Ca^{2+} transients in one of the 4 responder cells in 0[Ca^{2+}]out. In those 4 responder cells, the ΔF/F was reduced and the monoexponential decay phase was more (but not statistically significant) rapid than in control conditions (insert of Figure 66A). Indeed, as summarized in Table 9, the average of ΔF/F or AUC/F of responders (n=4) was slightly, even if not significantly, reduced. We supposed that, in the 4 out of 37 cells oscillating in 0[Ca^{2+}]out, the electrical field stimulation could induce a Ca^{2+} release from intracellular stores.

In the presence of TTX + A887826, only 12 out of 55 (21.8%) DRG neurons were "responders" (*P* = 0.012 *vs* control, χ^2 test) and, in a typical time course, we did not observe any Ca^{2+} increase (Figure 66A). The insert of the Figure 66A displays the trace of one of 12 responder cells in TTX + A887826. Among them, both ΔF/F and AUC/F were slightly (but not significantly) reduced (Table 9). In finding an explanation to the observation that 12 out of 55 of cells still oscillated in the presence of TTX plus A887826, we have to consider that A887826 block of TTX-resistant Na^+ currents is dependent on Nav1.8 channels being in the open state (Zhang X.F. *et al.*, 2010). In fact, A887826 potently (IC_{50} = 8 nM) inhibits TTX-resistant Na^+ currents in rat DRG neurons in a voltage-dependent way, being about 8-fold less potent at relatively hyperpolarized (Vm < -60 mV) membrane voltages in comparison to -40 mV-clamped cells (Zhang *et al.*, 2010).

The block of L+N-type VOCCs by verapamil (1 μM) + PD173212 (500 nM) induced a significant reduction of ΔF/F (Table 9, *P*=0.003, ANOVA followed by Bonferroni's test) without a significant decrease of AUC/F. The number of "responders" under these experimental conditions was 17 out of 37 cells investigated (45.9%, not significant *vs* control: *P*=0.658, χ^2 test).

Pre-incubation with Cl-IB-MECA significantly decreased the number of responder cells (17 out of 64: 23%; *P*=0.012, χ^2 test) as compared to control (Figure 66B). However, Ca^{2+} parameters of "responders" were not modified by this treatment (Table 9).

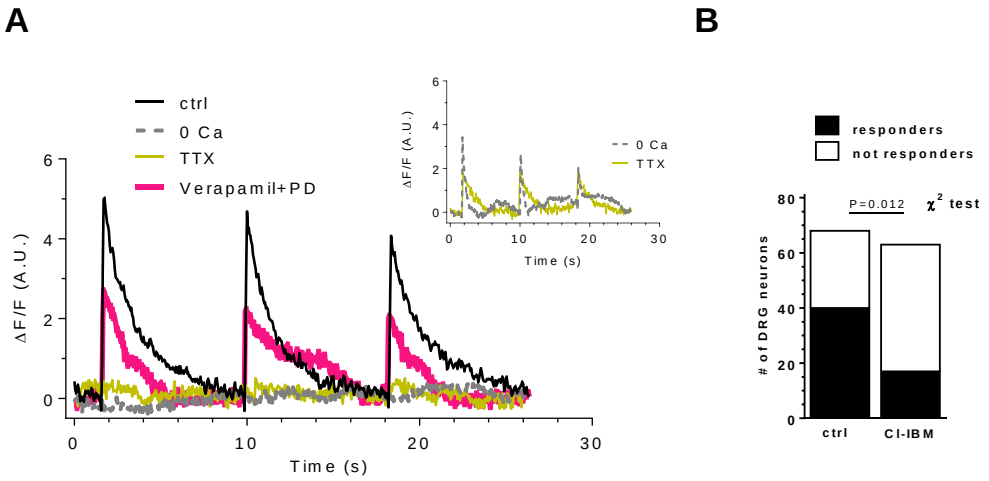

Figure 66: A_3AR stimulation reduces electrically-evoked and TTX-sensitive intracellular Ca^{2+} transients in isolated DRG neurons.
A. Typical time courses of Ca^{2+} transient induce in DRG neurons by 0.1 Hz electrical field stimulation in control condition (ctrl: black trace), extracellular free-Ca^{2+} solution (0[Ca^{2+}]out: dotted trace) or 1 µM Tetrodotoxin + 200 nM A887826 (TTX: grey trace). The insert depicts the time courses of a "responder" cell recorded in 0[Ca^{2+}]out (dotted trace) or TTX+A887826 (grey trace). B. Numbers of "responder" or "not-responder" DRG neurons to electrical field stimulation in control conditions or after pre-incubation with 30 nM Cl-IB-MECA (Cl-IBM). Statistical analysis was performed using χ2 test.

4.3 Discussion

In the present work, we investigated the expression and electrophysiological effects of adenosine A_3AR in primary sensory neurons. We report here first time evidence of A_3AR mRNA expression in the DRG, and we demonstrate that activation inhibits both pro-nociceptive N-type VOCC activation and AP firing in isolated DRG neurons.

A bulk of evidence indicates adenosine as a powerful analgesic compound in a number of *in vivo* animal models (Dickenson *et al.*, 2000) with a crucial role recognized for A_1AR activation. Of note, the A_3AR has recently gained attention as an interesting target in such conditions, because its activation causes pain relief without adverse side effects (Janes *et al.*, 2016).

In this study, we demonstrated by RT-PCR experiments that A_3AR mRNA is abundant in DRG homogenate, a result confirmed by immunocytochemical analysis showing receptor expression at neuronal level. We then explored the functional role of the A_3AR in DRG neurons by performing patch-clamp recording in the absence or presence of two different receptor agonists: the commercially available Cl-IB-MECA and the new highly selective A_3AR ligand MRS5980 (Fang *et al.*, 2015; Tosh *et al.*, 2014). Under basal (non-pharmacologically manipulated) conditions, A_3AR-

mediated effects on overall voltage-gated conductance consist of a reduction in total outward K^+ currents evoked by a ramp protocol. When analyzed in detail, the Cl-IB-MECA effect on K^+ currents was found to be dependent on the opening of Ca^{2+} channels, since it was prevented by the nonselective VOCC blocker Cd^{2+}. Among Ca^{2+}-activated K^+ currents (K_{Ca}), Cl-IB-MECA targeted SK and BK channels, which are known to be expressed in rat and mouse DRG neurons, (Mongan *et al.*, 2005; Pagadala *et al.*, 2013), because its effect was sensitive to the combination of the SK channel blocker apamin and the BK channel inhibitor TEA (200 μM).

Different VOCC types in DRG neurons have been described: P/Q- and N-types, encoded by Cav2.2 and Cav2.1, respectively, which are mainly involved in neurotransmitter release, and R-, L- and T-types, encoded by Cav2.3, Cav1.1-1.4 and Cav3.1-3.3, respectively (Schubert *et al.*, 1994.; Scroggs and Fox, 1992; Wilson *et al.*, 2000).

When VOCC-mediated currents were studied in isolation, A_3AR activation selectively inhibited N-type Ca^{2+} channels because the Cl-IB-MECA effect was prevented by the ω-CTX analogue PD173212 but not by the L-type blocker lacidipine.

Both A_3AR agonists inhibited VOCCs in the low nanomolar range, with MRS5980 being about 10-fold more potent than Cl-IB-MECA. In both cases, the selective A_3AR antagonist MRS1523 prevented the effect in a concentration-dependent manner, indicating that it was receptor-mediated. The reduction of K_{Ca} by A_3AR agonists was quantitatively lower (23.3% of ramp current inhibition at +80 mV in 100 nM Cl-IB-MECA) than Ca^{2+} current reduction (48.4% of Ca^{2+} current block at 0 mV in 100 nM Cl-IB-MECA), so the latter is expected to be the major mechanism to account for A_3AR-mediated pain control. This is in accordance with the notion that either BK or SK inhibition in DRG neurons is reported to increase cell excitability (Cao *et al.*, 2012; Chen *et al.*, 2009; Pagadala *et al.*, 2013), while, in the present work, a reduction of action potential firing was found upon A_3AR stimulation.

As known, A_1AR are also found to inhibit VOCCs in DRG neurons (Dolphin *et al.*, 1986). Consistent with this information, we observed a 24.8 ± 3.2 % Ca^{2+} current decrease in the presence of 1 μM CPA. The effect was not different from that observed in the presence of 10 μM concentration of the same compound, indicating that 1 μM CPA is enough to achieve maximal A_1AR activation in rat DRG neurons. More interestingly, the CPA-mediated Ca^{2+} current inhibition (24.8 ± 3.2 %) was significantly smaller compared to Cl-IB-MECA effect (44.1 ± 5.6 %) thus confirming a prominent functional role of A_3ARs on A_1ARs in this cell type.

When testing the effects of the endogenous agonist, adenosine-mediated inhibition of Ca^{2+} currents was either sensitive to the A_3AR blocker MRS1523 or to the A_1AR antagonist DPCPX. The results are consistent with a previous report demonstrating that 500 μM adenosine-induced Ca^{2+} signals in DRG neurons are prevented by either A_1 or A_3, but not A_{2A} or A_{2B}, AR antagonists (Zheng *et al.*, 2014).

It is well known that the Gi-coupled receptor, such as the A_3 or A_1AR subtype, can lead to inhibition of VOCC activation by a direct binding of the αi subunit to the channel protein in a number of cells

(Haas and Selbach, 2000; Schubert *et al.*, 1994). Here, we describe this phenomenon for the first time in DRG neurons. Furthermore, N-type channels are known to promote nociception by providing more than 60% of the neurotransmitter release by DRG neurons to lamina I dorsal horn neurons (Harding *et al.*, 1999; Heinke *et al.*, 2004). Previous observations demonstrate that N-type VOCCs blockers result in analgesia in a range of pain models (Gandini *et al.*, 2015; Lee, 2013; Vink and Alewood, 2012) and ziconotide, the first-choice compound among ω-CTX analogues, is approved as an intrathecal medication for chronic pain in the US (Adler and Lotz, 2017; Brookes *et al.*, 2017) and is under evaluation clinically. Of note, a direct block of N-type Ca^{2+} channels, as that achieved by ziconotide or ω-CTXs, is implicated in serious side effects (psychological symptoms such as neuropsychiatric, including depression, cognitive impairment, and hallucinations, anxiety, panic attacks, as well as ataxia, asthenia, headache, dysesthesia) (Lynch *et al.*, 2006), thus discouraging the perspective use of this compound clinically. Interestingly, an "indirect" VOCC modulation, as was accomplished by A_3AR activation, could represent a more suitable approach to pain control without adverse side effects.

Beyond VOCC inhibition, we also demonstrated that Cl-IB-MECA decreases in the number of action potentials elicited by a depolarizing ramp current injection in isolated DRG neurons. This could be another crucial mechanism by which A_3ARs exert pain relief, since sensitization to pain is described as a reduced threshold to noxious inputs due to increased action potential firing of primary sensory neurons. The Cl-IB-MECA effect was blocked by the A_3AR antagonist MRS1523 but not by the N-type Ca^{2+} channel blocker PD173212, demonstrating that N-type VOCC inhibition and firing frequency decrease are independent actions exerted by A_3ARs in rat DRG neurons. The mechanism by which Cl-IB-MECA inhibits DRG neuronal firing still needs further investigation and will be addressed in our future work.

Importantly, when we measured the intracellular Ca^{2+} rise following electrical field stimulation, we confirmed that neuronal Ca^{2+} spikes were significantly dampened by A_3 receptor activation. Thus, Cl-IB-MECA significantly reduced the number of cells responding to 0.1 Hz stimulation (from 60% of "responders" in control conditions to 26% in Cl-IB-MECA), even if it was not able to change the dynamic of Ca^{2+} rise ($\Delta F/F$ nor AUC/F) once Ca^{2+} spikes were triggered. Thus, the present data demonstrate that inhibition of DRG electrical activity might directly account for A_3AR-mediated pain control.

However, it must be pointed out that the above mentioned effects may not be the only mechanism by which A_3AR agonists exert analgesia. Data are present in the literature describing a peripheral effect of the A_3AR on cytokine release during chemotherapeutic-induced neuropathic pain (Janes *et al.*, 2014).

Concerning the neuronal population on which A_3AR agonists act, DRG neurons are a heterogeneous population of small-, medium- and large-sized cells. Among them, small- and medium-sized (cell diameter less than 30 µm) neurons responding to the TRPV1 agonist CPS and, possibly, to the TRPA1 agonist AITC are usually defined as nociceptors (Asai *et al.*, 2005; Fang *et al.*, 2005; Gold

et al., 1996; Lawson, 2002). We found that the vast majority of cells responding to Cl-IB-MECA were sensitive to both TRP compounds, even if a small fraction of A_3AR agonist-responding cells were insensitive to CPS or AITC (2 out of 13 and in 2 out of 7, respectively).

We conclude that the selective stimulation of the A_3AR inhibits N-type VOCC opening, leading to a reduction in neurotransmitter release, and reduces electrically-evoked excitation in isolated rat DRG neurons. Both these mechanisms may be important in accounting for the pain-relieving effect observed upon A_3AR activation and support the notion that an A_3AR-based therapy represents an important strategy to alleviate pain in different pathologies.

REFERENCES

References:

Abbracchio, M.P., Brambilla, R., Ceruti, S., Kim, H.O., von Lubitz, D.K., Jacobson, K.A., Cattabeni, F., 1995. G protein-dependent activation of phospholipase C by adenosine A3 receptors in rat brain. Mol. Pharmacol. 48, 1038–45.

Abbracchio, M.P., Burnstock, G., 1994. Purinoceptors: are there families of P2X and P2Y purinoceptors? Pharmacol. Ther. 64, 445–75.

Abdulla, F.A., Smith, P.A., 2001. Axotomy- and Autotomy-Induced Changes in Ca^{2+} and K^{+} Channel Currents of Rat Dorsal Root Ganglion Neurons. J. Neurophysiol. 85, 644–658. https://doi.org/10.1152/jn.2001.85.2.644

Abeliovich, A., Gitler, A.D., 2016. Defects in trafficking bridge Parkinson's disease pathology and genetics. Nature 539, 207–216. https://doi.org/10.1038/nature20414

Adachi, K., Kohara, T., Nakao, N., Arita, M., Chiba, K., Mishina, T., Sasaki, S., Fujita, T., 1995. Design, synthesis, and structure-activity relationships of 2-substituted-2-amino-1,3-propanediols: Discovery of a novel immunosuppressant, FTY720. Bioorg. Med. Chem. Lett. 5, 853–856. https://doi.org/10.1016/0960-894X(95)00127-F

Adair, T.H., 2005. Growth regulation of the vascular system: an emerging role for adenosine. Am. J. Physiol. Integr. Comp. Physiol. 289, R283–R296. https://doi.org/10.1152/ajpregu.00840.2004

Adler, J.A., Lotz, N.M., 2017. Intrathecal pain management: a team-based approach. J. Pain Res. 10, 2565–2575. https://doi.org/10.2147/JPR.S142147

Agresti, C., Meomartini, M.E., Amadio, S., Ambrosini, E., Serafini, B., Franchini, L., Volonté, C., Aloisi, F., Visentin, S., 2005. Metabotropic P2 receptor activation regulates oligodendrocyte progenitor migration and development. Glia 50, 132–144. https://doi.org/10.1002/glia.20160

Aitken, P.G., Fayuk, D., Somjen, G.G., Turner, D.A., 1999. Use of Intrinsic Optical Signals to Monitor Physiological Changes in Brain Tissue Slices. Methods 18, 91–103. https://doi.org/10.1006/meth.1999.0762

Aitken, P.G., Tombaugh, G.C., Turner, D.A., Somjen, G.G., 1998. Similar Propagation of SD and Hypoxic SD-Like Depolarization in Rat Hippocampus Recorded Optically and Electrically. J. Neurophysiol. 80, 1514–1521. https://doi.org/10.1152/jn.1998.80.3.1514

Akopov, S.E., Simonian, N.A., Grigorian, G.S., 1996. Dynamics of polymorphonuclear leukocyte accumulation in acute cerebral infarction and their correlation with brain tissue damage. Stroke 27, 1739–43.

Al-Majed, A.A., Sayed-Ahmed, M.M., Al-Omar, F.A., Al-Yahya, A.A., Aleisa, A.M., Al-Shabanah, O.A., 2006. Carnitine esters prevent oxidative stress damage and energy depletion following transient forebrain ischaemia in the rat hippocampus. Clin. Exp. Pharmacol. Physiol. 33, 725–33. https://doi.org/10.1111/j.1440-1681.2006.04425.x

Alberg, A.J., Armeson, K., Pierce, J.S., Bielawski, J., Bielawska, A., Visvanathan, K., Hill, E.G., Ogretmen, B., 2013. Plasma sphingolipids and lung cancer: a population-based, nested case-control study. Cancer Epidemiol. Biomarkers Prev. 22, 1374–82. https://doi.org/10.1158/1055-9965.EPI-12-1424

Albers, G.W., Goldstein, L.B., Hess, D.C., Wechsler, L.R., Furie, K.L., Gorelick, P.B., Hurn, P., Liebeskind, D.S., Nogueira, R.G., Saver, J.L., STAIR VII Consortium, 2011. Stroke Treatment Academic Industry Roundtable (STAIR) recommendations for maximizing the use of intravenous thrombolytics and expanding treatment options with intra-arterial and neuroprotective therapies. Stroke 42, 2645–50. https://doi.org/10.1161/STROKEAHA.111.618850

Allaman, I., Lengacher, S., Magistretti, P.J., Pellerin, L., 2003. A2B receptor activation promotes glycogen synthesis in astrocytes through modulation of gene expression. Am. J. Physiol. Cell Physiol. 284, C696-704. https://doi.org/10.1152/ajpcell.00202.2002

Allende, M.L., Bektas, M., Lee, B.G., Bonifacino, E., Kang, J., Tuymetova, G., Chen, W., Saba, J.D., Proia, R.L., 2011. Sphingosine-1-phosphate lyase deficiency produces a pro-inflammatory response while impairing neutrophil trafficking. J. Biol. Chem. 286, 7348–58. https://doi.org/10.1074/jbc.M110.171819

Almeida, R.G., Lyons, D.A., 2017. On Myelinated Axon Plasticity and Neuronal Circuit Formation and Function. J. Neurosci. 37, 10023–10034. https://doi.org/10.1523/jneurosci.3185-16.2017

Altman, J., 1962. Are new neurons formed in the brains of adult mammals? Science 135, 1127–8.

Altman, J., Das, G.D., 1965. Autoradiographic and histological evidence of postnatal hippocampal neurogenesis in rats. J. Comp. Neurol. 124, 319–35.

Amisten, S., Braun, O.Ö., Bengtsson, A., Erlinge, D., 2008. Gene expression profiling for the identification of G-protein coupled receptors in human platelets. Thromb. Res. 122, 47–57. https://doi.org/10.1016/j.thromres.2007.08.014

Anderson, W.W., Collingridge, G.L., 2001. The LTP Program: a data acquisition program for on-line analysis of long-term potentiation and other synaptic events. J. Neurosci. Methods 108, 71–83.

Asai, H., Ozaki, N., Shinoda, M., Nagamine, K., Tohnai, I., Ueda, M., Sugiura, Y., 2005. Heat and mechanical

hyperalgesia in mice model of cancer pain. Pain 117, 19–29. https://doi.org/10.1016/j.pain.2005.05.010
Ascherio, A., Zhang, S.M., Hernán, M.A., Kawachi, I., Colditz, G.A., Speizer, F.E., Willett, W.C., 2001. Prospective study of caffeine consumption and risk of Parkinson's disease in men and women. Ann. Neurol. 50, 56–63.
Astrup, J., Siesjö, B.K., Symon, L., 1981. Thresholds in cerebral ischemia — the ischemic penumbra. Stroke 12, 723–725. https://doi.org/10.1161/01.STR.12.6.723
Attali, B., Wang, N., Kolot, A., Sobko, A., Cherepanov, V., Soliven, B., 1997. Characterization of delayed rectifier Kv channels in oligodendrocytes and progenitor cells. J. Neurosci. 17, 8234–45.
Auluck, P.K., Bonini, N.M., 2002. Pharmacological prevention of Parkinson disease in Drosophila. Nat. Med. 8, 1185–1186. https://doi.org/10.1038/nm1102-1185
Balatoni, B., Storch, M.K., Swoboda, E.-M., Schönborn, V., Koziel, A., Lambrou, G.N., Hiestand, P.C., Weissert, R., Foster, C.A., 2007. FTY720 sustains and restores neuronal function in the DA rat model of MOG-induced experimental autoimmune encephalomyelitis. Brain Res. Bull. 74, 307–16. https://doi.org/10.1016/j.brainresbull.2007.06.023
Baraldi, P.G., Borea, P.A., 2000. New potent and selective human adenosine A(3) receptor antagonists. Trends Pharmacol. Sci. 21, 456–9.
Barer, R., 1953. Spectrophotometry of red cell suspensions. J. Physiol. 119, 52P–53P.
Barres, B.A., Koroshetz, W.J., Swartz, K.J., Chun, L.L., Corey, D.P., 1990. Ion channel expression by white matter glia: the O-2A glial progenitor cell. Neuron 4, 507–24.
Bartley, J., Soltau, T., Wimborne, H., Kim, S., Martin-Studdard, A., Hess, D., Hill, W., Waller, J., Carroll, J., 2005. BrdU-positive cells in the neonatal mouse hippocampus following hypoxic-ischemic brain injury. BMC Neurosci. 6, 15. https://doi.org/10.1186/1471-2202-6-15
Beckman, J.S., Koppenol, W.H., 1996. Nitric oxide, superoxide, and peroxynitrite: the good, the bad, and ugly. Am. J. Physiol. Physiol. 271, C1424–C1437. https://doi.org/10.1152/ajpcell.1996.271.5.C1424
Bergles, D.E., Roberts, J.D., Somogyi, P., Jahr, C.E., 2000. Glutamatergic synapses on oligodendrocyte precursor cells in the hippocampus. Nature 405, 187–91. https://doi.org/10.1038/35012083
Berne, R.M., 1963. Cardiac nucleotides in hypoxia: possible role in regulation of coronary blood flow. Am. J. Physiol. Content 204, 317–322. https://doi.org/10.1152/ajplegacy.1963.204.2.317
Betti, M., Catarzi, D., Varano, F., Falsini, M., Varani, K., Vincenzi, F., Dal Ben, D., Lambertucci, C., Colotta, V., 2018. The aminopyridine-3,5-dicarbonitrile core for the design of new non-nucleoside-like agonists of the human adenosine A2B receptor. Eur. J. Med. Chem. 150, 127–139. https://doi.org/10.1016/j.ejmech.2018.02.081
Beukers, M.W., Chang, L.C.W., von Frijtag Drabbe Künzel, J.K., Mulder-Krieger, T., Spanjersberg, R.F., Brussee, J., IJzerman, A.P., 2004. New, Non-Adenosine, High-Potency Agonists for the Human Adenosine A $_{2B}$ Receptor with an Improved Selectivity Profile Compared to the Reference Agonist *N* -Ethylcarboxamidoadenosine. J. Med. Chem. 47, 3707–3709. https://doi.org/10.1021/jm049947s
Beukers, M.W., den Dulk, H., van Tilburg, E.W., Brouwer, J., Ijzerman, A.P., 2000. Why are A(2B) receptors low-affinity adenosine receptors? Mutation of Asn273 to Tyr increases affinity of human A(2B) receptor for 2-(1-Hexynyl)adenosine. Mol. Pharmacol. 58, 1349–56.
Biber, K., Fiebich, B.L., Gebicke-Härter, P., van Calker, D., 1999. Carbamazepine-induced upregulation of adenosine A1-receptors in astrocyte cultures affects coupling to the phosphoinositol signaling pathway. Neuropsychopharmacology 20, 271–8. https://doi.org/10.1016/S0893-133X(98)00059-1
Bigaud, M., Dincer, Z., Bollbuck, B., Dawson, J., Beckmann, N., Beerli, C., Fishli-Cavelti, G., Nahler, M., Angst, D., Janser, P., Otto, H., Rosner, E., Hersperger, R., Bruns, C., Quancard, J., 2016. Pathophysiological Consequences of a Break in S1P1-Dependent Homeostasis of Vascular Permeability Revealed by S1P1 Competitive Antagonism. PLoS One 11, e0168252. https://doi.org/10.1371/journal.pone.0168252
Billich, A., Bornancin, F., Dévay, P., Mechtcheriakova, D., Urtz, N., Baumruker, T., 2003. Phosphorylation of the immunomodulatory drug FTY720 by sphingosine kinases. J. Biol. Chem. 278, 47408–15. https://doi.org/10.1074/jbc.M307687200
Björklund, O., Shang, M., Tonazzini, I., Daré, E., Fredholm, B.B., 2008. Adenosine A1 and A3 receptors protect astrocytes from hypoxic damage. Eur. J. Pharmacol. 596, 6–13. https://doi.org/10.1016/j.ejphar.2008.08.002
Boillée, S., Vande Velde, C., Cleveland, D.W., 2006. ALS: A Disease of Motor Neurons and Their Nonneuronal Neighbors. Neuron 52, 39–59. https://doi.org/10.1016/j.neuron.2006.09.018
Bona, E., Adén, U., Gilland, E., Fredholm, B.B., Hagberg, H., 1997. Neonatal cerebral hypoxia-ischemia: the effect of adenosine receptor antagonists. Neuropharmacology 36, 1327–38.
Bouhassira, D., Attal, N., 2016. Translational neuropathic pain research: A clinical perspective. Neuroscience 338, 27–35. https://doi.org/10.1016/j.neuroscience.2016.03.029
Brady, N.R., Elmore, S.P., van Beek, J.J.H.G.M., Krab, K., Courtoy, P.J., Hue, L., Westerhoff, H. V, 2004. Coordinated behavior of mitochondria in both space and time: a reactive oxygen species-activated wave of mitochondrial depolarization. Biophys. J. 87, 2022–34. https://doi.org/10.1529/biophysj.103.035097

Brand, A., Vissiennon, Z., Eschke, D., Nieber, K., 2001. Adenosine A(1) and A(3) receptors mediate inhibition of synaptic transmission in rat cortical neurons. Neuropharmacology 40, 85–95.

Brinkmann, V., 2007. Sphingosine 1-phosphate receptors in health and disease: Mechanistic insights from gene deletion studies and reverse pharmacology. Pharmacol. Ther. 115, 84–105. https://doi.org/10.1016/j.pharmthera.2007.04.006

Brinkmann, V., Davis, M.D., Heise, C.E., Albert, R., Cottens, S., Hof, R., Bruns, C., Prieschl, E., Baumruker, T., Hiestand, P., Foster, C.A., Zollinger, M., Lynch, K.R., 2002. The immune modulator FTY720 targets sphingosine 1-phosphate receptors. J. Biol. Chem. 277, 21453–7. https://doi.org/10.1074/jbc.C200176200

Brinley, F.J., Kandel, E.R., Marshall, W.H., 1960. potassium outflux from rabbit cortex during spreading depression. J. Neurophysiol. 23, 246–256. https://doi.org/10.1152/jn.1960.23.3.246

Brookes, M.E., Eldabe, S., Batterham, A., 2017. Ziconotide Monotherapy: A Systematic Review of Randomised Controlled Trials. Curr. Neuropharmacol. 15, 217–231.

Bruijn, L.I., Houseweart, M.K., Kato, S., Anderson, K.L., Anderson, S.D., Ohama, E., Reaume, A.G., Scott, R.W., Cleveland, D.W., 1998. Aggregation and motor neuron toxicity of an ALS-linked SOD1 mutant independent from wild-type SOD1. Science 281, 1851–4.

Brunkhorst, H., 2014. Revolutionary constitutions: Arendt's inversions of Heidegger. Eur. J. Cult. Polit. Sociol. 1, 283–298. https://doi.org/10.1080/23254823.2014.992120

Bruns, R.F., Fergus, J.H., 1990. Allosteric enhancement of adenosine A1 receptor binding and function by 2-amino-3-benzoylthiophenes. Mol. Pharmacol. 38, 939–49.

Bueno-Junior, L.S., Leite, J.P., 2018. Input Convergence, Synaptic Plasticity and Functional Coupling Across Hippocampal-Prefrontal-Thalamic Circuits. Front. Neural Circuits 12, 40. https://doi.org/10.3389/fncir.2018.00040

Burda, J.E., Sofroniew, M. V, 2014. Reactive gliosis and the multicellular response to CNS damage and disease. Neuron 81, 229–48. https://doi.org/10.1016/j.neuron.2013.12.034

Burke, S.P., Nadler, J. V, 1988. Regulation of glutamate and aspartate release from slices of the hippocampal CA1 area: effects of adenosine and baclofen. J. Neurochem. 51, 1541–51.

Burnstock, G., 1975. Comparative studies of purinergic nerves. J. Exp. Zool. 194, 103–133. https://doi.org/10.1002/jez.1401940108

Burnstock, G., Cocks, T., Kasakov, L., Wong, H.K., 1978. Direct evidence for ATP release from non-adrenergic, non-cholinergic ("purinergic") nerves in the guinea-pig taenia coli and bladder. Eur. J. Pharmacol. 49, 145–9. https://doi.org/10.1016/0014-2999(78)90070-5

Busserolles, J., Tsantoulas, C., Eschalier, A., López García, J.A., 2016. Potassium channels in neuropathic pain. Pain 157, S7–S14. https://doi.org/10.1097/j.pain.0000000000000368

Butt, A.M., Dinsdale, J., 2005. Opposing actions of fibroblast growth factor-2 on early and late oligodendrocyte lineage cells in vivo. J. Neuroimmunol. 166, 75–87. https://doi.org/10.1016/j.jneuroim.2005.05.015

Butt, A.M., Duncan, A., Hornby, M.F., Kirvell, S.L., Hunter, A., Levine, J.M., Berry, M., 1999. Cells expressing the NG2 antigen contact nodes of Ranvier in adult CNS white matter. Glia 26, 84–91.

Butt, A.M., Kiff, J., Hubbard, P., Berry, M., 2002. Synantocytes: New functions for novel NG2 expressing glia. J. Neurocytol. 31, 551–565. https://doi.org/10.1023/A:1025751900356

Buttini, M., Appel, K., Sauter, A., Gebicke-Haerter, P.J., Boddeke, H.W., 1996. Expression of tumor necrosis factor alpha after focal cerebral ischaemia in the rat. Neuroscience 71, 1–16.

Calabrese, M., Reynolds, R., Magliozzi, R., Castellaro, M., Morra, A., Scalfari, A., Farina, G., Romualdi, C., Gajofatto, A., Pitteri, M., Benedetti, M.D., Monaco, S., 2015. Regional Distribution and Evolution of Gray Matter Damage in Different Populations of Multiple Sclerosis Patients. PLoS One 10, e0135428. https://doi.org/10.1371/journal.pone.0135428

Calabresi, P., Picconi, B., Saulle, E., Centonze, D., Hainsworth, A.H., Bernardi, G., 2000. Is pharmacological neuroprotection dependent on reduced glutamate release? Stroke 31, 766–72; discussion 773.

Camerer, E., Regard, J.B., Cornelissen, I., Srinivasan, Y., Duong, D.N., Palmer, D., Pham, T.H., Wong, J.S., Pappu, R., Coughlin, S.R., 2009. Sphingosine-1-phosphate in the plasma compartment regulates basal and inflammation-induced vascular leak in mice. J. Clin. Invest. 119, 1871–9.

Canals, S., Larrosa, B., Pintor, J., Mena, M.A., Herreras, O., 2008. Metabolic challenge to glia activates an adenosine-mediated safety mechanism that promotes neuronal survival by delaying the onset of spreading depression waves. J. Cereb. Blood Flow Metab. 28, 1835–44. https://doi.org/10.1038/jcbfm.2008.71

Canter, R.G., Penney, J., Tsai, L.-H., 2016. The road to restoring neural circuits for the treatment of Alzheimer's disease. Nature 539, 187–196. https://doi.org/10.1038/nature20412

Cao, X.-H., Byun, H.-S., Chen, S.-R., Cai, Y.-Q., Pan, H.-L., 2010. Reduction in voltage-gated K+ channel activity in primary sensory neurons in painful diabetic neuropathy: role of brain-derived neurotrophic factor. J. Neurochem. 114, no-no. https://doi.org/10.1111/j.1471-4159.2010.06863.x

Cao, X.-H., Chen, S.-R., Li, L., Pan, H.-L., 2012. Nerve injury increases brain-derived neurotrophic factor levels to suppress BK channel activity in primary sensory neurons. J. Neurochem. 121, 944–953.

https://doi.org/10.1111/j.1471-4159.2012.07736.x

Cao, X.-H., Zhao, S.-S., Liu, D.-Y., Wang, Z., Niu, L.-L., Hou, L.-H., Wang, C.-L., 2011. ROS-Ca(2+) is associated with mitochondria permeability transition pore involved in surfactin-induced MCF-7 cells apoptosis. Chem. Biol. Interact. 190, 16–27. https://doi.org/10.1016/j.cbi.2011.01.010

Caplan, L.R., 1998. Stroke treatment: Promising but still struggling. J. Am. Med. Assoc. 279, 1304–1306. https://doi.org/10.1001/jama.279.16.1304

Carlton, S.M., Du, J., Tan, H.Y., Nesic, O., Hargett, G.L., Bopp, A.C., Yamani, A., Lin, Q., Willis, W.D., Hulsebosch, C.E., 2009. Peripheral and central sensitization in remote spinal cord regions contribute to central neuropathic pain after spinal cord injury. Pain 147, 265–276. https://doi.org/10.1016/j.pain.2009.09.030

Carpenter, K.J., Vithlani, M., Dickenson, A.H., 2000. Unaltered peripheral excitatory actions of nociceptin contrast with enhanced spinal inhibitory effects after carrageenan inflammation: an electrophysiological study in the rat. Pain 85, 433–41.

Cerbai, F., Lana, D., Nosi, D., Petkova-Kirova, P., Zecchi, S., Brothers, H.M., Wenk, G.L., Giovannini, M.G., 2012. The neuron-astrocyte-microglia triad in normal brain ageing and in a model of neuroinflammation in the rat hippocampus. PLoS One 7, e45250. https://doi.org/10.1371/journal.pone.0045250

Chang, A., Nishiyama, A., Peterson, J., Prineas, J., Trapp, B.D., 2000. NG2-positive oligodendrocyte progenitor cells in adult human brain and multiple sclerosis lesions. J. Neurosci. 20, 6404–12.

Chen, F., Qi, Z., Luo, Y., Hinchliffe, T., Ding, G., Xia, Y., Ji, X., 2014. Non-pharmaceutical therapies for stroke: mechanisms and clinical implications. Prog. Neurobiol. 115, 246–69. https://doi.org/10.1016/j.pneurobio.2013.12.007

Chen, J.-F., Eltzschig, H.K., Fredholm, B.B., 2013. Adenosine receptors as drug targets — what are the challenges? Nat. Rev. Drug Discov. 12, 265–286. https://doi.org/10.1038/nrd3955

Chen, S.-R., Cai, Y.-Q., Pan, H.-L., 2009. Plasticity and emerging role of BKCa channels in nociceptive control in neuropathic pain. J. Neurochem. 110, 352–62. https://doi.org/10.1111/j.1471-4159.2009.06138.x

Chen, S., He, R.R., 1999. Effect of intracarotid administration of adenosine on the activity of area postrema neurons in barodenervated rats. Sheng Li Xue Bao 51, 667–74.

Cheong, S.L., Federico, S., Venkatesan, G., Mandel, A.L., Shao, Y.-M., Moro, S., Spalluto, G., Pastorin, G., 2013. The A_3 adenosine receptor as multifaceted therapeutic target: pharmacology, medicinal chemistry, and in silico approaches. Med. Res. Rev. 33, 235–335. https://doi.org/10.1002/med.20254

Chiaravalloti, N.D., DeLuca, J., 2008. Cognitive impairment in multiple sclerosis. Lancet. Neurol. 7, 1139–51. https://doi.org/10.1016/S1474-4422(08)70259-X

Chiba, K., Yanagawa, Y., Masubuchi, Y., Kataoka, H., Kawaguchi, T., Ohtsuki, M., Hoshino, Y., 1998. FTY720, a novel immunosuppressant, induces sequestration of circulating mature lymphocytes by acceleration of lymphocyte homing in rats. I. FTY720 selectively decreases the number of circulating mature lymphocytes by acceleration of lymphocyte homing. J. Immunol. 160, 5037–44.

Choi, D.W., 1990. Possible mechanisms limiting N-methyl-D-aspartate receptor overactivation and the therapeutic efficacy of N-methyl-D-aspartate antagonists. Stroke 21, III20-2.

Choi, J.W., Gardell, S.E., Herr, D.R., Rivera, R., Lee, C.-W., Noguchi, K., Teo, S.T., Yung, Y.C., Lu, M., Kennedy, G., Chun, J., 2011. FTY720 (fingolimod) efficacy in an animal model of multiple sclerosis requires astrocyte sphingosine 1-phosphate receptor 1 (S1P1) modulation. Proc. Natl. Acad. Sci. 108, 751–756. https://doi.org/10.1073/pnas.1014154108

Cieślik, M., Czapski, G.A., Strosznajder, J.B., 2015. The Molecular Mechanism of Amyloid β42 Peptide Toxicity: The Role of Sphingosine Kinase-1 and Mitochondrial Sirtuins. PLoS One 10, e0137193. https://doi.org/10.1371/journal.pone.0137193

Coelho, R.P., Payne, S.G., Bittman, R., Spiegel, S., Sato-Bigbee, C., 2007. The immunomodulator FTY720 has a direct cytoprotective effect in oligodendrocyte progenitors. J. Pharmacol. Exp. Ther. 323, 626–35. https://doi.org/10.1124/jpet.107.123927

Collewijn, H., Harreveld, A. V, 1966. Membrane potential of cerebral cortical cells during reading depression and asyxia. Exp. Neurol. 15, 425–36.

Comi, G., Radaelli, M., Soelberg Sørensen, P., 2017. Evolving concepts in the treatment of relapsing multiple sclerosis. Lancet 389, 1347–1356. https://doi.org/10.1016/S0140-6736(16)32388-1

Compston, A., Coles, A., 2002. Multiple sclerosis. Lancet 359, 1221–1231. https://doi.org/10.1016/S0140-6736(02)08220-X

Cooper, A.A., Gitler, A.D., Cashikar, A., Haynes, C.M., Hill, K.J., Bhullar, B., Liu, K., Xu, K., Strathearn, K.E., Liu, F., Cao, S., Caldwell, K.A., Caldwell, G.A., Marsischky, G., Kolodner, R.D., Labaer, J., Rochet, J.-C., Bonini, N.M., Lindquist, S., 2006. -Synuclein Blocks ER-Golgi Traffic and Rab1 Rescues Neuron Loss in Parkinson's Models. Science (80-.). 313, 324–328. https://doi.org/10.1126/science.1129462

Coppi, E., Cellai, L., Maraula, G., Dettori, I., Melani, A., Pugliese, A.M., Pedata, F., 2015. Role of adenosine in oligodendrocyte precursor maturation. Front. Cell. Neurosci. 9, 155. https://doi.org/10.3389/fncel.2015.00155

Coppi, E., Cellai, L., Maraula, G., Pugliese, A.M., Pedata, F., 2013a. Adenosine A_2 A receptors inhibit delayed rectifier potassium currents and cell differentiation in primary purified oligodendrocyte cultures. Neuropharmacology 73, 301–10. https://doi.org/10.1016/j.neuropharm.2013.05.035

Coppi, E., Maraula, G., Fumagalli, M., Failli, P., Cellai, L., Bonfanti, E., Mazzoni, L., Coppini, R., Abbracchio, M.P., Pedata, F., Pugliese, A.M., 2013b. UDP-glucose enhances outward K^+ currents necessary for cell differentiation and stimulates cell migration by activating the GPR17 receptor in oligodendrocyte precursors. Glia 61, 1155–1171. https://doi.org/10.1002/glia.22506

Coppi, E., Pedata, F., Gibb, A.J., 2012. P2Y $_1$ receptor modulation of Ca^{2+} -activated K^+ currents in medium-sized neurons from neonatal rat striatal slices. J. Neurophysiol. 107, 1009–1021. https://doi.org/10.1152/jn.00816.2009

Coppi, E., Pugliese, A.M., Stephan, H., Müller, C.E., Pedata, F., 2007. Role of P2 purinergic receptors in synaptic transmission under normoxic and ischaemic conditions in the CA1 region of rat hippocampal slices. Purinergic Signal. 3, 203–19. https://doi.org/10.1007/s11302-006-9049-4

Corradetti, R., Lo Conte, G., Moroni, F., Passani, M.B., Pepeu, G., 1984. Adenosine decreases aspartate and glutamate release from rat hippocampal slices. Eur. J. Pharmacol. 104, 19–26.

Corsi, C., Melani, A., Bianchi, L., Pepeu, G., Pedata, F., 1999. Striatal A2A adenosine receptors differentially regulate spontaneous and K+-evoked glutamate release in vivo in young and aged rats. Neuroreport 10, 687–91.

Costenla, A.R., Lopes, L. V, de Mendonça, A., Ribeiro, J.A., 2001. A functional role for adenosine A3 receptors: modulation of synaptic plasticity in the rat hippocampus. Neurosci. Lett. 302, 53–7.

Costigan, M., Scholz, J., Woolf, C.J., 2009. Neuropathic Pain: A Maladaptive Response of the Nervous System to Damage. Annu. Rev. Neurosci. 32, 1–32. https://doi.org/10.1146/annurev.neuro.051508.135531

Couttas, T.A., Kain, N., Daniels, B., Lim, X.Y., Shepherd, C., Kril, J., Pickford, R., Li, H., Garner, B., Don, A.S., 2014. Loss of the neuroprotective factor Sphingosine 1-phosphate early in Alzheimer's disease pathogenesis. Acta Neuropathol. Commun. 2, 9. https://doi.org/10.1186/2051-5960-2-9

Crespo, A., El Maatougui, A., Biagini, P., Azuaje, J., Coelho, A., Brea, J., Loza, M.I., Cadavid, M.I., García-Mera, X., Gutiérrez-de-Terán, H., Sotelo, E., 2013. Discovery of 3,4-Dihydropyrimidin-2(1H)-ones As a Novel Class of Potent and Selective A2B Adenosine Receptor Antagonists. ACS Med. Chem. Lett. 4, 1031–6. https://doi.org/10.1021/ml400185v

Cristalli, G., Lambertucci, C., Marucci, G., Volpini, R., Dal Ben, D., 2008. A2A adenosine receptor and its modulators: overview on a druggable GPCR and on structure-activity relationship analysis and binding requirements of agonists and antagonists. Curr. Pharm. Des. 14, 1525–52.

Cunha, R.A., Johansson, B., Constantino, M.D., Sebastião, A.M., Fredholm, B.B., 1996. Evidence for high-affinity binding sites for the adenosine A2A receptor agonist [3H] CGS 21680 in the rat hippocampus and cerebral cortex that are different from striatal A2A receptors. Naunyn. Schmiedebergs. Arch. Pharmacol. 353, 261–71.

Cunha, R.A., Johansson, B., Fredholm, B.B., Ribeiro, J.A., Sebastião, A.M., 1995. Adenosine A2A receptors stimulate acetylcholine release from nerve terminals of the rat hippocampus. Neurosci. Lett. 196, 41–4.

Cunha, R.A., Johansson, B., van der Ploeg, I., Sebastião, A.M., Ribeiro, J.A., Fredholm, B.B., 1994. Evidence for functionally important adenosine A2a receptors in the rat hippocampus. Brain Res. 649, 208–16.

Daval, J.L., Nicolas, F., 1994. Opposite effects of cyclohexyladenosine and theophylline on hypoxic damage in cultured neurons. Neurosci. Lett. 175, 114–6.

Davies, I.B., 1995. Risk of stroke in asymptomatic carotid stenosis. Lancet (London, England) 345, 722.

Dawson, M.R.L., Polito, A., Levine, J.M., Reynolds, R., 2003. NG2-expressing glial progenitor cells: an abundant and widespread population of cycling cells in the adult rat CNS. Mol. Cell. Neurosci. 24, 476–88.

de Castro, F., Bribián, A., 2005. The molecular orchestra of the migration of oligodendrocyte precursors during development. Brain Res. Brain Res. Rev. 49, 227–41. https://doi.org/10.1016/j.brainresrev.2004.12.034

De Keyser, J., Sulter, G., Langedijk, M., Elting, J.W., van der Naalt, J., 1999. Management of acute ischaemic stroke. Acta Clin. Belg. 54, 302–5.

De Paoli, P., Cerbai, E., Koidl, B., Kirchengast, M., Sartiani, L., Mugelli, A., 2002. Selectivity of different calcium antagonists on T- and L-type calcium currents in guinea-pig ventricular myocytes. Pharmacol. Res. 46, 491–7.

Debanne, D., Guérineau, N.C., Gähwiler, B.H., Thompson, S.M., 1996. Paired-pulse facilitation and depression at unitary synapses in rat hippocampus: quantal fluctuation affects subsequent release. J. Physiol. 491 (Pt 1), 163–76.

Debien, E., Mayol, K., Biajoux, V., Daussy, C., De Aguero, M.G., Taillardet, M., Dagany, N., Brinza, L., Henry, T., Dubois, B., Kaiserlian, D., Marvel, J., Balabanian, K., Walzer, T., 2013. S1PR5 is pivotal for the homeostasis of patrolling monocytes. Eur. J. Immunol. 43, 1667–1675. https://doi.org/10.1002/eji.201343312

Deckert, J., Jorgensen, M.B., 1988. Evidence for pre- and postsynaptic localization of adenosine A1 receptors in the CA1 region of rat hippocampus: a quantitative autoradiographic study. Brain Res. 446, 161–4.

DeLuca, G.C., Yates, R.L., Beale, H., Morrow, S.A., 2015. Cognitive Impairment in Multiple Sclerosis: Clinical, Radiologic and Pathologic Insights. Brain Pathol. 25, 79–98. https://doi.org/10.1111/bpa.12220

Dennis, P.B., Jaeschke, A., Saitoh, M., Fowler, B., Kozma, S.C., Thomas, G., 2001. Mammalian TOR: a homeostatic ATP sensor. Science 294, 1102–5. https://doi.org/10.1126/science.1063518

Deshpande, J.K., Siesjö, B.K., Wieloch, T., 1987. Calcium Accumulation and Neuronal Damage in the Rat Hippocampus following Cerebral Ischemia. J. Cereb. Blood Flow Metab. 7, 89–95. https://doi.org/10.1038/jcbfm.1987.13

Deussen, A., 2000. Metabolic flux rates of adenosine in the heart. Naunyn. Schmiedebergs. Arch. Pharmacol. 362, 351–63.

Dewar, D., Underhill, S.M., Goldberg, M.P., 2003. Oligodendrocytes and Ischemic Brain Injury. J. Cereb. Blood Flow Metab. 23, 263–274. https://doi.org/10.1097/01.WCB.0000053472.41007.F9

Di Cesare Mannelli, L., Pacini, A., Corti, F., Boccella, S., Luongo, L., Esposito, E., Cuzzocrea, S., Maione, S., Calignano, A., Ghelardini, C., 2015. Antineuropathic Profile of N-Palmitoylethanolamine in a Rat Model of Oxaliplatin-Induced Neurotoxicity. PLoS One 10, e0128080. https://doi.org/10.1371/journal.pone.0128080

Di Cesare Mannelli, L., Zanardelli, M., Landini, I., Pacini, A., Ghelardini, C., Mini, E., Bencini, A., Valtancoli, B., Failli, P., 2016. Effect of the SOD mimetic MnL4 on in vitro and in vivo oxaliplatin toxicity: Possible aid in chemotherapy induced neuropathy. Free Radic. Biol. Med. 93, 67–76. https://doi.org/10.1016/j.freeradbiomed.2016.01.023

Di Filippo, M., Sarchielli, P., Picconi, B., Calabresi, P., 2008. Neuroinflammation and synaptic plasticity: theoretical basis for a novel, immune-centred, therapeutic approach to neurological disorders. Trends Pharmacol. Sci. 29, 402–12. https://doi.org/10.1016/j.tips.2008.06.005

Dib-Hajj, S.D., Black, J.A., Waxman, S.G., 2009. Voltage-gated sodium channels: therapeutic targets for pain. Pain Med. 10, 1260–9. https://doi.org/10.1111/j.1526-4637.2009.00719.x

Dickenson, A.H., Suzuki, R., Reeve, A.J., 2000. Adenosine as a Potential Analgesic Target in Inflammatory and Neuropathic Pains. CNS Drugs 13, 77–85. https://doi.org/10.2165/00023210-200013020-00001

Dirnagl, U., 2012. Pathobiology of injury after stroke: the neurovascular unit and beyond. Ann. N. Y. Acad. Sci. 1268, 21–25. https://doi.org/10.1111/j.1749-6632.2012.06691.x

Dirnagl, U., Iadecola, C., Moskowitz, M.A., 1999. Pathobiology of ischaemic stroke: an integrated view. Trends Neurosci. 22, 391–7.

Dixon, A.K., Gubitz, A.K., Sirinathsinghji, D.J., Richardson, P.J., Freeman, T.C., 1996. Tissue distribution of adenosine receptor mRNAs in the rat. Br. J. Pharmacol. 118, 1461–8.

Dixon, A.K., Widdowson, L., Richardson, P.J., 1997. Desensitisation of the adenosine A1 receptor by the A2A receptor in the rat striatum. J. Neurochem. 69, 315–21.

Dolphin, A.C., 2016. Voltage-gated calcium channels and their auxiliary subunits: physiology and pathophysiology and pharmacology. J. Physiol. 594, 5369–5390. https://doi.org/10.1113/JP272262

Dolphin, A.C., Forda, S.R., Scott, R.H., 1986. Calcium-dependent currents in cultured rat dorsal root ganglion neurones are inhibited by an adenosine analogue. J. Physiol. 373, 47–61.

Donati, C., Cencetti, F., Nincheri, P., Bernacchioni, C., Brunelli, S., Clementi, E., Cossu, G., Bruni, P., 2007. Sphingosine 1-phosphate mediates proliferation and survival of mesoangioblasts. Stem Cells 25, 1713–9. https://doi.org/10.1634/stemcells.2006-0725

Donoso, M.V., López, R., Miranda, R., Briones, R., Huidobro-Toro, J.P., 2005. A2B adenosine receptor mediates human chorionic vasoconstriction and signals through arachidonic acid cascade. Am. J. Physiol. Heart Circ. Physiol. 288, H2439-49. https://doi.org/10.1152/ajpheart.00548.2004

Drury, A.N., Szent-Györgyi, A., 1929. The physiological activity of adenine compounds with especial reference to their action upon the mammalian heart. J. Physiol. 68, 213–37.

Du, J., Fang, J., Wen, C., Shao, X., Liang, Y., Fang, J., 2017. The Effect of Electroacupuncture on PKMzeta in the ACC in Regulating Anxiety-Like Behaviors in Rats Experiencing Chronic Inflammatory Pain. Neural Plast. 2017, 1–13. https://doi.org/10.1155/2017/3728752

Dudek, S.M., Camp, S.M., Chiang, E.T., Singleton, P.A., Usatyuk, P.V., Zhao, Y., Natarajan, V., Garcia, J.G.N., 2007. Pulmonary endothelial cell barrier enhancement by FTY720 does not require the S1P1 receptor. Cell. Signal. 19, 1754–1764. https://doi.org/10.1016/J.CELLSIG.2007.03.011

Dukala, D.E., Soliven, B., 2016. S1P1 deletion in oligodendroglial lineage cells: Effect on differentiation and myelination. Glia 64, 570–82. https://doi.org/10.1002/glia.22949

Dunwiddie, T. V, Diao, L., Kim, H.O., Jiang, J.L., Jacobson, K.A., 1997. Activation of hippocampal adenosine A3 receptors produces a desensitization of A1 receptor-mediated responses in rat hippocampus. J. Neurosci. 17, 607–14.

Dux, E., Fastbom, J., Ungerstedt, U., Rudolphi, K., Fredholm, B.B., 1990. Protective effect of adenosine and a novel xanthine derivative propentofylline on the cell damage after bilateral carotid occlusion in the gerbil hippocampus. Brain Res. 516, 248–56.

Eckle, T., Faigle, M., Grenz, A., Laucher, S., Thompson, L.F., Eltzschig, H.K., 2008. A2B adenosine receptor dampens hypoxia-induced vascular leak. Blood 111, 2024–2035. https://doi.org/10.1182/blood-2007-10-

117044
Elmore, S., 2007. Apoptosis: a review of programmed cell death. Toxicol. Pathol. 35, 495–516. https://doi.org/10.1080/01926230701320337
Eltzschig, H.K., Ibla, J.C., Furuta, G.T., Leonard, M.O., Jacobson, K.A., Enjyoji, K., Robson, S.C., Colgan, S.P., 2003. Coordinated Adenine Nucleotide Phosphohydrolysis and Nucleoside Signaling in Posthypoxic Endothelium. J. Exp. Med. 198, 783–796. https://doi.org/10.1084/jem.20030891
Eltzschig, H.K., Thompson, L.F., Karhausen, J., Cotta, R.J., Ibla, J.C., Robson, S.C., Colgan, S.P., 2004. Endogenous adenosine produced during hypoxia attenuates neutrophil accumulation: coordination by extracellular nucleotide metabolism. Blood 104, 3986–3992. https://doi.org/10.1182/blood-2004-06-2066
Emery, B., 2010. Regulation of Oligodendrocyte Differentiation and Myelination. Science (80-.). 330, 779–782. https://doi.org/10.1126/science.1190927
English, C., Aloi, J.J., 2015. New FDA-Approved Disease-Modifying Therapies for Multiple Sclerosis. Clin. Ther. 37, 691–715. https://doi.org/10.1016/j.clinthera.2015.03.001
Erdmann, A.A., Gao, Z.-G., Jung, U., Foley, J., Borenstein, T., Jacobson, K.A., Fowler, D.H., 2005. Activation of Th1 and Tc1 cell adenosine A2A receptors directly inhibits IL-2 secretion in vitro and IL-2-driven expansion in vivo. Blood 105, 4707–14. https://doi.org/10.1182/blood-2004-04-1407
Fang, X., McMullan, S., Lawson, S.N., Djouhri, L., 2005. Electrophysiological differences between nociceptive and non-nociceptive dorsal root ganglion neurones in the rat in vivo. J. Physiol. 565, 927–43. https://doi.org/10.1113/jphysiol.2005.086199
Fang, Z.-Z., Tosh, D.K., Tanaka, N., Wang, H., Krausz, K.W., O'Connor, R., Jacobson, K.A., Gonzalez, F.J., 2015. Metabolic mapping of A3 adenosine receptor agonist MRS5980. Biochem. Pharmacol. 97, 215–23. https://doi.org/10.1016/j.bcp.2015.07.007
Farkas, E., Pratt, R., Sengpiel, F., Obrenovitch, T.P., 2008. Direct, live imaging of cortical spreading depression and anoxic depolarisation using a fluorescent, voltage-sensitive dye. J. Cereb. Blood Flow Metab. 28, 251–62. https://doi.org/10.1038/sj.jcbfm.9600569
Feoktistov, I., Biaggioni, I., 2011. Role of adenosine A(2B) receptors in inflammation. Adv. Pharmacol. 61, 115–44. https://doi.org/10.1016/B978-0-12-385526-8.00005-9
Feoktistov, I., Biaggioni, I., 1997. Adenosine A2B receptors. Pharmacol. Rev. 49, 381–402.
Feoktistov, I., Goldstein, A.E., Ryzhov, S., Zeng, D., Belardinelli, L., Voyno-Yasenetskaya, T., Biaggioni, I., 2002. Differential expression of adenosine receptors in human endothelial cells: role of A2B receptors in angiogenic factor regulation. Circ. Res. 90, 531–8.
Feoktistov, I., Ryzhov, S., Zhong, H., Goldstein, A.E., Matafonov, A., Zeng, D., Biaggioni, I., 2004. Hypoxia Modulates Adenosine Receptors in Human Endothelial and Smooth Muscle Cells Toward an A_{2B} Angiogenic Phenotype. Hypertension 44, 649–654. https://doi.org/10.1161/01.HYP.0000144800.21037.a5
Fernández-Fernández, D., Rosenbrock, H., Kroker, K.S., 2015. Inhibition of PDE2A, but not PDE9A, modulates presynaptic short-term plasticity measured by paired-pulse facilitation in the CA1 region of the hippocampus. Synapse 69, 484–496. https://doi.org/10.1002/syn.21840
Ferre, S., von Euler, G., Johansson, B., Fredholm, B.B., Fuxe, K., 1991. Stimulation of high-affinity adenosine A2 receptors decreases the affinity of dopamine D2 receptors in rat striatal membranes. Proc. Natl. Acad. Sci. U. S. A. 88, 7238–41.
Fiebich, B.L., Biber, K., Lieb, K., van Calker, D., Berger, M., Bauer, J., Gebicke-Haerter, P.J., 1996. Cyclooxygenase-2 expression in rat microglia is induced by adenosine A2a-receptors. Glia 18, 152–60. https://doi.org/10.1002/(SICI)1098-1136(199610)18:2<152:AID-GLIA7>3.0.CO;2-2
Field, M.J., Li, Z., Schwarz, J.B., 2007. Ca2+ channel alpha2-delta ligands for the treatment of neuropathic pain. J. Med. Chem. 50, 2569–75. https://doi.org/10.1021/jm060650z
Fields, R.D., 2015. A new mechanism of nervous system plasticity: activity-dependent myelination. Nat. Rev. Neurosci. 16, 756–67. https://doi.org/10.1038/nrn4023
Fields, R.D., Stevens-Graham, B., 2002. New Insights into Neuron-Glia Communication. Science (80-.). 298, 556–562. https://doi.org/10.1126/science.298.5593.556
Filipenko, I., Schwalm, S., Reali, L., Pfeilschifter, J., Fabbro, D., Huwiler, A., Zangemeister-Wittke, U., 2016. Upregulation of the S1P3 receptor in metastatic breast cancer cells increases migration and invasion by induction of PGE2 and EP2/EP4 activation. Biochim. Biophys. Acta - Mol. Cell Biol. Lipids 1861, 1840–1851. https://doi.org/10.1016/J.BBALIP.2016.09.005
Filippi, M., Rocca, M.A., Barkhof, F., Brück, W., Chen, J.T., Comi, G., DeLuca, G., De Stefano, N., Erickson, B.J., Evangelou, N., Fazekas, F., Geurts, J.J., Lucchinetti, C., Miller, D.H., Pelletier, D., Popescu, B.F.G., Lassmann, H., Attendees of the Correlation between Pathological MRI findings in MS workshop, 2012. Association between pathological and MRI findings in multiple sclerosis. Lancet Neurol. 11, 349–360. https://doi.org/10.1016/S1474-4422(12)70003-0
Ford, A., Castonguay, A., Cottet, M., Little, J.W., Chen, Z., Symons-Liguori, A.M., Doyle, T., Egan, T.M., Vanderah, T.W., De Koninck, Y., Tosh, D.K., Jacobson, K.A., Salvemini, D., 2015. Engagement of the

GABA to KCC2 Signaling Pathway Contributes to the Analgesic Effects of A 3 AR Agonists in Neuropathic Pain. J. Neurosci. 35, 6057–6067. https://doi.org/10.1523/JNEUROSCI.4495-14.2015

Foster, C.A., Howard, L.M., Schweitzer, A., Persohn, E., Hiestand, P.C., Balatoni, B., Reuschel, R., Beerli, C., Schwartz, M., Billich, A., 2007. Brain Penetration of the Oral Immunomodulatory Drug FTY720 and Its Phosphorylation in the Central Nervous System during Experimental Autoimmune Encephalomyelitis: Consequences for Mode of Action in Multiple Sclerosis. J. Pharmacol. Exp. Ther. 323, 469–475. https://doi.org/10.1124/jpet.107.127183

Fowler, J.C., 1992. Escape from inhibition of synaptic transmission during in vitro hypoxia and hypoglycemia in the hippocampus. Brain Res. 573, 169–73.

Fraser, H., Gao, Z., Ozeck, M.J., Belardinelli, L., 2003. N-[3-(R)-tetrahydrofuranyl]-6-aminopurine riboside, an A1 adenosine receptor agonist, antagonizes catecholamine-induced lipolysis without cardiovascular effects in awake rats. J. Pharmacol. Exp. Ther. 305, 225–31. https://doi.org/10.1124/jpet.102.046821

Fredholm, B.B., 1995. Purinoceptors in the nervous system. Pharmacol. Toxicol. 76, 228–39.

Fredholm, B.B., Arslan, G., Halldner, L., Kull, B., Schulte, G., Wasserman, W., 2000. Structure and function of adenosine receptors and their genes. Naunyn. Schmiedebergs. Arch. Pharmacol. 362, 364–74.

Fredholm, B.B., Dunwiddie, T. V, 1988. How does adenosine inhibit transmitter release? Trends Pharmacol. Sci. 9, 130–4.

Fredholm, B.B., IJzerman, A.P., Jacobson, K.A., Klotz, K.N., Linden, J., 2001. International Union of Pharmacology. XXV. Nomenclature and classification of adenosine receptors. Pharmacol. Rev. 53, 527–52.

Fredholm, B.B., IJzerman, A.P., Jacobson, K.A., Linden, J., Muller, C.E., 2011. International Union of Basic and Clinical Pharmacology. LXXXI. Nomenclature and Classification of Adenosine Receptors--An Update. Pharmacol. Rev. 63, 1–34. https://doi.org/10.1124/pr.110.003285

Fredholm, B.B., Zhang, Y., Van Der Ploeg, I., 1996. Adenosine A(2A) receptors mediate the inhibitory effect of adenosine on formyl-Met-Leu-Phe-stimulated respiratory burst in neutrophil leucocytes. Naunyn. Schmiedebergs. Arch. Pharmacol. 354, 262–267. https://doi.org/10.1007/BF00171056

Frenguelli, B.G., Wigmore, G., Llaudet, E., Dale, N., 2007. Temporal and mechanistic dissociation of ATP and adenosine release during ischaemia in the mammalian hippocampus. J. Neurochem. 101, 1400–13. https://doi.org/10.1111/j.1471-4159.2007.04425.x

Frey, U., Morris, R.G., 1997. Synaptic tagging and long-term potentiation. Nature 385, 533–6. https://doi.org/10.1038/385533a0

Fujita, T., Hirose, R., Yoneta, M., Sasaki, S., Inoue, K., Kiuchi, M., Hirase, S., Chiba, K., Sakamoto, H., Arita, M., 1996. Potent immunosuppressants, 2-alkyl-2-aminopropane-1,3-diols. J. Med. Chem. 39, 4451–9. https://doi.org/10.1021/jm960391l

Furukawa, K., Fu, W., Li, Y., Witke, W., Kwiatkowski, D.J., Mattson, M.P., 1997. The actin-severing protein gelsolin modulates calcium channel and NMDA receptor activities and vulnerability to excitotoxicity in hippocampal neurons. J. Neurosci. 17, 8178–86.

Fusco, I., Ugolini, F., Lana, D., Coppi, E., Dettori, I., Gaviano, L., Nosi, D., Cherchi, F., Pedata, F., Giovannini, M.G., Pugliese, A.M., 2018. The Selective Antagonism of Adenosine A2B Receptors Reduces the Synaptic Failure and Neuronal Death Induced by Oxygen and Glucose Deprivation in Rat CA1 Hippocampus in Vitro. Front. Pharmacol. 9, 399. https://doi.org/10.3389/fphar.2018.00399

Fusi, C., Materazzi, S., Benemei, S., Coppi, E., Trevisan, G., Marone, I.M., Minocci, D., De Logu, F., Tuccinardi, T., Di Tommaso, M.R., Susini, T., Moneti, G., Pieraccini, G., Geppetti, P., Nassini, R., 2014. Steroidal and non-steroidal third-generation aromatase inhibitors induce pain-like symptoms via TRPA1. Nat. Commun. 5, 5736. https://doi.org/10.1038/ncomms6736

Gaengel, K., Niaudet, C., Hagikura, K., Laviña, B., Muhl, L., Hofmann, J.J., Ebarasi, L., Nyström, S., Rymo, S., Chen, L.L., Pang, M.-F., Jin, Y., Raschperger, E., Roswall, P., Schulte, D., Benedito, R., Larsson, J., Hellström, M., Fuxe, J., Uhlén, P., Adams, R., Jakobsson, L., Majumdar, A., Vestweber, D., Uv, A., Betsholtz, C., 2012. The Sphingosine-1-Phosphate Receptor S1PR1 Restricts Sprouting Angiogenesis by Regulating the Interplay between VE-Cadherin and VEGFR2. Dev. Cell 23, 587–599. https://doi.org/10.1016/j.devcel.2012.08.005

Gallo-Rodriguez, C., Ji, X.D., Melman, N., Siegman, B.D., Sanders, L.H., Orlina, J., Fischer, B., Pu, Q., Olah, M.E., van Galen, P.J., 1994. Structure-activity relationships of N6-benzyladenosine-5'-uronamides as A3-selective adenosine agonists. J. Med. Chem. 37, 636–46.

Gallo, V., Mangin, J.-M., Kukley, M., Dietrich, D., 2008. Synapses on NG2-expressing progenitors in the brain: multiple functions? J. Physiol. 586, 3767–3781. https://doi.org/10.1113/jphysiol.2008.158436

Gallo, V., Zhou, J.M., McBain, C.J., Wright, P., Knutson, P.L., Armstrong, R.C., 1996. Oligodendrocyte progenitor cell proliferation and lineage progression are regulated by glutamate receptor-mediated K+ channel block. J. Neurosci. 16, 2659–70.

Gan, T.J., Habib, A.S., 2007. Adenosine as a Non-Opioid Analgesic in the Perioperative Setting. Anesth. Analg. 105, 487–494. https://doi.org/10.1213/01.ane.0000267260.00384.d9

Gandini, M.A., Sandoval, A., Felix, R., 2015. Toxins targeting voltage-activated Ca2+ channels and their

potential biomedical applications. Curr. Top. Med. Chem. 15, 604–16.
Gao, Y., Phillis, J.W., 1994. CGS 15943, an adenosine A2 receptor antagonist, reduces cerebral ischemic injury in the Mongolian gerbil. Life Sci. 55, PL61-5.
Gao, Z., Chen, T., Weber, M.J., Linden, J., 1999. A2B adenosine and P2Y2 receptors stimulate mitogen-activated protein kinase in human embryonic kidney-293 cells. cross-talk between cyclic AMP and protein kinase c pathways. J. Biol. Chem. 274, 5972–80.
Gassowska, M., Cieslik, M., Wilkaniec, A., Strosznajder, J.B., 2014. Sphingosine Kinases/Sphingosine-1-Phosphate and Death Signalling in APP-Transfected Cells. Neurochem. Res. 39, 645–652. https://doi.org/10.1007/s11064-014-1240-3
Gebicke-Haerter, P.J., Van Calker, D., Nörenberg, W., Illes, P., 1996. Molecular mechanisms of microglial activation. A. Implications for regeneration and neurodegenerative diseases. Neurochem. Int. 29, 1–12.
Gegelashvili, G., Robinson, M.B., Trotti, D., Rauen, T., 2001. Regulation of glutamate transporters in health and disease. Prog. Brain Res. 132, 267–86. https://doi.org/10.1016/S0079-6123(01)32082-4
Gessi, S., Merighi, S., Stefanelli, A., Fazzi, D., Varani, K., Borea, P.A., 2013. A(1) and A(3) adenosine receptors inhibit LPS-induced hypoxia-inducible factor-1 accumulation in murine astrocytes. Pharmacol. Res. 76, 157–70. https://doi.org/10.1016/j.phrs.2013.08.002
Gessi, S., Varani, K., Merighi, S., Cattabriga, E., Pancaldi, C., Szabadkai, Y., Rizzuto, R., Klotz, K.-N., Leung, E., Mac Lennan, S., Baraldi, P.G., Borea, P.A., 2005. Expression, Pharmacological Profile, and Functional Coupling of A2B Receptors in a Recombinant System and in Peripheral Blood Cells Using a Novel Selective Antagonist Radioligand, [3H]MRE 2029-F20. Mol. Pharmacol. 67, 2137–2147. https://doi.org/10.1124/mol.104.009225
Gibson, C.L., 2013. Cerebral ischemic stroke: is gender important? J. Cereb. Blood Flow Metab. 33, 1355–61. https://doi.org/10.1038/jcbfm.2013.102
Gilron, I., Watson, C.P.N., Cahill, C.M., Moulin, D.E., 2006. Neuropathic pain: a practical guide for the clinician. Can. Med. Assoc. J. 175, 265–275. https://doi.org/10.1503/cmaj.060146
Ginsberg, M.D., 2009. Current status of neuroprotection for cerebral ischemia: synoptic overview. Stroke 40, S111-4. https://doi.org/10.1161/STROKEAHA.108.528877
Ginsborg, B.L., Hirst, G.D., 1972. The effect of adenosine on the release of the transmitter from the phrenic nerve of the rat. J. Physiol. 224, 629–45.
Glickman, M., Malek, R.L., Kwitek-Black, A.E., Jacob, H.J., Lee, N.H., 1999. Molecular Cloning, Tissue-Specific Expression, and Chromosomal Localization of a Novel Nerve Growth Factor-Regulated G-Protein-Coupled Receptor, nrg-1. Mol. Cell. Neurosci. 14, 141–152. https://doi.org/10.1006/mcne.1999.0776
Gold, M.S., Dastmalchi, S., Levine, J.D., 1996. Co-expression of nociceptor properties in dorsal root ganglion neurons from the adult rat in vitro. Neuroscience 71, 265–75.
Goldberg, D.S., McGee, S.J., 2011. Pain as a global public health priority. BMC Public Health 11, 770. https://doi.org/10.1186/1471-2458-11-770
Golfier, S., Kondo, S., Schulze, T., Takeuchi, T., Vassileva, G., Achtman, A.H., Gräler, M.H., Abbondanzo, S.J., Wiekowski, M., Kremmer, E., Endo, Y., Lira, S.A., Bacon, K.B., Lipp, M., 2010. Shaping of terminal megakaryocyte differentiation and proplatelet development by sphingosine-1-phosphate receptor S1P $_4$. FASEB J. 24, 4701–4710. https://doi.org/10.1096/fj.09-141473
Gomes, C., Ferreira, R., George, J., Sanches, R., Rodrigues, D.I., Gonçalves, N., Cunha, R.A., 2013. Activation of microglial cells triggers a release of brain-derived neurotrophic factor (BDNF) inducing their proliferation in an adenosine A2A receptor-dependent manner: A2A receptor blockade prevents BDNF release and proliferation of microglia. J. Neuroinflammation 10, 780. https://doi.org/10.1186/1742-2094-10-16
Gonçalves, F.Q., Pires, J., Pliassova, A., Beleza, R., Lemos, C., Marques, J.M., Rodrigues, R.J., Canas, P.M., Köfalvi, A., Cunha, R.A., Rial, D., 2015. Adenosine A2b receptors control A1 receptor-mediated inhibition of synaptic transmission in the mouse hippocampus. Eur. J. Neurosci. 41, 878–88. https://doi.org/10.1111/ejn.12851
González-Fernández, E., Sánchez-Gómez, M.V., Pérez-Samartín, A., Arellano, R.O., Matute, C., 2014. A3 Adenosine receptors mediate oligodendrocyte death and ischemic damage to optic nerve. Glia 62, 199–216. https://doi.org/10.1002/glia.22599
Gonzalez, P., Rodríguez, F.J., 2017. Analysis of the expression of the Wnt family of proteins and its modulatory role on cytokine expression in non activated and activated astroglial cells. Neurosci. Res. 114, 16–29. https://doi.org/10.1016/j.neures.2016.08.003
Gordon, J.L., 1986. Extracellular ATP: effects, sources and fate. Biochem. J. 233, 309–19.
Gourine, A. V, Dale, N., Gourine, V.N., Spyer, K.M., 2004. Fever in systemic inflammation: roles of purines. Front. Biosci. 9, 1011–22.
Grafstein, B., 1956. locus of propagation of spreading cortical depression. J. Neurophysiol. 19, 308–316. https://doi.org/10.1152/jn.1956.19.4.308
Gräler, M.H., Bernhardt, G., Lipp, M., 1998. EDG6, a Novel G-Protein-Coupled Receptor Related to Receptors

for Bioactive Lysophospholipids, Is Specifically Expressed in Lymphoid Tissue. Genomics 53, 164–169. https://doi.org/10.1006/geno.1998.5491

Grant, M.B., Davis, M.I., Caballero, S., Feoktistov, I., Biaggioni, I., Belardinelli, L., 2001. Proliferation, migration, and ERK activation in human retinal endothelial cells through A(2B) adenosine receptor stimulation. Invest. Ophthalmol. Vis. Sci. 42, 2068–73.

Gu, L., Huang, B., Shen, W., Gao, L., Ding, Z., Wu, H., Guo, J., 2013. Early activation of nSMase2/ceramide pathway in astrocytes is involved in ischemia-associated neuronal damage via inflammation in rat hippocampi. J. Neuroinflammation 10, 109. https://doi.org/10.1186/1742-2094-10-109

Gutman, G.A., Chandy, K.G., Grissmer, S., Lazdunski, M., McKinnon, D., Pardo, L.A., Robertson, G.A., Rudy, B., Sanguinetti, M.C., Stühmer, W., Wang, X., 2005. International Union of Pharmacology. LIII. Nomenclature and molecular relationships of voltage-gated potassium channels. Pharmacol. Rev. 57, 473–508. https://doi.org/10.1124/pr.57.4.10

Haas, H.L., Selbach, O., 2000. Functions of neuronal adenosine receptors. Naunyn. Schmiedebergs. Arch. Pharmacol. 362, 375–81.

Habib, A.S., Minkowitz, H., Osborn, T., Ogunnaike, B., Candiotti, K., Viscusi, E., Gu, J., Creed, M.R., Gan, T.J., Adenosine Study Group, 2008. Phase 2, Double-blind, Placebo-controlled, Dose-Response Trial of Intravenous Adenosine for Perioperative Analgesia. Anesthesiology 109, 1085–1091. https://doi.org/10.1097/ALN.0b013e31818db88c

Hagberg, H., Andersson, P., Lacarewicz, J., Jacobson, I., Butcher, S., Sandberg, M., 1987. Extracellular adenosine, inosine, hypoxanthine, and xanthine in relation to tissue nucleotides and purines in rat striatum during transient ischemia. J. Neurochem. 49, 227–31.

Hait, N.C., Bellamy, A., Milstien, S., Kordula, T., Spiegel, S., 2007. Sphingosine kinase type 2 activation by ERK-mediated phosphorylation. J. Biol. Chem. 282, 12058–65. https://doi.org/10.1074/jbc.M609559200

Hammarberg, C., Schulte, G., Fredholm, B.B., 2003. Evidence for functional adenosine A3 receptors in microglia cells. J. Neurochem. 86, 1051–4.

Hannon, H.E., Atchison, W.D., 2013. Omega-conotoxins as experimental tools and therapeutics in pain management. Mar. Drugs 11, 680–99. https://doi.org/10.3390/md11030680

Harding, L.M., Beadle, D.J., Bermudez, I., 1999. Voltage-dependent calcium channel subtypes controlling somatic substance P release in the peripheral nervous system. Prog. Neuropsychopharmacol. Biol. Psychiatry 23, 1103–12.

Haroutunian, V., Katsel, P., Roussos, P., Davis, K.L., Altshuler, L.L., Bartzokis, G., 2014. Myelination, oligodendrocytes, and serious mental illness. Glia 62, 1856–1877. https://doi.org/10.1002/glia.22716

Harreveld, A. Van, Stamm, J.S., 1953. spreading cortical convulsions and depressions. J. Neurophysiol. 16, 352–366. https://doi.org/10.1152/jn.1953.16.4.352

Hart, M.L., Jacobi, B., Schittenhelm, J., Henn, M., Eltzschig, H.K., 2009. Cutting Edge: A2B Adenosine receptor signaling provides potent protection during intestinal ischemia/reperfusion injury. J. Immunol. 182, 3965–8. https://doi.org/10.4049/jimmunol.0802193

Haskó, G., Csóka, B., Németh, Z.H., Vizi, E.S., Pacher, P., 2009. A(2B) adenosine receptors in immunity and inflammation. Trends Immunol. 30, 263–70. https://doi.org/10.1016/j.it.2009.04.001

Haskó, G., Pacher, P., 2008. A $_{2A}$ receptors in inflammation and injury: lessons learned from transgenic animals. J. Leukoc. Biol. 83, 447–455. https://doi.org/10.1189/jlb.0607359

Hayashi, E., Kunitomo, M., Mori, M., Shinozuka, K., Yamada, S., 1978. The development of tachyphylaxis to electrical stimulation in guinea-pig ileal longitudinal muscles and the possible participation of adenosine and adenine nucleotides. Br. J. Pharmacol. 63, 457–64.

Hayashi, H., Iwata, M., Tsuchimori, N., Matsumoto, T., 2014. Activation of peripheral KCNQ channels attenuates inflammatory pain. Mol. Pain 10, 15. https://doi.org/10.1186/1744-8069-10-15

Hayashida, M., Fukuda, K., Fukunaga, A., 2005. Clinical application of adenosine and ATP for pain control. J. Anesth. 19, 225–235. https://doi.org/10.1007/s00540-005-0310-8

He, X., Huang, Y., Li, B., Gong, C.-X., Schuchman, E.H., 2010. Deregulation of sphingolipid metabolism in Alzheimer's disease. Neurobiol. Aging 31, 398–408. https://doi.org/10.1016/j.neurobiolaging.2008.05.010

Heemels, M.-T., 2016. Neurodegenerative diseases. Nature 539, 179–179. https://doi.org/10.1038/539179a

Heinke, B., Balzer, E., Sandkühler, J., 2004. Pre- and postsynaptic contributions of voltage-dependent Ca2+ channels to nociceptive transmission in rat spinal lamina I neurons. Eur. J. Neurosci. 19, 103–11.

Herreras, O., Somjen, G.G., 1993a. Propagation of spreading depression among dendrites and somata of the same cell population. Brain Res. 610, 276–82.

Herreras, O., Somjen, G.G., 1993b. Analysis of potential shifts associated with recurrent spreading depression and prolonged unstable spreading depression induced by microdialysis of elevated K+ in hippocampus of anesthetized rats. Brain Res. 610, 283–94.

Hettinger, B.D., Lee, A., Linden, J., Rosin, D.L., 2001. Ultrastructural localization of adenosine A2A receptors suggests multiple cellular sites for modulation of GABAergic neurons in rat striatum. J. Comp. Neurol.

431, 331–46.
Hille, B., n.d. Ionic channels: molecular pores of excitable membranes. Harvey Lect. 82, 47–69.
Hillion, J., Canals, M., Torvinen, M., Casado, V., Scott, R., Terasmaa, A., Hansson, A., Watson, S., Olah, M.E., Mallol, J., Canela, E.I., Zoli, M., Agnati, L.F., Ibanez, C.F., Lluis, C., Franco, R., Ferre, S., Fuxe, K., 2002. Coaggregation, cointernalization, and codesensitization of adenosine A2A receptors and dopamine D2 receptors. J. Biol. Chem. 277, 18091–7. https://doi.org/10.1074/jbc.M107731200
Hines, J.H., Ravanelli, A.M., Schwindt, R., Scott, E.K., Appel, B., 2015. Neuronal activity biases axon selection for myelination in vivo. Nat. Neurosci. 18, 683–9. https://doi.org/10.1038/nn.3992
Hinz, S., Lacher, S.K., Seibt, B.F., Müller, C.E., 2014. BAY60-6583 acts as a partial agonist at adenosine A2B receptors. J. Pharmacol. Exp. Ther. 349, 427–36. https://doi.org/10.1124/jpet.113.210849
Hoffman, C.J., Clark, F.J., Ochs, S., 1973. Intracortical impedance changes during spreading depression. J. Neurobiol. 4, 471–86. https://doi.org/10.1002/neu.480040508
Holgate, S.T., 2005. The Quintiles Prize Lecture 2004. The identification of the adenosine A2B receptor as a novel therapeutic target in asthma. Br. J. Pharmacol. 145, 1009–15. https://doi.org/10.1038/sj.bjp.0706272
Holloway, P.M., Gavins, F.N.E., 2016. Modeling Ischemic Stroke In Vitro: Status Quo and Future Perspectives. Stroke 47, 561–9. https://doi.org/10.1161/STROKEAHA.115.011932
Holz, R.W., Fisher, S.K., Siegel, G.J., Agranoff, B.W., Albers, R.W., 1999. asic Neurochemistry: Molecular, Cellular and Medical Aspects., Philadelphia: Lippincott-Raven. https://doi.org/10.1002/cne.22549
Honig, L.S., Rosenberg, R.N., 2000. Apoptosis and neurologic disease. Am. J. Med. 108, 317–30.
Hossmann, K.-A., 1994. Viability thresholds and the penumbra of focal ischemia. Ann. Neurol. 36, 557–565. https://doi.org/10.1002/ana.410360404
Huang, F., Wang, X., Ostertag, E.M., Nuwal, T., Huang, B., Jan, Y.-N., Basbaum, A.I., Jan, L.Y., 2013. TMEM16C facilitates Na(+)-activated K+ currents in rat sensory neurons and regulates pain processing. Nat. Neurosci. 16, 1284–90. https://doi.org/10.1038/nn.3468
Huang, M., Daly, J.W., 1974. Adenosine-elicited accumulation of cyclic AMP in brain slices: potentiation by agents which inhibit uptake of adenosine. Life Sci. 14, 489–503.
Huang, M., Daly, J.W., 1972. Accumulation of cyclic adenosine monophosphate in incubated slices of brain tissue. 1. Structure-activity relationships of agonists and antagonists of biogenic amines and of tricyclic tranquilizers and antidepressants. J. Med. Chem. 15, 458–62.
Huang, Q., Wu, L.-J., Tashiro, S.-I., Onodera, S., Ikejima, T., 2006. Elevated levels of DNA repair enzymes and antioxidative enzymes by (+)-catechin in murine microglia cells after oxidative stress. J. Asian Nat. Prod. Res. 8, 61–71. https://doi.org/10.1080/10286020500209087
Hussl, S., Boehm, S., 2006. Functions of neuronal P2Y receptors. Pflugers Arch. 452, 538–51. https://doi.org/10.1007/s00424-006-0063-8
Hutchison, K.A., Fox, I.H., 1989. Purification and characterization of the adenosine A2-like binding site from human placental membrane. J. Biol. Chem. 264, 19898–903.
Huwiler, A., Zangemeister-Wittke, U., 2018. The sphingosine 1-phosphate receptor modulator fingolimod as a therapeutic agent: Recent findings and new perspectives. Pharmacol. Ther. 185, 34–49. https://doi.org/10.1016/j.pharmthera.2017.11.001
Iadarola, J.M., Caudle, R.M., 1997. Good pain, bad pain. Science 278, 239–40.
Iadecola, C., 1997. Bright and dark sides of nitric oxide in ischemic brain injury. Trends Neurosci. 20, 132–9.
Iadecola, C., Anrather, J., 2011. The immunology of stroke: from mechanisms to translation. Nat. Med. 17, 796–808. https://doi.org/10.1038/nm.2399
Im, D.-S., Ungar, A.R., Lynch, K.R., 2000. Characterization of a Zebrafish (Danio rerio) Sphingosine 1-Phosphate Receptor Expressed in the Embryonic Brain. Biochem. Biophys. Res. Commun. 279, 139–143. https://doi.org/10.1006/BBRC.2000.3933
Imeri, F., Schwalm, S., Lyck, R., Zivkovic, A., Stark, H., Engelhardt, B., Pfeilschifter, J., Huwiler, A., 2016. Sphingosine kinase 2 deficient mice exhibit reduced experimental autoimmune encephalomyelitis: Resistance to FTY720 but not ST-968 treatments. Neuropharmacology 105, 341–350. https://doi.org/10.1016/j.neuropharm.2016.01.031
Jacobson, K.A., 1998. Adenosine A3 receptors: novel ligands and paradoxical effects. Trends Pharmacol. Sci. 19, 184–91.
Jaillard, C., Harrison, S., Stankoff, B., Aigrot, M.S., Calver, A.R., Duddy, G., Walsh, F.S., Pangalos, M.N., Arimura, N., Kaibuchi, K., Zalc, B., Lubetzki, C., 2005. Edg8/S1P5: an oligodendroglial receptor with dual function on process retraction and cell survival. J. Neurosci. 25, 1459–69. https://doi.org/10.1523/jneurosci.4645-04.2005
Jain, K.K., 2000. An evaluation of intrathecal ziconotide for the treatment of chronic pain. Expert Opin. Investig. Drugs 9, 2403–10. https://doi.org/10.1517/13543784.9.10.2403
Janes, K., Esposito, E., Doyle, T., Cuzzocrea, S., Tosh, D.K., Jacobson, K.A., Salvemini, D., 2014. A3 adenosine receptor agonist prevents the development of paclitaxel-induced neuropathic pain by modulating spinal glial-restricted redox-dependent signaling pathways. Pain 155, 2560–2567.

https://doi.org/10.1016/j.pain.2014.09.016
Janes, K., Symons-Liguori, A.M., Jacobson, K.A., Salvemini, D., 2016. Identification of A3 adenosine receptor agonists as novel non-narcotic analgesics. Br. J. Pharmacol. 173, 1253–67. https://doi.org/10.1111/bph.13446
Janes, K., Wahlman, C., Little, J.W., Doyle, T., Tosh, D.K., Jacobson, K.A., Salvemini, D., 2015. Spinal neuroimmune activation is independent of T-cell infiltration and attenuated by A3 adenosine receptor agonists in a model of oxaliplatin-induced peripheral neuropathy. Brain. Behav. Immun. 44, 91–99. https://doi.org/10.1016/j.bbi.2014.08.010
Jarvis, M.F., Schulz, R., Hutchison, A.J., Do, U.H., Sills, M.A., Williams, M., 1989. [3H]CGS 21680, a selective A2 adenosine receptor agonist directly labels A2 receptors in rat brain. J. Pharmacol. Exp. Ther. 251, 888–93.
Jenne, C.N., Enders, A., Rivera, R., Watson, S.R., Bankovich, A.J., Pereira, J.P., Xu, Y., Roots, C.M., Beilke, J.N., Banerjee, A., Reiner, S.L., Miller, S.A., Weinmann, A.S., Goodnow, C.C., Lanier, L.L., Cyster, J.G., Chun, J., 2009. T-bet-dependent S1P5 expression in NK cells promotes egress from lymph nodes and bone marrow. J. Exp. Med. 206, 2469–81. https://doi.org/10.1084/jem.20090525
Jensen, T.S., Baron, R., Haanpää, M., Kalso, E., Loeser, J.D., Rice, A.S.C., Treede, R.-D., 2011. A new definition of neuropathic pain. Pain 152, 2204–2205. https://doi.org/10.1016/j.pain.2011.06.017
Jeong, L.S., Jin, D.Z., Kim, H.O., Shin, D.H., Moon, H.R., Gunaga, P., Chun, M.W., Kim, Y.-C., Melman, N., Gao, Z.-G., Jacobson, K.A., 2003. N ^{6} -Substituted D-4‘-Thioadenosine-5‘-methyluronamides: Potent and Selective Agonists at the Human A $_{3}$ Adenosine Receptor. J. Med. Chem. 46, 3775–3777. https://doi.org/10.1021/jm034098e
Ji, X., Kim, Y.C., Ahern, D.G., Linden, J., Jacobson, K.A., 2001. [3H]MRS 1754, a selective antagonist radioligand for A(2B) adenosine receptors. Biochem. Pharmacol. 61, 657–63.
Ji, X.D., Gallo-Rodriguez, C., Jacobson, K.A., 1994. A selective agonist affinity label for A3 adenosine receptors. Biochem. Biophys. Res. Commun. 203, 570–6.
Jiang, X., Wang, X., 2004. Cytochrome C-mediated apoptosis. Annu. Rev. Biochem. 73, 87–106. https://doi.org/10.1146/annurev.biochem.73.011303.073706
Jin, X., Shepherd, R.K., Duling, B.R., Linden, J., 1997. Inosine binds to A3 adenosine receptors and stimulates mast cell degranulation. J. Clin. Invest. 100, 2849–2857. https://doi.org/10.1172/JCI119833
Johansson, B., Fredholm, B.B., 1995. Further characterization of the binding of the adenosine receptor agonist [3H]CGS 21680 to rat brain using autoradiography. Neuropharmacology 34, 393–403.
Johansson, B., Halldner, L., Dunwiddie, T. V, Masino, S.A., Poelchen, W., Giménez-Llort, L., Escorihuela, R.M., Fernández-Teruel, A., Wiesenfeld-Hallin, Z., Xu, X.J., Hårdemark, A., Betsholtz, C., Herlenius, E., Fredholm, B.B., 2001. Hyperalgesia, anxiety, and decreased hypoxic neuroprotection in mice lacking the adenosine A1 receptor. Proc. Natl. Acad. Sci. U. S. A. 98, 9407–12. https://doi.org/10.1073/pnas.161292398
Jung, C.G., Kim, H.J., Miron, V.E., Cook, S., Kennedy, T.E., Foster, C.A., Antel, J.P., Soliven, B., 2007. Functional consequences of S1P receptor modulation in rat oligodendroglial lineage cells. Glia 55, 1656–67. https://doi.org/10.1002/glia.20576
Káradóttir, R., Cavelier, P., Bergersen, L.H., Attwell, D., 2005. NMDA receptors are expressed in oligodendrocytes and activated in ischaemia. Nature 438, 1162–6. https://doi.org/10.1038/nature04302
Kataoka, H., Sugahara, K., Shimano, K., Teshima, K., Koyama, M., Fukunari, A., Chiba, K., 2005. FTY720, sphingosine 1-phosphate receptor modulator, ameliorates experimental autoimmune encephalomyelitis by inhibition of T cell infiltration. Cell. Mol. Immunol. 2, 439–48.
Kawasaki, K., Czéh, G., Somjen, G.G., 1988. Prolonged exposure to high potassium concentration results in irreversible loss of synaptic transmission in hippocampal tissue slices. Brain Res. 457, 322–9.
Kihara, Y., Maceyka, M., Spiegel, S., Chun, J., 2014. Lysophospholipid receptor nomenclature review: IUPHAR Review 8. Br. J. Pharmacol. 171, 3575–3594. https://doi.org/10.1111/bph.12678
Kim, D.S., Choi, J.O., Rim, H.D., Cho, H.J., 2002. Downregulation of voltage-gated potassium channel alpha gene expression in dorsal root ganglia following chronic constriction injury of the rat sciatic nerve. Brain Res. Mol. Brain Res. 105, 146–52.
Kim, H.J., Miron, V.E., Dukala, D., Proia, R.L., Ludwin, S.K., Traka, M., Antel, J.P., Soliven, B., 2011. Neurobiological effects of sphingosine 1-phosphate receptor modulation in the cuprizone model. FASEB J. 25, 1509–1518. https://doi.org/10.1096/fj.10-173203
Kim, Y.C., Ji, X., Melman, N., Linden, J., Jacobson, K.A., 2000. Anilide derivatives of an 8-phenylxanthine carboxylic congener are highly potent and selective antagonists at human A(2B) adenosine receptors. J. Med. Chem. 43, 1165–72.
King, B.F., 2002. 2-Chloro-N ^{6} -methyl-(*N*)-methanocarba-2′-deoxyadenosine-3′,5′-bisphosphate is a selective high affinity P2Y $_{1}$ receptor antagonist: Commentary on Boyer *et al* . Br. J. Pharmacol. 135, 1839–1840. https://doi.org/10.1038/sj.bjp.0704674
Kitagawa, H., Mori, A., Shimada, J., Mitsumoto, Y., Kikuchi, T., 2002. Intracerebral adenosine infusion improves neurological outcome after transient focal ischemia in rats. Neurol. Res. 24, 317–23.

https://doi.org/10.1179/016164102101199819
Kluck, R.M., Bossy-Wetzel, E., Green, D.R., Newmeyer, D.D., 1997. The release of cytochrome c from mitochondria: a primary site for Bcl-2 regulation of apoptosis. Science 275, 1132–6.
Knutson, P., Ghiani, C.A., Zhou, J.M., Gallo, V., McBain, C.J., 1997. K+ channel expression and cell proliferation are regulated by intracellular sodium and membrane depolarization in oligodendrocyte progenitor cells. J. Neurosci. 17, 2669–82.
Koeppen, M., Eckle, T., Eltzschig, H.K., 2011. Interplay of hypoxia and A2B adenosine receptors in tissue protection. Adv. Pharmacol. 61, 145–86. https://doi.org/10.1016/B978-0-12-385526-8.00006-0
Kolachala, V., Asamoah, V., Wang, L., Obertone, T.S., Ziegler, T.R., Merlin, D., Sitaraman, S. V., 2005. TNF-α upregulates adenosine 2b (A2b) receptor expression and signaling in intestinal epithelial cells: a basis for A2bR overexpression in colitis. Cell. Mol. Life Sci. 62, 2647–2657. https://doi.org/10.1007/s00018-005-5328-4
Kong, T., Westerman, K.A., Faigle, M., Eltzschig, H.K., Colgan, S.P., 2006. HIF-dependent induction of adenosine A2B receptor in hypoxia. FASEB J. 20, 2242–50. https://doi.org/10.1096/fj.06-6419com
Koscsó, B., Csóka, B., Selmeczy, Z., Himer, L., Pacher, P., Virág, L., Haskó, G., 2012. Adenosine augments IL-10 production by microglial cells through an A2B adenosine receptor-mediated process. J. Immunol. 188, 445–53. https://doi.org/10.4049/jimmunol.1101224
Kostopoulos, G.K., Limacher, J.J., Phillis, J.W., 1975. Action of various adenine derivatives on cerebellar Purkinje cells. Brain Res. 88, 162–5.
Kostopoulos, G.K., Phillis, J.W., 1977. Purinergic depression of neurons in different areas of the rat brain. Exp. Neurol. 55, 719–24.
Kovacs, K., Toth, A., Deres, P., Kalai, T., Hideg, K., Gallyas, F., Sumegi, B., 2006. Critical role of PI3-kinase/Akt activation in the PARP inhibitor induced heart function recovery during ischemia-reperfusion. Biochem. Pharmacol. 71, 441–52. https://doi.org/10.1016/j.bcp.2005.05.036
Kow, L.M., van Harreveld, A., 1972. Ion and water movements in isolated chicken retinas during spreading depression. Neurobiology 2, 61–9.
Krobitsch, S., Lindquist, S., 2000. Aggregation of huntingtin in yeast varies with the length of the polyglutamine expansion and the expression of chaperone proteins. Proc. Natl. Acad. Sci. U. S. A. 97, 1589–94.
Krump-Konvalinkova, V., Yasuda, S., Rubic, T., Makarova, N., Mages, J., Erl, W., Vosseler, C., Kirkpatrick, C.J., Tigyi, G., Siess, W., 2005. Stable Knock-Down of the Sphingosine 1-Phosphate Receptor S1P $_1$ Influences Multiple Functions of Human Endothelial Cells. Arterioscler. Thromb. Vasc. Biol. 25, 546–552. https://doi.org/10.1161/01.ATV.0000154360.36106.d9
Kull, B., Arslan, G., Nilsson, C., Owman, C., Lorenzen, A., Schwabe, U., Fredholm, B.B., 1999. Differences in the order of potency for agonists but not antagonists at human and rat adenosine A2A receptors. Biochem. Pharmacol. 57, 65–75.
Kuo, Y.-L., Cheng, J.-K., Hou, W.-H., Chang, Y.-C., Du, P.-H., Jian, J.-J., Rau, R.-H., Yang, J.-H., Lien, C.-C., Tsaur, M.-L., 2017. K^+ Channel Modulatory Subunits KChIP and DPP Participate in Kv4-Mediated Mechanical Pain Control. J. Neurosci. 37, 4391–4404. https://doi.org/10.1523/JNEUROSCI.1619-16.2017
Kuroda, Y., Saito, M., Kobayashi, K., 1976. Concomitant changes in cyclic AMP level and postsynaptic potentials of olfactory cortex slices induced by adenosine derivatives. Brain Res. 109, 196–201.
Lana, D., Cerbai, F., Di Russo, J., Boscaro, F., Giannetti, A., Petkova-Kirova, P., Pugliese, A.M., Giovannini, M.G., 2013. Hippocampal long term memory: effect of the cholinergic system on local protein synthesis. Neurobiol. Learn. Mem. 106, 246–57. https://doi.org/10.1016/j.nlm.2013.09.013
Lana, D., Iovino, L., Nosi, D., Wenk, G.L., Giovannini, M.G., 2016. The neuron-astrocyte-microglia triad involvement in neuroinflammaging mechanisms in the CA3 hippocampus of memory-impaired aged rats. Exp. Gerontol. 83, 71–88. https://doi.org/10.1016/j.exger.2016.07.011
Lana, D., Melani, A., Pugliese, A.M., Cipriani, S., Nosi, D., Pedata, F., Giovannini, M.G., 2014. The neuron-astrocyte-microglia triad in a rat model of chronic cerebral hypoperfusion: protective effect of dipyridamole. Front. Aging Neurosci. 6, 322. https://doi.org/10.3389/fnagi.2014.00322
Lana, D., Ugolini, F., Melani, A., Nosi, D., Pedata, F., Giovannini, M.G., 2017a. The neuron-astrocyte-microglia triad in CA3 after chronic cerebral hypoperfusion in the rat: Protective effect of dipyridamole. Exp. Gerontol. 96, 46–62. https://doi.org/10.1016/j.exger.2017.06.006
Lana, D., Ugolini, F., Nosi, D., Wenk, G.L., Giovannini, M.G., 2017b. Alterations in the Interplay between Neurons, Astrocytes and Microglia in the Rat Dentate Gyrus in Experimental Models of Neurodegeneration. Front. Aging Neurosci. 9, 296. https://doi.org/10.3389/fnagi.2017.00296
Langdon, D.W., 2011. Cognition in multiple sclerosis. Curr. Opin. Neurol. 24, 244–249. https://doi.org/10.1097/WCO.0b013e328346a43b
Laplante, M., Sabatini, D.M., 2012. mTOR signaling in growth control and disease. Cell 149, 274–93. https://doi.org/10.1016/j.cell.2012.03.017
Lappas, C.M., Rieger, J.M., Linden, J., 2005. A2A adenosine receptor induction inhibits IFN-gamma

production in murine CD4+ T cells. J. Immunol. 174, 1073–80.
Latini, S., Bordoni, F., Corradetti, R., Pepeu, G., Pedata, F., 1999a. Effect of A 2A adenosine receptor stimulation and antagonism on synaptic depression induced by *in vitro* ischaemia in rat hippocampal slices. Br. J. Pharmacol. 128, 1035–1044. https://doi.org/10.1038/sj.bjp.0702888
Latini, S., Bordoni, F., Corradetti, R., Pepeu, G., Pedata, F., 1998. Temporal correlation between adenosine outflow and synaptic potential inhibition in rat hippocampal slices during ischemia-like conditions. Brain Res. 794, 325–8.
Latini, S., Bordoni, F., Pedata, F., Corradetti, R., 1999b. Extracellular adenosine concentrations during *in vitro* ischaemia in rat hippocampal slices. Br. J. Pharmacol. 127, 729–739. https://doi.org/10.1038/sj.bjp.0702591
Latini, S., Pazzagli, M., Pepeu, G., Pedata, F., 1996. A2 adenosine receptors: their presence and neuromodulatory role in the central nervous system. Gen. Pharmacol. 27, 925–33.
Latini, S., Pedata, F., 2001. Adenosine in the central nervous system: release mechanisms and extracellular concentrations. J. Neurochem. 79, 463–84.
Lawson, S.N., 2002. Phenotype and function of somatic primary afferent nociceptive neurones with C-, Adelta- or Aalpha/beta-fibres. Exp. Physiol. 87, 239–44.
Leão, A.A.P., 1951. The slow voltage variation of cortical spreading depression of activity. Electroencephalogr. Clin. Neurophysiol. 3, 315–21.
Leão, A.A.P., 1947. Further observations on the spreading depression of activity in the cerebral cortex. J. Neurophysiol. 10, 409–14. https://doi.org/10.1152/jn.1947.10.6.409
Lectures on the diseases of the nervous system : Charcot, J. M. (Jean Martin), 1825-1893 : Free Download, Borrow, and Streaming : Internet Archive [WWW Document], n.d. URL https://archive.org/details/lecturesondiseas00char/page/n5 (accessed 10.24.18).
Lee, J.M., Zipfel, G.J., Choi, D.W., 1999. The changing landscape of ischaemic brain injury mechanisms. Nature 399, A7-14.
Lee, S., 2013. Pharmacological Inhibition of Voltage-gated Ca(2+) Channels for Chronic Pain Relief. Curr. Neuropharmacol. 11, 606–20. https://doi.org/10.2174/1570159X11311060005
Lemos, C., Pinheiro, B.S., Beleza, R.O., Marques, J.M., Rodrigues, R.J., Cunha, R.A., Rial, D., Köfalvi, A., 2015. Adenosine A2B receptor activation stimulates glucose uptake in the mouse forebrain. Purinergic Signal. 11, 561–9. https://doi.org/10.1007/s11302-015-9474-3
Leo, A.A.P., 1944. spreading depression of activity in the cerebral cortex. J. Neurophysiol. 7, 359–390. https://doi.org/10.1152/jn.1944.7.6.359
Levine, J.M., Reynolds, R., 1999. Activation and proliferation of endogenous oligodendrocyte precursor cells during ethidium bromide-induced demyelination. Exp. Neurol. 160, 333–47. https://doi.org/10.1006/exnr.1999.7224
Li, Q., Han, X., Lan, X., Hong, X., Li, Q., Gao, Y., Luo, T., Yang, Q., Koehler, R.C., Zhai, Y., Zhou, J., Wang, J., 2017. Inhibition of tPA-induced hemorrhagic transformation involves adenosine A2b receptor activation after cerebral ischemia. Neurobiol. Dis. 108, 173–182. https://doi.org/10.1016/j.nbd.2017.08.011
Limaye, V., Li, X., Hahn, C., Xia, P., Berndt, M.C., Vadas, M.A., Gamble, J.R., 2005. Sphingosine kinase-1 enhances endothelial cell survival through a PECAM-1-dependent activation of PI-3K/Akt and regulation of Bcl-2 family members. Blood 105, 3169–77. https://doi.org/10.1182/blood-2004-02-0452
Lin, Y., Phillis, J.W., 1992. Deoxycoformycin and oxypurinol: protection against focal ischemic brain injury in the rat. Brain Res. 571, 272–80.
Linden, J., Taylor, H.E., Robeva, A.S., Tucker, A.L., Stehle, J.H., Rivkees, S.A., Fink, J.S., Reppert, S.M., 1993. Molecular cloning and functional expression of a sheep A3 adenosine receptor with widespread tissue distribution. Mol. Pharmacol. 44, 524–32.
Linden, J., Thai, T., Figler, H., Jin, X., Robeva, A.S., 1999. Characterization of human A(2B) adenosine receptors: radioligand binding, western blotting, and coupling to G(q) in human embryonic kidney 293 cells and HMC-1 mast cells. Mol. Pharmacol. 56, 705–13.
Lipton, P., 1999. Ischemic Cell Death in Brain Neurons. Physiol. Rev. 79, 1431–1568. https://doi.org/10.1152/physrev.1999.79.4.1431
Little, J.W., Ford, A., Symons-Liguori, A.M., Chen, Z., Janes, K., Doyle, T., Xie, J., Luongo, L., Tosh, D.K., Maione, S., Bannister, K., Dickenson, A.H., Vanderah, T.W., Porreca, F., Jacobson, K.A., Salvemini, D., 2015. Endogenous adenosine A3 receptor activation selectively alleviates persistent pain states. Brain 138, 28–35. https://doi.org/10.1093/brain/awu330
Liu, J., Solway, K., Messing, R.O., Sharp, F.R., 1998. Increased neurogenesis in the dentate gyrus after transient global ischemia in gerbils. J. Neurosci. 18, 7768–78.
Livingston, M., Heaney, L.G., Ennis, M., 2004. Adenosine, inflammation and asthma--a review. Inflamm. Res. 53, 171–8. https://doi.org/10.1007/s00011-004-1248-2
Lo, E.H., 2008. A new penumbra: transitioning from injury into repair after stroke. Nat. Med. 14, 497–500. https://doi.org/10.1038/nm1735

Lopes, L. V, Cunha, R.A., Kull, B., Fredholm, B.B., Ribeiro, J.A., 2002. Adenosine A(2A) receptor facilitation of hippocampal synaptic transmission is dependent on tonic A(1) receptor inhibition. Neuroscience 112, 319–29.

Lopes, L. V, Rebola, N., Pinheiro, P.C., Richardson, P.J., Oliveira, C.R., Cunha, R.A., 2003. Adenosine A3 receptors are located in neurons of the rat hippocampus. Neuroreport 14, 1645–8. https://doi.org/10.1097/01.wnr.0000088406.04452.44

Love, S., 2003. Apoptosis and brain ischaemia. Prog. Neuropsychopharmacol. Biol. Psychiatry 27, 267–82. https://doi.org/10.1016/S0278-5846(03)00022-8

Lupica, C.R., Proctor, W.R., Dunwiddie, T. V, 1992. Presynaptic inhibition of excitatory synaptic transmission by adenosine in rat hippocampus: analysis of unitary EPSP variance measured by whole-cell recording. J. Neurosci. 12, 3753–64.

Lynch, S.S., Cheng, C.M., Yee, J.L., 2006. Intrathecal ziconotide for refractory chronic pain. Ann. Pharmacother. 40, 1293–300. https://doi.org/10.1345/aph.1G584

MacDonald, R.L., Skerritt, J.H., Werz, M.A., 1986. Adenosine agonists reduce voltage-dependent calcium conductance of mouse sensory neurones in cell culture. J. Physiol. 370, 75–90.

Macrez, R., Ali, C., Toutirais, O., Le Mauff, B., Defer, G., Dirnagl, U., Vivien, D., 2011. Stroke and the immune system: from pathophysiology to new therapeutic strategies. Lancet Neurol. 10, 471–480. https://doi.org/10.1016/S1474-4422(11)70066-7

Maenhaut, C., Van Sande, J., Libert, F., Abramowicz, M., Parmentier, M., Vanderhaegen, J.J., Dumont, J.E., Vassart, G., Schiffmann, S., 1990. RDC8 codes for an adenosine A2 receptor with physiological constitutive activity. Biochem. Biophys. Res. Commun. 173, 1169–78.

Magistretti, P.J., Hof, P.R., Martin, J.L., 1986. Adenosine stimulates glycogenolysis in mouse cerebral cortex: a possible coupling mechanism between neuronal activity and energy metabolism. J. Neurosci. 6, 2558–62.

Mah, H.D., Daly, J.W., 1976. Adenosine-dependent formation of cyclic AMP in brain slices. Pharmacol. Res. Commun. 8, 65–79.

Majumder, P., Trujillo, C.A., Lopes, C.G., Resende, R.R., Gomes, K.N., Yuahasi, K.K., Britto, L.R.G., Ulrich, H., 2007. New insights into purinergic receptor signaling in neuronal differentiation, neuroprotection, and brain disorders. Purinergic Signal. 3, 317–331. https://doi.org/10.1007/s11302-007-9074-y

Malek, R.L., Toman, R.E., Edsall, L.C., Wong, S., Chiu, J., Letterle, C.A., Van Brocklyn, J.R., Milstien, S., Spiegel, S., Lee, N.H., 2001. Nrg-1 belongs to the endothelial differentiation gene family of G protein-coupled sphingosine-1-phosphate receptors. J. Biol. Chem. 276, 5692–9. https://doi.org/10.1074/jbc.M003964200

Mandala, S., Hajdu, R., Bergstrom, J., Quackenbush, E., Xie, J., Milligan, J., Thornton, R., Shei, G.-J., Card, D., Keohane, C., Rosenbach, M., Hale, J., Lynch, C.L., Rupprecht, K., Parsons, W., Rosen, H., 2002. Alteration of lymphocyte trafficking by sphingosine-1-phosphate receptor agonists. Science 296, 346–9. https://doi.org/10.1126/science.1070238

Maragakis, N.J., Rothstein, J.D., 2004. Glutamate transporters: animal models to neurologic disease. Neurobiol. Dis. 15, 461–473. https://doi.org/10.1016/j.nbd.2003.12.007

Marcoli, M., Raiteri, L., Bonfanti, A., Monopoli, A., Ongini, E., Raiteri, M., Maura, G., 2003. Sensitivity to selective adenosine A1 and A2A receptor antagonists of the release of glutamate induced by ischemia in rat cerebrocortical slices. Neuropharmacology 45, 201–10.

Martínez-Fábregas, J., Díaz-Moreno, I., González-Arzola, K., Janocha, S., Navarro, J.A., Hervás, M., Bernhardt, R., Velázquez-Campoy, A., Díaz-Quintana, A., De la Rosa, M.A., 2014. Structural and functional analysis of novel human cytochrome C targets in apoptosis. Mol. Cell. Proteomics 13, 1439–56. https://doi.org/10.1074/mcp.M113.034322

Masino, S., Boison, D., 2013. Adenosine: A key link between metabolism and brain activity, Adenosine: A Key Link between Metabolism and Brain Activity. Springer. https://doi.org/10.1007/978-1-4614-3903-5

Matloubian, M., Lo, C.G., Cinamon, G., Lesneski, M.J., Xu, Y., Brinkmann, V., Allende, M.L., Proia, R.L., Cyster, J.G., 2004. Lymphocyte egress from thymus and peripheral lymphoid organs is dependent on S1P receptor 1. Nature 427, 355–360. https://doi.org/10.1038/nature02284

McDowell, G.C., Pope, J.E., 2016. Intrathecal Ziconotide: Dosing and Administration Strategies in Patients With Refractory Chronic Pain. Neuromodulation 19, 522–32. https://doi.org/10.1111/ner.12392

McIlwain, H., Pull, I., 1972. Release of adenine derivatives on electrical stimulation of superfused tissues from the brain. J. Physiol. 221, 9P–10P.

Melani, A., Corti, F., Stephan, H., Müller, C.E., Donati, C., Bruni, P., Vannucchi, M.G., Pedata, F., 2012. Ecto-ATPase inhibition: ATP and adenosine release under physiological and ischemic in vivo conditions in the rat striatum. Exp. Neurol. 233, 193–204. https://doi.org/10.1016/j.expneurol.2011.09.036

Melani, A., Gianfriddo, M., Vannucchi, M.G., Cipriani, S., Baraldi, P.G., Giovannini, M.G., Pedata, F., 2006. The selective A2A receptor antagonist SCH 58261 protects from neurological deficit, brain damage and activation of p38 MAPK in rat focal cerebral ischemia. Brain Res. 1073–1074, 470–80.

https://doi.org/10.1016/j.brainres.2005.12.010

Melani, A., Pantoni, L., Bordoni, F., Gianfriddo, M., Bianchi, L., Vannucchi, M.G., Bertorelli, R., Monopoli, A., Pedata, F., 2003. The selective A2A receptor antagonist SCH 58261 reduces striatal transmitter outflow, turning behavior and ischemic brain damage induced by permanent focal ischemia in the rat. Brain Res. 959, 243–50.

Melani, A., Pantoni, L., Corsi, C., Bianchi, L., Monopoli, A., Bertorelli, R., Pepeu, G., Pedata, F., 1999. Striatal outflow of adenosine, excitatory amino acids, gamma-aminobutyric acid, and taurine in awake freely moving rats after middle cerebral artery occlusion: correlations with neurological deficit and histopathological damage. Stroke 30, 2448–54; discussion 2455.

Melani, A., Turchi, D., Vannucchi, M.G., Cipriani, S., Gianfriddo, M., Pedata, F., 2005. ATP extracellular concentrations are increased in the rat striatum during in vivo ischemia. Neurochem. Int. 47, 442–8. https://doi.org/10.1016/j.neuint.2005.05.014

Meyer, P.T., Elmenhorst, D., Bier, D., Holschbach, M.H., Matusch, A., Coenen, H.H., Zilles, K., Bauer, A., 2005. Quantification of cerebral A1 adenosine receptors in humans using [18F]CPFPX and PET: an equilibrium approach. Neuroimage 24, 1192–204. https://doi.org/10.1016/j.neuroimage.2004.10.029

Meyerhof, W., Müller-Brechlin, R., Richter, D., 1991. Molecular cloning of a novel putative G-protein coupled receptor expressed during rat spermiogenesis. FEBS Lett. 284, 155–60.

Miron, V.E., Jung, C.G., Kim, H.J., Kennedy, T.E., Soliven, B., Antel, J.P., 2008. FTY720 modulates human oligodendrocyte progenitor process extension and survival. Ann. Neurol. 63, 61–71. https://doi.org/10.1002/ana.21227

Miyamota, M.D., Breckenridge, B.M., 1974. A cyclic adenosine monophosphate link in the catecholamine enhancement of transmitter release at the neuromuscular junction. J. Gen. Physiol. 63, 609–24.

Mizugishi, K., Yamashita, T., Olivera, A., Miller, G.F., Spiegel, S., Proia, R.L., 2005. Essential Role for Sphingosine Kinases in Neural and Vascular Development. Mol. Cell. Biol. 25, 11113–11121. https://doi.org/10.1128/MCB.25.24.11113-11121.2005

Mongan, L.C., Hill, M.J., Chen, M.X., Tate, S.N., Collins, S.D., Buckby, L., Grubb, B.D., 2005. The distribution of small and intermediate conductance calcium-activated potassium channels in the rat sensory nervous system. Neuroscience 131, 161–75. https://doi.org/10.1016/j.neuroscience.2004.09.062

Monopoli, A., Lozza, G., Forlani, A., Mattavelli, A., Ongini, E., 1998. Blockade of adenosine A2A receptors by SCH 58261 results in neuroprotective effects in cerebral ischaemia in rats. Neuroreport 9, 3955–9.

Moore, K.A., Nicoll, R.A., Schmitz, D., 2003. Adenosine gates synaptic plasticity at hippocampal mossy fiber synapses. Proc. Natl. Acad. Sci. U. S. A. 100, 14397–402. https://doi.org/10.1073/pnas.1835831100

Mori, M., Nishizaki, T., Okada, Y., 1992. Protective effect of adenosine on the anoxic damage of hippocampal slice. Neuroscience 46, 301–7.

Moriyama, K., Sitkovsky, M. V, 2010. Adenosine A2A receptor is involved in cell surface expression of A2B receptor. J. Biol. Chem. 285, 39271–88. https://doi.org/10.1074/jbc.M109.098293

Morley, P., Hogan, M.J., Hakim, A.M., 1994. Calcium-mediated mechanisms of ischemic injury and protection. Brain Pathol. 4, 37–47.

Moskowitz, M.A., Lo, E.H., Iadecola, C., 2010. The Science of Stroke: Mechanisms in Search of Treatments. Neuron 67, 181–198. https://doi.org/10.1016/j.neuron.2010.07.002

Motyl, J., Strosznajder, J.B., 2018. Sphingosine kinase 1/sphingosine-1-phosphate receptors dependent signalling in neurodegenerative diseases. The promising target for neuroprotection in Parkinson's disease. Pharmacol. Reports 70, 1010–1014. https://doi.org/10.1016/j.pharep.2018.05.002

Mu, A., Weinberg, E., Moulin, D.E., Clarke, H., 2017. Pharmacologic management of chronic neuropathic pain: Review of the Canadian pain society consensus statement. Can. Fam. Physician. https://doi.org/10.1016/j.pain.2009.05.014

Müller, C.E., Jacobson, K.A., 2011. Recent developments in adenosine receptor ligands and their potential as novel drugs. Biochim. Biophys. Acta - Biomembr. 1808, 1290–1308. https://doi.org/10.1016/j.bbamem.2010.12.017

Müller, M., Somjen, G.G., 2000. Na^+ Dependence and the Role of Glutamate Receptors and Na^+ Channels in Ion Fluxes During Hypoxia of Rat Hippocampal Slices. J. Neurophysiol. 84, 1869–1880. https://doi.org/10.1152/jn.2000.84.4.1869

Müller, M., Somjen, G.G., 1999. Intrinsic Optical Signals in Rat Hippocampal Slices During Hypoxia-Induced Spreading Depression-Like Depolarization. J. Neurophysiol. 82, 1818–1831. https://doi.org/10.1152/jn.1999.82.4.1818

Nassini, R., Fusi, C., Materazzi, S., Coppi, E., Tuccinardi, T., Marone, I.M., De Logu, F., Preti, D., Tonello, R., Chiarugi, A., Patacchini, R., Geppetti, P., Benemei, S., 2015. The TRPA1 channel mediates the analgesic action of dipyrone and pyrazolone derivatives. Br. J. Pharmacol. 172, 3397–411. https://doi.org/10.1111/bph.13129

Newell, D.W., Barth, A., Papermaster, V., Malouf, A.T., 1995. Glutamate and non-glutamate receptor mediated toxicity caused by oxygen and glucose deprivation in organotypic hippocampal cultures. J. Neurosci. 15, 7702–11.

Newman, G.C., Hospod, F.E., Trowbridge, S.D., Motwani, S., Liu, Y., 1998. Restoring adenine nucleotides in a brain slice model of cerebral reperfusion. J. Cereb. Blood Flow Metab. 18, 675–85. https://doi.org/10.1097/00004647-199806000-00010

Nishiyama, A., Chang, A., Trapp, B.D., 1999. NG2+ glial cells: a novel glial cell population in the adult brain. J. Neuropathol. Exp. Neurol. 58, 1113–24.

Nishiyama, A., Komitova, M., Suzuki, R., Zhu, X., 2009. Polydendrocytes (NG2 cells): multifunctional cells with lineage plasticity. Nat. Rev. Neurosci. 10, 9–22. https://doi.org/10.1038/nrn2495

Nishiyama, A., Watanabe, M., Yang, Z., Bu, J., 2002. Identity, distribution, and development of polydendrocytes: NG2-expressing glial cells. J. Neurocytol. 31, 437–455. https://doi.org/10.1023/A:1025783412651

North, R.A., 2002. Molecular Physiology of P2X Receptors. Physiol. Rev. 82, 1013–1067. https://doi.org/10.1152/physrev.00015.2002

Novgorodov, A.S., El-Alwani, M., Bielawski, J., Obeid, L.M., Gudz, T.I., 2007. Activation of sphingosine-1-phosphate receptor S1P5 inhibits oligodendrocyte progenitor migration. FASEB J. 21, 1503–1514. https://doi.org/10.1096/fj.06-7420com

O'Connor, S.E., Dainty, I.A., Leff, P., 1991. Further subclassification of ATP receptors based on agonist studies. Trends Pharmacol. Sci. 12, 137–141. https://doi.org/10.1016/0165-6147(91)90530-6

O'Kane, E.M., Stone, T.W., 1998. Interaction between adenosine A1 and A2 receptor-mediated responses in the rat hippocampus in vitro. Eur. J. Pharmacol. 362, 17–25.

O'Malley, H.A., Isom, L.L., 2015. Sodium Channel β Subunits: Emerging Targets in Channelopathies. Annu. Rev. Physiol. 77, 481–504. https://doi.org/10.1146/annurev-physiol-021014-071846

O'Regan, M.H., Simpson, R.E., Perkins, L.M., Phillis, J.W., 1992. The selective A2 adenosine receptor agonist CGS 21680 enhances excitatory transmitter amino acid release from the ischemic rat cerebral cortex. Neurosci. Lett. 138, 169–72.

O'Sullivan, S., 2017. Sphingosine-1-phosphate receptor therapies: Advances in clinical trials for CNS-related diseases. Neuropharmacology 113, 597–607. https://doi.org/10.1016/J.NEUROPHARM.2016.11.006

Obeidat, A.S., Andrew, R.D., 1998. Spreading depression determines acute cellular damage in the hippocampal slice during oxygen/glucose deprivation. Eur. J. Neurosci. 10, 3451–61.

Obrenovitch, T.P., 1995. The ischaemic penumbra: twenty years on. Cerebrovasc. Brain Metab. Rev. 7, 297–323.

Ochs, S., Hunt, K., 1960. Apical dendrites and propagation of spreading depression in cerebral cortex. J. Neurophysiol. 23, 432–444. https://doi.org/10.1152/jn.1960.23.4.432

Ong, W.Y., Levine, J.M., 1999. A light and electron microscopic study of NG2 chondroitin sulfate proteoglycan-positive oligodendrocyte precursor cells in the normal and kainate-lesioned rat hippocampus. Neuroscience 92, 83–95.

Ontaneda, D., Cohen, J.A., Amato, M.P., 2017. Clinical outcome measures for progressive MS trials. Mult. Scler. J. 23, 1627–1635. https://doi.org/10.1177/1352458517729465

Orr, A.G., Orr, A.L., Li, X.-J., Gross, R.E., Traynelis, S.F., 2009. Adenosine A2A receptor mediates microglial process retraction. Nat. Neurosci. 12, 872–878. https://doi.org/10.1038/nn.2341

Ortore, G., Martinelli, A., 2010. A2B receptor ligands: past, present and future trends. Curr. Top. Med. Chem. 10, 923–40.

Othman, T., Yan, H., Rivkees, S.A., 2003. Oligodendrocytes express functional A1 adenosine receptors that stimulate cellular migration. Glia 44, 166–72. https://doi.org/10.1002/glia.10281

Outeiro, T.F., Lindquist, S., 2003. Yeast Cells Provide Insight into Alpha-Synuclein Biology and Pathobiology. Science (80-.). 302, 1772–1775. https://doi.org/10.1126/science.1090439

Pagadala, P., Park, C.-K., Bang, S., Xu, Z.-Z., Xie, R.-G., Liu, T., Han, B.-X., Tracey, W.D., Wang, F., Ji, R.-R., 2013. Loss of NR1 Subunit of NMDARs in Primary Sensory Neurons Leads to Hyperexcitability and Pain Hypersensitivity: Involvement of Ca^{2+}-Activated Small Conductance Potassium Channels. J. Neurosci. 33, 13425–13430. https://doi.org/10.1523/jneurosci.0454-13.2013

Panjehpour, M., Castro, M., Klotz, K.-N., 2005. Human breast cancer cell line MDA-MB-231 expresses endogenous A_{2B} adenosine receptors mediating a Ca^{2+} signal. Br. J. Pharmacol. 145, 211–218. https://doi.org/10.1038/sj.bjp.0706180

Pantoni, L., Garcia, J.H., Gutierrez, J.A., 1996. Cerebral white matter is highly vulnerable to ischemia. Stroke 27, 1641–6; discussion 1647.

Pașca, S.P., 2018. The rise of three-dimensional human brain cultures. Nature 553, 437–445. https://doi.org/10.1038/nature25032

Passmore, G.M., Selyanko, A.A., Mistry, M., Al-Qatari, M., Marsh, S.J., Matthews, E.A., Dickenson, A.H., Brown, T.A., Burbidge, S.A., Main, M., Brown, D.A., 2003. KCNQ/M currents in sensory neurons: significance for pain therapy. J. Neurosci. 23, 7227–36.

Pchejetski, D., Bohler, T., Brizuela, L., Sauer, L., Doumerc, N., Golzio, M., Salunkhe, V., Teissié, J., Malavaud, B., Waxman, J., Cuvillier, O., 2010. FTY720 (fingolimod) sensitizes prostate cancer cells to radiotherapy by inhibition of sphingosine kinase-1. Cancer Res. 70, 8651–61.

https://doi.org/10.1158/0008-5472.CAN-10-1388
Pearson, T., Damian, K., Lynas, R.E., Frenguelli, B.G., 2006. Sustained elevation of extracellular adenosine and activation of A1 receptors underlie the post-ischaemic inhibition of neuronal function in rat hippocampus in vitro. J. Neurochem. 97, 1357–68. https://doi.org/10.1111/j.1471-4159.2006.03823.x
Pedata, F., Corsi, C., Melani, A., Bordoni, F., Latini, S., 2001. Adenosine extracellular brain concentrations and role of A2A receptors in ischemia. Ann. N. Y. Acad. Sci. 939, 74–84.
Pedata, F., Dettori, I., Coppi, E., Melani, A., Fusco, I., Corradetti, R., Pugliese, A.M., 2016. Purinergic signalling in brain ischemia. Neuropharmacology 104, 105–130. https://doi.org/10.1016/j.neuropharm.2015.11.007
Pedata, F., Gianfriddo, M., Turchi, D., Melani, A., 2005. The protective effect of adenosine A2A receptor antagonism in cerebral ischemia. Neurol. Res. 27, 169–74. https://doi.org/10.1179/016164105X21913
Pedata, F., Latini, S., Pugliese, A.M., Pepeu, G., 1993. Investigations into the adenosine outflow from hippocampal slices evoked by ischemia-like conditions. J. Neurochem. 61, 284–9.
Pedata, F., Melani, A., Pugliese, A.M., Coppi, E., Cipriani, S., Traini, C., 2007. The role of ATP and adenosine in the brain under normoxic and ischemic conditions. Purinergic Signal. 3, 299–310. https://doi.org/10.1007/s11302-007-9085-8
Pedata, F., Pepeu, G., Spignoli, G., 1984. Biphasic effect of methylxanthines on acetylcholine release from electrically-stimulated brain slices. Br. J. Pharmacol. 83, 69–73.
Pedata, F., Pugliese, A.M., Melani, A., Gianfriddo, M., 2003. A2A receptors in neuroprotection of dopaminergic neurons. Neurology 61, S49-50.
Peirs, C., Seal, R.P., 2016. Neural circuits for pain: Recent advances and current views. Science 354, 578–584. https://doi.org/10.1126/science.aaf8933
Peng, X., Hassoun, P.M., Sammani, S., McVerry, B.J., Burne, M.J., Rabb, H., Pearse, D., Tuder, R.M., Garcia, J.G.N., 2004. Protective Effects of Sphingosine 1-Phosphate in Murine Endotoxin-induced Inflammatory Lung Injury. Am. J. Respir. Crit. Care Med. 169, 1245–1251. https://doi.org/10.1164/rccm.200309-1258OC
Perez-Buira, S., Barrachina, M., Rodriguez, A., Albasanz, J.L., Martín, M., Ferrer, I., 2007. Expression levels of adenosine receptors in hippocampus and frontal cortex in argyrophilic grain disease. Neurosci. Lett. 423, 194–9. https://doi.org/10.1016/j.neulet.2007.06.049
Phillis, J.W., 2004. Adenosine and adenine nucleotides as regulators of cerebral blood flow: roles of acidosis, cell swelling, and KATP channels. Crit. Rev. Neurobiol. 16, 237–70.
Phillis, J.W., 1995. The effects of selective A1 and A2a adenosine receptor antagonists on cerebral ischemic injury in the gerbil. Brain Res. 705, 79–84.
Pitson, S.M., Moretti, P.A.B., Zebol, J.R., Lynn, H.E., Xia, P., Vadas, M.A., Wattenberg, B.W., 2003. Activation of sphingosine kinase 1 by ERK1/2-mediated phosphorylation. EMBO J. 22, 5491–500. https://doi.org/10.1093/emboj/cdg540
Pizzo, P.A., Clark, N.M., 2012. Alleviating suffering 101--pain relief in the United States. N. Engl. J. Med. 366, 197–9. https://doi.org/10.1056/NEJMp1109084
Plum, F., 2001. Neuroprotection in acute ischemic stroke. JAMA 285, 1760–1.
Popoli, P., Betto, P., Reggio, R., Ricciarello, G., 1995. Adenosine A2A receptor stimulation enhances striatal extracellular glutamate levels in rats. Eur. J. Pharmacol. 287, 215–7.
Popoli, P., Pepponi, R., 2012. Potential therapeutic relevance of adenosine A2B and A2A receptors in the central nervous system. CNS Neurol. Disord. Drug Targets 11, 664–74.
Poucher, S.M., Keddie, J.R., Singh, P., Stoggall, S.M., Caulkett, P.W., Jones, G., Coll, M.G., 1995. The in vitro pharmacology of ZM 241385, a potent, non-xanthine A2a selective adenosine receptor antagonist. Br. J. Pharmacol. 115, 1096–102.
Prescott, S.A., Ma, Q., De Koninck, Y., 2014. Normal and abnormal coding of somatosensory stimuli causing pain. Nat. Neurosci. 17, 183–191. https://doi.org/10.1038/nn.3629
Press, N.J., Taylor, R.J., Fullerton, J.D., Tranter, P., McCarthy, C., Keller, T.H., Brown, L., Cheung, R., Christie, J., Haberthuer, S., Hatto, J.D.I., Keenan, M., Mercer, M.K., Press, N.E., Sahri, H., Tuffnell, A.R., Tweed, M., Fozard, J.R., 2005. A new orally bioavailable dual adenosine A2B/A3 receptor antagonist with therapeutic potential. Bioorg. Med. Chem. Lett. 15, 3081–5. https://doi.org/10.1016/j.bmcl.2005.04.021
Prince, D.A., Stevens, C.F., 1992. Adenosine decreases neurotransmitter release at central synapses. Proc. Natl. Acad. Sci. U. S. A. 89, 8586–90.
Pugliese, A.M., Coppi, E., Spalluto, G., Corradetti, R., Pedata, F., 2006. A $_3$ adenosine receptor antagonists delay irreversible synaptic failure caused by oxygen and glucose deprivation in the rat CA1 hippocampus *in vitro*. Br. J. Pharmacol. 147, 524–532. https://doi.org/10.1038/sj.bjp.0706646
Pugliese, A.M., Coppi, E., Volpini, R., Cristalli, G., Corradetti, R., Jeong, L.S., Jacobson, K.A., Pedata, F., 2007. Role of adenosine A3 receptors on CA1 hippocampal neurotransmission during oxygen-glucose deprivation episodes of different duration. Biochem. Pharmacol. 74, 768–79. https://doi.org/10.1016/j.bcp.2007.06.003

Pugliese, A.M., Latini, S., Corradetti, R., Pedata, F., 2003. Brief, repeated, oxygen-glucose deprivation episodes protect neurotransmission from a longer ischemic episode in the in vitro hippocampus: role of adenosine receptors. Br. J. Pharmacol. 140, 305–14. https://doi.org/10.1038/sj.bjp.0705442

Pugliese, A.M., Traini, C., Cipriani, S., Gianfriddo, M., Mello, T., Giovannini, M.G., Galli, A., Pedata, F., 2009. The adenosine A2A receptor antagonist ZM241385 enhances neuronal survival after oxygen-glucose deprivation in rat CA1 hippocampal slices. Br. J. Pharmacol. 157, 818–30. https://doi.org/10.1111/j.1476-5381.2009.00218.x

Pull, I., McIlwain, H., 1972. Adenine derivatives as neurohumoral agents in the brain. The quantities liberated on excitation of superfused cerebral tissues. Biochem. J. 130, 975–81.

Ramkumar, V., Stiles, G.L., Beaven, M.A., Ali, H., 1993. The A3 adenosine receptor is the unique adenosine receptor which facilitates release of allergic mediators in mast cells. J. Biol. Chem. 268, 16887–90.

Rebola, N., Simões, A.P., Canas, P.M., Tomé, A.R., Andrade, G.M., Barry, C.E., Agostinho, P.M., Lynch, M.A., Cunha, R.A., 2011. Adenosine A2A receptors control neuroinflammation and consequent hippocampal neuronal dysfunction. J. Neurochem. 117, 100–11. https://doi.org/10.1111/j.1471-4159.2011.07178.x

Regehr, W.G., 2012. Short-term presynaptic plasticity. Cold Spring Harb. Perspect. Biol. 4, a005702. https://doi.org/10.1101/cshperspect.a005702

Richardson, W.D., Kessaris, N., Pringle, N., 2006. Oligodendrocyte wars. Nat. Rev. Neurosci. 7, 11–18. https://doi.org/10.1038/nrn1826

Riddy, D., Stamp, C., Sykes, D., Charlton, S., Dowling, M., 2012. Reassessment of the pharmacology of Sphingosine-1-phosphate S1P $_3$ receptor ligands using the DiscoveRx PathHunter^{TM} and Ca $^{2+}$ release functional assays. Br. J. Pharmacol. 167, 868–880. https://doi.org/10.1111/j.1476-5381.2012.02032.x

Rieger, J.M., Brown, M.L., Sullivan, G.W., Linden, J., Macdonald, T.L., 2001. Design, synthesis, and evaluation of novel A2A adenosine receptor agonists. J. Med. Chem. 44, 531–9.

Ritter, D.M., Zemel, B.M., Lepore, A.C., Covarrubias, M., 2015. Kv3.4 channel function and dysfunction in nociceptors. Channels 9, 209–217. https://doi.org/10.1080/19336950.2015.1056949

Rivkees, S.A., Price, S.L., Zhou, F.C., 1995. Immunohistochemical detection of A1 adenosine receptors in rat brain with emphasis on localization in the hippocampal formation, cerebral cortex, cerebellum, and basal ganglia. Brain Res. 677, 193–203.

Rosenblueth, A., García Ramos, J., 1966. Some phenomena usually associated with spreading depression. Acta Physiol. Lat. Am. 16, 141–79.

Rosenthal, W., Hescheler, J., Trautwein, W., Schultz, G., 1988. Control of voltage-dependent Ca2+ channels by G protein-coupled receptors. FASEB J. 2, 2784–90.

Rosin, D.L., Hettinger, B.D., Lee, A., Linden, J., 2003. Anatomy of adenosine A2A receptors in brain: morphological substrates for integration of striatal function. Neurology 61, S12-8.

Rosin, D.L., Robeva, A., Woodard, R.L., Guyenet, P.G., Linden, J., 1998. Immunohistochemical localization of adenosine A2A receptors in the rat central nervous system. J. Comp. Neurol. 401, 163–86.

Ross, G.W., Abbott, R.D., Petrovitch, H., Morens, D.M., Grandinetti, A., Tung, K.H., Tanner, C.M., Masaki, K.H., Blanchette, P.L., Curb, J.D., Popper, J.S., White, L.R., 2000. Association of coffee and caffeine intake with the risk of Parkinson disease. J. Am. Med. Assoc. 283, 2674–2679. https://doi.org/10.1001/jama.283.20.2674

Rothhammer, V., Kenison, J.E., Tjon, E., Takenaka, M.C., de Lima, K.A., Borucki, D.M., Chao, C.-C., Wilz, A., Blain, M., Healy, L., Antel, J., Quintana, F.J., 2017. Sphingosine 1-phosphate receptor modulation suppresses pathogenic astrocyte activation and chronic progressive CNS inflammation. Proc. Natl. Acad. Sci. U. S. A. 114, 2012–2017. https://doi.org/10.1073/pnas.1615413114

Saab, A.S., Tzvetanova, I.D., Nave, K.-A., 2013. The role of myelin and oligodendrocytes in axonal energy metabolism. Curr. Opin. Neurobiol. 23, 1065–72. https://doi.org/10.1016/j.conb.2013.09.008

Sachdeva, S., Gupta, M., 2013. Adenosine and its receptors as therapeutic targets: An overview. Saudi Pharm. J. SPJ Off. Publ. Saudi Pharm. Soc. 21, 245–53. https://doi.org/10.1016/j.jsps.2012.05.011

Saini, H.S., Coelho, R.P., Goparaju, S.K., Jolly, P.S., Maceyka, M., Spiegel, S., Sato-Bigbee, C., 2005. Novel role of sphingosine kinase 1 as a mediator of neurotrophin-3 action in oligodendrocyte progenitors. J. Neurochem. 95, 1298–310. https://doi.org/10.1111/j.1471-4159.2005.03451.x

Salter, M.W., 2014. Deepening understanding of the neural substrates of chronic pain. Brain 137, 651–653. https://doi.org/10.1093/brain/awu028

Salvatore, C.A., Jacobson, M.A., Taylor, H.E., Linden, J., Johnson, R.G., 1993. Molecular cloning and characterization of the human A3 adenosine receptor. Proc. Natl. Acad. Sci. U. S. A. 90, 10365–9.

Salvatore, C.A., Tilley, S.L., Latour, A.M., Fletcher, D.S., Koller, B.H., Jacobson, M.A., 2000. Disruption of the A(3) adenosine receptor gene in mice and its effect on stimulated inflammatory cells. J. Biol. Chem. 275, 4429–34.

Sampaio-Baptista, C., Johansen-Berg, H., 2017. White Matter Plasticity in the Adult Brain. Neuron 96, 1239–1251. https://doi.org/10.1016/j.neuron.2017.11.026

Sanchez, T., Estrada-Hernandez, T., Paik, J.-H., Wu, M.-T., Venkataraman, K., Brinkmann, V., Claffey, K.,

Hla, T., 2003. Phosphorylation and action of the immunomodulator FTY720 inhibits vascular endothelial cell growth factor-induced vascular permeability. J. Biol. Chem. 278, 47281–90. https://doi.org/10.1074/jbc.M306896200

Sandkühler, J., 2009. Models and Mechanisms of Hyperalgesia and Allodynia. Physiol. Rev. 89, 707–758. https://doi.org/10.1152/physrev.00025.2008

Sanna, M.G., Wang, S.-K., Gonzalez-Cabrera, P.J., Don, A., Marsolais, D., Matheu, M.P., Wei, S.H., Parker, I., Jo, E., Cheng, W.-C., Cahalan, M.D., Wong, C.-H., Rosen, H., 2006. Enhancement of capillary leakage and restoration of lymphocyte egress by a chiral S1P1 antagonist in vivo. Nat. Chem. Biol. 2, 434–41. https://doi.org/10.1038/nchembio804

Satoi, H., Tomimoto, H., Ohtani, R., Kitano, T., Kondo, T., Watanabe, M., Oka, N., Akiguchi, I., Furuya, S., Hirabayashi, Y., Okazaki, T., 2005. Astroglial expression of ceramide in Alzheimer's disease brains: A role during neuronal apoptosis. Neuroscience 130, 657–666. https://doi.org/10.1016/J.NEUROSCIENCE.2004.08.056

Sattin, A., Rall, T.W., 1970. The effect of adenosine and adenine nucleotides on the cyclic adenosine 3', 5'-phosphate content of guinea pig cerebral cortex slices. Mol. Pharmacol. 6, 13–23.

Sawynok, J., 2016. Adenosine receptor targets for pain. Neuroscience 338, 1–18. https://doi.org/10.1016/j.neuroscience.2015.10.031

Schaller, B., Graf, R., Jacobs, A.H., 2003. Ischaemic tolerance: a window to endogenous neuroprotection? Lancet 362, 1007–1008. https://doi.org/10.1016/S0140-6736(03)14446-7

Schindler, C.W., Karcz-Kubicha, M., Thorndike, E.B., Müller, C.E., Tella, S.R., Ferré, S., Goldberg, S.R., 2005. Role of central and peripheral adenosine receptors in the cardiovascular responses to intraperitoneal injections of adenosine A1 and A2A subtype receptor agonists. Br. J. Pharmacol. 144, 642–50. https://doi.org/10.1038/sj.bjp.0706043

Schindler, M., Harris, C.A., Hayes, B., Papotti, M., Humphrey, P.P., 2001. Immunohistochemical localization of adenosine A1 receptors in human brain regions. Neurosci. Lett. 297, 211–5.

Schmidt, C.O., Raspe, H., Kohlmann, T., 2010. Graded back pain revisited – Do latent variable models change our understanding of severe back pain in the general population? Pain 149, 50–56. https://doi.org/10.1016/j.pain.2010.01.025

Schnell, J.P., Croset, M., Dieumegard, D., Velasco, G., Siejka, J., 1983. Characterization of calcium implanted zirconia thin films. Nucl. Instruments Methods Phys. Res. 209–210, 1187–1191. https://doi.org/10.1016/0167-5087(83)90937-7

Scholfield, C.N., 1978. Depression of evoked potentials in brain slices by adenosine compounds. Br. J. Pharmacol. 63, 239–44.

Schubert, D., Tarikas, H., LaCorbiere, M., 1976. Neurotransmitter regulation of adenosine 3',5'-monophosphate in clonal nerve, glia, and muscle cell lines. Science 192, 471–3.

Schubert, P., Rudolphi, K.A., Fredholm, B.B., Yoichi, N., 1994. Modulation of nerve and glial function by adenosine-role in the development of ischemic damage. Int. J. Biochem. 26, 1227–1236. https://doi.org/10.1016/0020-711X(94)90092-2

Schulte, G., Fredholm, B.B., 2003. The G(s)-coupled adenosine A(2B) receptor recruits divergent pathways to regulate ERK1/2 and p38. Exp. Cell Res. 290, 168–76.

Schultz, J., 1975. Cyclic adenosine 3',5'-monophosphate in guinea-pig cerebral cortical slices: studies on the role of adenosine. J. Neurochem. 24, 1237–42.

Scroggs, R.S., Fox, A.P., 1992. Calcium current variation between acutely isolated adult rat dorsal root ganglion neurons of different size. J. Physiol. 445, 639–58.

Scroggs, R.S., Fox, A.P., 1991. Distribution of dihydropyridine and omega-conotoxin-sensitive calcium currents in acutely isolated rat and frog sensory neuron somata: diameter-dependent L channel expression in frog. J. Neurosci. 11, 1334–46.

Sebastião, A.M., Ribeiro, J.A., 1996. Adenosine A2 receptor-mediated excitatory actions on the nervous system. Prog. Neurobiol. 48, 167–89.

Sharp, F.R., Liu, J., Bernabeu, R., 2002. Neurogenesis following brain ischemia. Brain Res. Dev. Brain Res. 134, 23–30.

Shea, B.S., Brooks, S.F., Fontaine, B.A., Chun, J., Luster, A.D., Tager, A.M., 2010. Prolonged Exposure to Sphingosine 1–Phosphate Receptor-1 Agonists Exacerbates Vascular Leak, Fibrosis, and Mortality after Lung Injury. Am. J. Respir. Cell Mol. Biol. 43, 662–673. https://doi.org/10.1165/rcmb.2009-0345OC

Shimizu, H., Daly, J., 1970. Formation of cyclic adenosine 3',5'-monophosphate from adenosine in brain slices. Biochim. Biophys. Acta 222, 465–73.

Siesjö, B.K., Bengtsson, F., 1989. Calcium Fluxes, Calcium Antagonists, and Calcium-Related Pathology in Brain Ischemia, Hypoglycemia, and Spreading Depression: A Unifying Hypothesis. J. Cereb. Blood Flow Metab. 9, 127–140. https://doi.org/10.1038/jcbfm.1989.20

Simpson, R.E., O'Regan, M.H., Perkins, L.M., Phillis, J.W., 1992. Excitatory transmitter amino acid release from the ischemic rat cerebral cortex: effects of adenosine receptor agonists and antagonists. J. Neurochem. 58, 1683–90.

Siniscalchi, A., Rodi, D., Gessi, S., Campi, F., Borea, P.A., 1999. Early changes in adenosine A1 receptors in cerebral cortex slices submitted to in vitro ischemia. Neurochem. Int. 34, 517–22.

Snow, J.B., Zheng, J.B., Chang, R.K., 1983. Spatially and spectrally resolved multipoint coherent anti-Stokes Raman scattering from N(2) and O(2) flows. Opt. Lett. 8, 599–601.

Soliven, B., Ma, L., Bae, H., Attali, B., Sobko, A., Iwase, T., 2003. PDGF upregulates delayed rectifier via Src family kinases and sphingosine kinase in oligodendroglial progenitors. Am. J. Physiol. Physiol. 284, C85–C93. https://doi.org/10.1152/ajpcell.00145.2002

Soliven, B., Miron, V., Chun, J., 2011. The neurobiology of sphingosine 1-phosphate signaling and sphingosine 1-phosphate receptor modulators. Neurology 76, S9–S14. https://doi.org/10.1212/WNL.0b013e31820d9507

Soliven, B., Szuchet, S., Arnason, B.G., Nelson, D.J., 1988. Forskolin and phorbol esters decrease the same K+ conductance in cultured oligodendrocytes. J. Membr. Biol. 105, 177–86.

Soliven, B., Szuchet, S., Arnason, B.G.W., Nelson, D.J., 1989. Expression and Modulation of K⁺ Currents in Oligodendrocytes: Possible Role in Myelinogenesis. Dev. Neurosci. 11, 118–131. https://doi.org/10.1159/000111893

Somjen, G.G., 2001. Mechanisms of Spreading Depression and Hypoxic Spreading Depression-Like Depolarization. Physiol. Rev. 81, 1065–1096. https://doi.org/10.1152/physrev.2001.81.3.1065

Sontheimer, H., Kettenmann, H., 1988. Heterogeneity of potassium currents in cultured oligodendrocytes. Glia 1, 415–20. https://doi.org/10.1002/glia.440010609

Sontheimer, H., Perouansky, M., Hoppe, D., Lux, H.D., Grantyn, R., Kettenmann, H., 1989. Glial cells of the oligodendrocyte lineage express proton-activated Na+ channels. J. Neurosci. Res. 24, 496–500. https://doi.org/10.1002/jnr.490240406

Sperlágh, B., Zsilla, G., Baranyi, M., Illes, P., Vizi, E.S., 2007. Purinergic modulation of glutamate release under ischemic-like conditions in the hippocampus. Neuroscience 149, 99–111. https://doi.org/10.1016/j.neuroscience.2007.07.035

Spignoli, G., Pedata, F., Pepeu, G., 1984. A1 and A2 adenosine receptors modulate acetylcholine release from brain slices. Eur. J. Pharmacol. 97, 341–2.

Stemkowski, P.L., Noh, M., Chen, Y., Smith, P.A., 2015. Increased excitability of medium-sized dorsal root ganglion neurons by prolonged interleukin-1β exposure is K^+ channel dependent and reversible. J. Physiol. 593, 3739–3755. https://doi.org/10.1113/JP270905

Stemkowski, P.L., Smith, P.A., 2012. Long-term IL-1β exposure causes subpopulation-dependent alterations in rat dorsal root ganglion neuron excitability. J. Neurophysiol. 107, 1586–1597. https://doi.org/10.1152/jn.00587.2011

Stevens, B., Porta, S., Haak, L.L., Gallo, V., Fields, R.D., 2002. Adenosine: a neuron-glial transmitter promoting myelination in the CNS in response to action potentials. Neuron 36, 855–68.

Stoll, G., Jander, S., Schroeter, M., 1998. Inflammation and glial responses in ischemic brain lesions. Prog. Neurobiol. 56, 149–71.

Suen, D.-F., Norris, K.L., Youle, R.J., 2008. Mitochondrial dynamics and apoptosis. Genes Dev. 22, 1577–90. https://doi.org/10.1101/gad.1658508

Sun, K., Zhang, Y., Bogdanov, M. V., Wu, H., Song, A., Li, J., Dowhan, W., Idowu, M., Juneja, H.S., Molina, J.G., Blackburn, M.R., Kellems, R.E., Xia, Y., 2015. Elevated adenosine signaling via adenosine A2B receptor induces normal and sickle erythrocyte sphingosine kinase 1 activity. Blood 125, 1643–1652. https://doi.org/10.1182/blood-2014-08-595751

Sun, Y., Huang, P., 2016. Adenosine A2B Receptor: From Cell Biology to Human Diseases. Front. Chem. 4. https://doi.org/10.3389/fchem.2016.00037

Sutphen, R., Xu, Y., Wilbanks, G.D., Fiorica, J., Grendys, E.C., LaPolla, J.P., Arango, H., Hoffman, M.S., Martino, M., Wakeley, K., Griffin, D., Blanco, R.W., Cantor, A.B., Xiao, Y., Krischer, J.P., 2004. Lysophospholipids are potential biomarkers of ovarian cancer. Cancer Epidemiol. Biomarkers Prev. 13, 1185–91.

Suzuki, S., Enosawa, S., Kakefuda, T., Li, X.K., Mitsusada, M., Takahara, S., Amemiya, H., 1996. Immunosuppressive effect of a new drug, FTY720, on lymphocyte responses in vitro and cardiac allograft survival in rats. Transpl. Immunol. 4, 252–5.

Swanson, T.H., Drazba, J.A., Rivkees, S.A., 1995. Adenosine A1 receptors are located predominantly on axons in the rat hippocampal formation. J. Comp. Neurol. 363, 517–531. https://doi.org/10.1002/cne.903630402

Takagi, Y., Nozaki, K., Takahashi, J., Yodoi, J., Ishikawa, M., Hashimoto, N., 1999. Proliferation of neuronal precursor cells in the dentate gyrus is accelerated after transient forebrain ischemia in mice. Brain Res. 831, 283–7.

Takahashi, Y., Wu, J., Suzuki, K., Martinez-Redondo, P., Li, M., Liao, H.-K., Wu, M.-Z., Hernández-Benítez, R., Hishida, T., Shokhirev, M.N., Esteban, C.R., Sancho-Martinez, I., Belmonte, J.C.I., 2017. Integration of CpG-free DNA induces de novo methylation of CpG islands in pluripotent stem cells. Science 356, 503–508. https://doi.org/10.1126/science.aag3260

Takigawa, T., Alzheimer, C., 2002. Phasic and tonic attenuation of EPSPs by inward rectifier K+ channels in rat hippocampal pyramidal cells. J. Physiol. 539, 67–75.

Takigawa, T., Alzheimer, C., 1999. G protein-activated inwardly rectifying K+ (GIRK) currents in dendrites of rat neocortical pyramidal cells. J. Physiol. 517 (Pt 2), 385–90.

Tan, Z.Y., Donnelly, D.F., LaMotte, R.H., 2006. Effects of a Chronic Compression of the Dorsal Root Ganglion on Voltage-Gated Na^+ and K^+ Currents in Cutaneous Afferent Neurons. J. Neurophysiol. 95, 1115–1123. https://doi.org/10.1152/jn.00830.2005

Tanaka, E., Yamamoto, S., Kudo, Y., Mihara, S., Higashi, H., 1997. Mechanisms underlying the rapid depolarization produced by deprivation of oxygen and glucose in rat hippocampal CA1 neurons in vitro. J. Neurophysiol. 78, 891–902. https://doi.org/10.1152/jn.1997.78.2.891

Taylor, D.A., Stone, T.W., 1978. Neuronal responses to extracellularly applied cyclic AMP:Role of the adenosine receptor. Experientia 34, 481–2.

Taylor, J., Anderson, W.S., Brandt, J., Mari, Z., Pontone, G.M., 2016. Neuropsychiatric Complications of Parkinson Disease Treatments: Importance of Multidisciplinary Care. Am. J. Geriatr. Psychiatry 24, 1171–1180. https://doi.org/10.1016/j.jagp.2016.08.017

Thoreen, C.C., Chantranupong, L., Keys, H.R., Wang, T., Gray, N.S., Sabatini, D.M., 2012. A unifying model for mTORC1-mediated regulation of mRNA translation. Nature 485, 109–13. https://doi.org/10.1038/nature11083

Todd, A.J., 2010. Neuronal circuitry for pain processing in the dorsal horn. Nat. Rev. Neurosci. 11, 823–836. https://doi.org/10.1038/nrn2947

Tominaga, K., Shibata, S., Watanabe, S., 1992. A neuroprotective effect of adenosine A1-receptor agonists on ischemia-induced decrease in 2-deoxyglucose uptake in rat hippocampal slices. Neurosci. Lett. 145, 67–70.

Tonelli, F., Lim, K.G., Loveridge, C., Long, J., Pitson, S.M., Tigyi, G., Bittman, R., Pyne, S., Pyne, N.J., 2010. FTY720 and (S)-FTY720 vinylphosphonate inhibit sphingosine kinase 1 and promote its proteasomal degradation in human pulmonary artery smooth muscle, breast cancer and androgen-independent prostate cancer cells. Cell. Signal. 22, 1536–1542. https://doi.org/10.1016/J.CELLSIG.2010.05.022

Tong, C.-K., MacDermott, A.B., 2006. Both Ca2+-permeable and -impermeable AMPA receptors contribute to primary synaptic drive onto rat dorsal horn neurons. J. Physiol. 575, 133–44. https://doi.org/10.1113/jphysiol.2006.110072

Torrance, N., Ferguson, J.A., Afolabi, E., Bennett, M.I., Serpell, M.G., Dunn, K.M., Smith, B.H., 2013. Neuropathic pain in the community: More under-treated than refractory? Pain 154, 690–699. https://doi.org/10.1016/j.pain.2012.12.022

Torrance, N., Smith, B.H., Bennett, M.I., Lee, A.J., 2006. The Epidemiology of Chronic Pain of Predominantly Neuropathic Origin. Results From a General Population Survey. J. Pain 7, 281–289. https://doi.org/10.1016/j.jpain.2005.11.008

Torres, V.I., Vallejo, D., Inestrosa, N.C., 2017. Emerging Synaptic Molecules as Candidates in the Etiology of Neurological Disorders. Neural Plast. 2017, 1–25. https://doi.org/10.1155/2017/8081758

Tosh, D.K., Finley, A., Paoletta, S., Moss, S.M., Gao, Z.-G., Gizewski, E.T., Auchampach, J.A., Salvemini, D., Jacobson, K.A., 2014. In Vivo Phenotypic Screening for Treating Chronic Neuropathic Pain: Modification of *C* 2-Arylethynyl Group of Conformationally Constrained A_3 Adenosine Receptor Agonists. J. Med. Chem. 57, 9901–9914. https://doi.org/10.1021/jm501021n

Touzani, O., Roussel, S., MacKenzie, E.T., 2001. The ischaemic penumbra. Curr. Opin. Neurol. 14, 83–8.

Traini, C., Pedata, F., Cipriani, S., Mello, T., Galli, A., Giovannini, M.G., Cerbai, F., Volpini, R., Cristalli, G., Pugliese, A.M., 2011. P2 receptor antagonists prevent synaptic failure and extracellular signal-regulated kinase1/2 activation induced by oxygen and glucose deprivation in rat CA1 hippocampus in vitro. Eur. J. Neurosci. 33, 2203–2215. https://doi.org/10.1111/j.1460-9568.2011.07667.x

Treede, R.-D., Jensen, T.S., Campbell, J.N., Cruccu, G., Dostrovsky, J.O., Griffin, J.W., Hansson, P., Hughes, R., Nurmikko, T., Serra, J., 2008. Neuropathic pain: Redefinition and a grading system for clinical and research purposes. Neurology 70, 1630–1635. https://doi.org/10.1212/01.wnl.0000282763.29778.59

Trincavelli, M.L., Marroni, M., Tuscano, D., Ceruti, S., Mazzola, A., Mitro, N., Abbracchio, M.P., Martini, C., 2004. Regulation of A2B adenosine receptor functioning by tumour necrosis factor a in human astroglial cells. J. Neurochem. 91, 1180–90. https://doi.org/10.1111/j.1471-4159.2004.02793.x

Trincavelli, M.L., Melani, A., Guidi, S., Cuboni, S., Cipriani, S., Pedata, F., Martini, C., 2008. Regulation of A(2A) adenosine receptor expression and functioning following permanent focal ischemia in rat brain. J. Neurochem. 104, 479–90. https://doi.org/10.1111/j.1471-4159.2007.04990.x

Tsantoulas, C., Zhu, L., Shaifta, Y., Grist, J., Ward, J.P.T., Raouf, R., Michael, G.J., McMahon, S.B., 2012. Sensory neuron downregulation of the Kv9.1 potassium channel subunit mediates neuropathic pain following nerve injury. J. Neurosci. 32, 17502–13. https://doi.org/10.1523/JNEUROSCI.3561-12.2012

Tsokas, P., Ma, T., Iyengar, R., Landau, E.M., Blitzer, R.D., 2007. Mitogen-activated protein kinase upregulates the dendritic translation machinery in long-term potentiation by controlling the mammalian target of rapamycin pathway. J. Neurosci. 27, 5885–94. https://doi.org/10.1523/JNEUROSCI.4548-

06.2007

Unal-Cevik, I., Kilinç, M., Gürsoy-Ozdemir, Y., Gurer, G., Dalkara, T., 2004. Loss of NeuN immunoreactivity after cerebral ischemia does not indicate neuronal cell loss: a cautionary note. Brain Res. 1015, 169–74. https://doi.org/10.1016/j.brainres.2004.04.032

van Calker, D., Müller, M., Hamprecht, B., 1979. Adenosine regulates via two different types of receptors, the accumulation of cyclic AMP in cultured brain cells. J. Neurochem. 33, 999–1005.

van der Klein, P.A., Kourounakis, A.P., IJzerman, A.P., 1999. Allosteric modulation of the adenosine A(1) receptor. Synthesis and biological evaluation of novel 2-amino-3-benzoylthiophenes as allosteric enhancers of agonist binding. J. Med. Chem. 42, 3629–35. https://doi.org/10.1021/jm991051d

van Doorn, R., Lopes Pinheiro, M.A., Kooij, G., Lakeman, K., van het Hof, B., van der Pol, S.M.A., Geerts, D., van Horssen, J., van der Valk, P., van der Kam, E., Ronken, E., Reijerkerk, A., de Vries, H.E., 2012. Sphingosine 1-phosphate receptor 5 mediates the immune quiescence of the human brain endothelial barrier. J. Neuroinflammation 9, 133. https://doi.org/10.1186/1742-2094-9-133

Van harreveld, A., SCHADE, J.P., 1959. Chloride movements in cerebral cortex after circulatory arrest and during spreading depression. J. Cell. Comp. Physiol. 54, 65–84.

van Muijlwijk-Koezen, J.E., Timmerman, H., van der Goot, H., Menge, W.M.P.B., Frijtag von Drabbe Künzel, J., de Groote, M., IJzerman, A.P., 2000. Isoquinoline and Quinazoline Urea Analogues as Antagonists for the Human Adenosine A_3 Receptor. J. Med. Chem. 43, 2227–2238. https://doi.org/10.1021/jm000002u

Varani, K., Portaluppi, F., Gessi, S., Merighi, S., Ongini, E., Belardinelli, L., Borea, P.A., 2000. Dose and time effects of caffeine intake on human platelet adenosine A(2A) receptors : functional and biochemical aspects. Circulation 102, 285–9.

Vartanian, T., Szuchet, S., Dawson, G., Campagnoni, A.T., 1986. Oligodendrocyte adhesion activates protein kinase C-mediated phosphorylation of myelin basic protein. Science 234, 1395–8.

Vessey, D.A., Kelley, M., Zhang, J., Li, L., Tao, R., Karliner, J.S., 2007. Dimethylsphingosine and FTY720 inhibit the SK1 form but activate the SK2 form of sphingosine kinase from rat heart. J. Biochem. Mol. Toxicol. 21, 273–279. https://doi.org/10.1002/jbt.20193

Vink, S., Alewood, P.F., 2012. Targeting voltage-gated calcium channels: developments in peptide and small-molecule inhibitors for the treatment of neuropathic pain. Br. J. Pharmacol. 167, 970–89. https://doi.org/10.1111/j.1476-5381.2012.02082.x

von Lubitz, D.K., 1999. Adenosine and cerebral ischemia: therapeutic future or death of a brave concept? Eur. J. Pharmacol. 371, 85–102.

Von Lubitz, D.K., Lin, R.C., Jacobson, K.A., 1995. Cerebral ischemia in gerbils: effects of acute and chronic treatment with adenosine A2A receptor agonist and antagonist. Eur. J. Pharmacol. 287, 295–302.

Vyskocil, F., Kritz, N., Bures, J., 1972. Potassium-selective microelectrodes used for measuring the extracellular brain potassium during spreading depression and anoxic depolarization in rats. Brain Res. 39, 255–9.

Walzer, T., Chiossone, L., Chaix, J., Calver, A., Carozzo, C., Garrigue-Antar, L., Jacques, Y., Baratin, M., Tomasello, E., Vivier, E., 2007. Natural killer cell trafficking in vivo requires a dedicated sphingosine 1-phosphate receptor. Nat. Immunol. 8, 1337–1344. https://doi.org/10.1038/ni1523

Wang, J., Huxley, V.H., 2006. Adenosine A2A receptor modulation of juvenile female rat skeletal muscle microvessel permeability. Am. J. Physiol. Heart Circ. Physiol. 291, H3094-105. https://doi.org/10.1152/ajpheart.00526.2006

Wang, M., Obrenovitch, T.P., Urenjak, J., 2003. Effects of the nitric oxide donor, DEA/NO on cortical spreading depression. Neuropharmacology 44, 949–57.

Wang, S., Kee, N., Preston, E., Wojtowicz, J.M., 2005. Electrophysiological correlates of neural plasticity compensating for ischemia-induced damage in the hippocampus. Exp. brain Res. 165, 250–60. https://doi.org/10.1007/s00221-005-2296-8

Watson, C., Long, J.S., Orange, C., Tannahill, C.L., Mallon, E., McGlynn, L.M., Pyne, S., Pyne, N.J., Edwards, J., 2010. High Expression of Sphingosine 1-Phosphate Receptors, S1P1 and S1P3, Sphingosine Kinase 1, and Extracellular Signal-Regulated Kinase-1/2 Is Associated with Development of Tamoxifen Resistance in Estrogen Receptor-Positive Breast Cancer Patients. Am. J. Pathol. 177, 2205–2215. https://doi.org/10.2353/AJPATH.2010.100220

Waxman, S.G., Zamponi, G.W., 2014. Regulating excitability of peripheral afferents: emerging ion channel targets. Nat. Neurosci. 17, 153–63. https://doi.org/10.1038/nn.3602

Wei, W., Du, C., Lv, J., Zhao, G., Li, Z., Wu, Z., Haskó, G., Xie, X., 2013. Blocking A2B adenosine receptor alleviates pathogenesis of experimental autoimmune encephalomyelitis via inhibition of IL-6 production and Th17 differentiation. J. Immunol. 190, 138–46. https://doi.org/10.4049/jimmunol.1103721

Welsh, T.G., Kucenas, S., 2018. Purinergic signaling in oligodendrocyte development and function. J. Neurochem. 145, 6–18. https://doi.org/10.1111/jnc.14315

West, S.J., Bannister, K., Dickenson, A.H., Bennett, D.L., 2015. Circuitry and plasticity of the dorsal horn – Toward a better understanding of neuropathic pain. Neuroscience 300, 254–275.

https://doi.org/10.1016/j.neuroscience.2015.05.020
White, P.J., Rose'Meyer, R.B., Hope, W., 1996. Functional characterization of adenosine receptors in the nucleus tractus solitarius mediating hypotensive responses in the rat. Br. J. Pharmacol. 117, 305–8.
Williamson, A. V, Compston, D.A., Randall, A.D., 1997. Analysis of the ion channel complement of the rat oligodendrocyte progenitor in a commonly studied in vitro preparation. Eur. J. Neurosci. 9, 706–20.
Wilson, S.M., Toth, P.T., Oh, S.B., Gillard, S.E., Volsen, S., Ren, D., Philipson, L.H., Lee, E.C., Fletcher, C.F., Tessarollo, L., Copeland, N.G., Jenkins, N.A., Miller, R.J., 2000. The status of voltage-dependent calcium channels in alpha 1E knock-out mice. J. Neurosci. 20, 8566–71.
Windrem, M.S., Nunes, M.C., Rashbaum, W.K., Schwartz, T.H., Goodman, R.A., McKhann, G., Roy, N.S., Goldman, S.A., 2004. Fetal and adult human oligodendrocyte progenitor cell isolates myelinate the congenitally dysmyelinated brain. Nat. Med. 10, 93–97. https://doi.org/10.1038/nm974
Wu, L.G., Saggau, P., 1994. Adenosine inhibits evoked synaptic transmission primarily by reducing presynaptic calcium influx in area CA1 of hippocampus. Neuron 12, 1139–48.
Wyss-Coray, T., 2016. Ageing, neurodegeneration and brain rejuvenation. Nature 539, 180–186. https://doi.org/10.1038/nature20411
Xaus, J., Mirabet, M., Lloberas, J., Soler, C., Lluis, C., Franco, R., Celada, A., 1999. IFN-gamma up-regulates the A2B adenosine receptor expression in macrophages: a mechanism of macrophage deactivation. J. Immunol. 162, 3607–14.
Xiao, Y., Yang, X.-F., Xu, M.-Y., 2007. Effect of acetylcholine on pain-related electric activities in hippocampal CA1 area of normal and morphinistic rats. Neurosci. Bull. 23, 323–328. https://doi.org/10.1007/s12264-007-0048-4
Xu, K., Bastia, E., Schwarzschild, M., 2005. Therapeutic potential of adenosine A(2A) receptor antagonists in Parkinson's disease. Pharmacol. Ther. 105, 267–310. https://doi.org/10.1016/j.pharmthera.2004.10.007
Yaar, R., Jones, M.R., Chen, J.-F., Ravid, K., 2005. Animal models for the study of adenosine receptor function. J. Cell. Physiol. 202, 9–20. https://doi.org/10.1002/jcp.20138
Yamamoto, A., Lucas, J.J., Hen, R., 2000. Reversal of Neuropathology and Motor Dysfunction in a Conditional Model of Huntington's Disease. Cell 101, 57–66. https://doi.org/10.1016/S0092-8674(00)80623-6
Yamashima, T., Tonchev, A.B., Borlongan, C. V, 2007. Differential response to ischemia in adjacent hippocampalsectors: neuronal death in CA1 versus neurogenesis in dentate gyrus. Biotechnol. J. 2, 596–607. https://doi.org/10.1002/biot.200600219
Yang, D., Zhang, Y., Nguyen, H.G., Koupenova, M., Chauhan, A.K., Makitalo, M., Jones, M.R., St Hilaire, C., Seldin, D.C., Toselli, P., Lamperti, E., Schreiber, B.M., Gavras, H., Wagner, D.D., Ravid, K., 2006. The A2B adenosine receptor protects against inflammation and excessive vascular adhesion. J. Clin. Invest. 116, 1913–23. https://doi.org/10.1172/JCI27933
Yang, J., Liu, X., Bhalla, K., Kim, C.N., Ibrado, A.M., Cai, J., Peng, T.I., Jones, D.P., Wang, X., 1997. Prevention of apoptosis by Bcl-2: release of cytochrome c from mitochondria blocked. Science 275, 1129–32.
Yao, Y., Sei, Y., Abbracchio, M.P., Jiang, J.-L., Kim, Y.-C., Jacobson, K.A., 1997. Adenosine A3Receptor Agonists Protect HL-60 and U-937 Cells from Apoptosis Induced by A3Antagonists. Biochem. Biophys. Res. Commun. 232, 317–322. https://doi.org/10.1006/bbrc.1997.6290
Yawo, H., Chuhma, N., 1993. Preferential inhibition of omega-conotoxin-sensitive presynaptic Ca2+ channels by adenosine autoreceptors. Nature 365, 256–8. https://doi.org/10.1038/365256a0
Yekkirala, A.S., Roberson, D.P., Bean, B.P., Woolf, C.J., 2017. Breaking barriers to novel analgesic drug development. Nat. Rev. Drug Discov. 16, 545–564. https://doi.org/10.1038/nrd.2017.87
Yoon, M.H., Bae, H.B., Choi, J. Il, 2005. Antinociception of Intrathecal Adenosine Receptor Subtype Agonists in Rat Formalin Test. Anesth. Analg. 101, 1417–1421. https://doi.org/10.1213/01.ANE.0000180994.10087.6F
Yoon, M.H., Bae, H.B., Choi, J. Il, Kim, S.J., Chung, S.T., Kim, C.M., 2006. Roles of Adenosine Receptor Subtypes in the Antinociceptive Effect of Intrathecal Adenosine in a Rat Formalin Test. Pharmacology 78, 21–26. https://doi.org/10.1159/000094762
Yoshii, F., Moriya, Y., Ohnuki, T., Ryo, M., Takahashi, W., 2017. Neurological safety of fingolimod: An updated review. Clin. Exp. Neuroimmunol. 8, 233–243. https://doi.org/10.1111/cen3.12397
Young, A.R., Ali, C., Duretête, A., Vivien, D., 2007. Neuroprotection and stroke: time for a compromise. J. Neurochem. 103, 1302–1309. https://doi.org/10.1111/j.1471-4159.2007.04866.x
Yu, L., Huang, Z., Mariani, J., Wang, Y., Moskowitz, M., Chen, J.-F., 2004. Selective inactivation or reconstitution of adenosine A2A receptors in bone marrow cells reveals their significant contribution to the development of ischemic brain injury. Nat. Med. 10, 1081–7. https://doi.org/10.1038/nm1103
Zablocki, J.A., Wu, L., Shryock, J., Belardinelli, L., 2004. Partial A(1) adenosine receptor agonists from a molecular perspective and their potential use as chronic ventricular rate control agents during atrial fibrillation (AF). Curr. Top. Med. Chem. 4, 839–54.
Zeilhofer, H.U., Wildner, H., Yévenes, G.E., 2012. Fast Synaptic Inhibition in Spinal Sensory Processing and Pain Control. Physiol. Rev. 92, 193–235. https://doi.org/10.1152/physrev.00043.2010

Zemann, B., Kinzel, B., Müller, M., Reuschel, R., Mechtcheriakova, D., Urtz, N., Bornancin, F., Baumruker, T., Billich, A., 2006. Sphingosine kinase type 2 is essential for lymphopenia induced by the immunomodulatory drug FTY720. Blood 107, 1454–8. https://doi.org/10.1182/blood-2005-07-2628

Zetterström, T., Fillenz, M., 1990. Adenosine agonists can both inhibit and enhance in vivo striatal dopamine release. Eur. J. Pharmacol. 180, 137–43.

Zhang, H., Jarjour, A.A., Boyd, A., Williams, A., 2011. Central nervous system remyelination in culture--a tool for multiple sclerosis research. Exp. Neurol. 230, 138–48. https://doi.org/10.1016/j.expneurol.2011.04.009

Zhang, L., Wang, X., Bullock, A.J., Callea, M., Shah, H., Song, J., Moreno, K., Visentin, B., Deutschman, D., Alsop, D.C., Atkins, M.B., Mier, J.W., Signoretti, S., Bhasin, M., Sabbadini, R.A., Bhatt, R.S., 2015. Anti-S1P Antibody as a Novel Therapeutic Strategy for VEGFR TKI-Resistant Renal Cancer. Clin. Cancer Res. 21, 1925–1934. https://doi.org/10.1158/1078-0432.CCR-14-2031

Zhang, Q., Zhou, P., Chen, Z., Li, M., Jiang, H., Gao, Z., Yang, H., 2013. Dynamic PIP2 interactions with voltage sensor elements contribute to KCNQ2 channel gating. Proc. Natl. Acad. Sci. U. S. A. 110, 20093–8. https://doi.org/10.1073/pnas.1312483110

Zhang, X.-F., Shieh, C.-C., Chapman, M.L., Matulenko, M.A., Hakeem, A.H., Atkinson, R.N., Kort, M.E., Marron, B.E., Joshi, S., Honore, P., Faltynek, C.R., Krafte, D.S., Jarvis, M.F., 2010. A-887826 is a structurally novel, potent and voltage-dependent Na(v)1.8 sodium channel blocker that attenuates neuropathic tactile allodynia in rats. Neuropharmacology 59, 201–7. https://doi.org/10.1016/j.neuropharm.2010.05.009

Zhang, Y., Yu, Q., Lai, T., Yang, Y., Li, G., Sun, S., 2013. Effects of small interfering RNA targeting sphingosine kinase-1 gene on the animal model of Alzheimer's disease. J. Huazhong Univ. Sci. Technol. [Medical Sci. 33, 427–432. https://doi.org/10.1007/s11596-013-1136-5

Zhao, Z., Francis, C.E., Ravid, K., 1997. An A3-subtype adenosine receptor is highly expressed in rat vascular smooth muscle cells: its role in attenuating adenosine-induced increase in cAMP. Microvasc. Res. 54, 243–52. https://doi.org/10.1006/mvre.1997.2044

Zheng, L., Chen, J., Huang, Y., Wang, Y., Yang, H., Zhang, Y., Xie, S., 2014. Evidence for A1 and A3 receptors mediating adenosine-induced intracellular calcium release in the dorsal root ganglion neurons by using confocal microscopy imaging. Lasers Med. Sci. 29, 1209–1215. https://doi.org/10.1007/s10103-013-1511-2

Zhou, A.-M., Li, W.-B., Li, Q.-J., Liu, H.-Q., Feng, R.-F., Zhao, H.-G., 2004. A short cerebral ischemic preconditioning up-regulates adenosine receptors in the hippocampal CA1 region of rats. Neurosci. Res. 48, 397–404. https://doi.org/10.1016/j.neures.2003.12.010

Zhou, Q.Y., Li, C., Olah, M.E., Johnson, R.A., Stiles, G.L., Civelli, O., 1992. Molecular cloning and characterization of an adenosine receptor: the A3 adenosine receptor. Proc. Natl. Acad. Sci. U. S. A. 89, 7432–6.

Zimmermann, H., Braun, N., Kegel, B., Heine, P., 1998. New insights into molecular structure and function of ecto-nucleotidases in the nervous system. Neurochem. Int. 32, 421–425. https://doi.org/10.1016/S0197-0186(97)00126-5

Zylka, M.J., 2011. Pain-relieving prospects for adenosine receptors and ectonucleotidases. Trends Mol. Med. 17, 188–196. https://doi.org/10.1016/j.molmed.2010.12.006